

Distribution Agreement

In presenting this thesis or dissertation as a partial fulfillment of the requirements for an advanced degree from Emory University, I hereby grant to Emory University and its agents the non-exclusive license to archive, make accessible, and display my thesis or dissertation in whole or in part in all forms of media, now or hereafter known, including display on the world wide web. I understand that I may select some access restrictions as part of the online submission of this thesis or dissertation. I retain all ownership rights to the copyright of the thesis or dissertation. I also retain the right to use in future works (such as articles or books) all or part of this thesis or dissertation.

DocuSigned by:
Signature: *Adrian Richard Demeritte*
FC476977ED15498...

Adrian Richard Demeritte
Name

7/12/2023 | 4:20 PM EDT
Date


Title TOTAL SYNTHESIS AND BIOLOGICAL EVALUATION OF NATURAL
PRODUCT MIMICS TOWARDS FUNGAL PATHOGENS

Author Adrian Richard Demeritte

Degree Doctor of Philosophy

Program Chemistry

Approved by the Committee

DocuSigned by:

8EA00928FE1F483...

William Wuest

Advisor

DocuSigned by:

4B23808931874CD...

Simon Blakey

Committee Member

DocuSigned by:

CE29A64E7A6B4A6...

Frank McDonald

Committee Member

Committee Member

Committee Member

Committee Member

Accepted by the Laney Graduate School:

Kimberly Jacob Arriola, Ph.D, MPH
Dean, James T. Laney Graduate School

Date

**TOTAL SYNTHESIS AND BIOLOGICAL EVALUATION OF NATURAL PRODUCT
MIMICS TOWARDS FUNGAL PATHOGENS**

By

Adrian R. Demeritte

B.A., Saint John's College, 2016

Advisor:

William M. Wuest, PhD.

Committee:

Frank McDonald, PhD

Simon Blakey, PhD

An abstract of
A dissertation submitted to the faculty of the
James T. Laney School of Graduate Studies of Emory University
In partial fulfillment of the requirements for the degree of
Doctor of Philosophy
In Chemistry
2023

Abstract

TOTAL SYNTHESIS AND BIOLOGICAL EVALUATION OF NATURAL PRODUCT MIMICS TOWARDS FUNGAL PATHOGENS

By: Adrian Demeritte

Natural products possess a wide range of bioactivities with potential for therapeutic usage. Often, these natural products are manufactured by certain organisms to make them competitive in their own environments. One can assume that a greater variety of secondary metabolites with novel structures are produced in environments with a larger biodiversity, as to provide producers with a selective advantage against competing organisms, induce antimicrobial effects against pathogenic microbes, or even to act as an adaptation to nonbiological impacts (such as light or elevated temperature). In several cases, these secondary metabolites derive their antimicrobial properties from mimicking natural cofactors. Synthetic chemists have fostered these properties by way of analog development, thereby utilizing novel scaffolds from natural products to reveal, enhance, or maintain bioactivity. The first chapter covers this idea specifically towards antifungal compounds. Pathogenic fungi are particularly capable of resistance development as a large percentage of our current armamentarium targets ergosterol synthesis in some way.

The second chapter covers the synthesis of phenolic bisabolene compounds isolated from deep sea sediment which display impressive activity against the causative agent in black rot in cruciferous vegetables, *Alternaria brassicae*. As all current inhibitors possess the same mechanism of action, there is a dire need for compounds with novel scaffolds to either overcome point mutations or provide alternative methods to inhibit growth. This chapter goes into the modular synthetic design mimicking the scaffold of the natural product penicaculin A, whose mechanism of action is currently unknown and may possess a novel pharmacophore for *Alternaria brassicae* inhibition. A key transformation through a theoretical pharmacophore containing intermediate is leveraged for analog development. Results show that peniciaculin A may act as a ubiquinone mimic at the Q_o site of the cytochrome *bc*₁ complex.

The third chapter covers the synthesis of 4-hydroxypyridinones which may owe their activity to an underutilized mechanism of action by inhibiting the Q_i site of the cytochrome *bc*₁ complex; specifically in their implication towards the invasive indoor pathogen *Aspergillus fumigatus*. The antifungal activity of 4-hydroxy-2-pyridione class of natural products remains thoroughly unexplored despite promising reports in the literature. This chapter first goes into diverted synthesis of a small group of 4-hydroxypyridinone natural products ilicicolin H, oxysporidinone, sambutoxin and septoriamycin A. The latter hints to the potential for these natural products to adopt different binding poses in the Q_i site of the pocket enabling a 'kingdom switch'. This chapter then covers efforts towards the synthesis of chimeric compounds which may aide in circumventing antifungal resistance through 4-pyridinone compounds which may not only mimic ilicicolin H through a simplified scaffold, but also possess a dual mechanism of action by leveraging the bioactivity of chromene.

Acknowledgements

I would like to acknowledge my advisor, Prof. William Wuest for always pushing me apply myself, and to be more confident in my knowledge of science. In many ways Bill, as he's endearingly called, can be seen as someone who asks a lot of others. I've realized that this comes from a place of respect as people only ask of you what they think you're capable of. Originally, I did not believe I had the capability to be in graduate school. However, it's because of people like Bill who've reminded me that one's current place is never a mistake and that validity does indeed exist in the moment itself.

I aspire to one day have but a fraction of the passion that Prof. Simon Blakey and Prof. Frank McDonald have towards not only furthering their own enthusiasm for science but instilling those values in others as well. Time and time again I've seen student's perspectives on chemistry shift because of conversations with these two concerning anything from the minute, to field changing ideas, and everything in between. To you all, please keep inspiring students even if you don't fully grasp your effect on them.

I could not have asked for a more supportive committee or chemistry department in general. Emory immediately outweighs other schools for recruitment weekend. Looking back, those students always left with positive outlooks without even meeting people like Dr. Fred Strobel who was always eager to help in the mass-spec room or Steve Krebs who would stop his day to genuinely ask how things were going before gesturing towards a box of donuts or freshly made French toast. Others who provide unsung support to students like Dr. Antonio Braithwaite or Kira Walsh, make being at Emory so much more than what it is on the surface or what you can see in a weekend visit.

I'd like to thank my previous advisors Dr. Thomas Nicholas Jones and Dr. Kate Graham at the College of Saint Benedict/ Saint John's University for sparking and fostering my initial interest in chemistry. Without you, I probably would have continued my plans to pursue a graduate level degree in another field, or perhaps never submit my applications in the first place.

I'd also like to acknowledge my original office mates and friends in the Wuest Lab, Dr. Justin Shapiro and Dr. Ana (Jaramillo) Cheng. You both eased the adjustment to graduate school and I'm incredibly thankful to have both of you in my life. I look forward to future trips, conversations, and finally getting to the rest of the to-do list still posted in our original office today. I'm thankful for others in the lab who served mentors and companions throughout my journey. Having learned so much from individuals like Dr. Erika Csatory, Dr. Kelly Robinson, Dr. Amber Scharnow in subgroups then leading my own was such an emboldening experience. Of course, one of the benefits of the Wuest lab would be general culture, so I'd like to thank everyone for their support in every situation.

To my graduate student mentor, Dr. Ingrid Wilt, thank you for standing by me throughout graduate school and always wanting to support me. Our dynamic always mimicked that of colleagues and I'll appreciate the conversations on science, life, music, and animated movies for what they were. To my first undergraduate mentee Alejandro McDonald, thank you for bringing a much-needed reminder of Caribbean culture to Bay 2. As time goes on, I hope we continue our lunch sessions to keep each other up to date on our endeavors and to continue encouraging one another. I'll always believe in your ability to impress yourself. To my first graduate mentee Ricardo Cruz, continue to blossom into an amazing chemist. Though getting you to open up at first was a challenge, I enjoy the ability to pop in and share a laugh whenever to lighten the mood if chemistry isn't going as planned. I'll cherish our bond as I continue my journey through science.

I'd like to thank the friends I've made outside of lab in graduate school for everything. From some of my best friends and former roommates like Quincy Mckoy and David Laws to others like Paul Beasly, Ayda Gonzalez, Tamra Blue, Alyssa Johnson, Dr. Ordy Manuel Gnewou and Dr. Brea Emmanuel; all of our memories from graduate school will be cherished. I'm happy to have started my graduate school journey with you all and I wish you the best in your future endeavors.

To my friends outside of graduate school, thank you for reminding me that scientific outcomes do not determine the worth of a person. Regardless of how many times a reaction didn't work, I was always 'Adrian' to Calvin Pratt, Kaal Ferguson, Theo Moss and Taylor D. Merfeld. To my mother Ramona Demeritte and sister Amethyst Demeritte, thank you for continually being my support system from so far away. To my father Fealy Demeritte, thank you for instilling values of hard work and perseverance in me. Had you still been here today I know you'd be proud. Lastly, I'd like to acknowledge and thank my fiancé Dr. Lovell Murphy for everything along this journey. You've been my rock since day one for all the ups and downs of my day-to-day life here and I can't express how much I appreciate you pushing me to be the best version of myself.

Table of Contents

1. Chapter 1: Natural Products

| | |
|--|-----------|
| 1.1. The importance of discourse in science, from cave walls to island porches | 1 |
| 1.2. Natural Products: the spices of life are secondary metabolites..... | 2 |
| 1.3. Antifungal Compounds | 3 |
| 1.3.1. Antifungal natural products and derivatives and their mechanism of action..... | 3 |
| 1.3.2. Antifungals not based on natural products..... | 6 |
| 1.4. Issues with the current toolbox | 7 |
| 1.5. Why mimic natural products | 8 |
| 1.6. Examples of antifungals mimicking natural products from the literature..... | 9 |
| 1.7. Examples of DTS strategies in the Wuest Lab..... | 11 |
| 1.8. Ubiquinone: a lesser utilized target..... | 14 |
| 1.9. Chapters..... | 15 |
| 1.10. Chapter 1 references..... | 16 |

2. Chapter 2: Total synthesis and biological evaluation of

| | |
|--|-----------|
| <i>antifungal phenolic bisabolenes.....</i> | 21 |
| 2.1. Introduction | 21 |

| | |
|---|----|
| 2.1.1. Blight and economic impact of fungal pathogens | 21 |
| 2.1.2. The pesticide problem | 22 |
| 2.1.3. Penciaculin A: a potential new hope..... | 24 |
| 2.1.4. Previous Approaches..... | 26 |
| 2.1.4.1 Previous synthesis of penciaculin A..... | 29 |
| 2.2. Results and discussion..... | 30 |
| 2.2.1. Synthesis by way of Aggarwal borylation (1,2 migration)..... | 30 |
| 2.2.2. Synthesis by asymmetric Grignard..... | 33 |
| 2.2.3. Synthesis by lithium halogen exchange..... | 35 |
| 2.2.3.1. Testing previous methods..... | 35 |
| 2.2.3.2. Synthesis of linchpin intermediate..... | 37 |
| 2.2.3.3. Lithium halogen exchange..... | 43 |
| 2.2.4. Aryl coupling | 48 |
| 2.2.5. Analog Design | 53 |
| 2.2.5.1 Ethyl acrylate analogs..... | 55 |
| 2.2.5.2 Enone derivatives..... | 56 |
| 2.2.6. Antimicrobial activity | 57 |
| 2.3. Conclusions and future directions..... | 60 |

| | |
|--|----|
| 2.4. Chapter 2 references..... | 62 |
| 3. Chapter 3: Progress towards the total synthesis of 4-hydroxypyridinones..... | 67 |
| 3.1. Introduction..... | 67 |
| 3.1.1. Silent killers | 67 |
| 3.1.2. The current toolbox has redundant tools | 69 |
| 3.1.3. 4-Hydroxypyridinones may provide alternative mechanisms for tackling this issue..... | 69 |
| 3.2. Results and discussion..... | 72 |
| 3.2.1. Synthesis of pyridinone core..... | 74 |
| 3.2.2. Coupling of western fragments..... | 78 |
| 3.2.3. C-3 functionalization | 80 |
| 3.2.3.1. Metalation then insertion into electrophiles..... | 80 |
| 3.2.3.2. Suzuki oxidative cleave tandem | 82 |
| 3.2.4. Revisiting the oxysporidinone western fragment | 83 |
| 3.2.5. Ongoing strategies for allylboration towards homoallylic alcohols..... | 84 |
| 3.2.6. Chimera compounds..... | 86 |
| 3.3. Conclusions | 92 |
| 3.4. Chapter 3 references..... | 92 |

| | |
|--|------------|
| 4. Chapter 4. Experimental details..... | 96 |
| 4.1. Fungal growth inhibition assays..... | 96 |
| 4.2. Chemistry: General notes..... | 97 |
| 4.3. Chemistry Synthesis procedures and characterization..... | 99 |
| 4.3.1. Chapter 2..... | 99 |
| 4.3.2. Chapter 3..... | 144 |
| 4.4. SI references..... | 165 |
| 5. Appendix..... | 167 |
| 5.1. Appendix chapter 2..... | 167 |
| 5.2. Appendix chapter 3..... | 198 |

Table of Schemes

| | |
|---|-----------|
| Scheme 2.1: Synthesis of Aggarwal borylation precursor | 31 |
| Scheme 2.2: Synthesis of (S,S)-ligand required for asymmetric Grignard | 34 |
| Scheme 2.3: Asymmetric Grignard addition to 2.2 | 34 |
| Scheme 2.4: Synthesis of Ito's aldehyde towards (+)-sydonol..... | 36 |
| Scheme 2.5: Diastereoselective nucleophilic addition | 44 |
| Scheme 2.6: Continued synthetic route towards peniciaculin A..... | 47 |
| Scheme 2.7: Synthesis of brominated and borylated aryl coupling partners | 49 |
| Scheme 2.8: Continued synthesis towards penciaculin A (post monodeprotection) | 52 |
| Scheme 2.9: Proposed hydrogenation of 2.36 to 2.1..... | 54 |
| Scheme 2.10: Synthetic route towards ethyl acrylate analogs | 56 |
| Scheme 2.11: Synthetic route towards enone and methoxy ketone analogs | 57 |
| Scheme 3.1: Synthesis of pyridinone core through Vilsmeier cyclization..... | 75 |
| Scheme 3.2: Synthesis of methylated pyridinone core..... | 76 |
| Scheme 3.3: Synthesis of N-hydroxylated pyridinone core..... | 77 |
| Scheme 3.4: Regioselective halogenation of pyridinone core | 78 |
| Scheme 3.5: Suzuki Miyaura of standard aryl boronic acids | 78 |
| Scheme 3.6: Synthetic route to boronic ester coupling partner for oxysporidinone | 79 |

| | |
|---|-----------|
| Scheme 3.7: Synthetic route towards ‘Bpin swapped’ coupling reaction | 80 |
| Scheme 3.8: Suzuki oxidative cleavage tandem | 83 |
| Scheme 3.9: Coupling of trifluoroborate salt | 84 |
| Scheme 3.10 : Synthetic reactions towards boronic ester 3.32..... | 85 |
| Scheme 3.11: Conditions for [3,3]-sigmatropic rearrangement | 86 |
| Scheme 3.12: Synthetic routes to homoallylic alcohol tandem partners | 91 |
| Scheme 3.13: Tandem Prins/ Friedel Crafts cyclization..... | 91 |

Table of Figures

| | |
|--|----|
| Figure 1.1: Fungal cell with major antifungal sites | 3 |
| Figure 1.2: Structures of polyene antifungals | 4 |
| Figure 1.3: Structures of allylamine natural product antifungals | 5 |
| Figure 1.4: Structures of members of the echinocandin family | 6 |
| Figure 1.5: Structures of azole antifungals | 7 |
| Figure 1.6: Antifungals from the sampangine scaffold | 10 |
| Figure 1.7: Antifungal developed from α -Mangostin | 11 |
| Figure 1.8: Progression towards simplified Carolacton analog..... | 12 |
| Figure 1.9: Baulamycins and their derivatives..... | 14 |
| Figure 1.10: Cyt <i>bc</i> ₁ complex with Q cycle of ubiquinone | 15 |
| Figure 2.1: Pharmacophore map of typical QoI fungicides | 23 |
| Figure 2.2: Structure of peniciculin A with QoI scaffold mapped on | 25 |
| Figure 2.3: Aggarwal methodology to set tertiary alcohols..... | 27 |
| Figure 2.4: Gilheany's tridentate ligand to set tertiary alcohols | 28 |
| Figure 2.5: Key disconnection for Yajima's synthesis of peniciculin A | 29 |
| Figure 2.6: Retrosynthetic disconnections for synthesis 3.1 by 1,2-migration | 30 |
| Figure 2.7: Retrosynthetic disconnections for synthesis of 3.1 by | |

| | |
|---|----|
| asymmetric Grignard | 33 |
| Figure 2.8: Retrosynthetic disconnections for synthesis of 3.1 through | |
| Diastereoselective nucleophilic addition | 35 |
| Figure 2.9: Structure of linchpin intermediate | 37 |
| Figure 2.10: Theoretical rearrangement of tertiary alcohol under acidic conditions | 41 |
| Figure 2.11: ¹ HNMR of linchpin overlap | 43 |
| Figure 2.12: Proposed model for diastereoselective nucleophilic addition | 45 |
| Figure 2.13: Peniciaculin analogs docked in cyt <i>bc₁</i> | 55 |
| Figure 2.14: Bioactivity of synthesized peniciaculin analogs | 58 |
| Figure 2.15: Future proposed analogs mimicking the peniciaculin A scaffold | 61 |
| Figure 3.1: Structure of target 4-hydroxypyridinones | 70 |
| Figure 3.2: SAR map of 4-hydroxypyridinone scaffold along with binding results | 73 |
| Figure 3.3: Retrosynthetic example on oxysporidinone | 74 |
| Figure 3.4: Breakdown of synthetic strategy using dihalogenated pyridinone | 77 |
| Figure 3.5: Rmanchandran's [3,3]-sigmatropic rearrangement to | |
| benzylic homoallylic alcohols | 85 |
| Figure 3.6: Structures of docked polycyclic chromene pyridinones | 88 |
| Figure 3.7: Overlapped structure of best chimera analogs without constraints | 89 |

Figure 3.8: Structures of best fitting chimera analogs with hydrogen

bonding constraint90

Table of Tables

| | |
|---|----|
| Table 2.1: Optimization of 1,2-migration..... | 32 |
| Table 2.2: Benzylic oxidation conditions | 32 |
| Table 2.3: Optimization of diastereoselective Grignard addition | 36 |
| Table 2.4: Coupling conditions with benzylic oxygen as the nucleophile | 38 |
| Table 2.5: Coupling conditions with azodicarboxylates | 39 |
| Table 2.6: Conditions for optimization of benzylic bromination | 40 |
| Table 2.7: Conditions for optimization of benzylic coupling | 42 |
| Table 2.8: Optimization of lithium halogen exchange | 46 |
| Table 2.9: Optimization of aryl coupling | 51 |
| Table 3.1: Suzuki conditions attempted for coupling oxysporidinone Western fragment..... | 79 |
| Table 3.2: Conditions for metalating at the C-3 position | 81 |

List of Abbreviations

Ab *Alternaria brassicae*

Ac acetyl

AIBN azobisisobutyronitrile

APCI atmospheric pressure chemical ionization

Ar aryl

Bn benzyl

Boc *tert*-butyloxycarbonyl

Bu butyl

Ccpa carbon catabolite control protein

CBS Corey-Bakshi-Shibata

Cbz carboxybenzyl

CFU colony forming unit

DBU 1,8-diazabicycloundec-7-ene

D₂O deuterium oxide

1,2-DCE 1,2-dichloroethane

DCM dichloromethane

DIBAL-H diisobutylaluminum hydride

DIPEA *N,N*-diisopropylethylamine

DMAD dimethyl acetylenedicarboxylate

DMAP *N,N*-4-(dimethylamino)pyridine

DMF *N,N*-dimethylformamide

dppf 1,1'-bis(diphenylphosphino)ferrocene

d.r. diastereomeric ratio

DTS diverted total synthesis

EDG electron-donating group

ee enantiomeric excess

Et ethyl

equiv equivalents

ESI electrospray ionization

EWG electron-withdrawing group

Fmoc Fluorenylmethyloxycarbonyl

h hours

HA hospital acquired

HAT hydrogen atom transfer

HPLC high performance liquid chromatography

HRMS high-resolution mass spectrometry

HWE Horner-Wadsworth Emmons

IDM iron deficient media

IFI invasive fungal infection

IPA invasive pulmonary aspergillosis

IR infrared spectroscopy

IRM iron rich media

L ligand

LAH lithium aluminum hydride

LDA lithium diisopropylamide

LLS longest linear sequence

Me methyl

MIC minimum inhibitory concentration

min minutes

mmol millimoles

MoA mechanism of action

MOM methoxymethyl

MRSA methicillin resistant *Staphylococcus aureus*

Ms mesyl

MS molecular sieves

NBS *N*-bromosuccinimide

NPs natural products

NMR nuclear magnetic resonance

nr no reaction

OMe methoxy

PG protecting group

Ph phenyl

Pr propyl

PTLC preparatory thin layer chromatography

PTSA *p*-toluenesulfonic acid

Qi quinone inside

Qo quinone outside

QiI quinone inside inhibitor

QoI quinone outside inhibitor

SAR structure activity relationship

SAM sambutoxin

SEP septoriamycin

OXY oxysporidinone

SDH succinate dehydrogenase

SDHI succinate dehydrogenase inhibitor

SEM trimethylsilylethoxymethyl

TBAF tetrabutylammonium fluoride

TBAI tetrabutylammonium iodide

TBS *tert*-butyldimethylsilyl

TBDPS *tert*-Butyldiphenylsilyl

TEA triethylamine

temp temperature

Tf trifluoromethanesulfonyl

THF tetrahydrofuran

TIPS triisopropylsilyl

TLC thin layer chromatography

TMEDA *N,N,N',N'*-tetramethylethylenediamine

TS transition state

Chapter 1: Natural Products.

1.1. The Importance of Discourse in Science, from Cave Walls to Island Porches

Discourse has a timeless role on the center stage of progression throughout history. This powerful tool has shaped individual and collective understanding towards a honed sense of the minute, amplified the impact of the unseen, and highlighted the importance of argumentation (based on evidence) to persuade. Indeed, scientific achievement, and dissemination thereof, would be stunted without discourse.

This discourse can be written or spoken and can take form by way of conversation, literature review or even artistic representation. The earliest signs of such discourse can be traced all the way back to depictions on cave walls or clay tablets. Though the content was vast, knowledge related to the preservation of health, well-being, and good harvest was guaranteed to be recorded, emboldened throughout time, and passed down from generation to generation. For instance, depictions of oils from *Cupressus sempervirens* (Cypress) and *Commiphora* species (myrrh) can be found on clay tablets in cuneiform from Mesopotamia thousands of years ago.¹ Not surprisingly, these oils and plants are still used today to treat coughs, colds, and inflammation. This same trend can be seen throughout history. Indeed, whether it be through ancient Egyptian, Babylonian or Indian records, through any of the Chinese Dynasties, or even during the Dark and Middle Ages, there is some illustration, and discourse thereof, of medicine and the impact of the minute molecules all around us.²

Growing up on an island, this discourse took its shape in the form of folklore. Countless stories from those of yesteryear were told on screened in porches about the medicinal effects of certain plants or cocktails from the garden. These tales about “bush medicine” carried powerful

implications of the capabilities of the tiny molecules in the plants that inhabit the region.³⁻⁷ Rather than scrutinize which herb works better for coughs or aches one may wonder why they work at all.

1.2. Natural Products: The Spices of Life are Secondary Metabolites

Such discourse has played a vital role in the diffusion of knowledge on natural products throughout time. Natural products (NPs) have been reported to exhibit a wide range of medicinally relevant bioactivities and therefore play a dominant role in the discovery and development process towards lead compounds for human medicine. These pharmaceutically relevant small molecules bridge an important gap in antipathogenic, anticancer, anti-inflammatory and immunomodulatory efforts that nonchemical therapeutic practices could not accomplish alone. Also known as secondary metabolites due their mechanism of synthesis or specialized metabolites due to their potential use in primary life sustaining roles, these compounds are synthesized mainly by bacteria, fungi and plants and can be unique to an organism or a specific taxonomic group. There are various reviews on NPs from these organisms in the literature, in fact the *SuperNatural 2* general database estimates there are over 326,000 known NPs to date.⁸ Bioactive secondary metabolites can have a variety of effects towards the survival of their parent organisms by acting as necessitating factors to attract, deter, or kill other organisms.⁹ In turn, one can assume that a greater variety of secondary metabolites with novel structures provide producers with a selective advantage against competing organisms, induce antimicrobial effects against pathogenic microbes, or even to act as an adaptation to environmental impacts or stimuli. In many cases NPs owe their success in drug discovery to their structural diversity and therefore crucial to increase the potential for the identification of biologically relevant molecules.¹⁰

1.3 Antifungal Compounds

1.3.1 Antifungal Natural Products and Derivatives and Their Mechanisms of Action

Several antifungal agents have been derived from natural products for clinical use. One of the earliest antifungal natural products to show selective inhibitory activity against fungi was griseofulvin. Derived from *Penicillium griseofulvum*, this polyketide was shown to prevent mitosis by binding to tubulin.¹¹ This antifungal was not only one of the first to gain FDA-approval, but it was also the first to be used widely used to treat superficial fungal infections.¹²

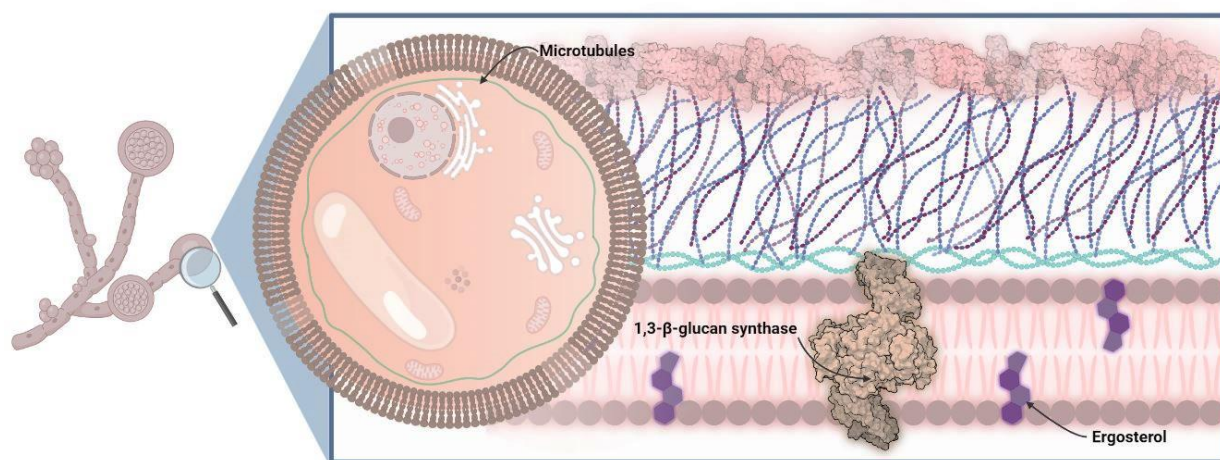


Figure 1.1: Fungal cell with major targets for common antifungals highlighted. Note that many of the major fungicides on the market today target ergosterol in some capacity. Figure constructed in Biorender.com.

The natural product polyenes gained notoriety in the 1950s and have been a staple in treating systemic infections ever since. These compounds also represent one of the major structural classes of antifungal natural products. Though nystatin (previously fungicin) was the first polyenic compound with known antifungal activity the most well-known natural product polyene came about in 1955 by way of amphotericin B.^{13,14} These large bacterial macrocyclic lactones are produced by members of the *Streptomyces* species and have the broadest spectrum of activity of any clinically useful antifungal compounds. Compounds in this class associate with the main sterol in fungal cell membranes (ergosterol) and cause membrane disruption, increased permeability, leakage of cytoplasmic contents and ultimately cell death.^{15–17} Since then, more than 200 polyene

antifungals have been discovered, with amphotericin B, nystatin and natamycin being most commonly used in antifungal therapy.^{18,19} While these fungicidal molecules are still used they suffer from a significant drawback, namely significant nephrotoxicity due to the off target effects of ergosterol binding and pore formation within the cell membrane.^{18,20} Though lipid-based formulations of amphotericin B maintain broad spectrum activity and a lower incidence of nephrotoxicity, higher costs for these formulations limit their usage.²¹

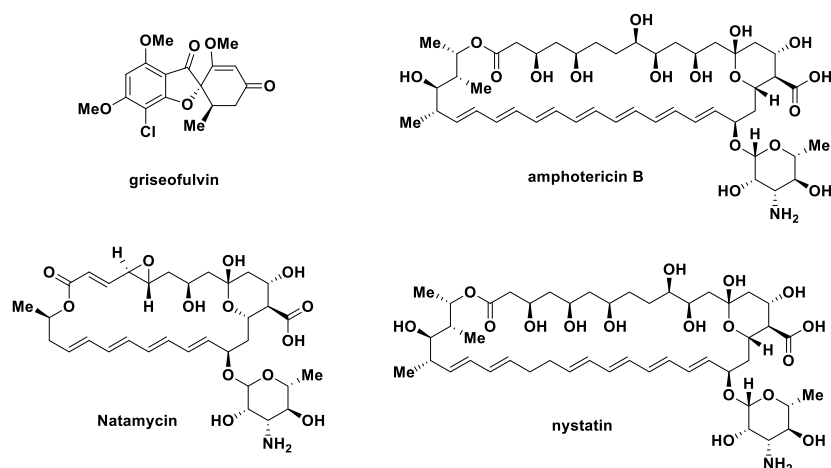


Figure 1.2: Structures of polyene antifungals.

Another group of known natural product derived antifungals comes from a small set of semisynthetic compounds known as the allylamines. These compounds contain a natural product pharmacophore that mimics a portion of squalene, and thereby target the squalene epoxidase in a reversible, noncompetitive manner, inhibiting an early stage of ergosterol biosynthesis and thereby affecting membrane structure and function.²² Examples from this class came in the 1980's with naftifine being developed as an allylamine agent for topical use and terbinafine being used as a widespread antifungal for dermatophyte infections after improvements for systemic bioavailability.^{23,24}

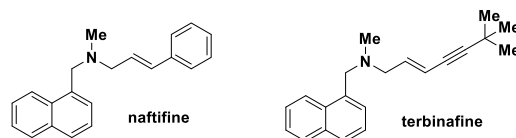


Figure 1.3: Structures of allylamine natural product antifungals.

Though the azoles came before them, in the early 2000's the echinocandins provided other natural product based fungal inhibitors. The echinocandins are fungal lipopeptide natural products that affect the biosynthesis of the fungal cell wall through non-competitive inhibition of 1,3- β -glucan synthase encoded by *FKSI*.²⁵ This enzyme is responsible for the production of β -1,3-glucan, a critical cell wall component of many pathogenic fungi. The echinocandins have a rather limited antifungal spectrum and the pharmacokinetics of the natural products are well are not favorable, thus semisynthetic derivatives have been prepared over the years to allow for clinical use: caspofungin (synthesized from pneumocandin B₀), anidulafungin (synthesized from echinocandin B), and micafungin (synthesized from FR901379).²⁶ This modified class of antifungals is often used to treat systemic fungal infections as they have a relatively good safety profile with low toxicity and few drug-drug interactions.²⁷ One major limitation, however, is the requirement of intravenous administration due to poor bioavailability resulting from their large size and weight.

1.3.2 Antifungals not based on Natural Products

Another major class of fungal inhibitors not based on natural products are azoles. Azoles are the most widely used antifungals and are synthetic compounds that reversibly inhibit cytochrome P450 enzyme 51 (eburicol 14 α -demethylase), which is responsible for demethylation of lanosterol in the synthesis towards ergosterol, leading to cytotoxic depletion of ergosterol.²⁸ The first azole imidazole derivatives (clotrimazole and miconazole) were discovered in the 1960s and were marketed as topical alternatives to griseovulvin and nystatin for cutaneous and mucocutaneous infections.²⁹ Traction for azoles greatly increased after ketoconazole, a miconazole

derivative, was introduced in 1981 for greater oral availability.³⁰ This broad spectrum antifungal was soon modified to attenuate its toxicity profile and eventually newer triazoles like fluconazole and itraconazole were brought to the market with improved safety panels became the universal option for azole treatment.³¹ It should be noted that though lanosterol demethylase also plays an important role in cholesterol synthesis in mammals, the antifungal efficacy of azoles show moderate specificity for the fungal enzyme over the mammalian counterpart.³²

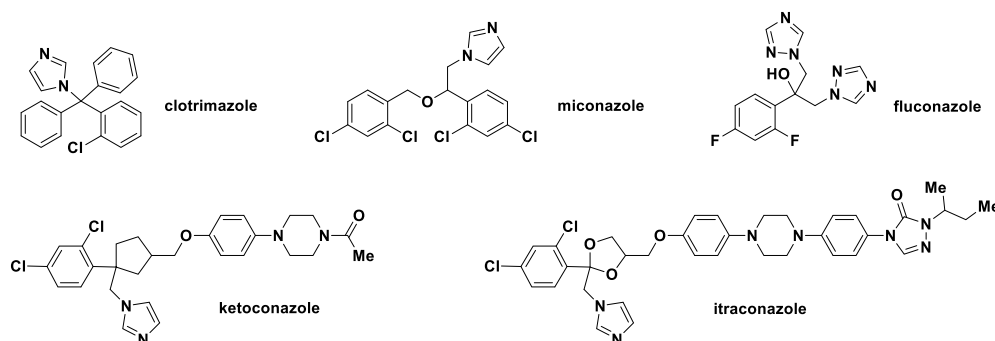


Figure 1.5: Structures of azole antifungals. Ketoconazole and itraconazole are typically administered as a racemic mixture.

1.4 Issues with the Current Toolbox

A cursory glance at the current armamentarium for antifungals reveals a common mechanism of action (MoA). The near universal focus on the disruption of cell membrane integrity by the accumulation of sterol precursors and the reduction of ergosterol, has led to the emergence of resistance in many cases. For instance, resistance in azoles often involves alteration or overexpression of the drug target gene (*ERG11/cyp51A/cyp51B*). In many cases, point mutations in *Candida* and *Aspergillus* close to the heme-binding site of the enzyme result in a loss of azole activity.³³ Separately, *ERG3* mutations can lead to the accumulation of alternative sterols through ergosterol depletion and often result in cross-resistance to azoles and polyenes. Additionally, induction of efflux-related genes like *CDR1*, *CDR2*, and *MDR1* have also been associated with

clinical azole resistance in several *Candida* species.^{34–36} Echinocandin resistance most commonly stems from mutations in highly conserved regions of the Fsk subunits in the target enzyme glucan synthase.³⁷ Alarming, these mutations in hot-spot regions of the gene typically impart cross-resistance to all of the echinocandin drugs.³⁸ This common mechanism of action and the potential for the development of cross resistance due to targeting the same biosynthetic pathway, highlights the alarming need for compounds with alternative MoAs or further expansion of bioactive scaffolds to circumvent resistance due to point mutations.

1.5 Why Mimic Natural Products

Though most directly obtained through harvesting from their natural sources, this process can at times be tedious, time consuming and expensive.³⁹ Moreover, supply can be greatly outweighed by demand, or can be inconsistent due to varied biosynthesis caused by conditions differing from the ecological environment of the producing organism. Total synthesis serves to fill in that gap. Throughout the years, a wide variety of NPs with medicinally relevant bioactivities have been synthesized in academic research labs and pharmaceutical companies around the world.^{40,41} In many cases, total synthesis was combined with a greater exploration of chemical space through the production of corresponding analogs of target NPs which, themselves, could increase the number of bioactive compounds for therapeutic usage but also ultimately expand understanding of the mechanism of action for their respective NPs.^{42,43}

While efforts in natural product isolation help to generate new lead molecules for drug discovery and development, analog production offers an alternative, as well as an extension, to the classical drug discovery pipeline by providing a basis for further chemical and biological studies on bioactive secondary metabolites. There can be many takeaways from analog development. For instance, the creation of a dimensionally similar minimized scaffold may maintain or even improve

biological activity while overcoming limitations of synthetic accessibility, viability in approach, or analysis capabilities. Alternatively, one may discover or introduce new and exciting biological properties through varied structural modifications.

1.6 Examples of Antifungals Mimicking Natural Products from the Literature

There are quite a few examples of antifungal natural products which have benefitted from analog development. Sampangine is a copyrine alkaloid first isolated from the bark of *Cananga odorata* in 1986.⁴⁴ This compound found to have potent antifungal activity that was later linked to the reduction of cellular oxygen, the induction of reactive oxygen species (ROS), and alterations in heme biosynthesis.⁴⁵ It's believed that these qualities arise from a quinone-like redox cycling mechanism that consumes oxygen and produces high levels of cellular ROS. Analog development by Jiang and coauthors through a scaffold hopping and ring replacement lead to several successful analogs which could be accessed in five steps and retained, or improved activity and overall water solubility compared to the parent natural product.⁴⁶ These two compounds represent good starting points for the development of new generation of antifungal agents as they exhibit excellent antifungal activity against a variety of fungal pathogens, like fluconazole resistant isolates, and also benefit from low toxicity and strong inhibitory effects on fungal biofilms.⁴⁶

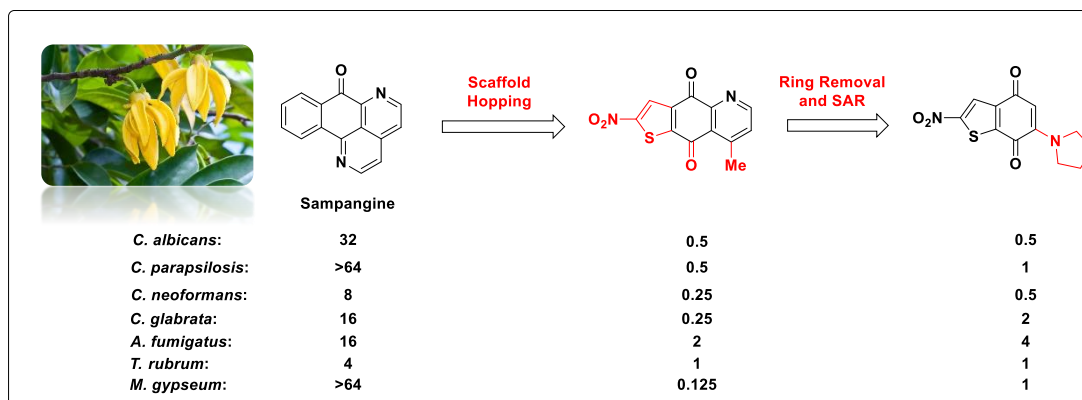


Figure 1.6: Antifungals developed from the sampangine natural product isolated from *Cananga odorata* (left). Sampangine scaffold is shown along with relevant antifungal activity. Values shown are for MIC₈₀ experiments with values given in µg/ mL.

α -Mangostin is the major xanthone derivative extracted from the skin of mangosteen and has a wide range of pharmacological properties though its antifungal activity was found to be negligible (MIC values up to 1 mg/mL).^{47–51} Lin and coauthors sought to create semisynthetic derivatives to mimic antimicrobial peptides which have an amphipathic structure and primarily kill fungal cells by disrupting the cell membrane.⁵² Their hypothesis was that these mangostin derivatives could circumvent the downfalls of antimicrobial peptides, namely lack of selectivity, enzymatic degradation and high production cost through their cationic amphiphilic nature.^{53,54} Lin and coauthors found that arginine residue coupled xanthones were much more active against species of *C. albicans*, *Aspergillus* and *Fusarium* strains. In some cases activities were comparable to and even better than known antifungals caspofungin and natamycin. The indicated analog was not only nontoxic against human corneal fibroblasts at concentrations up to IC₅₀ of 64.1 μ g/ mL but in resistance studies some species of *C. albicans* failed to develop drug resistance even after 27 passages, aptly both improving the activity of α -Mangostin while attenuating the drawbacks of antimicrobial peptides.

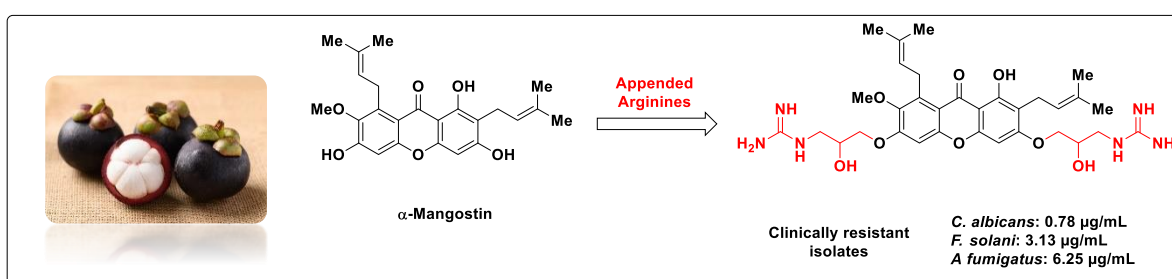


Figure 1.7: Antifungal developed from the xanthone derivative α -Mangostin from the skin of mangosteen. Antifungal activities shown are against resistant clinical isolates.

1.7. Examples of DTS Strategies in the Wuest Lab

Natural product researchers have looked toward unique ecosystems to discover secondary metabolites with excellent biological activities to use in society.⁵⁵ Diverted total synthesis (DTS) is a specific strategy in natural product synthesis that our group has leveraged toward the efficient synthesis of bioactive natural products of interest. DTS utilizes strategic retrosynthetic design to build complex natural products from simple building blocks through a convergent manner, which in themselves can serve as starting points of synthetic analogs. This can greatly simplify synthetic campaigns for structure-activity relationship (SAR) efforts of biologically interesting compounds.

In the Wuest lab we focus on the diversification and target identification of antimicrobial natural products enabled by total synthesis. One specific example from the can be seen in the total synthesis of the natural product carolacton. Carolacton is a secondary metabolite isolated from the myxobacterium *Sorangium cellulosum*, with the ability to affect *Streptococcus mutans* cells transitioning to a biofilm at nanomolar concentrations. After completing the total synthesis of this molecule in 2014, elucidation of the cause of biofilm-specific activity in *S. mutans* was limited through molecular genetic techniques as the bioactivity of carolacton was monitored by LIVE/DEAD staining and CFU/mL counts which have to low throughput analysis of carolacton-treated cells.⁵⁶ We sought to promote further analysis of the activity of carolacton by creating a simplified analog of this natural product with quantifiable biofilm inhibitory activity. In 2017 we were able to demonstrate that a simplified analog, named C3, inhibited 50% of biofilm formation with an IC_{50} of 63 μM .⁵⁷ It is significant to note that this initial observation of biofilm inhibition was the first instance of a quantifiable IC_{50} value for carolacton or its analogs. This finding also showed the importance of chain length and, in a follow up paper in 2019, we were able to simplify the carolacton side chain while oversaturating the carolacton macrocycle to produce a drastically simplified analog, (+)-aklyl. This analog not only maintained activity with an IC_{50} of 44 μM but

also allowed for the first observance of a minimum inhibitory concentration (MIC) value for any compound structurally related to carolacton at 250 μM .⁵⁸ This analog effectuated the preliminary screening of *S. mutans* mutants, aiding in the identification of a carbon catabolite control protein (CcpA) as the putative target of (+)-alkyl. Hence, this analog provided an additional tool for which further biological data could be garnered in future assays. Carolacton's story illustrates an important takeaway from analog development, namely the production of a simplified scaffold which not only maintained bioactivity, but also provided an additional means of analysis through that simplification.

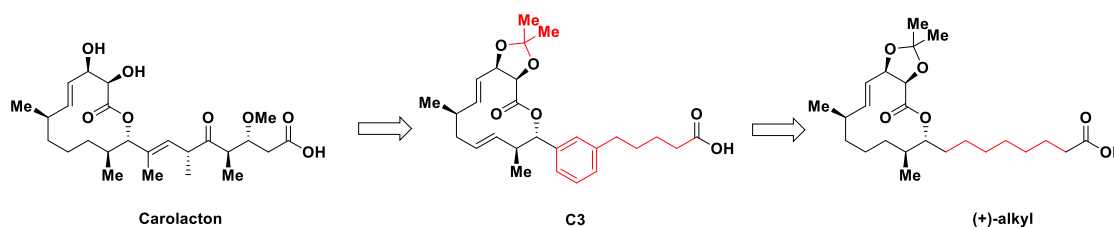


Figure 1.8: Progression towards simplified Carolacton analog (+)-2.

Another example from our group comes from our synthesis of baulamycins A and B. The baulamycins were isolated from an extract derived from *Streptomyces tempisquensis* (Playa Grande, Costa Rica) and were shown to inhibit in vitro bacterial iron acquisition.⁵⁹ The initial isolation paper of these compounds showed discrepancies in their broad spectrum activity, particularly against *Staphylococcus aureus* in both iron rich and iron depleted media (IRM and IDM respectively). This inconsistency, along with ambiguity in absolute and relative stereochemistry of baulamycin A and B, prompted our efforts to leverage diverted total synthesis (DTS) toward a better understanding of the biological mode of action of these compounds. Through the total synthesis of the baulamycins along with eight rationally designed analogs (A-

H) (**Figure 9**), we were able to identify a common chemotype as well as attribute broad spectrum activity in iron-rich media to nonselective membrane lysis which was further supported by uptake experiments.⁶⁰ Moreover, the simplified analog (-)-F provided improved potency with an MIC of 8 μ M in both IRM and IDM when compared to values of baulamycin A (125 μ M and 125 μ M) and baulamycin B (500 μ M and 250 μ M). This ability to discern previously unknown mechanisms of action represents yet another important takeaway from analog development. These aspects, when applied to already potent bioactive small molecules, can lead to the discovery of previously unknown information regarding MoA or even the discovery of more easily accessible natural product derivatives which maintain necessary bioactivity. Not included in this short section, but of equal importance, are methods and strategies to improve solubility, stability, absorption, and dissolution of bioactive secondary metabolites which are pertinent when it comes to the bioavailability of these NPs in human medicine. Indeed, synthesis of analogs and SAR development provides a powerful method for lead drug discovery.

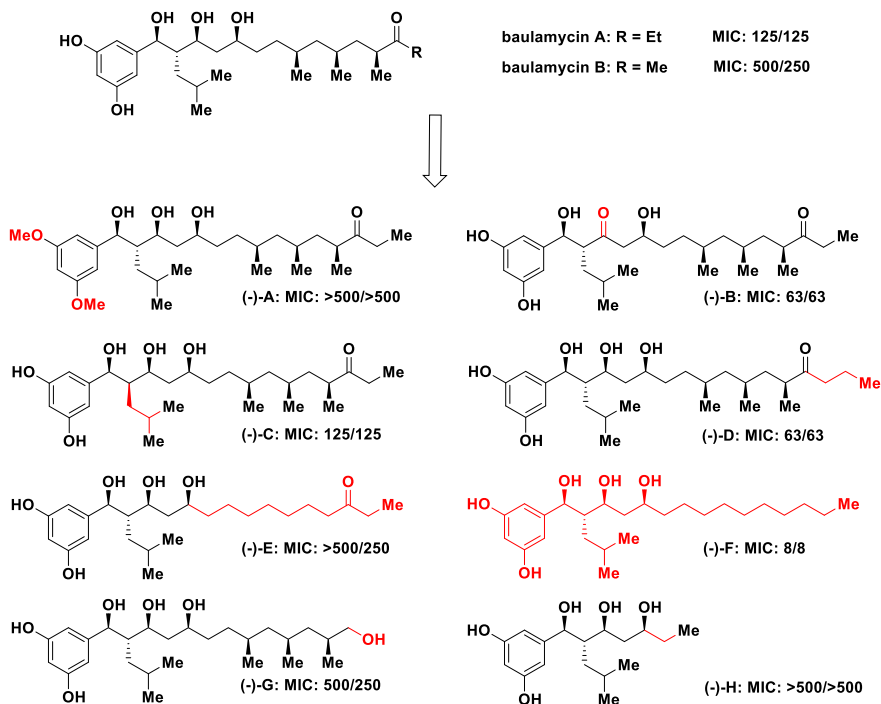


Figure 1.9: Baulamycins A and B along with 8 analog derivatives used in MOA identification. The two MIC values (in μM) refer to iron rich media and iron depleted media respectively (*S. aureus* SH1000).

1.8 Ubiquinone a Lesser Utilized Target

As said before inspiration for lead drug development stems from mimicking natural cofactors of target enzymes. For example, ubiquinone (coenzyme q10) is a lipid-soluble compound composed of a redox active quinoid moiety and a hydrophobic tail (**Figure 1.10**). This coenzyme plays an important role in energy production in both bacteria and the mitochondria in a redox reaction known as the Q cycle via complex III (cyt *bc*₁) in the electron transport chain.⁶¹ This cycle takes place in two distinct binding sites on the cytochrome b subunit: the ubiquinol-oxidation (Q_o) site and the ubiquinone-reduction (Q_i) site. The role of these two sites in electron transport chain makes them attractive targets for drug development by taking advantage of the ubiquitous binding affinity of this cofactor via use of ubiquinone mimics with a broad spectrum of activity.⁶² Even though some pathogens have developed resistance in part due to mutations on mitochondrial genes in these sites, mutations tend to come with some fitness costs. Moreover, development of natural product-inspired, structurally unique inhibitors helps circumvent resistance through novel pharmacophores and in some cases lead to entirely new mechanisms of action. I've focused the majority of my doctoral work on the development of structurally unique inhibitors is needed to keep pace with the likely emergence of resistant pathogens.

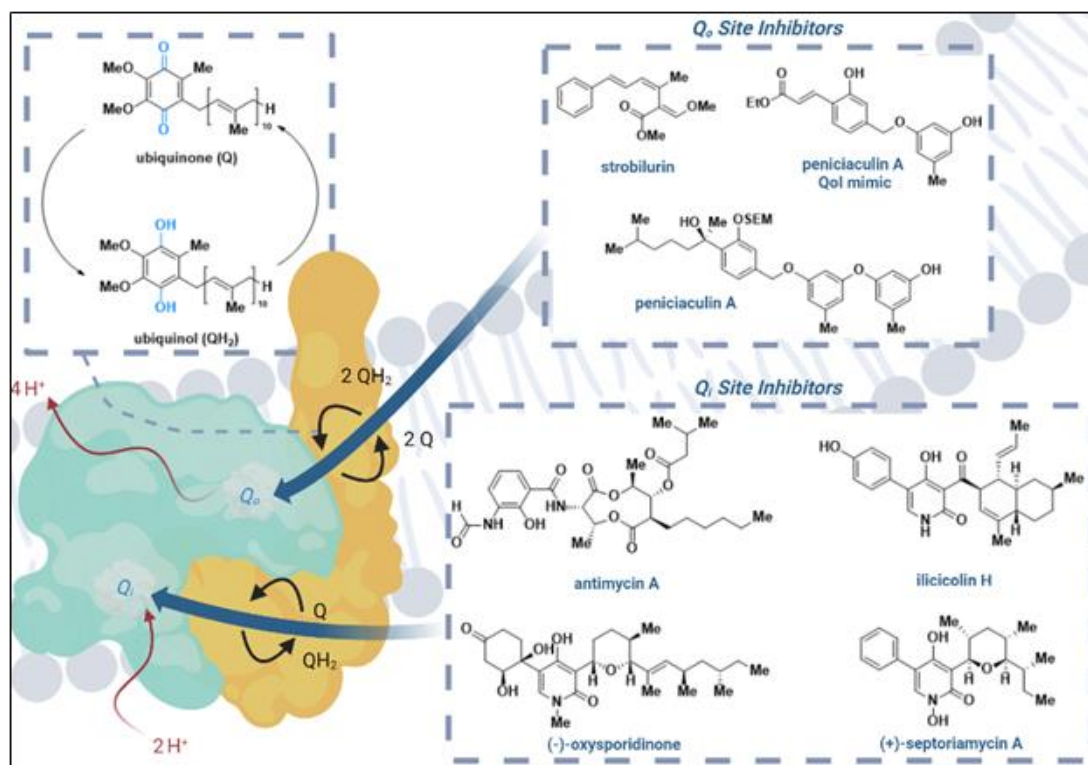


Figure 1.10. Cyt *bc*₁ complex shown highlighting the Q cycle of ubiquinone and the roles of the Q_o and Q_i sites in this process. The strobilurins are known to target the Q_o site and peniciculin A/analogues are proposed to as well. Antimycin A is known to target the Q_i site and 4-hydroxypyridinones (-)-oxysporidinone and (+)-septoriamycin A are proposed to as well.

1.9 Chapters

The second chapter covers synthetic efforts towards the total synthesis of peniciculin A, a phenolic bisabolane type sesquiterpenoid identified from a culture of *P. aculeatum*, as well as the synthesis and biological evaluation of several analogs to probe SAR. Here I demonstrate why I believe that these molecules mimic known QoIs targeting the Q_o site of the *bc*₁ complex. This chapter also has a short section on future synthetic analogs planned.

The third chapter covers synthetic efforts towards several pyran-containing 4-hydroxypyridinones like ilicicolin H, (-)-oxysporidinone and (+)-septoriamycin A. I hypothesize that these target the Q_i site of the *bc*₁ complex. In this chapter I demonstrate how to I plan leverage DTS toward a better understanding of the biological MoA of these compounds as well as their

simplification. This chapter also has a short section detailing the continued synthesis of these natural products and derivatives.

1.10. Chapter 1 References

- (1) Cragg, G. M.; Newman, D. J. Biodiversity: A Continuing Source of Novel Drug Leads. *Pure Appl. Chem.* **2005**, *77* (1), 7–24.
- (2) Shokeir, A. A.; Hussein, M. I. The Urology of Pharaonic Egypt. *BJU Int.* **1999**, *84* (7), 755–761.
- (3) Vujicic, T.; Cohall, D. Knowledge, Attitudes and Practices on the Use of Botanical Medicines in a Rural Caribbean Territory. *Front. Pharmacol.* **2021**, *12*, 2919.
- (4) Whistler, W. A. Traditional and Herbal Medicine in the Cook Islands. *J. Ethnopharmacol.* **1985**, *13* (3), 239–280.
- (5) Miyamoto, K.; Ehara, H.; Thaman, R.; Veitayaki, J.; Yoshida, T.; Kobayashi, H. Traditional Knowledge of Medicinal Plants on Gau Island, Fiji: Differences between Sixteen Villages with Unique Characteristics of Cultural Value. *J. Ethnobiol. Ethnomed.* **2021**, *17* (1), 1–14.
- (6) Halberstein, R. A. Traditional Botanical Remedies on a Small Caribbean Island: Middle (Grand) Caicos, West Indies. **2007**, *3* (3), 227–239.
- (7) Richey-Abbey, L. R. Bush Medicine in the Family Islands: The Medical Ethnobotany of Cat Island and Long Island, Bahamas. *Dissertation; Miami University.* **2012**, 1–301.
- (8) Banerjee, P.; Erehman, J.; Gohlke, B. O.; Wilhelm, T.; Preissner, R.; Dunkel, M. Super Natural II-a Database of Natural Products. *Nucleic Acids Res.* **2015**, *43* (D1), D935–D939.
- (9) Petersen, L.-E.; Kellermann, M. Y.; Schupp, P. J. Secondary Metabolites of Marine Microbes: From Natural Products Chemistry to Chemical Ecology. *YOUMARES 9 - The Oceans: Our Research, Our Future* **2020**, 159–180.
- (10) Hong, J. Natural Product Diversity and Its Role in Chemical Biology and Drug Discovery. *Curr. Opin. Chem. Biol.* **2012**, *15* (3), 350–354.
- (11) Oxford, A. E.; Raistrick, H.; Simonart, P. Studies in the Biochemistry of Micro-Organisms: Griseofulvin, C₁₇H₁₇O₆Cl, a Metabolic Product of *Penicillium Griseo-Fulvum* Dierckx. *Biochem. J.* **1939**, *33* (2), 240–248.
- (12) Odds, F. C. Antifungal Agents: Their Diversity and Increasing Sophistication. *Mycologist* **2003**, *17* (2), 51–55.
- (13) Dutcher, J. D. The Discovery and Development of Amphotericin B. *Dis. Chest.* **1968**, *54*, 296–298.
- (14) Dismukes, W. E. Introduction to Antifungal Drugs. *Clin. Infect. Dis.* **2000**, *30* (4), 653–657.
- (15) Cheah, H.-L.; Lim, V.; Sandai, D. Inhibitors of the Glyoxylate Cycle Enzyme ICL1 in *Candida Albicans* for Potential Use as Antifungal Agents. *PLoS One* **2014**, *9* (4), e95951.

- (16) Gallis, H. A.; Drew, R. H.; Pickard, W. W. Amphotericin B: 30 Years of Clinical Experience. *Rev. Infect. Dis.* **1990**, *12* (2), 308–329.
- (17) Bolard, J. How Do the Polyene Macrolide Antibiotics Affect the Cellular Membrane Properties? *Biochim. Biophys. Acta-Biomembr.* **1986**, *864* (3–4), 257–304.
- (18) Zotchev, S. Polyene Macrolide Antibiotics and Their Applications in Human Therapy. *Curr. Med. Chem.* **2003**, *10* (3), 211–223.
- (19) Dixon, D. M.; Walsh, T. J. Antifungal Agents. *Medical Microbiology* **1996**, chpt. 76.
- (20) Carolus, H.; Pierson, S.; Lagrou, K.; Van Dijck, P. Amphotericin B and Other Polyenes—Discovery, Clinical Use, Mode of Action and Drug Resistance. *J. Fungi* **2020**, *6* (4), 321–342.
- (21) Dupont, B. Overview of the Lipid Formulations of Amphotericin B. *J. Antimicrob. Chemother.* **2002**, *49* (suppl_1), 31–36.
- (22) Petranyi, G.; Ryder, N. S.; Stütz, A. Allylamine Derivatives: New Class of Synthetic Antifungal Agents Inhibiting Fungal Squalene Epoxidase. *Science* **1984**, *224* (4654), 1239–1241.
- (23) Monk, J. P.; Brogden, R. N. Naftifine: A Review of Its Antimicrobial Activity and Therapeutic Use in Superficial Dermatomycoses. *Drugs* **1991**, *42* (4), 659–672.
- (24) Leyden, J. Pharmacokinetics and Pharmacology of Terbinafine and Itraconazole. *J. Am. Acad. Dermatol.* **1998**, *38* (5), S42–S47.
- (25) Onishi, J.; Meinz, M.; Thompson, J.; Curotto, J.; Dreikorn, S.; Rosenbach, M.; Douglas, C.; Abruzzo, G.; Flattery, A.; Kong, L.; Cabello, A.; Vicente, F.; Pelaez, F.; Diez, M. T.; Martin, I.; Bills, G.; Giacobbe, R.; Dombrowski, A.; Schwartz, R.; Morris, S.; Harris, G.; Tsipouras, A.; Wilson, K.; Kurtz, M. B. Discovery of Novel Antifungal (1,3)- β -D-Glucan Synthase Inhibitors. *Antimicrob. Agents Chemother.* **2000**, *44* (2), 368–377.
- (26) Patil, A.; Majumdar, S. Echinocandins in Antifungal Pharmacotherapy. *J. Pharm. and Pharmacol.* **2017**, *69* (12), 1635–1660.
- (27) Denning, D. W. Echinocandin Antifungal Drugs. *Lancet* **2003**, *362* (9390), 1142–1151.
- (28) Sheehan, D. J.; Hitchcock, C. A.; Sibley, C. M. Current and Emerging Azole Antifungal Agents. *Clin. Microbiol. Rev.* **1999**, *12* (1), 40–79.
- (29) Allen, D.; Wilson, D.; Drew, R.; Perfect, J. Azole Antifungals: 35 Years of Invasive Fungal Infection Management. *Expert Rev. Anti-Infect. Ther.* **2015**, *13* (6), 787–798.
- (30) Heeres, J.; Backx, L. J. J.; Mostmans, J. H.; Van Cutsem, J. Antimycotic Imidazoles. Part 4. Synthesis and Antifungal Activity of Ketoconazole, a New Potent Orally Active Broad-Spectrum Antifungal Agent. *J. Med. Chem.* **1979**, *22* (8), 1003–1005.
- (31) Maertens, J. A. History of the Development of Azole Derivatives. *Clin. Microbiol. and Infect.* **2004**, *10* (SUPPL. 1), 1–10.

- (32) Koltin, Y.; Hitchcock, C. A. The Search for New Triazole Antifungal Agents. *Curr. Opin. Chem. Biol.* **1997**, *1* (2), 176–182.
- (33) Revie, N. M.; Iyer, K. R.; Robbins, N.; Cowen, L. E. Antifungal Drug Resistance: Evolution, Mechanisms and Impact. *Curr. Opin. Microbiol.* **2018**, *45*, 70–76.
- (34) Sanglard, D.; Kuchler, K.; Ischer, F.; Pagani, J. L.; Monod, M.; Bille, J. Mechanisms of Resistance to Azole Antifungal Agents in *Candida Albicans* Isolates from AIDS Patients Involve Specific Multidrug Transporters. *Antimicrob. Agents Chemother.* **1995**, *39* (11), 2378–2386.
- (35) Sanglard, D.; Ischer, F.; Monod, M.; Bille, J. Cloning of *Candida Albicans* Genes Conferring Resistance to Azole Antifungal Agents: Characterization of CDR2, a New Multidrug ABC Transporter Gene. *Microbiology* **1997**, *143* (2), 405–416.
- (36) Morschhäuser, J.; Barker, K. S.; Liu, T. T.; Blaß-Warmuth, J.; Homayouni, R.; Rogers, P. D. The Transcription Factor Mrr1p Controls Expression of the MDR1 Efflux Pump and Mediates Multidrug Resistance in *Candida Albicans*. *PLoS Pathog.* **2007**, *3* (11), 1603–1616.
- (37) Park, S.; Kelly, R.; Kahn, J. N.; Robles, J.; Hsu, M. J.; Register, E.; Li, W.; Vyas, V.; Fan, H.; Abruzzo, G.; Flattery, A.; Gill, C.; Chrebet, G.; Parent, S. A.; Kurtz, M.; Teppler, H.; Douglas, C. M.; Perlin, D. S. Specific Substitutions in the Echinocandin Target Fks1p Account for Reduced Susceptibility of Rare Laboratory and Clinical *Candida* Sp. Isolates. *Antimicrob. Agents Chemother.* **2005**, *49* (8), 3264–3273.
- (38) Perlin, D. S. Resistance to Echinocandin-Class Antifungal Drugs. *Drug. Resist Updat.* **2007**, *10* (3), 130.
- (39) Yao, Z.-J.; Huang, P.-Q.; Richard, H. *Efficiency in Natural Product Total Synthesis*; Wiley, **2018**.
- (40) Nicolaou, K. C.; Rigol, S. Perspectives from Nearly Five Decades of Total Synthesis of Natural Products and Their Analogues for Biology and Medicine. *Nat. Prod. Rep.* **2020**.
- (41) Baran, P. S. Natural Product Total Synthesis: As Exciting as Ever and Here to Stay. *J. Am. Chem. Soc.* **2018**, *140* (14), 4751–4755.
- (42) Bebbington, M. W. P. Natural Product Analogues: Towards a Blueprint for Analogue-Focused Synthesis. *Chem. Soc. Rev.* **2017**, *46* (16), 5059–5109.
- (43) Crane, E. A.; Gademann, K. Capturing Biological Activity in Natural Product Fragments by Chemical Synthesis. *Angew. Chem. Int. Ed.* **2016**, *55* (12), 3882–3902.
- (44) Rao, J. U. M.; Giri, G. S.; Hanumaiah, T.; Rao, K. V. J. Sampangine, a New Alkaloid from *Cananga Odorata*. *J. Nat. Prod.* **1986**, *49* (2), 346–347.
- (45) Mahdi, F.; Morgan, J. B.; Liu, W.; Agarwal, A. K.; Jekabsons, M. B.; Liu, Y.; Zhou, Y. D.; Nagle, D. G. Sampangine (a Cypripine Alkaloid) Exerts Biological Activities through Cellular Redox Cycling of Its Quinone and Semiquinone Intermediates. *J. Nat. Prod.* **2015**, *78* (12), 3018–3023.
- (46) Jiang, Z.; Liu, N.; Hu, D.; Dong, G.; Miao, Z.; Yao, J.; He, H.; Jiang, Y.; Zhang, W.; Wang, Y.; Sheng, C. The Discovery of Novel Antifungal Scaffolds by Structural Simplification of the Natural Product Sampangine. *ChemComm* **2015**, *51* (78), 14648–14651.

- (47) Kaomongkolgit, R.; Jamdee, K.; Chaisomboon, N. Antifungal Activity of Alpha-Mangostin against *Candida Albicans*. *J. Oral. Sci.* **2009**, *51* (3), 401–406.
- (48) Upegui, Y.; Robledo, S. M.; Gil Romero, J. F.; Quiñones, W.; Archbold, R.; Torres, F.; Escobar, G.; Nariño, B.; Echeverri, F. In Vivo Antimalarial Activity of α -Mangostin and the New Xanthone δ -Mangostin. *Phytother. Res.* **2015**, *29* (8), 1195–1201.
- (49) Mahabusarakam, W.; Proudfoot, J.; Taylor, W.; Croft, K. Inhibition of Lipoprotein Oxidation by Prenylated Xanthenes Derived from Mangostin. *Free. Radic. Res.* **2009**, *33* (5), 643–659.
- (50) Koh, J. J.; Qiu, S.; Zou, H.; Lakshminarayanan, R.; Li, J.; Zhou, X.; Tang, C.; Saraswathi, P.; Verma, C.; Tan, D. T. H.; Tan, A. L.; Liu, S.; Beuerman, R. W. Rapid Bactericidal Action of Alpha-Mangostin against MRSA as an Outcome of Membrane Targeting. *Biochim. Biophys. Acta-Biomembr.* **2013**, *1828* (2), 834–844.
- (51) Shan, T.; Cui, X. J.; Li, W.; Lin, W. R.; Lu, H. W.; Li, Y. M.; Chen, X.; Wu, T. α -Mangostin Suppresses Human Gastric Adenocarcinoma Cells in Vitro via Blockade of Stat3 Signaling Pathway. *Acta Pharmacol. Sin.* **2014**, *35* (8), 1065–1073.
- (52) Lin, S.; Ling Wendy Sin, W.; Koh, J.-J.; Lim, F.; Wang, L.; Cao, D.; Beuerman, R. W.; Ren, L.; Liu, S. Semisynthesis and Biological Evaluation of Xanthone Amphiphilics as Selective, Highly Potent Antifungal Agents to Combat Fungal Resistance. *J. Med. Chem.* **2017**, *60*, 10135–10150.
- (53) Ivankin, A.; Livne, L.; Mor, A.; Caputo, G. A.; Degrado, W. F.; Meron, M.; Lin, B.; Gidalevitz, D. Role of the Conformational Rigidity in de Novo Design of Biomimetic Antimicrobial Compounds. *Angew. Chem. Int. Ed.* **2010**, *49* (45), 8465.
- (54) Méndez-Samperio, P. Peptidomimetics as a New Generation of Antimicrobial Agents: Current Progress. *Infect. Drug Resist.* **2014**, *7*, 237.
- (55) Keohane, C. E.; Steele, A. D.; Wuest, W. M. The Rhizosphere Microbiome: A Playground for Natural Product Chemists. *Synlett* **2015**, *26* (20), 2739–2744.
- (56) Hallside, M. S.; Brzozowski, R. S.; Wuest, W. M.; Phillips, A. J. A Concise Synthesis of Carolacton. *Org. Lett.* **2014**, *16* (4), 1148–1151.
- (57) Solinski, A. E.; Koval, A. B.; Brzozowski, R. S.; Morrison, K. R.; Fraboni, A. J.; Carson, C. E.; Eshraghi, A. R.; Zhou, G.; Quivey, R. G.; Voelz, V. A.; Buttarro, B. A.; Wuest, W. M. Diverted Total Synthesis of Carolacton-Inspired Analogs Yields Three Distinct Phenotypes in *Streptococcus Mutans* Biofilms. *J. Am. Chem. Soc.* **2017**, *139* (21), 7188–7191.
- (58) Solinski, A. E.; Scharnow, A. M.; Fraboni, A. J.; Wuest, W. M. Synthetic Simplification of Carolacton Enables Chemical Genetic Studies in *Streptococcus Mutans*. *ACS Infect. Dis.* **2019**, *5* (8), 1480–1486.
- (59) Tripathi, A.; Schofield, M. M.; Chlipala, G. E.; Schultz, P. J.; Yim, I.; Newmister, S. A.; Nusca, T. D.; Scaglione, J. B.; Hanna, P. C.; Tamayo-Castillo, G.; Sherman, D. H. Baulamycins A and B, Broad-Spectrum Antibiotics Identified as Inhibitors of Siderophore Biosynthesis in *Staphylococcus Aureus* and *Bacillus Anthracis*. *J. Am. Chem. Soc.* **2014**, *136* (4), 1579–1586.
- (60) Steele, A. D.; Ernouf, G.; Lee, Y. E.; Wuest, W. M. Diverted Total Synthesis of the Baulamycins and Analogues Reveals an Alternate Mechanism of Action. *Org. Lett.* **2018**, *20* (4), 1126–1129.

- (61) Erecińska, M.; Chance, B.; Wilson, D. F.; Dutton, P. L. Aerobic Reduction of Cytochrome b 566 in Pigeon-Heart Mitochondria (Succinate-Cytochrome C1 Reductase-Stopped-Flow Kinetics). *PNAS* **1972**, *69* (1), 50–54.
- (62) Zuccolo, M.; Kunova, A.; Musso, L.; Forlani, F.; Pinto, A.; Vistoli, G.; Gervasoni, S.; Cortesi, P.; Dallavalle, S. Dual-Active Antifungal Agents Containing Strobilurin and SDHI- Based Pharmacophores. *Sci. Rep.* **2019**, *9*, 11377.

Chapter 2: Total Synthesis and Biological Evaluation of Antifungal Phenolic Bisabolenes.

Disclaimer: The original project was proposed by Dr. Ingrid K. Wilt. Adrian R. Demeritte assisted with the refocusing of project goals towards the target scaffold. Dr. Ingrid K Wilt completed synthesis of the Gilheany inspired methods towards the ketone derivatives. Adrian R Demeritte utilized Gilheany inspired methods towards sydonol-like intermediates. Adrian R. Demeritte proposed and completed the synthesis of intermediates generated from the diastereoselective nucleophilic addition route. Dr. Ingrid K. Wilt assisted, at times, with throughput of material through **2.29**, however all yields indicated are that of Adrian R. Demeritte. Dr. Ingrid K. Wilt completed the synthesis of the ketone derivatives describe in **Section 2.2.5.2** unless otherwise stated. Adrian R. Demeritte proposed synthesis of the ethyl acrylate derivates and performed it. Only compounds synthesized by Adrian R. Demeritte are reported in the SI. Collaborators at Corteva Agriscience screened a panel of compounds for herbicidal, insecticidal, and fungicidal activity. Results of the fungicidal data are reported in **Section 2.6**.

2.1. Introduction**2.1.1. Blight and Economic Impact of Fungal Pathogens**

The cultivation of cruciferous vegetables is a multibillion-dollar industry worldwide and currently places 5th in global production as major vegetable crops. For example, in 2016 world production of broccoli and cauliflower was 25 million metric tons, valued at \$13.9 billion, with the USA alone contributing 1.3 million metric tons to worldwide production, valued at \$1.65 billion.¹ While lucrative, dark leaf spotting of brassicas, also known as black spot or *Alternaria* blight, is a major bottleneck of the global production of cultivated oilseed crops, head cabbage, broccoli, cauliflower, and other important crops from the Brassicaceae family.^{2,3} The causative agents of this disease are the various *Alternaria* species including *A. brassicae* (cruciferous

vegetables), *A. brassicola* (potato), *A. alternata* (tomato) and *A. solani* (tomato). These pathogens are known to infect host plant cells at all stages of development and cause large necrotic lesions which drastically reduce photosynthetic efficiency, hasten the plant senescence, and lead to collapse and death of plants under high pathogen pressure.⁴ In fact, black spotting has led to 15 to 70% losses of product, by both infection of seeds/seedlings and of the fully grown produce.⁵ Once infected, crops do not store well and in cases where full senescence is not realized before harvesting, production loss still occurs due to the excising of visually unappealing produce.² Alarmingly *A. brassicae* (*Ab*), boasting the largest host range of the aforementioned pathogens, is present in 33 states across the USA which ranks 3rd and 6th for the global production broccoli/cauliflower and cabbage/ other brassicas respectively.^{1,6} Thus, the threat of yield losses poses important agricultural economic issues necessitating the use of protective fungicides.

2.1.2. The Pesticide Problem

The agricultural industry hinges upon the use of pesticides for efficient production of common fruits and vegetables. Such pesticides are used to treat and prevent various diseases caused by bacteria, fungi, nematodes and viruses which can damage crops and thus have major economic impact. In many cases, inspiration for the chemical structure of these compounds comes from mimicking natural cofactors of target enzymes. For example, ubiquinone (coenzyme q10) is a lipid-soluble compound composed of a redox active quinoid moiety and a hydrophobic tail. This coenzyme plays an important role in energy production in the mitochondria by accepting electrons in complex II (succinate dehydrogenase) and is reproduced in complex III (cyt *bc*₁) through the oxidation of ubiquinol.⁷ The latter enzyme is considered to be an essential component of the respiratory chain. Hence, to date, most commonly used pesticides take advantage of the ubiquitous binding affinity of this cofactor via production and use of ubiquinone mimics with a broad

spectrum of activity with complex 3 inhibitors being the most common ubiquinone mimics used commercially.^{8,9} Many complex III inhibitors act as quinone outside inhibitors (QoI's) by targeting this quinol oxidation site. In fact, all fungicides effective against *Ab* interfere with ATP production by acting as QoI fungicides and these compounds (eg. azoxystrobin, kresoxim-methyl) represent one of the most important classes of agricultural fungicides due to their broad activity (**Figure 2.1**).¹⁰

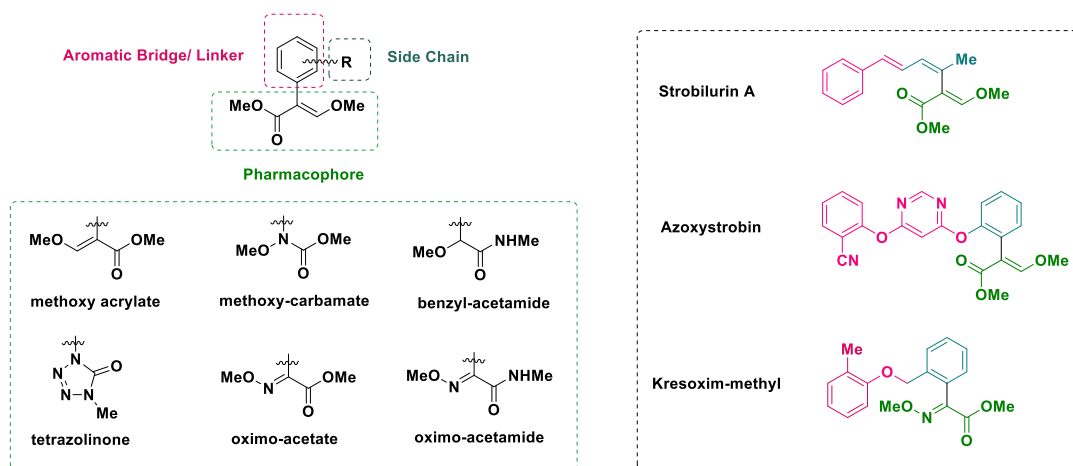


Figure 2.1: (Top Left) Structure mapping of typical QoI fungicides. As shown structures usually have some active pharmacophore, linked by an aromatic bridge for stability as well as a side chain to improve lipophilicity. **(Bottom Left)** Known pharmacophores for QoI inhibitors at the Q_o site of the cyt *bc₁* complex. **(Right)** structures of strobilurin A, the first isolated Q_o site inhibitor. Azoxystrobin and Kresoxim-methyl are also shown as they are commonly used commercially available QoIs.

QoIs first came about thanks to two natural products isolated from the fungus *Strobilurus tenacellus*, namely strobilurin A and B.¹¹ These compounds were first brought to market in 1996 and extensive analog design for stability and potency have led to 10 major strobilurin fungicides being on the market to date.¹² This analog design also allowed for the identification of identified several pharmacophores that maintain QoI activity, though one of the most predominantly used pharmacophores to date is methyl methoxyacrylate moiety. Other pharmacophores from QoIs considered to be analogs of strobilurin are methoxyacetamide, methoxycarbamates, oximinoacetates, oximinoacetamides, azazolidinedones, dihydrodioxazines, imidazolinones, and

bearylcarbamates.⁸ A modification made to enhance UV stability is the addition of a central linking ring, and this motif is nearly omnipresent motif in synthetic in modern QoI fungicides.¹³ Though extensive chemical diversity provides differing binding modes within the Q_o site for each pharmacophore it should be noted, however, that QoI fungicides have a high risk of resistance development in their target pathogens due to their site-specific mode of action with cross resistance already being observed due to point mutations.¹⁴ These mutations disrupt the binding mode of most QoIs by introducing additional steric interactions with their central ring and quelling their antifungal capabilities.⁹ Though there are less common point mutations in other species, for example F129L in *A. solani*, the most frequently observed mutation is G143A in the Q_o site of cytochrome *b*.^{15,16} Thankfully, not all hope is lost, as an example of success in QoI development comes by way of the recently approved QoI metyltetraprole tetrazolinone (Pavecto).^{17,18} Therefore natural product agrochemicals have the potential to broaden the scope of organic fungicides by affording novel binding modes through innovative QoI chemotypes, thereby providing unique mechanisms of action to combat rising resistance to QoI fungicides.

2.1.3. Peniciaculin A: A Potential New

In tandem with this ongoing dilemma, natural product researchers have given considerable attention to unique ecosystems in hopes of discovering secondary metabolites with promising biological activities. Recently, several phenolic bisabolene sesquiterpenes with a wide range of activity were identified from a culture of *Penicillium aculeatum*, a fungus isolated from deep sea sediments. Peniciaculin A exhibited activity against *Ab* (MIC=0.5 µg/mL) with a chemical structure that mimicked known QoI's, and by way ubiquinone, however all other co-isolates were far less bioactive to *Ab*.¹⁹ Interestingly, even co-isolates with near identical structural motifs to

that of known QoIs showed far less activity including ‘co-isolate 5’ (MIC= 32 $\mu\text{g/mL}$) (**Figure 2.2**).

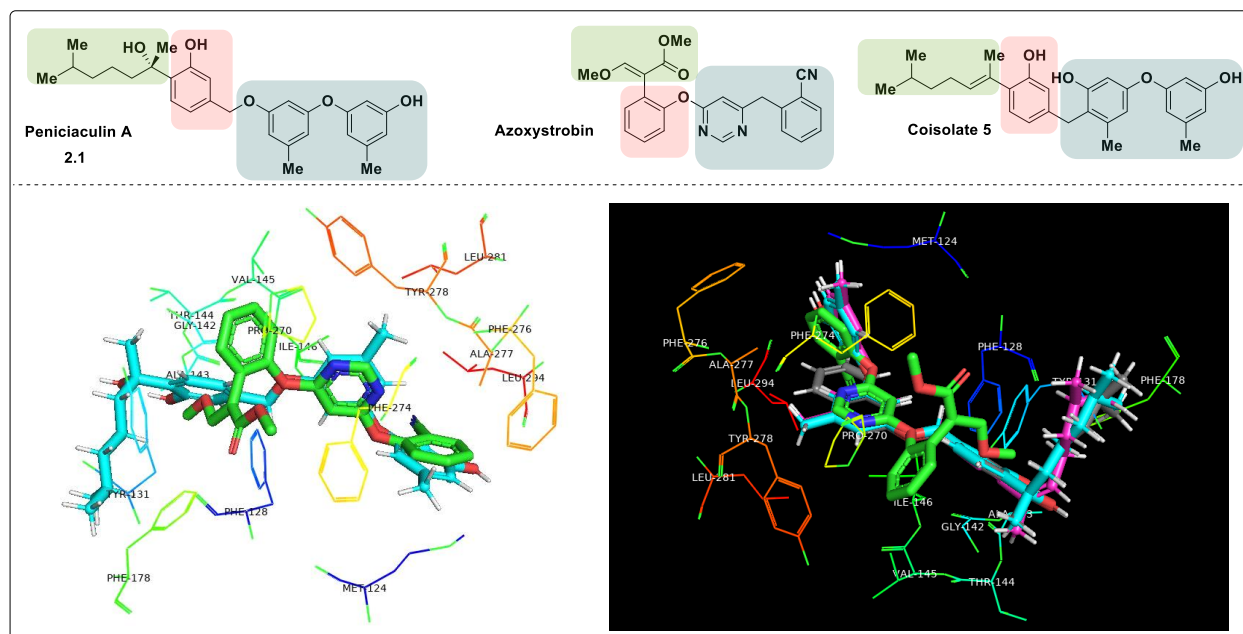


Figure 2.2: (Top) Structure of peniciaculin A mapped onto prototypical QoI scaffold (green: pharmacophore, red: aromatic ring, blue: sidechain). The structure of azoxystrobin is also shown for reference. **(Bottom left)** Structure of peniciaculin A (cyan) bound in bovine *bc1* with azoxystrobin (green). Favorable overlapping with pi-stacking residues has been highlighted. The pharmacophore of **2.1** occupies a slightly different space, this could potentially render G143A point mutations ineffective against this compound. **(Bottom right)** Overlap of **2.1** and other co-isolates in the binding pocket. Notably, co-isolate 5 bears a similar QoI type scaffold but lacks activity towards *Ab*.

Molecular modelling of these isolated compounds in a structurally similar quinol oxidation site show overlap with crucial residues in the active site for the binding of known QoI's including PHE274, PHE128, ILE146, PRO270, PHE129 and may even show better overlap with additional pi-slip stacking to residues like TYR270 (**Figure 2.2**).⁸ Hence, peniciaculin A may be able to adapt an alternative binding mode than azoxystrobin and could even help circumvent resistance in G143A mutants as well. Together, this information suggests that peniciaculin A may either be the Goldie-locks chemical of the bunch and hence possess some narrow spectrum activity towards *bc1* in *Ab* or, better yet, drive its activity by means of some previously undiscovered mechanism. Further investigation of these sesquiterpenes show potential for identification of unique

mechanisms of action for the inhibition of *Ab* towards combating current issues with rising pesticide resistance, prompting efforts towards their synthesis.

2.1.4. Previous Approaches

Tetrasubstituted centers are a widely encountered motif in natural products and pharmaceuticals, making their asymmetric synthesis is of particular importance.²⁰ Though the synthesis of enantiopure secondary alcohols can be readily accomplished, many of these strategies do not apply for tertiary alcohols.^{21–23} That said, the key step in the synthesis of these phenolic bisabolenes is the preparation of the chiral enantiopure tertiary alcohol motif.

In 2008, Aggarwal and coauthors demonstrated the potential of a converting secondary alcohols to quaternary stereogenic centers with high selectivity.²⁴ Namely, Aggarwal shows that conversion of a secondary alcohol to a secondary carbamate, can undergo stereoretentive or stereoinvertive insertion post lithiation depending on whether a boronic ester or borane was used respectively. This is followed by transmetallation with alkyl substituted pinacolato boron and 1,2-migration to form borylated intermediates. Subsequent oxidation then furnished the tertiary alcohol at the benzylic center (**Figure 2.3**). In 2012, Aggarwal applied this methodology towards the enantioselective synthesis of the bisabolene family of sesquiterpenes shown.²⁵ Though Aggarwal notes that sterics appear to not influence enantioselectivity, he does not comment on the extent to which sterics of nearby functional groups can limit reaction rate overall. It should be noted that though many examples of using this methodology to create tertiary alcohols are given, across both papers neither have both a tertiary alcohol at the benzylic center and an ortho phenol substituent present. Moreover, protecting group usage was fairly limited as phenols were only capped with methoxy protecting groups.

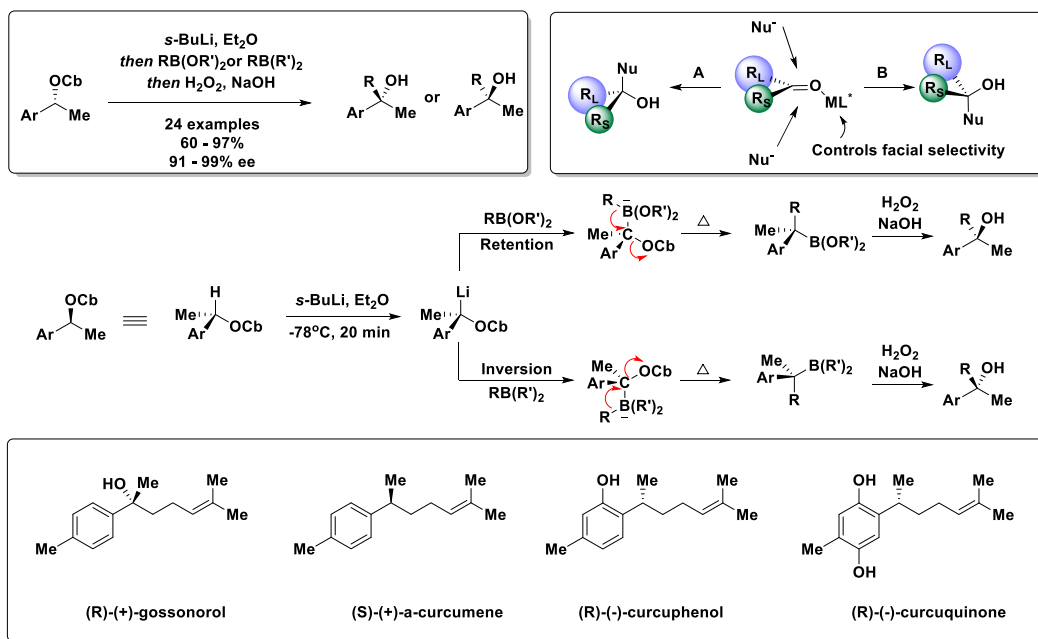


Figure 2.3: Aggarwal methodology to set tertiary alcohol from carbamoylated secondary alcohol. Aggarwal notes that selectivity here no longer relies on the different steric properties of similar-sized groups but rather whether the reaction of the chiral carbenoid occurs with retention or inversion. Thus, there is a higher potential greater enantioselective outcome.

An attractive method for the asymmetric synthesis of any compound involves the simple addition or removal of an additive to impart or alter chirality of the target compound. In 2017, the Gilheany Lab embarked on expanding knowledge on direct asymmetric organomagnesium additions to carbonyls, specifically towards the synthesis of tertiary alcohols.²⁶ Gilheany found that using the diamine tridentate ligand shown overcomes the shortcomings of previously reported bidentate ligands, most notably, low selectivity.²⁶ Namely, this ligand overcomes Schlenk-type dynamic interconversion through matching the maximum number of coordination sites on magnesium in the simplest halogen bridged aggregate.²⁷ When tested, stoichiometric use of this ligand allowed for the synthesis of tertiary alcohols with high enantiomeric excess (*ee*) as shown. This method was even employed in a formal asymmetric synthesis of vitamin E, though its ketone is slightly farther away from the arene. Though a large amount of the ligand is required Gilheany notes that recovery of the ligand from silica column is possible and can be recycled for future runs

as well. We envisioned that this method could either be used for late-stage synthesis of the tertiary alcohol or perhaps for quick synthesis of the natural product from readily available starting materials. This would also allow for quick analog production to further probe whether the peniciaculin tertiary alcohol is a novel pharmacophore.

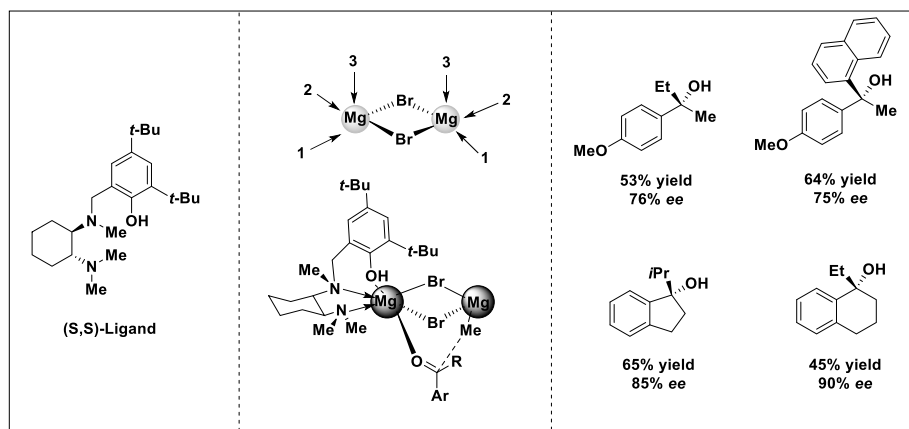


Figure 2.4: (Left) Tridentate ligand proposed by Gilheany and coauthors to test concept. (Middle) Ligand drawn in transition state showing three potential coordination sites on each metal center, along with design applied in relevant reaction. (Right) Examples from Gilheany's substrate scope showing products with varied Grignards on different benzylic ketones used.

Lastly, in 2008 Ito and coauthors successfully utilized a chiral imidazolidinone to preferentially set tertiary benzylic alcohols towards the synthesis of (+)-curcutetraol and (+)-sydonol with high selectivity.²⁸

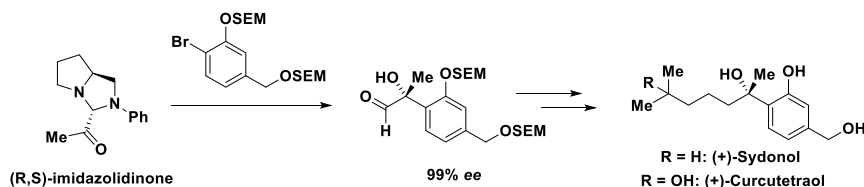


Figure 2.4: Ito's strategy towards the total synthesis of phenolic bisabolones.

I envisioned that use of chiral asymmetric nucleophilic addition could produce the tertiary alcohol of **2.1** in a highly selective manner while allowing for facile analog development by leveraging the reactivity of the homoallylic aldehyde revealed post hydrolysis.

2.1.4.1 Previous synthesis of Peniciaculin A

During our synthetic efforts and after sending out analogs to Corteva Agriscience™ for biological testing Yajima and coauthors published a total synthesis of peniciaculin A and several other phenolic bisabolenes.²⁹ Methodology along the route involves construction of the tertiary alcohol via a Sharpless asymmetric dihydroxylation reaction, followed by a SmI₂-mediated Julia olefination then cross metathesis to install the alkyl chain. Aryl installation relies on a key Suzuki Miyaura coupling a commercially available aryl iodide and boronic acid. First, it should be noted that a large majority of the synthetic progress in this chapter was completed before this paper was published and will be reported as such. Secondly, no information the biological evaluation, analog design and rationale, or discussion on the mechanism of action of peniciaculin A was included in Yajima's publication. The route we developed described below allows for rapid analog design and examines key structures in the peniciaculin scaffold which allow for activity towards our QoI hypothesis.

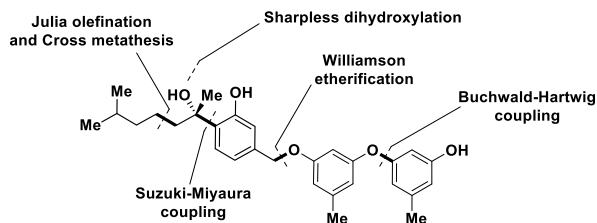


Figure 2.5: Key disconnections for Yajima synthesis of **2.1** in 2021.

2.2. Results and Discussion

2.2.1. Synthesis by way of Aggarwal borylation (1,2 migration)

In our initial efforts towards the total synthesis of peniciaculin A, we envisioned splitting the molecule into two major fragments. One 'phenol core' fragment unfunctionalized at the

benzylic site and another diaryl ether fragment which could be coupled together through functionalization at the benzylic site and subsequent substitution with the preformed diaryl ether. For the tertiary alcohol and phenolic bisabolene moieties in the prior, we opted to use the key 1,2 migration followed by in situ oxidation of a homologated borane developed by Aggarwal and coauthors to set the tetrasubstituted center from a commercially available 2-hydroxy-4-methylacetophenone. The diaryl ring could be readily formed from coupling two orcinol synthons.

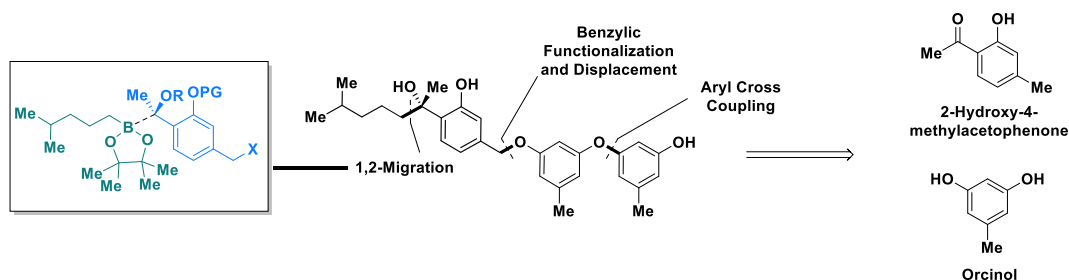
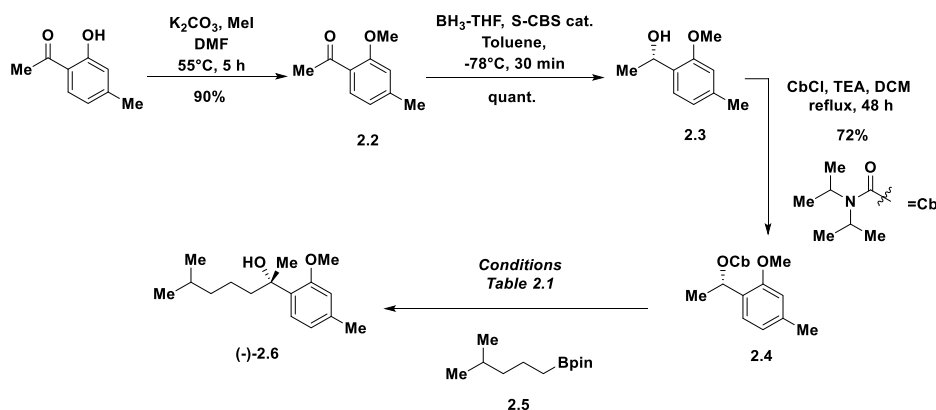


Figure 2.6: Retrosynthetic disconnections for synthesis of **2.1** through 1,2 migration.

This enantioselective route towards the synthesis of peniciaculin A commences with the methyl protection of 2-hydroxy-4-methylacetophenone in good yield. Then stereoselective Corey-Bakshi-Shibata (CBS) reduction of the ketone using (R)-(+)-2-methyl-CBS-oxazaborolidine primes the then carbamoylated secondary alcohol for the stereoretentive 1,2-migration previously mentioned.^{30,31} Unfortunately, utilizing initially reported conditions by Aggarwal yielded no product. Several optimizations were made in order to promote this reaction. First, Aggarwal has demonstrated that the use of a Lewis acid like $\text{MgBr}_2 \cdot \text{OEt}_2$ can promote 1,2-migration.³² Moreover, if added with methanol, lithiated carbamates could be protonated preventing racemization of the stereocenter.³³ As this reaction is extremely moisture sensitive, freshly prepared pinacol boronate ester, freshly distilled Et_2O , and *s*-BuLi titrated the same day were all required to produce the desired tertiary alcohol. At first, combination of the aforementioned produced the desired tertiary alcohol in 11% yield. Rotations of both the starting material and

recovered starting material were tested for epimerization and showed no negligible change. Increasing the equivalents of $\text{MgBr}_2 \cdot \text{OEt}_2$ along with allowing the reaction to warm to room temperature and stir overnight improved yields to 30% (**Table 2.1**). In all cases, a small percentage (~5%) of borylated intermediate was isolated showing that yields could theoretically improve, however increasing time spent in oxidizing conditions only led to decomposition of the intended product. This also indicated that the rate limiting step was insertion of the lithiated carbamate into the pinacol borate.



Scheme 2.1: Synthesis of Aggarwal borylation precursor.

Table 2.1: Optimization of 1,2 migration.

| Entry | Conditions | Result |
|-------|---|---------------|
| 1 | i. <i>s</i> -BuLi (1.1 equiv), Et ₂ O (0.25 M), -78°C, 15 min ii. (2.5) (1.5 equiv) 1.0 M in Et ₂ O, -78°C to rt, 2 h iii. 2 M NaOH _(aq) (7.0 equiv), H ₂ O ₂ (11.8 equiv), THF (0.15 M), 0°C to rt, 2 h | No reaction |
| 2 | i. <i>s</i> -BuLi (1.5 equiv), Et ₂ O (0.25 M), -78°C, 15 min ii. (2.5) (1.5 equiv) 1.0 M in Et ₂ O, -78°C to rt, 2 h iii. MgBr ₂ •OEt ₂ (1.5 equiv) 0.30 M in MeOH, rt, 2 h iv. 2 M NaOH _(aq) (7.0 equiv), H ₂ O ₂ (11.8 equiv), THF (0.15 M), 0°C to rt, o/n | 11% 2.6 |
| 3 | i. <i>s</i> -BuLi (1.5 equiv), Et ₂ O (0.25 M), -78°C, 15 min ii. (2.5) (1.5 equiv) 1.0 M in Et ₂ O, -78°C to rt, 2 h iii. MgBr ₂ •OEt ₂ (4.0 equiv) 0.30 M in MeOH, rt, o/n iv. 2 M NaOH _(aq) (7.0 equiv), H ₂ O ₂ (11.8 equiv), THF (0.15 M), 0°C to rt, o/n | 30% 2.6 |
| 4 | i. <i>s</i> -BuLi (1.5 equiv), Et ₂ O (0.25 M), -78°C, 15 min ii. (2.5) (1.5 equiv) 1.0 M in Et ₂ O, -78°C to rt, 2 h iii. MgBr ₂ •OEt ₂ (4.0 equiv) 0.30 M in MeOH, rt, o/n iv. 2 M NaOH _(aq) (7.0 equiv), H ₂ O ₂ (11.8 equiv), THF (0.15 M), 0°C to rt, 48 h | Decomposition |

Though there is precedent for creating a tetrasubstituted center without an ortho phenol, along with precedent for a 1,2-alkyl migration with a methyl capped phenol to produce a trisubstituted center, there was no substrate used to produce a tetrasubstituted center with an ortho methyl capped phenol. This finding led us to assume that even a minimalistic methyl capped hydroxyl group could hinder product formation if ortho to the migrating chain. We reasoned if utilization of the stereoinvertive pathway with an alkyl borane would circumvent issues with selectivity.

Table 2.2: Benzylic oxidation conditions on **2.6**.

| Entry | Oxidation Condition | Result |
|-------|---------------------------------------|---------------|
| 1 | SeO ₂ , <i>t</i> -BuOOH | No Reaction |
| 2 | KMnO ₄ | No Reaction |
| 3 | PCC | No Reaction |
| 4 | DDQ | No Reaction |
| 5 | O ₂ , <i>s</i> -BuLi, EDTA | No Reaction |
| 6 | KBr, oxone, NMO | No Reaction |
| 7 | NBS, AIBN <i>then</i> NaOH | Decomposition |

To test this theory, we hypothesized utilizing the previously indicated sequence of reactions towards carbamoyl **2.3** without substitution at the ortho position of the aryl ring, though synthetic efforts at another site on the molecule halted efforts here. Specifically, we simultaneously began efforts to oxidize the benzylic position of the aryl ring on (-)-**2.6**, and unfortunately all methods

resulted in either destruction of the molecule or little to no product formation due to a lack of reactivity at the aforementioned position. Given the number of necessary preceding steps along with the meticulous care needed to effectuate a low yielding key step, efforts in an alternative direction were encouraged, particularly in utilizing an alternative starting material with a higher oxidation state at the benzylic position of the aryl ring.

2.2.2. Synthesis by Asymmetric Grignard

Concurrently, we were also interested in introducing the tertiary center by utilizing a stoichiometric amount of chiral ligand for an asymmetric Grignard. Retrosynthetically, the route to achieve this was similar to the prior intended with selective inserted into methoxy protected ketone **2.2**.

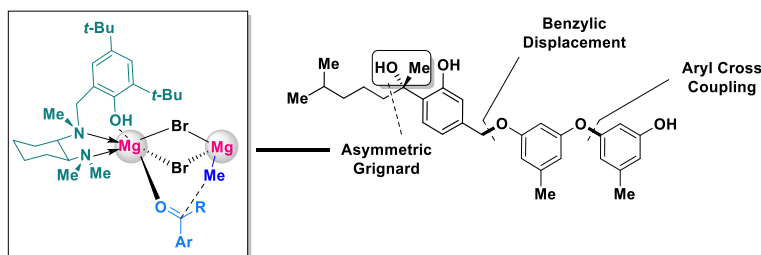
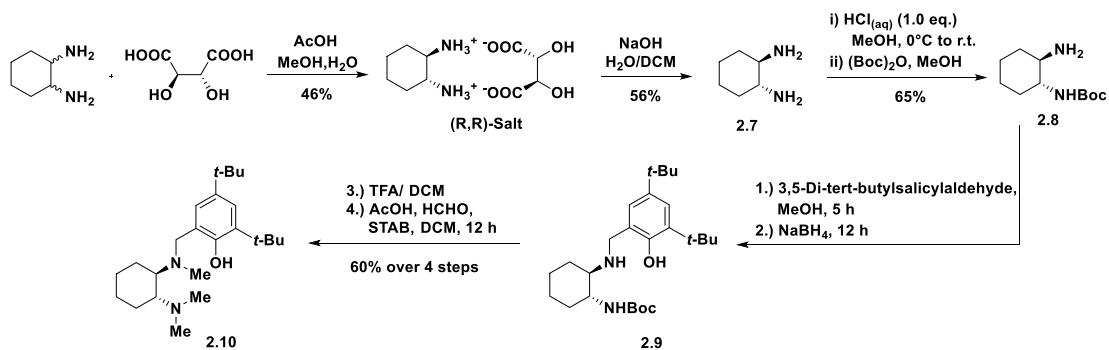


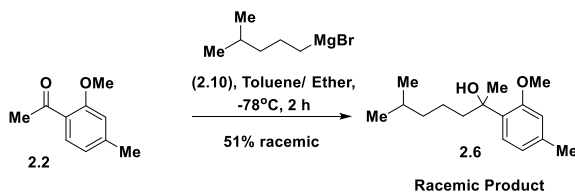
Figure 2.7: Retrosynthetic disconnections for synthesis of **2.1** through an asymmetric Grignard .

We envisioned usage of ligand **2.10** in combination with the desired Grignard reagent formed from 1-bromo-4-methylpentane, to set the tetrasubstituted centers present in the target compound. The proposed advantage of this route involved use of a similar substrate for both enantioselective and racemic syntheses of the target phenolic bisabolenes along with future analogs and we sought to incorporate this goal in further synthetic efforts.



Scheme 2.2: Synthesis of (S,S)-ligand required for asymmetric Grignard.

Synthesis of ligand **2.10** was completed in moderate yield compared to those published by Bieszcza *et al.* (**Scheme 2.2**).²⁶ Preliminary experiments with this ligand were conducted in tetrahydrofuran (THF) however, little to no enantioselectivity was observed most likely due to the strong coordinating ability of the solvent. Further replacing THF with a mixture of toluene/ether saw little to no product formation, presumed to be caused by solubility issues with the chosen Grignard and/or moisture present in either of the two solvents (**Scheme 2.3**). Even then, lack of high asymmetric induction required some separatory technique thereafter, which is less than ideal for an enantioselective synthesis and in turn provided little benefit over a total racemic synthesis. Having encountered oxidative in combination with current issues with current lack of selectivity with the current method I was inspired to radically redesign the current synthetic route.



Scheme 2.3: Asymmetric Grignard addition to **2.2**.

2.2.3. Synthesis by Lithium Halogen Exchange

2.2.3.1. Testing previous methods

Having countered several oxidation, functionalization, and asymmetric induction issues in prior routes I was motivated to drastically redesign the synthesis of this molecule to make it more modular and synthetically accessible for analog development. I wanted to maintain the main potential benefit of the aforementioned synthetic route, namely the use of a reusable chiral source that could be swapped out to produce either enantiomer of the tertiary alcohol. I was inspired Ito's use of a chiral imidazolidinone in a diastereoselective nucleophilic addition towards the synthesis of (+)-sydonol. Retrosynthetically, the side chain of this molecule could be accessed through a Wittig olefination of the pendent aldehyde.

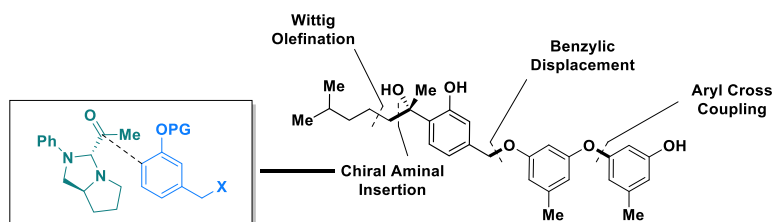
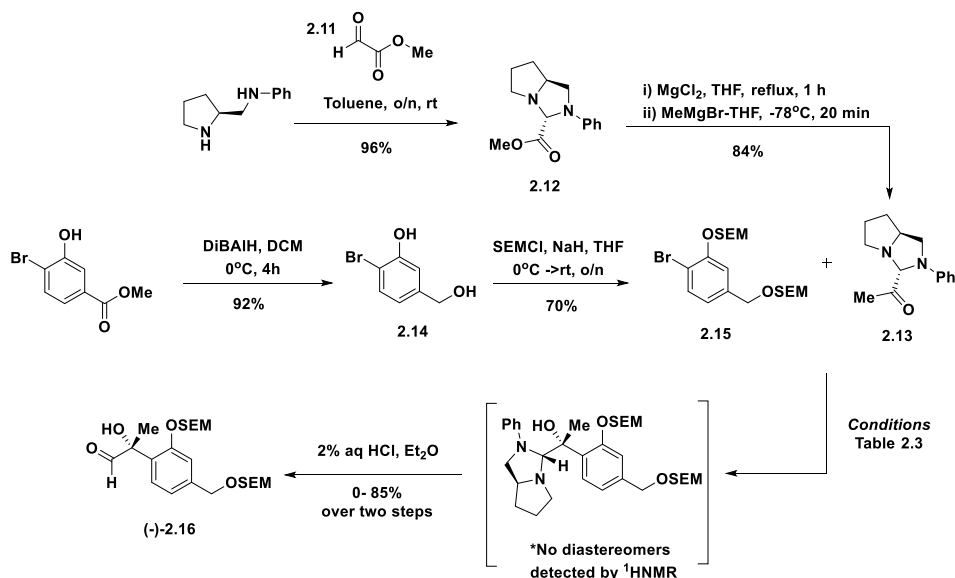


Figure 2.8: Retrosynthetic disconnections for the synthesis of **2.1** through diastereoselective addition.

I first utilized Ito and coauthors conditions on substrate **2.15** for baseline results. Chiral imidazolidinone (*R*, *S*) could either be synthesized from commercially available (*S*)-(+)-2-(anilinomethyl)pyrrolidine in 2 steps or in 5-steps from *N*-Boc-*L*-proline.³⁴ As (*R*)-(-)-2-(anilinomethyl)pyrrolidine was commercially available the (*S*,*R*) enantiomer was synthesized from *N*-Boc-*D*-proline in a similar manner.



Scheme 2.4: Synthesis of key aldehyde utilized in Ito's synthesis of sydonol. Synthesis of (S,R)-2.13 is also detailed.

Conditions reported by Ito and coauthors required two equivalents of aryl bromide **2.15** and used 2.5 equivalents of magnesium to generate the Grignard species.²⁸ Following those conditions gave product (-)-**2.16** in 0-55% yield with the chiral imidazolidinone as the limiting reagent. Bumping the equivalents of Mg⁰ to six improved the yield of this reaction to 85% though the yield still varied with the major byproduct being protodehalogenation of the aryl bromide upon protic quenching of the diastereoselective addition of the nucleophile. Increasing the length of time of this reaction did not improve yields.

Table 2.3: Optimization of diastereoselective Grignard addition on **2.15**.

| Entry | Conditions | Result |
|-------|---|------------|
| 1 | i. Mg ⁰ (2.5 equiv), Dibromoethane (0.5 equiv), THF, reflux, 2 h ii. 2.13 (2.0 equiv), -78°C, 2 h | 0-55% 2.16 |
| 2 | i. Mg ⁰ (6.0 equiv), Dibromoethane (0.5 equiv), THF, reflux, 3 h ii. 2.13 (2.0 equiv), -78°C, 2 h | 0-85% 2.16 |
| 3 | i. Mg ⁰ (6.0 equiv), Dibromoethane (0.5 equiv), THF, reflux, 3 h ii. 2.13 (2.0 equiv), -78°C, 5 h | 0-83% 2.16 |

2.2.3.2. Synthesis of Linchpin Intermediate

Further molecular docking studies of the peniciculin A in the binding site of the cytochrome *bc*₁ complex revealed the importance of pi stacking of the aryl ring just off the benzylic center of the phenol core and PHE274 and PHE128 in the cytochrome *bc*₁ complex. Thus, I wanted to design a synthetic route focused on an advanced intermediate which already possessed both this aryl ring as well as the phenol core. This intermediate, henceforth referred to as the linchpin intermediate would serve as the starting point for analogs in the series with the best chance of retaining activity. Moreover, largescale synthesis of this intermediate would circumvent troublesome oxidation optimizations for future analogs as well.

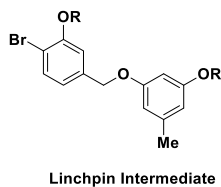
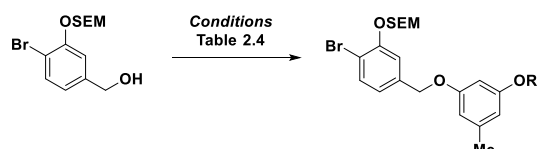
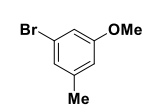
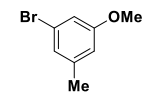
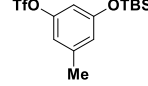


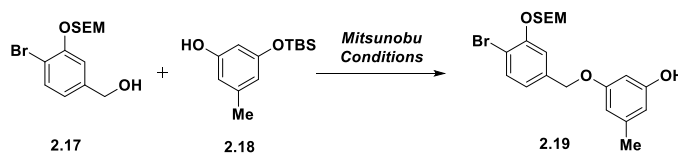
Figure 2.9: Structure of linchpin intermediate to be used as the central moiety in future synthetic efforts.

I explored various methods for installation of a monoaryl fragment at the benzylic center. Unfortunately, S_NAr reactions using various bases and sulfonyl transfer reactions did not give any intended protected linchpin intermediate.

Table 2.4: Coupling conditions with benzylic oxygen as nucleophile.

|  | | | |
|--|---|--|-------------|
| Entry | Aryl Ring | Conditions | Result |
| 1 |  | K ₂ CO ₃ , DMF, 25°C, 24 h | No Reaction |
| 2 |  | Cs ₂ CO ₃ , DMF, 100°C, 16 h | No Reaction |
| 3 |  | DMF, K ₂ CO ₃ , 100°C, 16 h | No Reaction |

Thinking these results stemmed from the lack of reactivity of the benzylic alcohol, I hypothesized that switching this oxygen to be the leaving group instead the nucleophile would promote intended coupling. Mesylation and displacement by monoprotected orcinol gave no intended product, however Mitsunobu reaction using triphenylphosphine and DIAD gave the intended protected linchpin intermediate in low yield and also resulted in TBS deprotection. Additionally, purification of the reaction was arduous as there were up to 10 species present in the crude material of this reaction. I took inspiration from a recently published article at the time and utilized a water soluble Mitsunobu-reagent made in house azidocarbonyl dimorpholide (ADDM) in an effort to improve purification and yield.³⁵ Though purification was greatly simplified utilizing this reagent, with both triphenylphosphine and tributylphosphine a decrease in overall yield was observed.

Table 2.5: Coupling conditions with azodicarboxylates using benzylic oxygen as the electrophile.

| Entry | Conditions | Result |
|-------|---|--------------------------------|
| 1 | DIAD, PPh ₃ , THF, 25°C, o/n | 33% 2.19 Messy Purification |
| 2 | DIAD, PBu ₃ , THF, 25°C, o/n | 25% 2.19 Messy Purification |
| 3 | ADDM, PPh ₃ , THF, 25°C, o/n | 16% 2.19 |
| 4 | ADDM, PBu ₃ , THF, 25°C, o/n | 11% 2.19 |

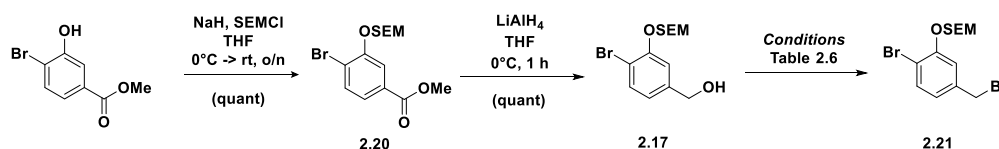
Though another protecting group could have been used in order to further prevent potential silyl migration, in all cases a stronger protecting group like a methyl cap may have caused issues during deprotection as use of elevated equivalents of BBr₃ could not only deprotect the methyl capped orcinol, but removed the orcinol fragment entirely.³⁶ Taken together I questioned whether could be a more robust method for generating this linchpin intermediate, with facilely labile protecting groups.

I first reasoned that coupling both the phenol core and orcinol fragment could be improved by increasing the reactivity of the leaving group at the benzylic center. Secondly, I hypothesized that use of a suitable base stable silyl protecting group on a monoprotected orcinol fragment would be ideal for both stability in a S_NAr and subsequent reactions but would also allow for easy removal via standard conditions.

My intended route commenced with the SEM protection of commercially available methyl-4-bromo-3-hydroxybenzoate in quantitative yield. Upon coupling, this would differentiate the phenol from the benzylic alcohol and avoid potential dimerization of the aryl bromide. Next, reduction of the methyl ester to the benzylic alcohol with a solution of DIBALH resulted in near

quantitative yield however, only SEM truncation was observed when scaling up the reaction. Thankfully, slow addition of the ester to a cooled solution of LAH for just one hour gave near quantitative yields of benzylic alcohol **2.17**. We found that functional group interconversion of **2.17** to the benzylic bromide gave primarily SEM truncation under standard Appel conditions (**Table 2.6**, entry 1). Bromination with PBr_3 on a small scale gave modest yields of the intended benzylic bromide but primarily resulted in SEM truncation upon scale up (**Table 2.6**, entry 3). I found that modified Appel conditions using NBS as the electrophile source of bromide gave quantitative conversion on both small and large scales (**Table 2.6**, entry 4). Note that it is crucial that the NBS is added slowly to a cooled reaction solution to avoid SEM truncation as higher temperatures or reacting for longer than an hour at 0°C promotes this. It should also be noted that these first three steps can produce near quantitative conversion to the benzyl bromide without the need for a column until after the third step.

Table 2.6: Conditions for optimization of benzylic bromination.



| Entry | Conditions | Scale | Result |
|-------|---|--------|-----------------|
| 1 | CBr_4 , PPh_3 , DCM, 0°C , 20 min | 100 mg | SEM Truncation |
| 2 | PBr_3 , DCM, 0°C , 1 h | 50 mg | 70% 2.21 |
| 3 | PBr_3 , DCM, 0°C , 1 h | 1.2 g | SEM Truncation |
| 4 | NBS, PPh_3 , DCM, 0°C , 1 h | 3.0 g | 90% 2.21 |

With benzylic bromide in hand, I attempted several coupling conditions with a monoprotected orcinol protected fragment to produce the linchpin intermediate needed. Choice of protecting groups here was limited given substrate issues with the native benzyl ether mentioned

prior as well as the potential for elimination of the tertiary alcohol under acidic conditions once set (**Figure 2.10**).

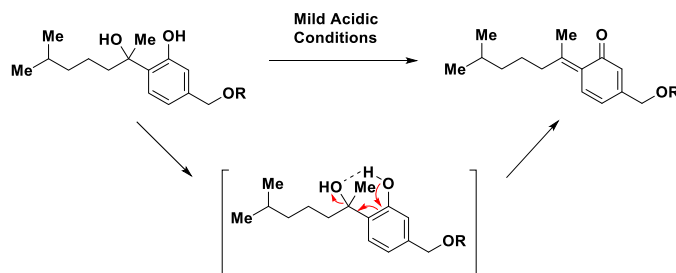
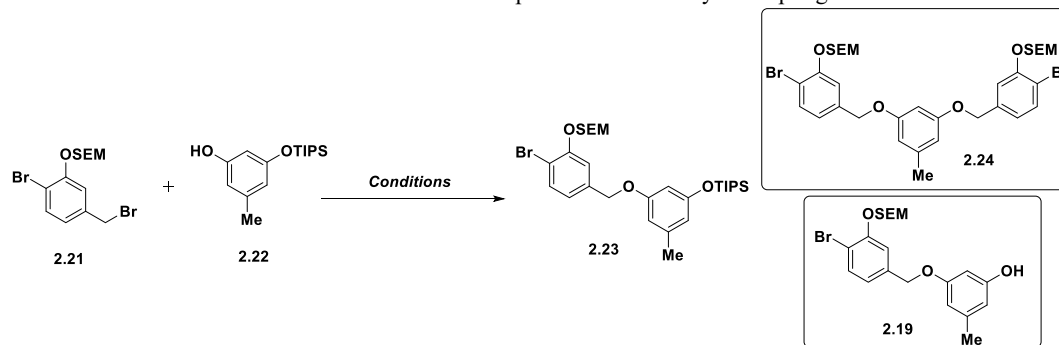


Figure 2.10: Potential rearrangement of benzylic tertiary alcohol in acidic conditions.

The protecting group chosen in all cases was TIPS as it could be easily removed with fluorinated species and provided more base stability than other silyl protecting groups tested (TMS, TBDPS etc.) in all reaction conditions without the presence of benzyl bromide. Moreover, TIPS could be selectively removed in the presence of SEM for late stage diaryl coupling towards peniciaculin A and analogs. Initially, tetrabutylammonium bromide (TBAB) assisted displacement was attempted but primarily TIPS deprotected orcinol, facilitated by potassium phosphate, was isolated with minimal coupling product.

Table 2.7: Conditions for optimization of benzylic coupling.

| Entry | Conditions | TIPS Deprotected Orcinol | Dimer 2.24 | TIPS Deprotected Linchpin 2.19 | Linchpin 2.23 |
|-------|--|--------------------------|------------|--------------------------------|---------------|
| 1 | TBAB, K ₃ PO ₄ , H ₂ O, 25°C, o/n | 100% | - | - | - |
| 2 | K ₂ CO ₃ , DMF, 80°C, 3 h | - | 26% | 38% | - |
| 3 | K ₂ CO ₃ , DMF, 25°C, 12 h | - | 21% | 11% | 68% |
| 4 | K ₂ CO ₃ , DMF, 25°C, 8 h | - | 10% | - | 86% |
| 5 | K ₂ CO ₃ , DMF, 25°C, 0°C, 20 h | - | - | - | 61% |

Reagents were switched out and using potassium carbonate while heating primarily formed triaryl intermediate **2.24** along with TIPS deprotected linchpin **2.19** (Table 2.7, entry 2). Running this reaction without heating at room temperature for 12 hours gave near full conversion from starting material with mono-TIPS protected orcinol as the limiting reagent to a 68% yield of intended protected linchpin intermediate with 21% of dimerized side product (Table 2.7, entry 3). Reducing reaction time to 8 hours improved yields of the intended linchpin intermediate to 86% conversion with the remaining material being dimerized intermediate (Table 2.7, entry 4). The presence of this intermediate made purification difficult, but not impossible. In an effort to prevent formation of this byproduct, the reaction was conducted overnight in a fridge at 4°C (Table 2.7, entry 5). Here, no dimerized product was formed as TIPS deprotection was hindered, however, purification was greatly complicated due to the starting benzylic bromide and protected linchpin intermediate coeluting during flash chromatography. Though small amounts of this byproduct could be carried through subsequent steps in order to differentiate the RFs of the aforementioned,

metalation and product formation would be greatly hindered due to side reactions with metalating reagents. Further, ^1H NMR spectra taken on lower MHz instruments show overlap of aryl these peaks, erroneously giving assurance of pure product. Taking all of the previously mentioned into account use of the conditions from entry 4, **Table 2.7** were used going forward.

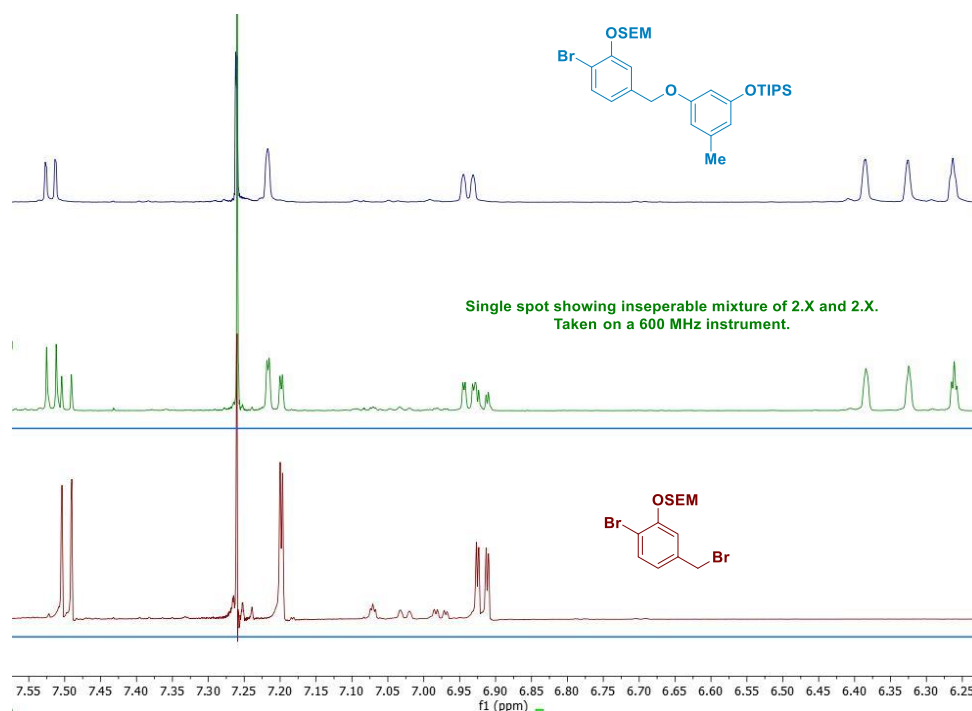


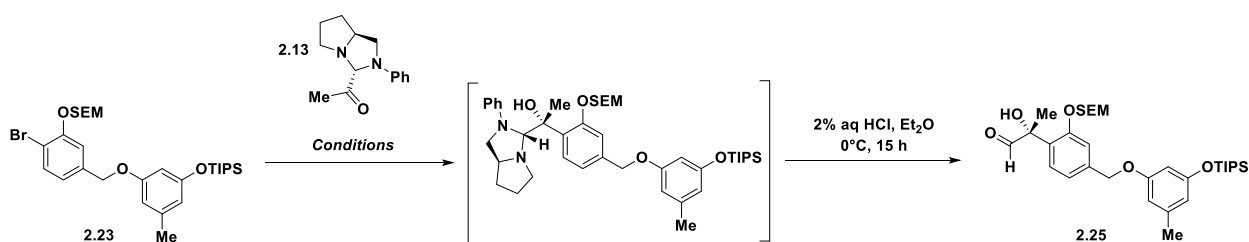
Figure 2.11: ^1H NMRs showing shifts of benzylic bromide **2.21** and linchpin intermediate **2.23**. Spectra taken on lower MHz instruments show significant overlap of **2.21** and **2.23**.

2.2.3.3. Lithium-Halogen Exchange

Initial attempts to utilize the conditions reported by Ito and coauthors to form target the tertiary alcohol **2.25** were unsuccessful (**Table 2.8**, entry 1).³⁴ In all cases, little to no target aldehyde was formed. Moreover, product yields, if any, were respective to the imidazolidinone as the limiting reagent, meaning that yields relative to the linchpin intermediate **2.23** were halved as two equivalents of this aryl bromide were required. The major product in all cases was the protodebrominated **2.26**, with zero recovery of the linchpin **2.23**. I attempted to optimize Grignard

formation through the addition of 4Å molecular sieves, activation of Mg^0 with additional equivalents of dibromoethane, use of freshly distilled solvent, increasing reaction times and altering equivalents of key reagents to no avail. This was particularly interesting given that use of Ito's substrate as the aryl bromide, produced the tertiary alcohol in a variable, but more consistent manner.

Comparing results from reactions ran in tandem, I wanted to determine where the disparity in product formation between both reactions came from. A closer inspection of the ^1H NMR of both starting bromides revealed that the benzylic protons of **2.23** were more deshielded than the benzylic protons of **2.15** (4.94 ppm vs 4.74 ppm respectively). I hypothesized that rather than nucleophilic addition into the chiral imidazolidinone, the Grignard species was simply deprotonating at the benzylic position at a faster rate in substrate **2.23** than that of **2.15**. Alternatively, the aryl Grignard of this species may not be reactive enough as Grignard nucleophiles tend suffer from decreased nucleophilicity due to the more covalent nature of the Mg-C bond. This is likely further exacerbated by the sterically hindered nature of the imidazolidinone electrophile.



Scheme 2.5: Diastereoselective nucleophilic addition.

Taken together, I proposed using a lithium halogen exchange to produce a lithiated organometallic compound, which has a greater ionic character than a Grignard of the same species, to promote nucleophilic attack of linchpin **2.23**. A potential concern was that diastereoselectivity

could suffer depending on the favored transition state during nucleophilic addition as desired *anti*-addition was promoted by chelation of the proline nitrogen and carbonyl with divalent magnesium (Figure 2.12). As lithium is monovalent, such chelation would not be possible.

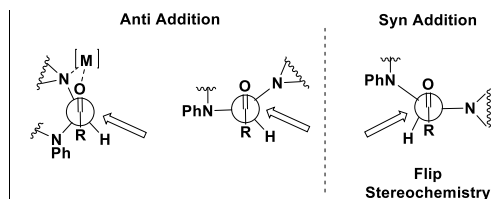
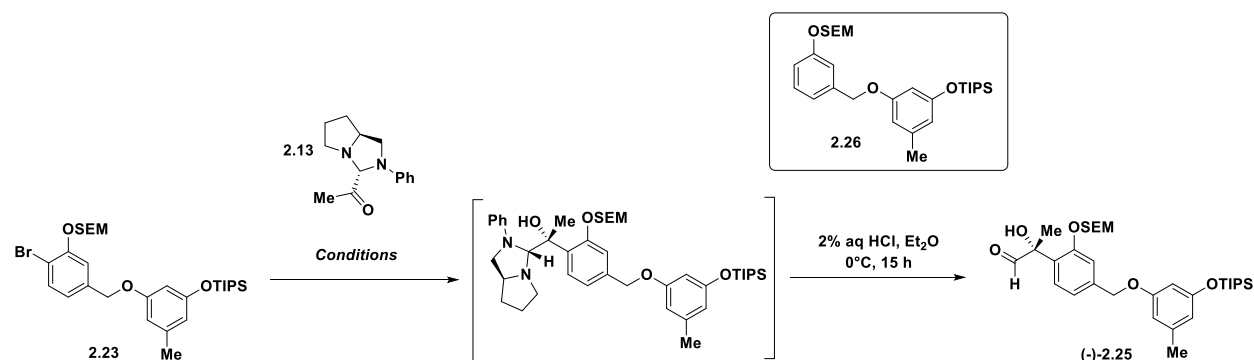


Figure 2.12: Proposed model for diastereoselective nucleophilic addition.

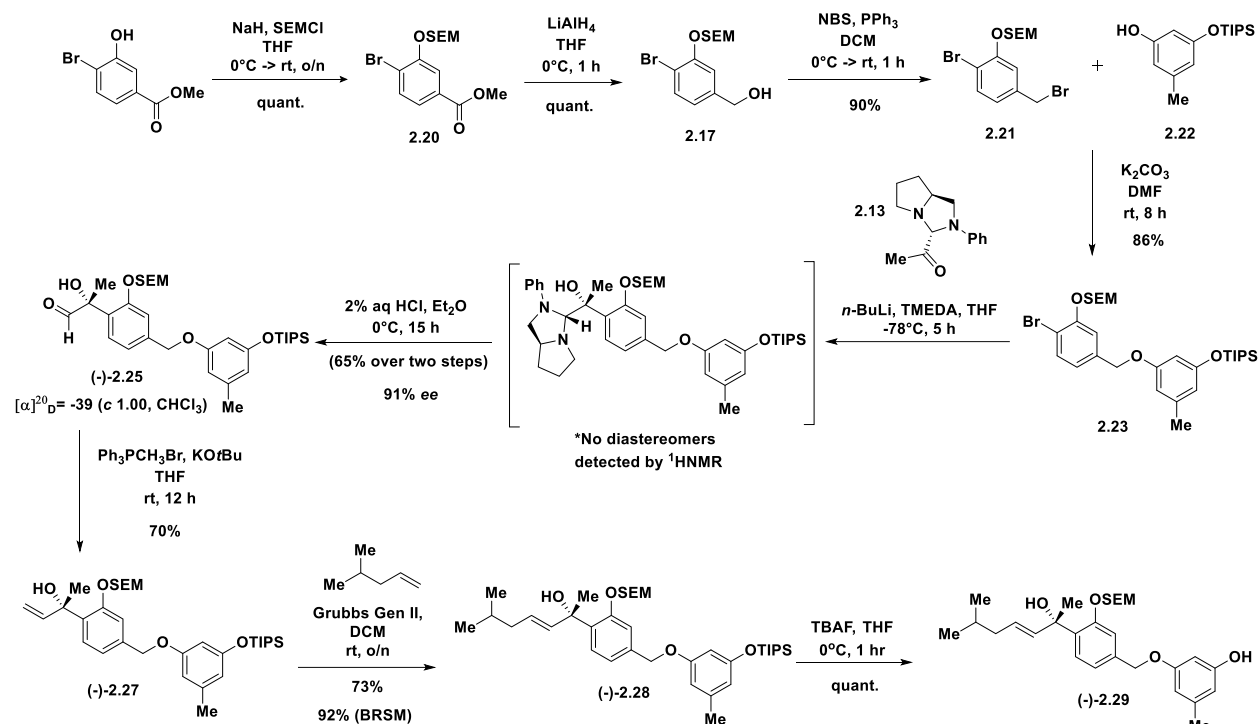
Additionally, as the conditions previously reported by Ito were reliant on two equivalents of aryl bromide for suitable yields, I sought to use the linchpin aryl bromide **2.23** as the limiting reagent to evade unnecessary protodebromination of the advanced intermediate. Optimization of the lithium halogen exchange began by treating one equivalent of aryl bromide with *n*-BuLi at -78°C to produce the lithiated species, followed reaction with the chiral imidazolidinone **2.13** at -78°C in an effort to form the benzylic tertiary alcohol. Unfortunately, no intended product was recovered and instead only protodebromination was observed (Table 2.8, entry 2). I opted to utilize TMEDA to stabilize the lithiated species and treatment of aryl bromide with this reagent before addition of *n*-BuLi gave 34% of the intended tertiary alcohol after hydrolysis with mild acid (Table 2.8, entry 3). This experiment was repeated with bromide **2.15**. Comparing optical rotations of product generated using Grignard and lithium halogen exchange conditions both indicated that the *anti*-addition of the metalated species were observed due to preferred Felkin-Ahn confirmation adopted by the imidazolidinone. The directions of these rotations were also consistent with previously synthesized homobenzylic aldehyde using Ito's substrate.

Table 2.8: Optimization of lithium halogen exchange.



| Entry | Conditions | Protodehalogenation 2.26 | Aldehyde 2.25 |
|-------|--|-----------------------------|------------------|
| 1 | i. Mg^0 (6.0 equiv), 2.23 (2.0 equiv), Dibromoethane (0.5 equiv), THF (0.5 M) reflux, 2 h ii. 2.13 (1.0 equiv), -78°C , 5 h | - | - |
| 2 | i. <i>n</i> -BuLi (1.25 equiv), 2.23 (1.0 equiv), THF (0.1 M), -78°C , 1.5 h ii. 2.13 (1.5 equiv), -78°C , 5 h | 38% | - |
| 3 | i. <i>n</i> -BuLi (1.25 equiv), 2.23 (1.0 equiv), TMEDA (1.25 equiv), THF (0.1 M), -78°C , 1.5 h ii. 2.13 (1.5 equiv), -78°C , 5 h | 66% | 34% |
| 4 | i. <i>n</i> -BuLi (1.25 equiv), 2.23 (1.0 equiv), TMEDA (1.25 equiv), THF (0.1 M), -78°C , 1.5 h ii. 2.13 (1.5 equiv), -78°C , 5 h | 35% | 65% |
| 5 | i. <i>n</i> -BuLi (1.25 equiv), 2.23 (1.0 equiv), TMEDA (1.25 equiv), THF (0.1 M), -78°C , 1.5 h ii. 2.13 (1.5 equiv), -78°C , 18 h | 24% | 76% |

I wanted to further investigate the source of the protodebrominated linchpin intermediate. I hypothesized that though anhydrous solvent was used, perhaps minute quantities of H_2O in the reaction was the cause of protodebromination of the lithiated linchpin intermediate. I found that addition of 4\AA molecular sieves increased the yield of intended product by two-fold (Table 2.8, entry 4). These reaction conditions were also utilized to perform a lithium halogen exchange into DMF where near full conversion to intended product was observed. This result led me to question whether steric incompatibility with the chiral imidazolidinone was the cause of the limited reactivity observed. Thus, when the lithium halogen exchange ran for 18 hours at -78°C , we found that yields intended product were slightly raised to 76% (Table 2.8, entry 5). It should be noted that no diastereomers were observed ^1H NMR in all cases. Moreover, enantiomeric excess for this reaction was determined to be 91%, in favor of the *anti*-stereoselective product, but likely is higher due to the aldehyde degrading on the column from successive runs.



Scheme 2.6: Continued synthetic route towards 2.1. Here aldehyde **2.25** was found to be unstable and either immediately stored in a freezer or converted to alkene **2.27**.

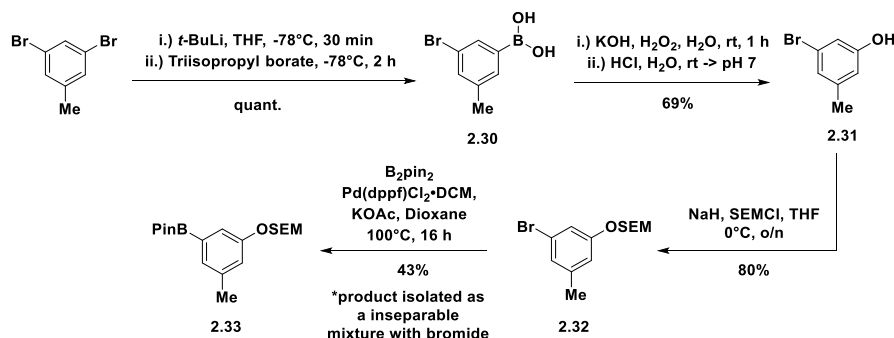
Hydrolysis of the aminal in mild acid required careful control of temperature as performing the reaction above 0°C could result in elimination of the benzylic alcohol. Reacting overnight in an ice chest unmasks aldehyde **(-)-2.25**. It should be noted that the starting pyrrolidine could be isolated from the aqueous layer and reused in subsequent reactions if desired. Attempts to directly perform a Wittig homologation on this aldehyde were unsuccessful. I believe this may be due to steric clash with the SEM protecting group of the phenol. Instead, a smaller methyl Wittig was utilized to generate a terminal alkene in good yield. Serendipitously, this strategy allows for facile analog development through cross metathesis with different alkyl chains to further probe the binding pocket of the cytochrome bc_1 complex. Towards penicillin A, cross metathesis with excess 4-methyl-1-pentene using Grubbs II generation catalyst installed the alkyl side chain, a transformation assumedly owed to Ruthenium's longer bond angle compared to that of phosphorus

for the direct Wittig. Intended product was separated with preparative thin layer chromatography (PTLC) and selective TIPS deprotection at 0°C provided free phenol (-)-**2.29** in good yield.

2.2.4. Aryl Coupling

Several reported conditions were tested for biaryl formation. First, we were interested in coupling the free phenol with an aryl halide through Buchwald conditions. These were generally unsuccessful with TBS protected aryl triflates. Attempts to convert to the more reactive aryl bromide were also met with challenges. Palladium catalyzed conversion from the aryl triflate directly to the aryl bromide yielded no product and Miyaura borylation followed by bromination with CuBr₂ was also unsuccessful in my hands. At this point, I realized that conversion from orcinol required several steps and protecting groups would need to be appended via a low yielding monoprotection at the start requiring either several steps to generate each substrate or, necessitating a deprotection, reprotection strategy for screening.

Given that this final aryl coupling towards peniciaculin A could be troublesome considering lability of the benzylic alcohol I wanted to come up with a concise route to easily generate functionalized aryl rings for testing coupling conditions to append aryl rings to free phenol scaffolds along our reaction route. I found that commercially available 3,5-dibromotoluene could cleanly be converted to the boronic acid through a monolithium-halogen exchange with *t*-BuLi at -78°C followed by reaction with triisopropylborate.³⁷ Oxidation with KOH and H₂O₂ converts this boronic acid to bromophenol **2.31** in 84% yield over two steps. At this point various protecting groups could be appended, and in this SEM was chosen for ease in global deprotection as well as base stability. This aryl bromide would then be used for subsequent diaryl ether couplings with the protected truncated saturated natural product.



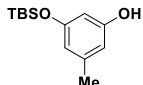
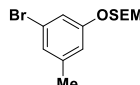
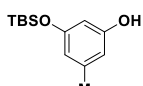
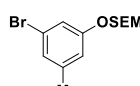
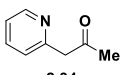
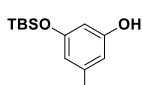
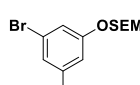
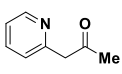
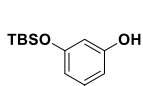
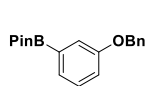
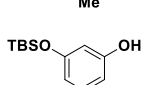
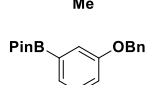
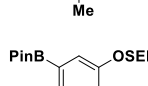
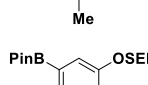
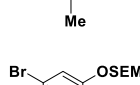
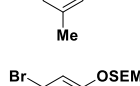
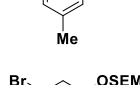
Scheme 2.7: Synthesis of brominated and borylated aryl coupling partners.

I first attempted to furnishing the diaryl ether through a copper catalyzed Ullman reaction. Unfortunately, all efforts towards combining functionalized aryl fragments by Ullman coupling were unsuccessful including metal free, ligand inclusive and forcing conditions utilizing various protecting groups.³⁸ In these cases, I hypothesized that use of Cs_2CO_3 would give the best chances for success as cesium phenoxide is relatively soluble in organic solvent and may also enhance the solubility of the proposed intermediate $[\text{Cu}(\text{OAr})_2]^-$. I also attempted this reaction with $\text{KO}t\text{-Bu}$ in case this reaction instead followed a free radical path during the aryl halide activation step, however this also led to little product formation.^{39,40} In some cases a (2-pyridyl)- acetone ligand was incorporated to improve activation of the aryl halide through a $\text{Cu}(\text{I})$ complex with the additive ligand as an intermediate.⁴¹ Unfortunately, this reaction also gave no conversion at lower temperatures (**Table 2.9**, entry 2) and under forcing conditions only showed decomposition of starting materials(**Table 2.9**, entry 3).

Aryl bromide **2.32** was converted to the corresponding aryl boronic ester aryl boronic ester through a palladium catalyzed Miyaura borylation to access another option for diaryl coupling via copper catalyzed Chan Lam reaction. While inseparable, but usable, mixtures with the corresponding bromide were isolated when SEM was the protecting group for this reaction borylation with benzyl protected bromide had no such issues (**2.51**). Initially, standard conditions

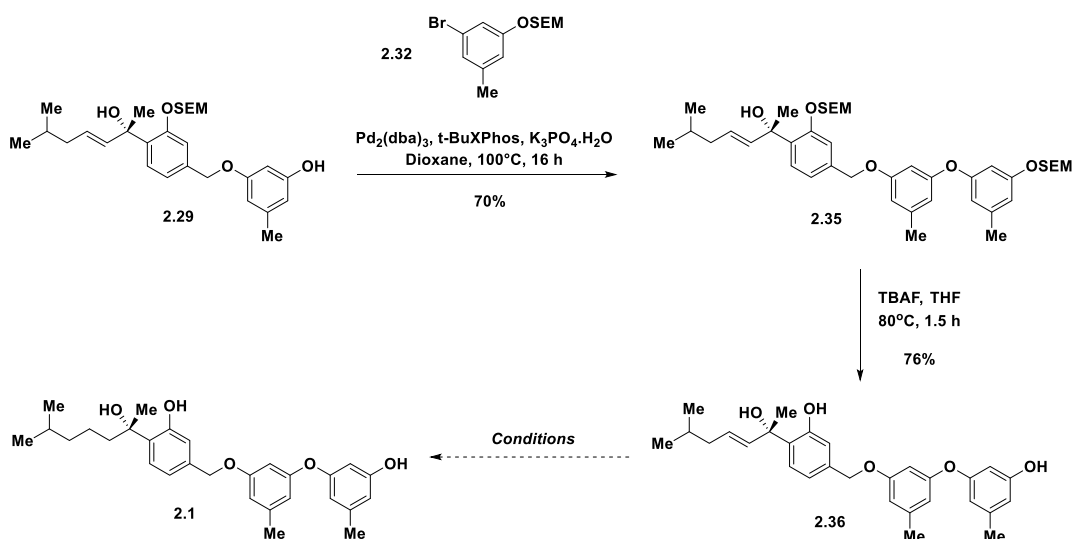
were employed using triethyl amine for both the boronic acid and boronic ester of the aryl halide and yielded little discernable product (**Table 2.9**, entry 4). I sought to circumvent this by taking inspiration from the Watson and Stahl groups studies towards better understanding the intricacies of Cu-based oxidative coupling reactions like the Chan Lam.^{42,43} Watson found that AcO^-/AcOH as well as pinacol generated in the reaction inhibited product formation with both amine and alcohol nucleophiles by forming inactive complexes with Cu(II) . They found that addition of B(OH)_3 not added in the sequestering of AcO^-/AcOH to form stable more stable borates, but also formed stable boric acid esters with pinacol. Moreover, Watson noted that B(OH)_3 also promotes oxidation of Cu(I) to Cu(II) in an effective manner preventing further nonproductive side reactions with the Cu(I) species. Formation of this active species (Cu(II)) is also promoted under dry air or O_2 atmosphere as these conditions allow for the re-oxidation of Cu(I) to Cu(II) .^{42,44} Taken together, I applied this knowledge to my Chan Lam couplings and saw modest yields on aryl rings (**Table 2.9**, entry 5) (Product is **2.9.5** in SI). When applied to **2.29** I saw addition of the Bpin aryl fragment via ^1H NMR but decomposition of the intended product (**Table 2.9**, entry 7). I assumed that this was due to the lability of the tertiary alcohol in acidic conditions as previously indicated, as using these conditions with another substrate garnered a modest yield of intended product (**Table 2.9**, entry 6).

Table 2.9: Optimization of aryl coupling.

| Entry | Phenol | Aryl Boronic Ester/ Halide | Additive | Conditions | Result |
|-------|---|---|---|---|-----------------|
| 1 |  |  | - | KOtBu, DMSO, 100°C, o/n | No Reaction |
| 2 |  |  |  2.34 | CuBr (10 mol%), Cs ₂ CO ₃ , DMSO, 90°C, o/n | 5% Coupling |
| 3 |  |  |  2.34 | CuBr (10 mol%), Cs ₂ CO ₃ , DMSO, 120°C, o/n | Decomposition |
| 4 |  |  | Molecular sieves | Et ₃ N, Cu(OAc) ₂ (1.0 equiv), DCM, rt, 24- 48 h | 17-28% Coupling |
| 5 |  |  | Molecular sieves | B(OH) ₃ , Cu(OAc) ₂ (1.0 equiv), MeCN, 80°C, 24 h | 53% Coupling |
| 6 | 2.49 |  | Molecular sieves | B(OH) ₃ , Cu(OAc) ₂ (1.0 equiv), MeCN, 80°C, 72 h | 30% Coupling |
| 7 | 2.29 |  | Molecular sieves | B(OH) ₃ , Cu(OAc) ₂ (1.0 equiv), MeCN, 80°C, 24 h | Decomposition |
| 8 | 2.29 |  | - | Pd ₂ (dba) ₃ (4 mol%), tBuXPhos (16 mol%), K ₃ PO ₄ Dioxane, 100°C, 16 h | No Reaction |
| 9 | 2.29 |  | - | Pd ₂ (dba) ₃ (4 mol%), tBuXPhos (16 mol%), K ₃ PO ₄ Dioxane : H ₂ O (99:1), 100°C, 16 h | 22-44% Coupling |
| 10 | 2.29 |  | Finely Crush K ₃ PO ₄ ·H ₂ O | Pd ₂ (dba) ₃ (4 mol%), tBuXPhos (16 mol%), K ₃ PO ₄ ·H ₂ O Dioxane, 100°C, 16 h | 70% Coupling |

Recently Schutzenmeister and coworkers synthesized anti-MRSA diaryl ethers through palladium catalyzed C-O bond couplings from functionalized orcinol fragments.⁴⁵ Several procedures using standard Cu- and Pd-based conditions were also attempted, and all failed to yield the desired product, primarily resulting in either decomposition or no conversion materials (Table 2.9, entry 7). Schutzenmeister found that a certain amount of water was required for the aryl ether coupling to occur after a screening for solvents and bases, found success with using K₃PO₄·H₂O in dioxane. Attempting this reaction using just K₃PO₄ resulted in no product formed. This implies

that this small amount of water is critical for some step in the catalytic cycle, most likely the ligand exchange of the bromine on the Pd(II) for the incoming oxygen nucleophile on the truncated natural product. Use of a solution of (99:1) Dioxane:H₂O gave inconsistent conversion of starting material to intended product. Using the hydrate indicated by Schutzenmeister and coworkers give intended product in good yield. It should be noted that this reaction is heterogeneous; if K₃PO₄·H₂O is not crushed into a very fine powder paired with good stirring the reaction will not proceed. This base is hygroscopic, crushing it should either be done quickly or under inert atmosphere. Moreover, if the reaction continued past the 16–20-hour window decomposition of the product increases, resulting in loss of starting material.

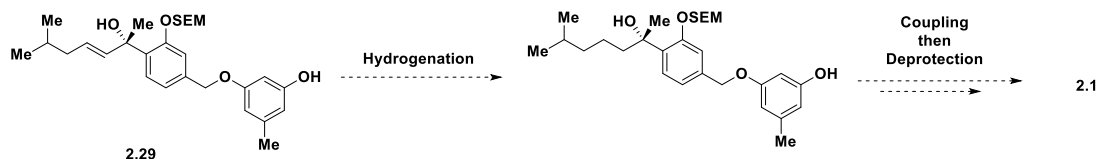


Scheme 2.8: Continued synthesis toward **2.1**.

Though the full peniciaculin carbon skeleton was in hand attempts to completely characterize these compounds with additional aryl rings were met with some challenges. First, in some cases, HRMS analysis of product **2.35** showed loss of the tertiary alcohol presumably due to expulsion from either rearrangement from the proximal alkene or expulsion from the benzylic methyl driven by the preferential formation of a conjugated system. Structural motifs from either of these options could be found in coisolated natural products with **2.1** (*i.e.* coisolate 5, coisolate

10).¹⁹ Moreover, though global SEM deprotection of **2.35** using an excess of dried TBAF and DBU (over 4Å molecular sieves) produced **2.36** in good yield, further instability issues ensued due to freeing the proximal phenol. The instability of polyphenolic compounds due to heat and light is well studied, and as indicated prior, could also result in degradation of material through rearrangement to expel the tertiary alcohol.^{46–49} The combination of the aforementioned led to the degradation of **2.36** over time. This instability combined with having a small amount of material made it difficult to acquire ¹³C NMR spectra of these compounds. Attempts to hydrogenate **2.36** towards the natural product were met with several challenges. As stated prior, peniciculin A has a native benzylic bond present limiting use of conventional conditions for hydrogenation to the natural product. Hydrogenation with Lindlar's catalyst gave minor and incomplete conversion to the target natural product.⁵⁰ It should also be noted that purification of the target natural product was difficult due to the similar polarity of the deprotected product as well as the presence of degraded byproducts. Moreover, this reaction gave irreproducible yields in future runs. Increasing the reaction pressure to 40 psi also gave no conversion of starting material towards product, and instead, in some cases, fully degraded product was isolated from a cumulation of the aforementioned. Hydrogenation was also attempted utilizing a copper-cobalt catalytic system as this method allows for careful and controlled introduction of hydrogen to the *in situ* generated catalyst limiting potential benzylic cleavage, though conversion to intended product was not seen.⁵¹ I hypothesize that these instability issues stem from the alkene present in the western fragment of this molecule furthering potential tertiary hydroxyl expulsion towards a conjugated system. As Yajima did not see such degradation issues, hydrogenation of the truncated peniciculin scaffold would be most ideal as **2.29** was found to be bench stable as an amorphous solid. Therefore, prior explored hydrogenation conditions, or use of a more efficient hydrogenation catalyst like Adams

catalyst in the case of Yajima *et al.*, or Shenvi hydrogenation could be employed prior to palladium coupling to circumvent these issues.^{29,52}



Scheme 2.9: Proposed hydrogenation reroute of **2.29** to **2.1**.

2.2.5. Analog Design

We set out to answer several questions through rational analog design using the peniciaculin scaffold. Generally, our strategy was based on truncation of the orcinol fragment to determine whether activity could be retained in a simplified molecule. Not only would this shave down steps to a bioactive compound but would also better mimic the molecular size of known QoI fungicides. Notably, molecular docking showed the potential for peniciaculin analogs to exhibit pi stacking interactions around their central ring mimicking favorable interactions in the cytochrome *bc₁* binding pocket like those seen in azoxystrobin at PHE274 and potential interactions at PHE128 as well. We also wanted to probe the importance of the tertiary alcohol to further validate its potential as a novel pharmacophore. This was completed in two ways, through replacement of the tertiary alcohol with a ketone moiety as well and complete replacement of the alkyl side chain. It should also be noted, as previously mentioned, derivatives of dirocinol with substitution at one phenol exhibited potent antibacterial activity against MRSA.⁴⁵ Similar activity was observed by Chen and coauthors towards various species of bacteria.⁵³ We hypothesized similar activity may exist against fungal species of interest. While we questioned whether omission of the pharmacophore and central ring would alter bioactivity as these derivatives would mimic the

central ring and sidechain of known QoIs, most likely such compounds would have a membrane perturbing mechanism of action as opposed to a specific target.

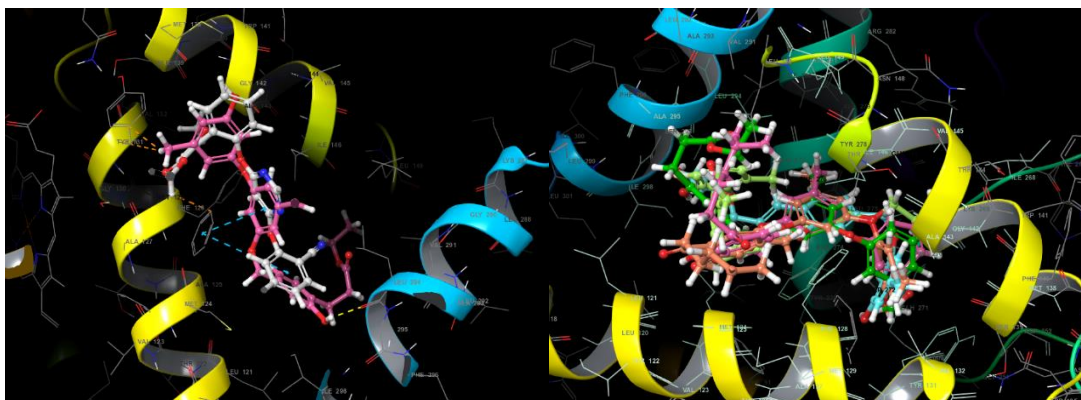
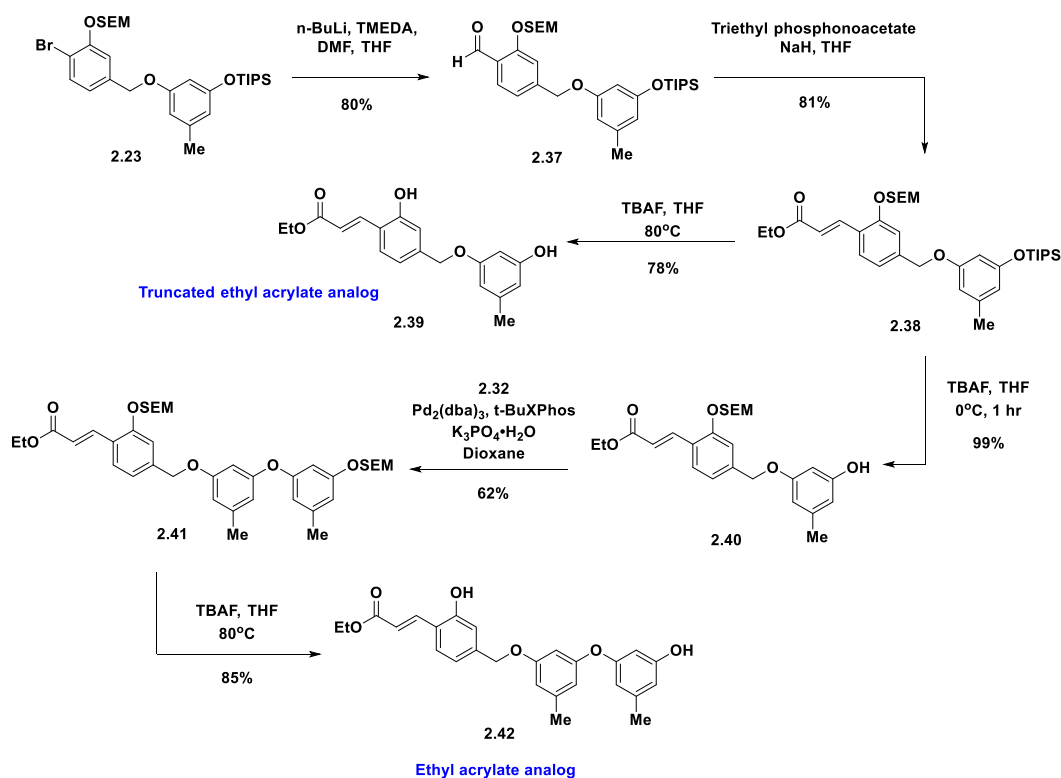


Figure 2.13: (Left) Example of peniciculin analog overlapped with axozystrobin in binding pocket, favorable pi-stacking interactions are shown. (Right) Overlap of target ligands to fully probe pi stacking potential in binding pocket.

2.2.5.1. Ethyl acrylate Analogs

Analogues were derived from linchpin intermediate **2.23**. A lithium halogen exchange followed by nucleophilic addition into DMF smoothly furnished aldehyde **2.37** in good yield. Horner-Wadsworth Emmons (HWE) reaction with that aldehyde gave **2.38** which could either be globally deprotected to give truncated analog **2.39** or selectively TIPS deprotected for subsequent coupling. Palladium catalyzed Buchwald coupling with aryl bromide **2.32** followed by global SEM deprotection gives triaryl acrylate analog **2.42**. Here, we sought to expand on the known QoI space by utilizing a more simplified enone at the benzylic position. Though it is similar methyl methoxy acrylate moieties seen in other QoI's it differs by possessing a less reactive covalent trap.⁸ It should be noted that much like **2.36**, stability of **2.39** and **2.42** varied in NMR solvents these compounds were soluble in due to the potential for rearrangement. Currently, acetone is the best choice for either of these compounds, though degradation of **2.42** appears more rapid in deuterated solvent than that of **2.39**.

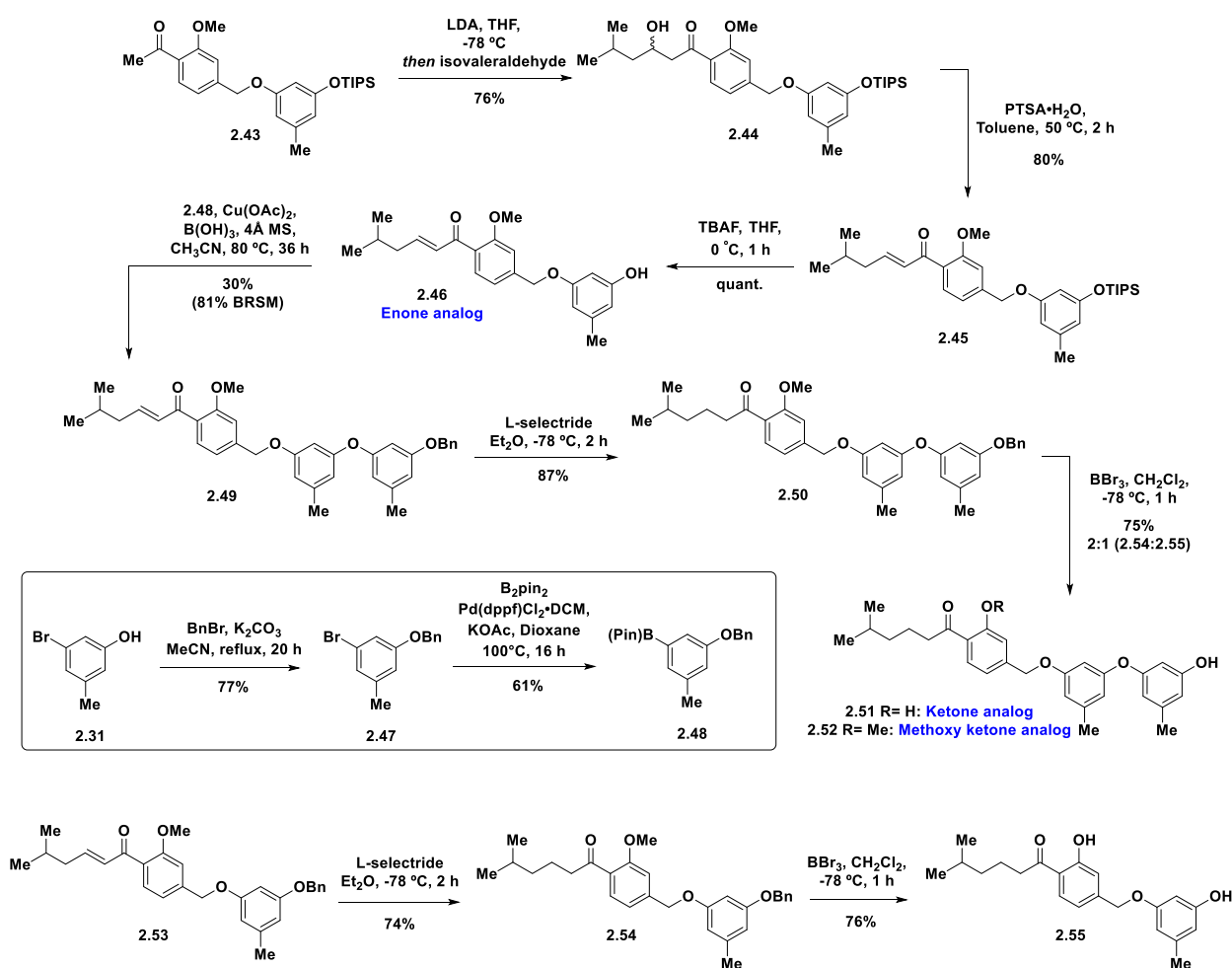


Scheme 2.10: Synthetic route towards ethyl acrylate analogs

2.2.5.2. Enone Derivatives

We also wanted to probe the importance of the tertiary alcohol through the synthesis of enone derivatives indicated. Aldol condensation with isovaleraldehyde resulted in enone **2.45**. TIPS deprotection produced enone analog **2.46**. Chan-Lam coupling of free phenol **2.49** with aryl pinacol boronate **2.48** resulted in the full triaryl scaffold **2.49**. Although palladium catalyzed Buchwald coupling was also attempted with aryl bromide **2.32**, no desired product was isolated. Deprotection with BBR_3 at -78°C after enone reduction by 1,4-addition with L-selectride resulted in the desired triaryl ketone analog **2.51** and benzyl deprotected triaryl **2.52**. Efforts to produce solely the global deprotected product **2.51** resulted in byproduct formation (*i.e.* benzyl ether cleavage and decomposition). Unfortunately, we also found full deprotected substrate **2.51** rapidly decomposed when subjected to various purification methods including silica column

chromatography, high performance liquid chromatography (HPLC), and mass guided purification and was thus not suitable for biological evaluation. For the truncated analogs, aldol condensation followed by chemoselective 1,4-reduction furnished of the desired ketone side chain **2.54**. Global deprotection under Lewis acidic conditions produced truncated ketone analog **2.55**.

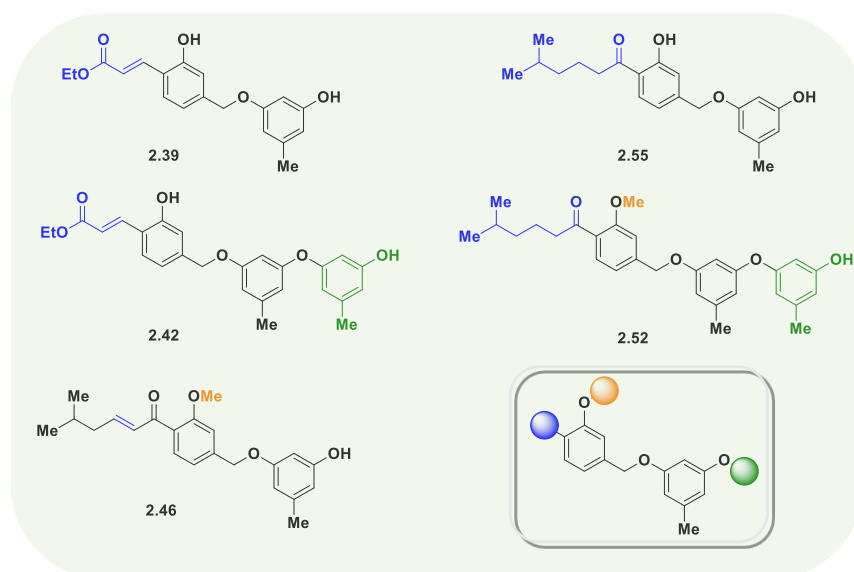


Scheme 2.11: Synthetic route towards enone and methoxy ketone analogs.

2.2.6. Antimicrobial activity

A small panel of analogs from this project were tested for their fungicidal, insecticidal and herbicidal activity by Corteva Agriscience™. Unfortunately, *A.brassicae* was not available as a

strain during the time of testing, however we expected to observe some activity in other strains of opportunistic fungi if these compounds had a similar mechanism of action.



| Compound | Corn Smut (USTIMA) | Rice Blast (PYRIOR) | <i>Pythium irregulare</i> (PYTHIR) | Late blight of potatoes/ tomatoes (MC4100) | Anthracnose of curcubits (COLLA) |
|----------|-----------------------|------------------------|---------------------------------------|---|-------------------------------------|
| 2.39 | 40 | 100 | 100 | 100 | 30 |
| 2.42 | 20 | 55 | 30 | 5 | 40 |
| 2.55 | 25 | - | - | - | 25 |
| 2.52 | 25 | 30 | - | - | 15 |
| 2.46 | 10 | 40 | 20 | 20 | 30 |

Figure 2.14: Activity of synthesized analogs based on the on the peniciaculin scaffold. Activity is reported as percent inhibition at 5 $\mu\text{g/mL}$.

Due to their similar mechanism of action, QoIs usually exhibit a broad spectrum of antifungal activity. Hence, we reasoned that all analogs should be assessed against a group of plant-pathogenic fungi despite peniciaculin only being tested on against *A. brassicae* in its isolation paper. Still, there are many other plant pathogenic fungi which bottleneck the agricultural industry. Highlighted are results from some of these pathogens, including *Ustilago maydis*, *Magnaporthe grisea*, *Phytophthora infestans*, *Pythium irregulare*, and *Colletotrichum orbiculare*.

Corn smut is typically caused by the fungus *U. maydis*, and targets corn (maize) and teosinte plants resulting in distortion in the appearance of heavily infected plants, though it is typically not fatal. The infection initially appears as whitish galls that later rupture and release dark spores capable of infecting other corn plants. Ironically, to some it's known as a delicacy, though it's effects still overall decrease food and biofuel supply.⁵⁴ Rice, which feeds half of the world's population, is hampered by rice blast disease caused by the heterothallic ascomycetous pathogen *P. oryzae*. This fungus is a major constraint on global rice cultivation and hinders production by approximately 10 to 30 percent yearly.⁵⁵ *P. infestans* is a soil-borne oomycetes or water mold and the causative agent of potato blight. It is most infamously known due to it's role in the Irish potato famine.⁵⁶ *P. irregulare* is also a water mold that causes damping off and root rot of plants which causes non-germination, stunted growth or negligent growth after germination, and decaying and death of seedlings at the soil level, thereby constraining both nursery and field settings.^{57,58} *C. orbiculare* causes wilting and stem lesions in cucurbit crops resulting in reduced yield, sour taste, and the demise of the entire plant.⁵⁹

Incorporation of a simplified QoI pharmacophore mimic in **2.39** and **2.42** through use of an ethyl acrylate moiety resulted in broad spectrum activity against fungal pathogens. Not only does this give a potentially new more simplified QoI pharmacophore, but it also suggests that the phenol core and diaryl fragment of peniciculin A mimic the central ring and side chain portions of known QoIs. Notably, truncated ethyl acrylate analog **2.39** was found to be more potent against target pathogenic fungi across the board compared to the full triaryl **2.42**. This could indicate that the monoaryl ether may be the optimal side chain length for the *bc*₁ binding pocket. Analogs which directly tested the importance of the tertiary alcohol, namely **2.46**, **2.52** and **2.55** only showed minor antifungal activity, with no discernable trend. This result is particularly interesting as one

would expect similar reactivity to **2.39** and **2.42** depending on the mechanism of action for **2.46** (e.g, covalent trap). These results suggest that the tertiary alcohol of peniciaculin A is indeed required for activity. Alternatively, **2.55** could undergo quinone formation through elimination of the tertiary alcohol as previously proposed, however this would not explain a lack of reactivity in some coisolates in the isolation paper. Lastly, this could suggest that the tertiary alcohol of peniciaculin A is acting as a novel pharmacophore.

2.3 Conclusions and Future Directions

Biological data collected support our initial hypothesis that peniciaculin A is acting as a QoI with novel tertiary alcohol pharmacophore. Substitution of the tertiary alcohol with an ethyl acrylate moiety by way of analogs **2.39** and **2.42** resulted in broad spectrum activity towards target pathogens tested. Notably, **2.39** was more potent towards nearly every fungal pathogen tested compared to **2.42** indicating that future studies should employ truncated analogs. To this effect, truncated analogs of both enantiomers of peniciaculin A could be facially generated using chemistry already developed. Additionally, further docking studies show that saturated analogs of **2.39** and **2.42** both have greatly improved docking scores, further indicating that some different mechanism of action may be at play for these two compounds. These have also been synthesized and require chromatographical purification for future testing. As analogs **2.46**, **2.52** and **2.55** did not show meaningful activity reinforcing the potential of peniciaculin A possessing a novel pharmacophore. Currently truncated analogs are being prepared for testing against *A. brassicae*.

To ensure the continuation of this project, I've written an NSF grant I've written an NSF grant detailing future bisabolene endeavors. In the distant future, analogs will leverage total synthesis of peniciaculin A through linchpin intermediate **2.23**, which will be adopted for facile access to additional analogs (**Figure 2.15. A**). Protection of commercially available

hydroxybenzoate followed by subsequent reduction and subjection to modified Appel conditions gives our key benzylic bromide. A variety of heteroatom-substituted (Y) functionalized aryl rings will be appended using displacement conditions employed in our synthesis of peniciaculin A analogs. As we hypothesize that the biaryl rings mimic ubiquinone, we will employ known bioisosteres of cyt *bc*₁ QoI compounds in our DTS (**Figure 2.15. B**: Musso, strobilurin, Sovran).^{60–62} The alkyl side chain can then be installed and modified to probe the importance of the hydrophobic pocket. Concurrently, we will also construct analogs bearing our simplified ethyl acrylate moiety to serve as a control based on its initial biological activity.

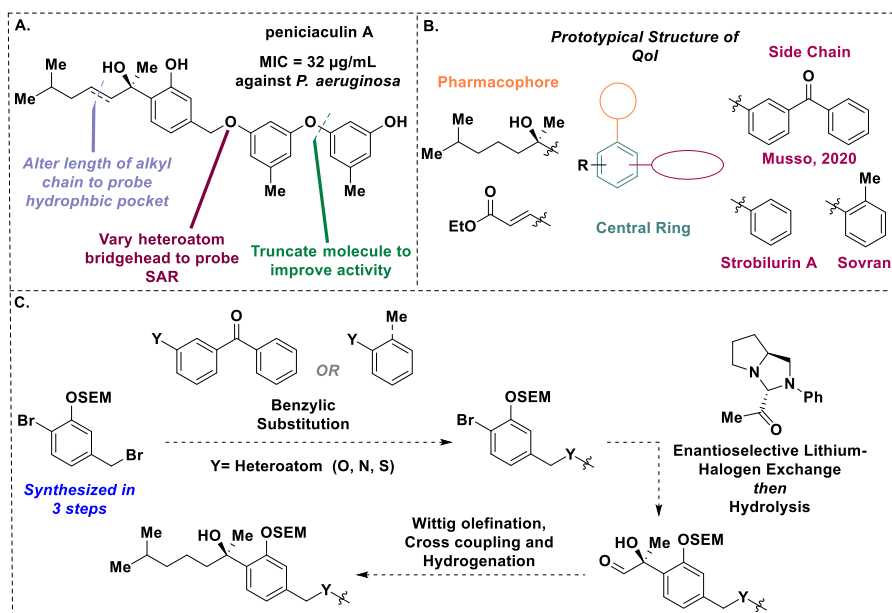


Figure 2.15: (A) Structure of peniciaculin A with intended changes to probe *Ps* activity. (B) Prototypical structure of known QoIs mapped onto intended peniciaculin A derivatives. Side chain modifications here are inspired by other QoIs. (C) Abbreviated synthetic route for the synthesis of target peniciaculin analogs.

2.4. Chapter 2 References

- (1) FAOSTAT. <http://www.fao.org/faostat/en/#data/QC> (accessed 2023-03-12).
- (2) Nowicki, M.; Nowakowska, M.; Niezgoda, A.; Kozik, E. Alternaria Black Spot of Crucifers: Symptoms, Importance of Disease, and Perspectives of Resistance Breeding. *Veg. Crop. Res. Bull.* **2012**, *76* (1), 5–19.
- (3) Shrestha, S. K.; Munk, L.; Mathur, S. B. Role of Weather on *Alternaria* Leaf Blight Disease and Its Effect on Yield and Yield Components of Mustard. *Nepal Agriculture Research Journal* **1970**, *6*, 62–72.
- (4) Nowakowska, M.; Wrzesińska, M.; Kamiński, P.; Szczechura, W.; Lichocka, M.; Tartanus, M.; Kozik, E. U.; Nowicki, M. *Alternaria Brassicicola* – Brassicaceae Pathosystem: Insights into the Infection Process and Resistance Mechanisms under Optimized Artificial Bio-Assay. *Eur. J. Plant. Pathol.* **2019**, *153* (1), 131–151.
- (5) Kumar, D.; Maurya, N.; Bharati, Y. K.; Kumar, A.; Srivastava, K.; Chand, G.; Kushwaha, C.; Singh, S. K. Alternaria Blight of Oilseed Brassicas : A Comprehensive Review. *Afr. J. Microbiol. Res.* **2014**, *8* (30), 2816–2829.
- (6) EPPO Global Database. https://www.eppo.int/RESOURCES/eppo_databases/global_database (accessed 2023-03-12).
- (7) Chow, C. K. Dietary Coenzyme Q 10 and Mitochondrial Status Port Chain , Where It Accepts Electrons from Complexes I and II and Plays. *Meth. Enzymol.* **2004**, *382* (1996), 105–112.
- (8) Zuccolo, M.; Kunova, A.; Musso, L.; Forlani, F.; Pinto, A.; Vistoli, G.; Gervasoni, S.; Cortesi, P.; Dallavalle, S. Dual-Active Antifungal Agents Containing Strobilurin and SDHI- Based Pharmacophores. *Sci. Rep.* **2019**, *9*, 11377.
- (9) Zeng, F.; Arnao, E.; Zhang, G.; Olaya, G.; Wullschlegel, J.; Sierotzki, H.; Ming, R.; Bluhm, B. H.; Bond, J. P.; Fakhoury, A. M.; Bradley, C. A. Characterization of Quinone Outside Inhibitor Fungicide Resistance in *Cercospora Sojina* and Development of Diagnostic Tools for Its Identification. *Plant. Dis.* **2015**, *99* (4), 544–550.
- (10) Bartlett, D. W.; Clough, J. M.; Godwin, J. R.; Hall, A. A.; Hamer, M.; Parr-Dobrzanski, B. The Strobilurin Fungicides. *Pest. Manag. Sci.* **2002**, *58* (7), 649–662.
- (11) Schramm, G.; Steglich, W.; Anke, T.; Oberwinkler, F. ANTIBIOTICS FROM BASIDIOMYCETES, III. STROBILURIN A AND B, ANTIFUNGAL METABOLITES FROM STROBILURUS TENACELLUS. *Chem. Inf.-Dienst.* **1978**, *9* (43), 2779–2784.
- (12) Morton, V.; Staub, T. A Short History of Fungicides. *APSnet Feature Articles* **2008**.
- (13) Feng, Y.; Huang, Y.; Zhan, H.; Bhatt, P.; Chen, S. An Overview of Strobilurin Fungicide Degradation: Current Status and Future Perspective. *Front. Microbiol.* **2020**, *11*, 389.
- (14) Gisi, U.; Sierotzki, H.; Cook, A.; Mccaffery, A. Mechanisms Influencing the Evolution of Resistance to Qo Inhibitor Fungicides. *Pest Manag. Sci.* **2002**, *867*, 859–867.
- (15) Kraiczy, P.; Haase, U.; Gencic, S.; Flindt, S.; Anke, T.; Brandt, U.; Von Jagow, G. The Molecular Basis for the Natural Resistance of the Cytochrome Bc1 Complex from Strobilurin-Producing Basidiomycetes to Center Qp Inhibitors. *Eur. J. Biochem.* **1996**, *235* (1–2), 54–63.

- (16) Nottensteiner, M.; Absmeier, C.; Zellner, M. QoI Fungicide Resistance Mutations in *Alternaria Solani* and *Alternaria Alternata* Are Fully Established in Potato Growing Areas in Bavaria and Dual Resistance against SDHI Fungicides Is Upcoming. *Gesunde. Pflanzen.* **2019**, *71* (3), 155–164.
- (17) Arakawa, A.; Kasai, Y.; Yamazaki, K.; Iwahashi, F. Features of Interactions Responsible for Antifungal Activity against Resistant Type Cytochrome Bc1: A Data-Driven Analysis Based on the Binding Free Energy at the Atomic Level. *PLoS One* **2018**, *13* (11), e0207673.
- (18) Matsuzaki, Y.; Yoshimoto, Y.; Arimori, S.; Kiguchi, S.; Harada, T.; Iwahashi, F. Discovery of Metyltetraprole: Identification of Tetrazolinone Pharmacophore to Overcome QoI Resistance. *Bioorg. Med. Chem.* **2020**, *28* (1), 115211.
- (19) Li, X.; Li, X.; Xu, G.; Zhang, P.; Wang, B. Antimicrobial Phenolic Bisabolanes and Related Derivatives from *Penicillium Aculeatum* SD-321, a Deep Sea Sediment-Derived Fungus. *J. Nat. Prod.* **2015**, *78*, 844–849.
- (20) Wu, Z. Enantioselective Synthesis of Natural Products Containing Tertiary Alcohols and Contributions to a Total Synthesis of Phorbasin B., **2015**.
- (21) Christoffers, J.; Baro, A. *Quaternary Stereocenters: Challenges and Solutions for Organic Synthesis*; Wiley-VCH, **2006**.
- (22) Pu, L.; Yu, H. Bin. Catalytic Asymmetric Organozinc Additions to Carbonyl Compounds. *Chem. Rev.* **2001**, *101* (3), 757–824.
- (23) Shibasaki, M.; Kanai, M. Asymmetric Synthesis of Tertiary Alcohols and α -Tertiary Amines via Cu-Catalyzed C–C Bond Formation to Ketones and Ketimines. *Chem. Rev.* **2008**, *108* (8), 2853–2873.
- (24) Stymiest, J. L.; Bagutski, V.; French, R. M.; Aggarwal, V. K. Enantiodivergent Conversion of Chiral Secondary Alcohols into Tertiary Alcohols. *Nature* **2008**, *456* (7223), 778–783.
- (25) Aggarwal, V. K.; Ball, L. T.; Carobene, S.; Connelly, R. L.; Hesse, M. J.; Partridge, B. M.; Roth, P.; Thomas, S. P.; Webster, M. P. Application of the Lithiation–Borylation Reaction to the Rapid and Enantioselective Synthesis of the Bisabolane Family of Sesquiterpenes. *ChemComm* **2012**, *48* (74), 9230–9232.
- (26) Bieszczad, B.; Gilheany, D. G. Asymmetric Grignard Synthesis of Tertiary Alcohols through Rational Ligand Design. *Angew. Chem. Int. Ed.* **2017**, *56* (15), 4272–4276.
- (27) Seyferth, D. The Grignard Reagents. *Organometallics* **1931**, *28*, 1598–1605.
- (28) Ito, S.; Zhang, C.; Hosoda, N.; Asami, M. Asymmetric Total Synthesis of (+)-Curcutetraol and (+)-Sydonol. *Tetrahedron* **2008**, *64* (42), 9879–9884.
- (29) Yajima, A.; Shirakawa, I.; Shiotani, N.; Ueda, K.; Murakawa, H.; Saito, T.; Katsuta, R.; Ishigami, K. Practical Synthesis of Aromatic Bisabolanes: Synthesis of 1,3,5-Bisabolatrien-7-ol, Peniciaculin A and B, and Hydroxysydonic Acid. *Tetrahedron* **2021**, *92*, 132253.
- (30) Bagutski, V.; French, R. M.; Aggarwal, V. K. Full Chirality Transfer in the Conversion of Secondary Alcohols into Tertiary Boronic Esters and Alcohols Using Lithiation–Borylation Reactions. *Angew. Chem. Int. Ed.* **2010**, *49* (30), 5142–5145.

- (31) Nave, S.; Sonawane, R. P.; Elford, T. G.; Aggarwal, V. K. Protodeboronation of Tertiary Boronic Esters: Asymmetric Synthesis of Tertiary Alkyl Stereogenic Centers. *J. Am. Chem. Soc.* **2010**, *132* (48), 17096–17098.
- (32) Althaus, M.; Mahmood, A.; Suárez, J. R.; Thomas, S. P.; Aggarwal, V. K. Application of the Lithiation-Borylation Reaction to the Preparation of Enantioenriched Allylic Boron Reagents and Subsequent in Situ Conversion into 1,2,4-Trisubstituted Homoallylic Alcohols with Complete Control over All Elements of Stereochemistry. *J. Am. Chem. Soc.* **2010**, *132* (11), 4025–4028.
- (33) Scott, H. K.; Aggarwal, V. K. Highly Enantioselective Synthesis of Tertiary Boronic Esters and Their Stereospecific Conversion to Other Functional Groups and Quaternary Stereocentres. *Chem. Eur. J.* **2011**, *17* (47), 13124–13132.
- (34) Zhang, C.; Ito, S.; Hosoda, N.; Asami, M. First Asymmetric Total Synthesis of (+)-Curcutetraol. *Tetrahedron Lett.* **2008**, *49* (16), 2552–2554.
- (35) Lanning, M. E.; Fletcher, S. Azodicarbonyl Dimorpholide (ADDM): An Effective, Versatile, and Water-Soluble Mitsunobu Reagent. *Tetrahedron Lett.* **2013**, *54* (35), 4624–4628.
- (36) Perali, R. S.; Mandava, S.; Chunduri, V. R. An Unexpected Migration of O-Silyl Group under Mitsunobu Reaction Conditions. *Tetrahedron Lett.* **2011**, *52* (23), 3045–3047.
- (37) Zhao, C.; Wu, M.; Huang, Z. Process for Preparing 3-Methyl-5-Methoxybenzenesulfonyl Chloride. Faming Zhuanli Shenqing: China 2017, p 11pp.
- (38) Yang, S.; Wu, C.; Ruan, M.; Yang, Y.; Zhao, Y.; Niu, J.; Yang, W.; Xu, J. Metal- and Ligand-Free Ullmann-Type C-O and C-N Coupling Reactions Promoted by Potassium Tert-Butoxide. *Tetrahedron Lett.* **2012**, *53* (33), 4288–4292.
- (39) Yang, S.; Wu, C.; Ruan, M.; Yang, Y.; Zhao, Y.; Niu, J.; Yang, W.; Xu, J. Metal- and Ligand-Free Ullmann-Type C-O and C-N Coupling Reactions Promoted by Potassium Tert-Butoxide. *Tetrahedron Lett.* **2012**, *53* (33), 4288–4292.
- (40) Yanagisawa, S.; Ueda, K.; Taniguchi, T.; Itami, K. Potassium T-Butoxide Alone Can Promote the Biaryl Coupling of Electron-Deficient Nitrogen Heterocycles and Haloarenes. *Org. Lett.* **2008**, *10* (20), 4673–4676.
- (41) Zhang, Q.; Wang, D.; Wang, X.; Ding, K. (2-Pyridyl)Acetone-Promoted Cu-Catalyzed O-Arylation of Phenols with Aryl Iodides, Bromides, and Chlorides. *J. Org. Chem.* **2009**, *74* (18), 7187–7190.
- (42) King, A. E.; Ryland, B. L.; Brunold, T. C.; Stahl, S. S. Kinetic and Spectroscopic Studies of Aerobic Copper(II)-Catalyzed Methoxylation of Arylboronic Esters and Insights into Aryl Transmetalation to Copper(II). *Organometallics* **2012**, *31* (22), 7948–7957.
- (43) Vantourout, J. C.; Miras, H. N.; Isidro-Llobet, A.; Sproules, S.; Watson, A. J. B. Spectroscopic Studies of the Chan-Lam Amination: A Mechanism-Inspired Solution to Boronic Ester Reactivity. *J. Am. Chem. Soc.* **2017**, *139* (13), 4769–4779.

- (44) King, A. E.; Brunold, T. C.; Stahl, S. S. Mechanistic Study of Copper-Catalyzed Aerobic Oxidative Coupling of Arylboronic Esters and Methanol: Insights into an Organometallic Oxidase Reaction. *J. Am. Chem. Soc.* **2009**, *131* (14), 5044–5045.
- (45) Boehlich, G. J.; de Vries, J.; Geismar, O.; Gudzuhn, M.; Streit, W. R.; Wicha, S. G.; Schützenmeister, N. Total Synthesis of Anti-MRSA Active Diorcinols and Analogues. *Chem. Eur. J.* **2020**, *26* (44), 9846–9850.
- (46) Ferreyra, S.; Bottini, R.; Fontana, A. Temperature and Light Conditions Affect Stability of Phenolic Compounds of Stored Grape Cane Extracts. *Food Chem.* **2023**, *405*, 134718.
- (47) Oliver, S.; Vittorio, O.; Cirillo, G.; Boyer, C. Enhancing the Therapeutic Effects of Polyphenols with Macromolecules. *Polym. Chem.* **2016**, *7* (8), 1529–1544.
- (48) Cao, H.; Saroglu, O.; Karadag, A.; Diaconeasa, Z.; Zoccatelli, G.; Conte-Junior, C. A.; Gonzalez-Aguilar, G. A.; Ou, J.; Bai, W.; Zamarioli, C. M.; de Freitas, L. A. P.; Shpigelman, A.; Campelo, P. H.; Capanoglu, E.; Hii, C. L.; Jafari, S. M.; Qi, Y.; Liao, P.; Wang, M.; Zou, L.; Bourke, P.; Simal-Gandara, J.; Xiao, J. Available Technologies on Improving the Stability of Polyphenols in Food Processing. *Food Front.* **2021**, *2* (2), 109–139.
- (49) Deng, J.; Yang, H.; Capanoglu, E.; Cao, H.; Xiao, J. Technological Aspects and Stability of Polyphenols. *Polyphenols: Properties, Recovery, and Applications* **2018**, 295–323.
- (50) Ghosh, A. K.; Krishnan, K. CHEMOSELECTIVE CATALYTIC HYDROGENATION OF ALKENES BY LINDLAR CATALYST. *Tetrahedron Lett.* **1998**, *39* (9), 947.
- (51) Ficker, M.; Svenningsen, S. W.; Larribeau, T.; Christensen, J. B. Inexpensive and Rapid Hydrogenation Catalyst from CuSO₄/CoCl₂ — Chemoselective Reduction of Alkenes and Alkynes in the Presence of Benzyl Protecting Groups. *Tetrahedron Lett.* **2018**, *59* (12), 1125–1129.
- (52) Iwasaki, K.; Wan, K. K.; Oppedisano, A.; Crossley, S. W. M.; Shenvi, R. A. Simple, Chemoselective Hydrogenation with Thermodynamic Stereocontrol. *J. Am. Chem. Soc.* **2014**, *136* (4), 1300–1303.
- (53) Chen, M.; Shao, C. L.; Fu, X. M.; Xu, R. F.; Zheng, J. J.; Zhao, D. L.; She, Z. G.; Wang, C. Y. Bioactive Indole Alkaloids and Phenyl Ether Derivatives from a Marine-Derived *Aspergillus* Sp. Fungus. *J. Nat. Prod.* **2013**, *76* (4), 547–553.
- (54) Ferris, A. C.; Walbot, V. Understanding *Ustilago Maydis* Infection of Multiple Maize Organs. *J. Fungi* **2021**, *7* (1), 1–9.
- (55) Wang, J.; Li, L.; Chai, R.; Zhang, Z.; Qiu, H.; Mao, X.; Hao, Z.; Wang, Y.; Sun, G. Succinyl-Proteome Profiling of *Pyricularia Oryzae*, a Devastating Phytopathogenic Fungus That Causes Rice Blast Disease. *Sci. Rep.* **2019**, *9* (1), 1–11.
- (56) Kroon, L. P. N. M.; Brouwer, H.; De Cock, A. W. A. M.; Govers, F. The Genus *Phytophthora* Anno 2012. *Phytopathology* **2012**, *102* (4), 348–364.
- (57) You, X. D.; Zhao, H.; Tojo, M. First Report of *Pythium Irregulare* Causing Damping-Off on Soybean in Japan. *Plant Dis.* **2019**, *103* (10), 2696–2696.

- (58) Arora, H.; Sharma, A.; Sharma, S.; Haron, F. F.; Gafur, A.; Sayyed, R. Z.; Datta, R. Pythium Damping-Off and Root Rot of Capsicum Annuum L.: Impacts, Diagnosis, and Management. *Microorganisms* **2021**, *9* (4), 1–17.
- (59) Kubo, Y.; Takano, Y. Dynamics of Infection-Related Morphogenesis and Pathogenesis in Colletotrichum Orbiculare. *J. Gen. Plant Pathol.* **2013**, *79* (4), 233–242.
- (60) Musso, L.; Fabbrini, A.; Dallavalle, S. Natural Compound-Derived Cytochrome Bc1 Complex Inhibitors as Antifungal Agents. *Molecules* **2020**, *25* (19), 1–28.
- (61) Anke, T.; Jürgen Hecht, H.; Schramm, G.; Steglich, W. Antibiotics from Basidiomycetes. Ix) Oudemansin, an Antifungal Antibiotic from Oudemansiella Mucida (Schrader Ex Fr.) Hoehnel (Agaricales). *J. Antibiot. (Tokyo)* **1979**, *32* (11), 1112–1117.
- (62) Ypema, H. L.; Gold, R. E. Kresoxim - Methyl: Modification of a Naturally Occurring Compound to Produce a New Fungicide. *Plant Dis.* **1999**, *83* (1), 4–19.

Chapter 3: Progress Towards the Total Synthesis of 4-hydroxypyridinones

Disclaimer: Work on this project was completed in conjunction with Ricardo Cruz. Adrian Demeritte conceptualized the project. Ricardo Cruz aided in the synthesis of the western fragments of these 4-hydroxypyridinones with guidance from Adrian Demeritte. Coupling conditions of the pyridinone and western fragments were also discussed and completed in conjunction with Ricardo Cruz, though Ricardo Cruz performed said coupling reactions. Synthesis of pyridinone cores, pyran intermediates, C-3 functionalization and chimera studies were conceptualized by and performed by Adrian Demeritte.

3.1 Introduction

3.1.1 Silent Killers

Fungi are everywhere. From the hard-to-reach corners in homes, to the leaves on the trees that line one's daily route to work, and even down to the first deep breath after waking up in the morning; everyone is constantly inhaling fungal spores. It's estimated that humans inhale 1000 to 10 billion vegetative spores on a daily basis.¹ For some, these ubiquitous aeroallergens pose little threat at all, while millions of others develop pulmonary and nasal allergies to these airborne fungal particles. To those with weakened immune systems, however, much deadlier complications may arise.

One of the most abundant genera in this cocktail of mold conidia is *Aspergillus*, with *Aspergillus fumigatus* being most ubiquitous fungal species within the environment.² The survivability of *A. fumigatus* cannot be understated. This species thrives in conditions with a wide range of pH or temperature and can even tolerate dehydration or freezing for long periods of time. Moreover, conidia from this species can be dispersed by even slight air currents due to their size

and weight, all while being protected from ultraviolet irradiation due to the melanin in their cell wall.³ It should then come as no surprise that this species is the most predominant cause of mold infections in humans.² Although conidia can be easily cleared by counteracting host mechanisms in the lung, *A. fumigatus* possesses a large arsenal to complicate this process. For example, once inside the respiratory tract mucociliary clearance is avoided due to the miniscule size of the conidia of *A. fumigatus*, while melanin in the cell wall garners resistance to reactive oxygen species and destruction by host cells.⁴ Additionally, exposed negatively charged sialic acid on conidia contribute to pathogenicity by enhancing adhesion to basal lamina proteins and therefore improve rates of infection.⁵ It's therefore easy to see how *A. fumigatus* can cause issues for the immunocompetent, while being deadly to the immunocompromised.

Invasive pulmonary aspergillosis (IPA) is a deadly fungal infection towards immunocompromised individuals primarily caused by indoor pathogen *A. fumigatus*. Because this fungus is ubiquitous, individuals in hospitals are particularly at risk and there are an estimated 200,000 cases of IPA each year. Realistically, however, some experts believe that this is an underestimate.⁶ Indeed, IPA is a major contributor to morbidity and mortality in this population. Strikingly, even improvements in sanitization with the recent COVID-19 pandemic have not quelled these numbers as IPA has also been recognized as a severe complication of SARS-CoV-2 infection in ICU patients, affecting 18%–39% of cases and resulting in a mortality rate of up to 50%.^{7–10} Unfortunately, these numbers become even more daunting in regards to leukemia patients who boast a 80-90% mortality rate when complications with IPA are involved.¹¹ It's no wonder then that both the CDC and WHO have designated *A. fumigatus* as high priority health concerns due to various factors, including global mortality rates, diagnostic availability, and reports of antifungal resistance.¹²

3.1.2 The Current Toolbox has Redundant Tools

Aspergilloma is currently treated with commonly prescribed azoles which target the *cyp51A* gene, interrupt ergosterol biosynthesis, promote the accumulation of 14a-methylsterols and consequently impair fungal growth through altered cell permeability and stability. Though in some cases mortality rates have been brought down to 30% or lower, environmental effects ensure that invasive aspergilloma still boasts a strikingly high mortality rate.¹³ For instance extensive use of azoles in various fields such as agriculture, industry, and clinics has created selective pressure and allowed the emergence of azole-resistant *A. fumigatus* in various environments.¹⁴ Frighteningly, azole-resistant invasive aspergillosis can be caused in patients who have never taken azoles if they come into contact with resistant spores. This is further exacerbated by the presence of azole resistant strains carrying *cyp51* or TR₃₄/L98H mutations resulting in mortality rates of up to 88% and, according to all studies to date, full treatment failure.¹⁵ Thus, there is a dire need for small molecules with novel mechanisms of action to serve as chemical probes towards combating this prevalent deadly opportunistic pathogen.

3.1.3 4-Hydroxypyridinones may provide alternative mechanisms for tackling this issue

A lesser explored strategy for targeting fungal machinery revolves around inhibiting the cytochrome *bc*₁ Q_i site. As cytochrome c is a ubiquitous protein present across all kingdoms of life one could easily identify how concerns of selectivity may arise.¹⁶ Ilicicolin H (**3.1**) is a 4-hydroxy-2-pyridinone originally isolated from the ascomycete *Cylindrocladium ilicicola* and exhibited potent broad spectrum antifungal activity towards various pathogens, namely one *A. fumigatus* (0.08 µg/mL).¹⁷ The biological mechanism of action was ultimately determined to be highly kingdom-selective inhibition fungal oxidoreductase, specifically the Q_i site of the mitochondrial cyt *bc*₁ reductase. Remarkably, **3.1** demonstrated 1000-fold selectivity for fungal versus

mammalian cytochrome.¹⁸ Antimycin, a natural product from various species of *Streptomyces*, is a known potent inhibitor of the Q_i site of the mitochondrial cyt *bc*₁ reductase. In fact, antimycin stoichiometrically binds to isolated cytochrome from fungi, mammals, and bacteria. Previous studies have confirmed this preference for binding fungal enzyme and indicated that there are sufficient structural differences between fungal, bacterial, and mammalian center Q_i sites to permit drug design toward a single essential enzyme target, thereby minimizing the likelihood of side effects.¹⁹

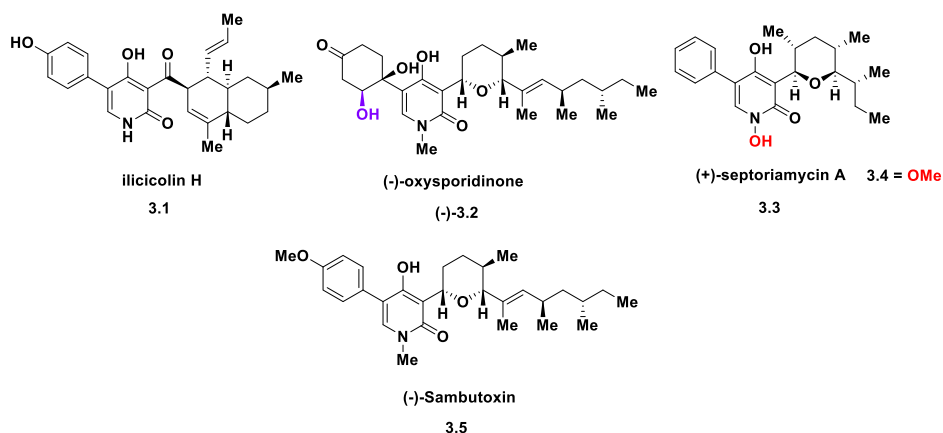


Figure 3.1: Structures of target 4-hydroxypyridinones.

Towards this end, computational binding studies of ilicicolin H using a homology model with antimycin as the native inhibitor were conducted and showed a few significant differences. Most notably, overlay of ilicicolin H indicated that the structural requirement for the observed antifungal activity involved the 5-aryl-4-hydroxy-2-pyridone buried deep in the binding pocket with the lipophilic right-hand side outside of the binding pocket and towards the lipid bilayer.¹⁸ The homology model suggested that the binding mode of ilicicolin H has some similarities but also differences relative to antimycin binding. This provides valuable insight to SAR and fungal specificity of ilicicolin H, demonstrating that small perturbations in the structure may alter species selectivity.

Similar hydroxypyridones like (-)-sambuxtoin (**3.5**) were found to strongly inhibit both succinate and NADH cytochrome c oxidoreductase, as well as DHQ oxidase, at very low concentrations and must therefore bind at either cytochrome b or c1.^{20,21} Still, biological testing of **3.5** against microbes of interest remain largely unexplored. A related 4-hydroxy-2-pyridinone, (-)-oxysporidinone (**3.2**), was found to possess potent activity towards and found to have low $\mu\text{g/mL}$ MIC values against a range of agriculturally relevant fungi, particularly *A. fumigatus* ($\text{IC}_{50} = 2 \mu\text{g/mL}$). Interestingly, its epimer (purple) possesses an 18-fold decrease in activity towards this pathogen (**Figure 3.1**).^{22,23} Not only does this hint that this stereocenter is critical to the activity of oxysporidinone, but this also indicates the left side of the molecule could be the pharmacophore in the hypothetical binding pocket of the unknown target. Based on the chemical homology, I hypothesize that oxysporidinone, along with other closely related 4-hydroxypyridinones, act as Q_i inhibitors.

Though these 4-hydroxypyridones target fungi due to limited testing in the literature, I hypothesize that there may be a facile way to change kingdom selectivity towards bacteria due to the slight differences in the cytochrome bc_1 binding pockets. For instance, the *N*-hydroxylated pyridone septoriamycin A (**3.3**), isolated from the ascomycete *Septoria pistaciarum*, was found to have a broad spectrum of anticancer, antibiotic, antiplasmodial, and antifungal activities.^{24,25} Compound **3.3** was found to have promising IC_{50} values against *C. albicans* ($12.07 \mu\text{g/mL}$) and *A. fumigatus* ($8.76 \mu\text{g/mL}$), whereas values greater than $20 \mu\text{g/mL}$ were observed against both *Staphylococcus aureus* and MRSA. Interestingly, the *O*-methyl analog of compound **3.3** (**3.4**) was found to have values greater than $20 \mu\text{g/mL}$ against *C. albicans* and *A. fumigatus*, whereas *S. aureus* and MRSA had IC_{50} values of 2.99 and $5.00 \mu\text{g/mL}$. Although the biological mechanism of action of compounds **3.3** and **3.4** remain unelucidated, it is reasonable to hypothesize it is similar

to that of compounds **3.1** and **3.5** based on structural similarity. Combined with the finding of activity-switching following methylation of the *N*-hydroxyl of compound **3.3**, this seems to suggest a chemically facile method for tuning mitochondrial cytochrome selectivity from one microbial kingdom to another. Taken together, I hypothesize that these 4-hydroxypyridinones may be acting in a similar manner, and through leveraging diverted total synthesis, could yield important chemical tools for developing potent cyt *bc*₁ reductase inhibitors of and other important pathogens.

3.2 Results and Discussion

To me, the important facet of these molecules is their potential ability to function in the same binding pocket without having putative motifs necessary for binding. As indicated by Singh and coauthors, the lipophilic side of ilicicolin H the molecule hangs outside of the binding pocket, leading me to hypothesize if alterations to the pyran rings of this family of molecules would greatly alter activity.¹⁸ Preliminary binding studies were conducted in bovine and bacterial cytochrome *bc*₁ reductase to examine how slight structural modifications in ilicicolin H, sambutoxin, septoriamycin A, and oxysporidinone affect overall binding relative to a known cytochrome inhibitor, antimycin A. Results of pyran methylation, N-functionalization through methylation, hydroxylation or methoxylation, and modification of pyran orientation confirmed that slight modification in structure could tune activity and in some cases completely change the orientation of the pyridinone in the binding pocket. More specifically, findings confirmed that while the aliphatic region lacks importance for binding, the stereochemical configurations within the tetrahydropyran ring and the methyl substitution pattern are crucial. In some cases, changing either of these two variables could dramatically affect how these molecules sit within the binding pocket; giving further credence to the potential to produce derivatives with a ‘kingdom switch’. Based on

these results, we sought to develop a highly divergent synthetic strategy to access the various pyridinone scaffolds of interest.

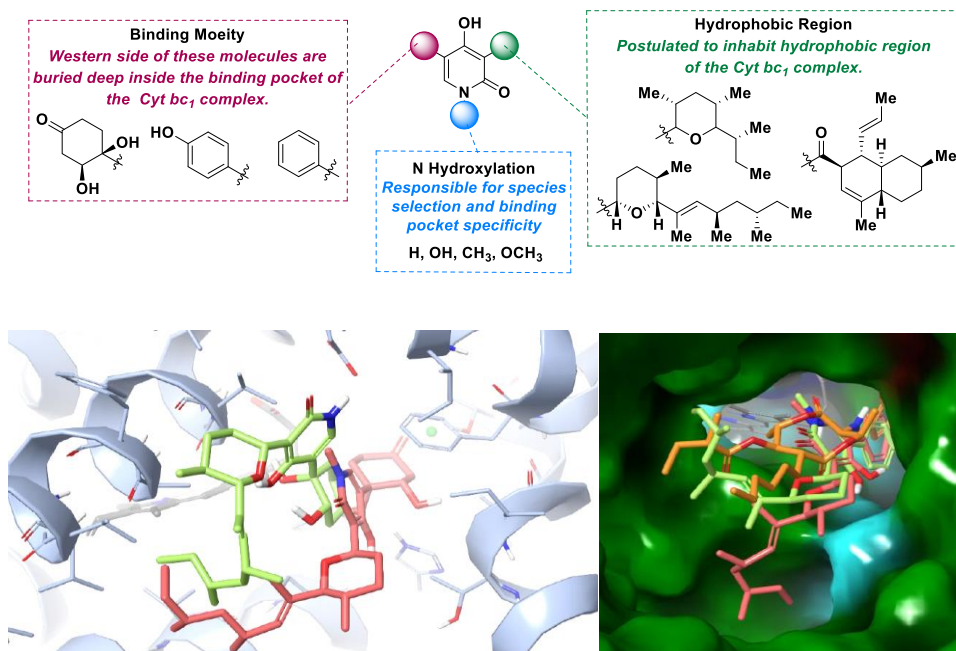


Figure 3.2: (Top) SAR map of related 4-hydroxysporidinone motifs compared to that of iliciolin H. (Bottom) Molecular docking of N-functionalized oxysporidinone in *Rhodobacter sphaeroides* cyt bc₁ Q_i site. Hydroxylation (red molecule, left image) changes the conformation of oxysporidinone (unfunctionalized, green, left image) in binding pocket and reduces docking score in bovine while increasing docking score in bacteria. Flipping the pyran ring provides better access to hydrophobic pocket near lipophilic region (red molecule is pyran flipped, right image).

Retrosynthetically, I first envisioned synthesizing a highly functionalized pyridinone ring through a Vilsmeier cyclization. It should be noted that C-H functionalization of pyridine rings at the C-4 position is difficult, and therefore either interconversion from another group or direct installation of the heteroatom or functional group of interest is required for facile synthesis. Importantly, N-functionalization could vary before intramolecular cyclization depending on the analog of interest (**Figure 3.2**, top). The pyridinone reactivity could then be leveraged through sequential functionalization at C-5 position with aryl or vinyl boronic acid of choice, followed by enantioselective alkylation with a deactivated Grignard reagent at the C-3 aldehyde to provide a secondary aryl alcohol with high selectivity. Use of the appropriate ligand here is crucial, though

enantiomeric enrichment with Birman's catalyst could occur if necessary as enantiopure material is required to limit production of diastereomers during the rhenium catalyzed Prins cyclization. I envision that this reaction will set all stereocenters on the pyran ring in facile manner. It should be noted that the stereochemistry of the alkyl chain of (-)-oxysporidinone is unknown, hence I seek to utilize an iterative, reagent controlled homologation sequence employing chiral stannanes to allow for quick access to any combination of the stereogenic centers to establish the correct structure of (-)-oxysporidinone. Barton-McCombie deoxygenation, followed by deprotection with mild acid, then selective demethylation with DABCO should furnish pyridinone of choice, but below the aforementioned is mapped on to oxysporidinone.

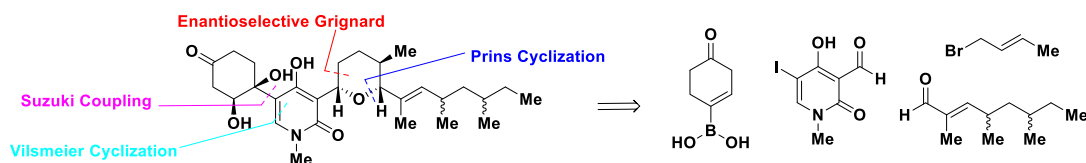
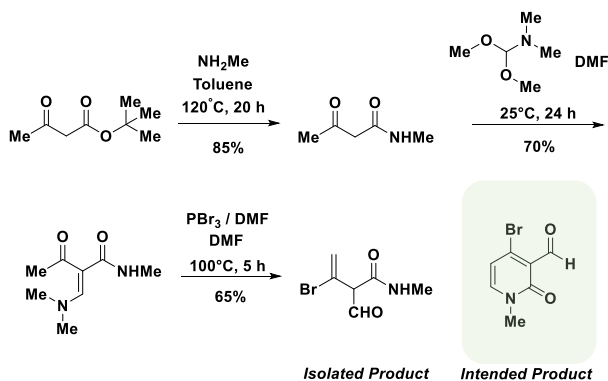


Figure 3.3: Retrosynthetic breakdown of one of the long term targets of this project 3.2.

3.2.1 Synthesis of Pyridinone Core

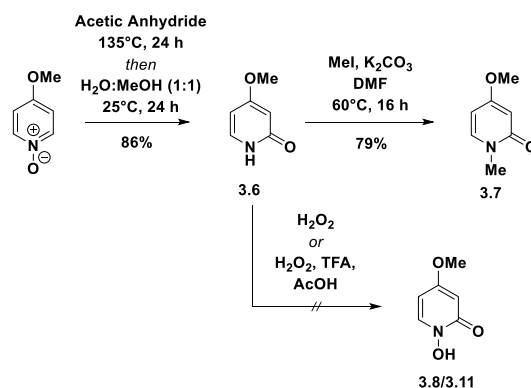
Initial attempts to produce the central highly functionalized 2-pyridinone fragment involved reaction of a β -keto amide with N,N-dimethylformamide dimethyl acetal to afford the corresponding enaminone. Though the Vilsmeier cyclization of this reagent was an attractive method to quickly access the 2-pyridinone core bearing functional handles, only product attributing to a single Vilsmeier reaction was recovered even after prolonged reaction times (**Scheme 3.1**). Unfortunately, this reaction was attempted with both PBr_3 and POCl_3 and yielded little to no intended product. Presumably, this is due to the altered electronics of the enaminone as this reaction is primarily with aryl substituted amides.²⁶



Scheme 3.1: Synthesis of pyridinone core through Vilsmeier cyclization.

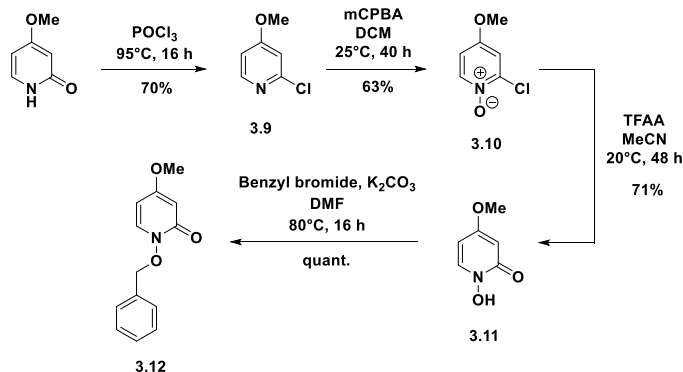
There were a few distinct issues with this strategy. First, displacement of the halogen in the 4 position could be difficult as strongly basic conditions are required which may be incompatible with the aldehyde at the 2 position. Second, this method doesn't allow for the synthesis of N-hydroxylated intermediates in a diverted manner as N-functionalization occurs at amidation step, requiring parallel syntheses for analog development.

With this in mind, I opted to employ a modular route towards the synthesis of the pyridinone core. I found that the central ring can be synthesized in good yield by remote oxidation and rearrangement of pyridine N-oxide with acetic anhydride, followed by tautomerization to the corresponding pyridinone in water to give pyridinone **3.6**. For the N-methylated targets and analogs, subsequent methylation with methyl iodide gives the dimethylated pyridinone core **3.7**. It should be noted that aqueous workup should be avoided for either of these steps due to the polarity of the pyridinone product. For the N-hydroxylated analogs, initial attempts to use H₂O₂ directly on the free nitrogen of the pyridinone gave no discernable product. Attempts to hydroxylate prophetically with acetic acid and TFA as additives were also largely unsuccessful. Presumably in the case of the latter, only TFA salts of **3.6** were formed.



Scheme 3.2: Synthesis of methylated pyridinone core with failed conditions for hydroxylated variant.

Due to the significant hazards associated with this reaction, I proposed a safer but slightly longer route. 2-chloro-4-methoxypyridine could be synthesized directly from **3.6** in heated neat reaction with POCl_3 to give halogenated pyridine **3.9**. Oxidation with mCPBA furnished the corresponding N-oxide **3.10** in modest yield. Increasing equivalents of mCPBA or increasing reaction times did not improve product yields. It should be noted that this product tarnishes quickly to a brown viscous liquid in air or light, and therefore should either be used immediately or stored appropriately in a freezer. Oxidation and rearrangement of the chlorinated pyridine N-oxide using TFAA gives the hydroxylated pyridinone **3.11** in modest yield. Several things should be noted for this reaction. First, the reaction should be completed in aluminum foil to prevent degradation of the starting material. Next, the addition of solid sodium bicarbonate followed by methanol addition is essential for quenching as addition of saturated sodium bicarbonate, followed by extraction with DCM, leads to full loss of starting material to the aqueous layer. Subsequent benzylation with benzyl bromide gives the benzyl protected hydroxylated pyridinone **3.12** in good yield.



Scheme 3.3: Synthesis of N-hydroxylated pyridinone core.

At this point I sought to leverage the reactivity of the pyridinone ring for selective functionalization. I envisioned utilizing a dihalogenation strategy for a selective Suzuki-Miyaura reaction at the iodine on the C-5 position towards accessing septoriamycin (phenyl), sambutoxin (4-methoxyphenyl), and oxysporidinone (cyclohexenone). The bromine on C-3 could be used in a selective Grignard reaction with a homoallylic aldehyde to produce a homoallylic alcohol primed for a Prins cyclization, setting all stereocenters in a facile manner.

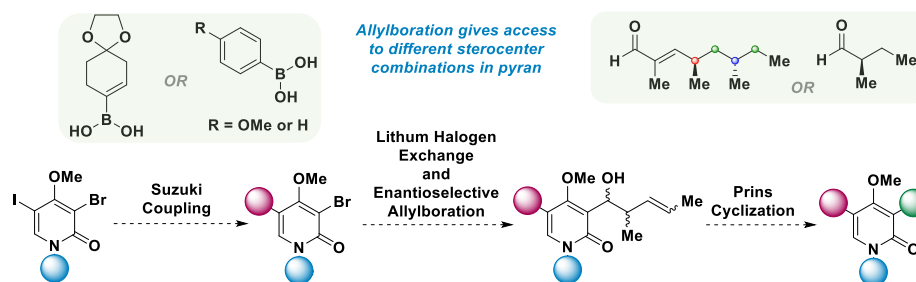
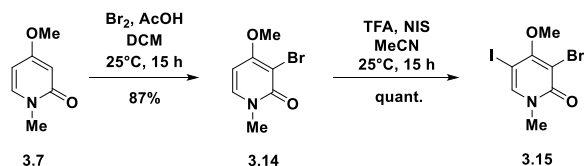


Figure 3.4: Breakdown of synthetic strategy using a dihalogenated pyridinone.

Bromination of **3.7** in a 4:1 solution of DCM: AcOH gave monobrominated product **3.14** in 87% yield. I should note that this reaction should not be ran longer than 24 hours as dibrominated byproduct **3.13** is produced as reaction time increases. Percentages of this dibrominated byproduct can be as high as 30% after 48 hours. Additionally, care should be taken when removing excess bromine on the rotovap as increased temperatures can greatly increase the production of this dibrominated product. From here, regioselective iodination with NIS then cleanly furnishes the

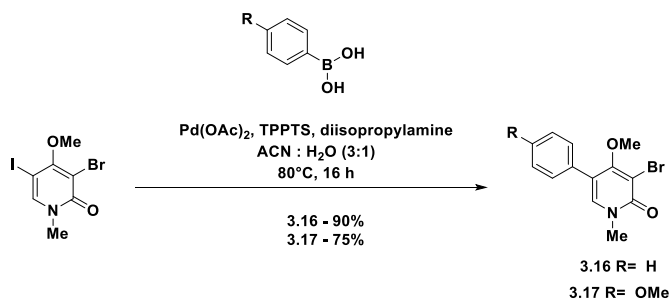
highly functionalized pyridinone central ring. In a similar manner, regioselective bromination with NBS followed by iodination with NIS can quickly furnished the pyridinone core for the hydroxylated analogs.



Scheme 3.4: Regioselective halogenation of pyridinone core.

3.2.2 Coupling of Western Fragments

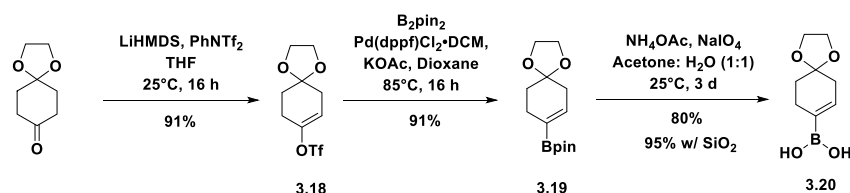
With the pyridinone cores in hand, we began scouting conditions for coupling the western fragments of our target molecules. Gratifyingly, standard Suzuki-Miyaura coupling conditions efficiently gave access to the septoriamycin (**3.3**, **3.4**) and sambutoxin (**3.5**) core scaffolds at the C-5 iodine using commercially available arylboronic acids. As the boronic acid needed for synthesis of the western fragment of oxysporidinone is commercially unavailable, we sought to make it.



Scheme 3.5: Suzuki Miyuara of standard aryl boronic acids.

Commercially available monoprotected 1,4-cyclohexanedione was converted to vinyl triflate **3.18** in the presence of phenyltriflimide in 91% yield. Miyaura borylation under standard conditions gives vinyl boronate **3.19**. Coupling of this boronate to the functionalized Bpin was unsuccessful using a variety of solvents, palladium sources and ligands. Hydrolysis of the Bpin to

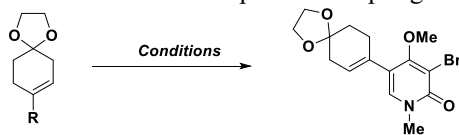
the more reactive boronic acid was possible, but a method inclusive of preserving the acetal protecting group was necessary. Conversion with sodium periodate was slow but garnered the intended boronic acid in good yield. We assumed there might be a good way speed up this reaction, assuming that slower conversion rates were due to the heterogenous nature of the reaction. We found that silica could be used as a solid support for sodium periodate to improve reaction times by increasing surface area and dispersion of the reagent.



Scheme 3.6: Synthetic route to the boronic ester coupling partner towards synthesis of **3.2**.

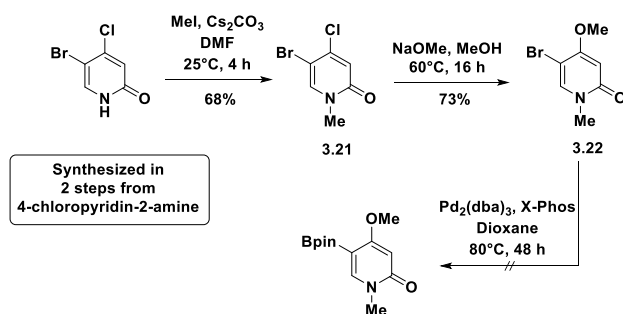
Using this method, though **3.20** could be quantitatively produced in less than 16 hours on small scale this result transferred poorly upon scale up. All attempts to couple this boronic acid were also unsuccessful and, in many cases, the deiodinated product at the C-5 position was isolated as a byproduct.

Table 3.1: Suzuki conditions attempted for coupling of **3.20** towards **3.2**.



| Entry | Organoboron | Pd Source | Base | Ligand | Solvent | Temperature | Product |
|-------|--------------------|---|---------------------------------|-------------------------|---------------------------|-------------|---------|
| 1 | Bpin | Pd(OAc) ₂ | DIPA | TPPTS, PPh ₃ | MeCN:H ₂ O | 80°C | - |
| 2 | B(OH) ₂ | Pd(OAc) ₂ | DIPA | TPPTS, PPh ₃ | MeCN:H ₂ O | 80°C | - |
| 3 | Bpin | Pd(OAc) ₂ | DIPA | TPPTS | MeCN:H ₂ O | 80°C | - |
| 4 | B(OH) ₂ | Pd(OAc) ₂ | DIPA | TPPTS | MeCN:H ₂ O | 80°C | - |
| 5 | Bpin | Pd(PPh ₃) ₄ | Na ₂ CO ₃ | - | dioxane:H ₂ O | 100°C | Trace |
| 6 | B(OH) ₂ | Pd(PPh ₃) ₄ | Na ₂ CO ₃ | - | dioxane: H ₂ O | 100°C | Trace |
| 7 | Bpin | Pd(OAc) ₂ | K ₂ CO ₃ | PPh ₃ | toluene : EtOH | 100°C | Trace |
| 8 | B(OH) ₂ | Pd(PPh ₃)Cl ₂ | K ₂ CO ₃ | - | DMF | 80°C | - |
| 9 | B(OH) ₂ | Pd(PPh ₃)Cl ₂ ·DCM | Na ₂ CO ₃ | - | dioxane:H ₂ O | 80°C | - |

We reasoned that our lack of success in coupling this fragment may be due to the methoxy substituent on C-4 sterically blocking addition to C-5. To test this, successful reaction conditions for commercially available boronic acids were tested on 4-chloropyridinone **3.21** reasoning that a smaller ortho substituent could boost conversion to the desired product. This chlorine could then easily be converted to the desired methoxy substituent via S_NAr . Unfortunately, this pivot also failed to produce any coupled species, indicating that the lack of reactivity could stem from electronic rather than steric factors. We also attempted to produce boronate species of the pyridinone core however final Miyaura borylation was unsuccessful.



Scheme 3.7: Synthetic route towards 'Bpin swapped' coupling reaction.

3.2.3 C-3 Functionalization

3.2.3.1 Metalation then Insertion into Electrophiles

With the western fragments for both septoriamycin and sambutoxin in hand we focused our effort on C-3 functionalization through a metalation strategy. I envisioned accessing a benzylic ketone through metalation a subsequent reaction with an electrophile of choice. Weinreb amide **3.24** was used as the initial coupling partner and was synthesized in 37% yield over two steps. Initial attempts to metalate with isopropyl magnesium bromide and *n*-BuLi on **3.7**, **3.16** and **3.17** were largely unsuccessful and returned inseparable mixtures of starting materials and protodebrominated products. As lithiation with *n*-BuLi required lower temperatures to prevent side

reactions, I wondered if incorporating a more selective metalating reagent would aide in full conversion of the brominated starting material. Knochel and coworkers found that the use of salt additives improved both the rate and efficiency of metalation, and upon switching to TurboGrignard saw full conversion of the starting material to protodehalogenated **3.26**.²⁷

Table 3.2: Grouped conditions for metalation towards synthesis of homoallylic alcohols. No conditions gave discernable product.

| Parameter | Pyridinone (EQ) | Coupling Partner | Metalating Reagent (EQ) | Metalation Time /Temp | Temperature/ Reaction Time | Result |
|------------|--------------------|--|--|-----------------------|------------------------------|--|
| Conditions | 3.14, 3.16 or 3.17 | Weinreb Amide, Acyl chloride, Aldehyde | TurboGrignard, Irosopyl magnesium bromide, <i>n</i> -BuLi, Activated Zinc, | 30 min to 1 hr | -78°C to rt 30 min to o/n | Protodehalogenation, Ethoxide Elimination or no reaction |

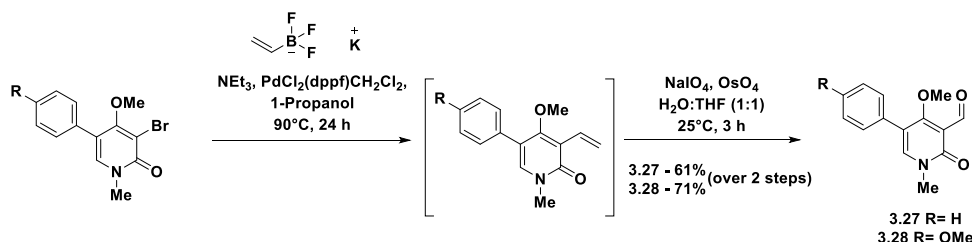
Though I had achieved full conversion of the starting material, I wanted to investigate the cause for protodebromination rather than insertion into the Weinreb electrophile. A D₂O quench of the reaction indicated that protodebromination occurs during the reaction and not during the workup. I hypothesized that this observation stemmed from incompatibility of with coupling partner. I assumed this was due to preferential deprotonation at the alpha position of the Weinreb, which is, likely further preferred by the steric bulk of the incoming metalated pyridinone. A closer inspection of observed byproducts revealed that an amide byproduct **3.25** was present in all crude mixtures with the Weinreb amide. This was further confirmed through LCMS analysis. This amide byproduct can be formed when a highly basic or sterically hindered nucleophiles prefers to

deprotonate at the methoxide moiety on the Weinreb amide, followed by elimination to release formaldehyde and the amide byproduct. With this in mind, I attempted to improve the reactivity of the coupling partner by utilizing the acyl chloride or aldehyde of **3.24**. Unfortunately, neither of these partners appreciably improved yields and protodebrominated starting material was universally the major byproduct presumably due to the *alpha*-deprotonation previously mentioned. A modified Negishi coupling was attempted using freshly activated zinc however only starting material returned was returned and so this route was quickly abandoned. I hypothesized that some combination of the aforementioned substrate issues were responsible and sought other coupling partners. Using DMF to trap the metalated intermediate towards converting the C-3 functional group to an aldehyde finally resulted in an isolatable product, albeit in very low yield. A closer inspection of the literature indicated that protodehalogenation could also result from deprotonation at the pyridinone methyl. Though, this deprotonation could be controlled with temperature, metalation would also suffer given results from previous experiments. Given the various potential sites of deprotonation, perceived bulkiness of the incoming nucleophile, issues in metalation at lower temperatures, issues with coelution during purification and incompatibility with various coupling partners I opted to find a more efficient route to formylate the C-3 site.

3.2.3.2 Suzuki Oxidative Cleavage Tandem

Further analysis of the byproducts from the Suzuki-Miyaura couplings on the septoriamycin and sambutoxin scaffolds revealed a byproduct, coupled at both the C-5 and C-3 positions. Given this side product I hypothesized that a cross coupling strategy could circumvent side reactions present with the metalation strategies previous mentioned. I envisioned formylating the C-3 position of these scaffolds through Suzuki-Miyaura coupling with vinyltrifluoroborate, followed by oxidative cleavage of the pendant alkene. Serendipitously, Suzuki-Miyaura coupling

with vinyltrifluoroboronate for one hour, followed by oxidative cleavage with osmium tetroxide and sodium periodate for 3 hours furnished intended aldehyde in good yield. Importantly the remaining mass balance composed of the starting aryl bromide as opposed to protodebromination as previously seen. As recovery of starting material was a result of incomplete coupling, extending reaction times to 24 hours followed by a slightly longer oxidative cleavage showed complete conversion to the formylated **3.27** or **3.28** in both cases. Isolated yields were notably lower, presumably due to potential loss of material during work up, though TLC shows spot to spot conversion.

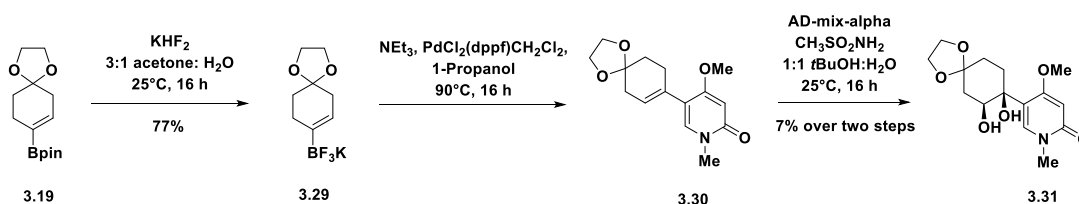


Scheme 3.8: Suzuki Oxidative Cleavage tandem for formylation of pyridinone at C-3.

3.2.4. Revisiting the Oxysporidinone Western Fragment

Successful results from the C-3 Suzuki oxidative cleavage experiments prompted us to revisit the oxysporidinone western scaffold. We proposed that use of a trifluoroborate salt could circumvent issues with reactivity here, accommodating for electronic issues seen previously with this fragment. Treatment of **3.20** with KHF_2 gave the desired trifluoroborate salt **3.29**, in moderate yield, with extraction with boiling acetonitrile greatly improving yields. Reaction of trifluoroborate salt **3.29** with dihalogenated pyridinone **3.15** yielded equal portions of intended product, protodehalogenated (indicating insertion into palladium but potential elimination by some proton source in the reaction) and starting material. We reasoned performing the next step in the reaction, namely an asymmetric dihydroxylation, could increase the polarity of intended product, making it

separable from the crude mixture. Standard asymmetric dihydroxylation of this crude mixture using additive methanesulfonamide gave good conversion to the desired diol **3.31** by LC-MS and HRMS analysis, but isolated yields were poor. Efforts in the immediate future are currently ongoing to improve these yields for future C-3 functionalization.



Scheme 3.9: Coupling of trifluoroborate salt **3.29** towards the western fragment of **3.2**.

3.2.5 Ongoing strategies for Allylboration Towards Homoallylic Alcohols

With formylated fragments in hand we then focused our attention towards forming the homoallylic alcohol necessary for the Prins cyclization. It was also at this point that I started to take interest in tandem reactions to achieve this transformation.²⁸ Initially, I envisioned synthesizing the homoallylic alcohol in a facile manner through 3,3-sigmatropic rearrangement proposed by Ramachandran and coauthors.²⁹ Importantly, Ramachandran notes that both temperature and equivalents of aldehyde are crucial for this reaction. With one equivalent of the aldehyde at -78°C typical crotylboration occurs, but with a slight excess of aldehyde at room temperature a [3,3]-sigmatropic rearrangement occurs to give homoallylic alcohol of choice (**Figure 3.5**). I hypothesized that this reaction could be beneficial for generating methylated derivatives at both sites indicated on the pyran, allowing for facile analog synthesis. It should also be noted that Ramachandran has another method where pyrans could directly be synthesized through a one-pot allyl-/crotylboration-Prins cyclization which could also prove to be useful in towards analog development.³⁰

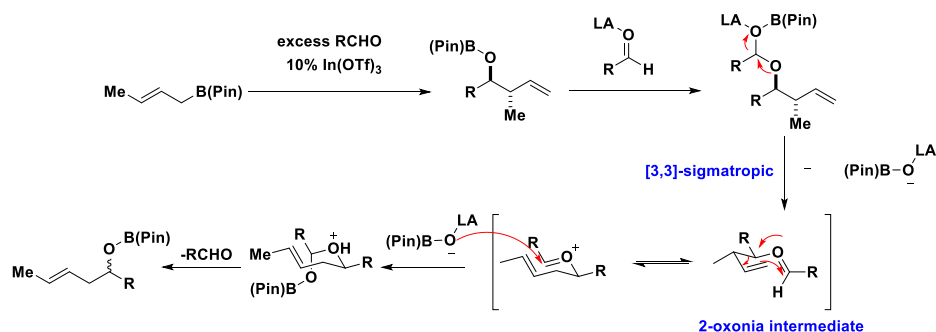
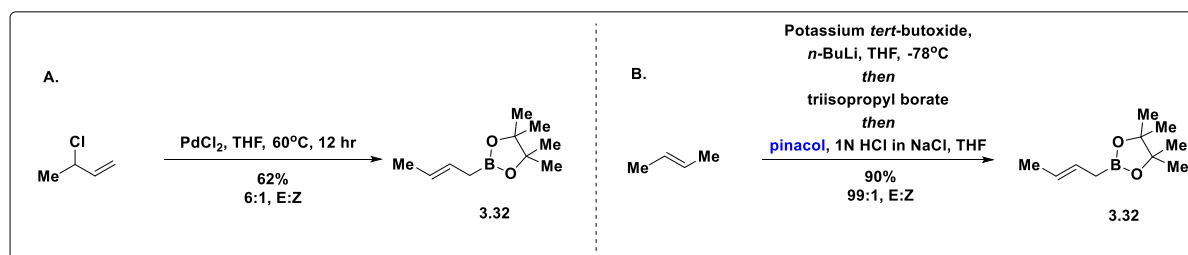


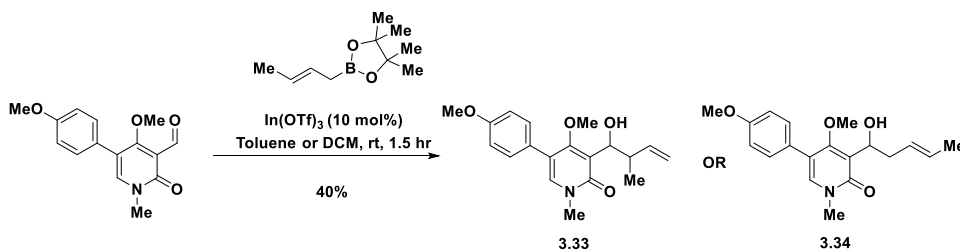
Figure 3.5: Ramachandran's [3,3]-sigmatropic rearrangement in the presence of excess aldehyde to give homoallylic alcohols.

Initial attempts to selectively produce the *trans*-crotylboronic acid pinacol ester **3.32** were unsuccessful as mixtures of both the *E* and *Z* alkenes could be seen by ^1H NMR. Preparing this reagent from *trans* butene instead yielded only the *trans* product **3.32**. Importantly, this provides modularity as workup with a bulkier pinacol could provide an avenue of selectivity by way of more widely used crotylation methods (Roush, Leighton, etc.).



Scheme 3.10: Reactions towards synthesizing boronic ester **3.32**.

With this reagent in hand, I carried out the borylation using conditions described by Ramachandran and only recovered crotylation product **3.33**. As coordination of the boronate species to the aldehyde is required for this transformation, I reasoned that the aldehyde's limited solubility in toluene may be hindering the crucial step. Rerunning these conditions in both acetonitrile and DCM still yielded solely crotylation product. Given issues with this method I opted to directly synthesize a chiral boronic ester to generate enantioenriched homoallylic alcohols as future synthetic plans involved a stereoselective rearrangement.



Scheme 3.11: Conditions for [3,3] sigmatropic rearrangement to homoallylic alcohol **3.34**.

It should be noted that crotylboration here can still be leveraged through cross metathesis to access functionalized crotyl groups towards the synthesis of septoriamycin A analogs. In 2010, Roush and Chen described an eloquent method to selectively allylborylate aldehydes through chiral transfer from a known chiral borylate.³¹ Specifically, Roush and Chen describe how selectivity is achieved by avoiding a less preferred pseudo axial positioning of the alpha substituent mediated by BF₃•Et₂O, promoting E over Z selectivity. Currently, both enantiomers of allylboronate indicated are being synthesized for use in such reactions.

3.2.6 Chimera Compounds

In an effort to fully explore the three-dimensional space of this binding pocket I also proposed synthesizing simplified mimics of ilicicolin H. As said before, this natural product is known to be a potent inhibitor of the Q_i site of the cytochrome *bc*₁ complex and possesses broad spectrum antifungal activity. Though this compound has been synthesized before, it's synthesis was lengthy and relied upon an aldol condensation-dehydration with a highly functionalized aldehyde coupling partner followed by a Diels-Alder cycloaddition towards the finished ilicicolin H scaffold.³² Given my hypothesis that the functionality on the eastern fragment of these pyridinones should not greatly alter activity, I sought to produce compounds which mimics ilicicolin H's scaffold in a synthetically facile manner. Moreover, I desired to leverage the

reactivity of the aldehyde intermediate already synthesized towards their production in a diverted manner.

To maximize the potential for success I wanted to further refine design of the simplified decalin based on the scaffolds of other bioactive small molecules. Survey of the literature shows a surplus of pyridinone containing natural products with decalin moieties incorporating the C-4 oxygen.^{33–36} Though many of them have not been synthesized, compounds which have been made struggle with selectivity issues in their routes and have often required complex coupling partners much like ilicicolin H. Thankfully, some require commercially available natural products as starting points allowing for ease of synthesis due to chiral pool availability, however, in many cases opposite enantiomers of those natural products are not commercially available and therefore require increased synthetic effort. As an expansion to these polycyclic pyridinone natural products, Kamauchi and coauthors found that some polycyclic chromene derivatives greatly inhibited hyphal and biofilm formation in *C. albicans*.³⁷ Taken together, I questioned whether a simplified chromene like moiety attached to the C-3 position of the pyridinone ring could mimic the ilicicolin H scaffold.

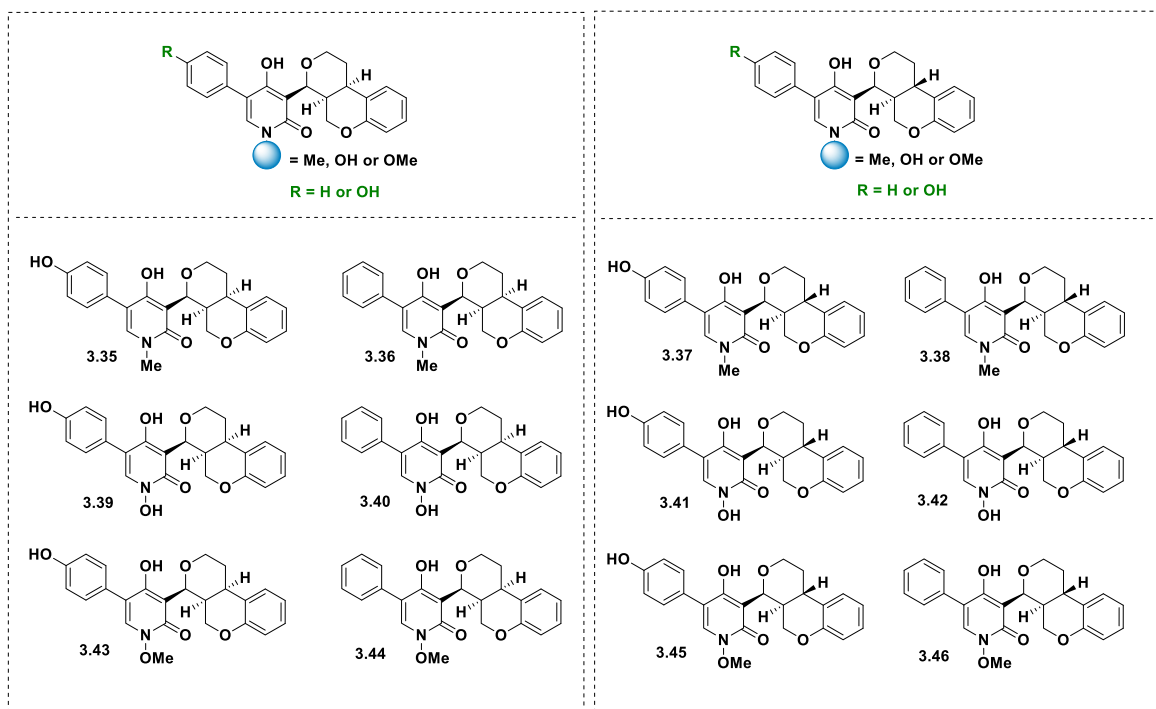


Figure 3.6: Structures of docked polycyclic chromene pyridinones.

I hypothesized that by leveraging the aldehyde of intermediates like **3.27** or **3.28**, a Prins cyclization could occur without the need for stereoselective functionalization, as stereochemistry would be directed by the alkene of the incoming group. Such linked polycyclic pyridinone compounds have yet to be seen in the literature and could possess unknown activity beyond the potential of mimicking the ilicicolin H scaffold. An additional benefit to this strategy would be the potential to produce a novel chimeric-like compound. Interest in the design of hybrid bifunctional compounds (chimeras) has improved in recent years and involves the merging the pharmacophores of active molecules with different mechanisms of action to simultaneously inhibit multiple targets thereby improving bioactivity through a combination approach.^{38,39} This method also aids in lowering the risk of resistance due to the multiple mechanisms of action for these compounds. A few examples of these dual active have already been produced and have seen some success in antifungal compounds, even though this concept is relatively new.^{40–43}

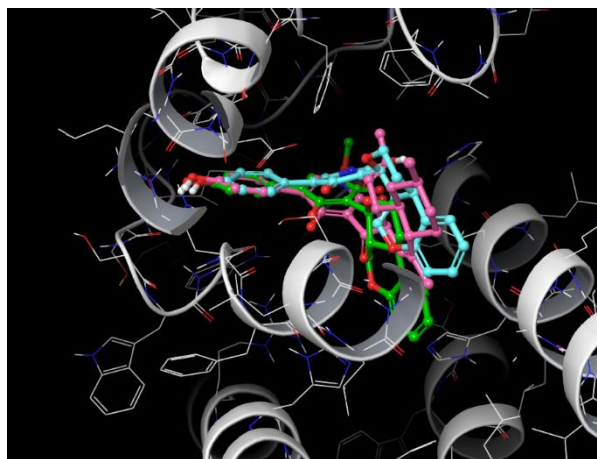


Figure 3.7: Overlapped structures of best fitting analogs with ilicicolin H. Docking scores are as follows: ilicicolin H (**3.1**) (green) (-6.473 kcal/mol), analog **3.41** (pink) (-6.197 kcal/mol) and **3.38** (cyan) (-6.041 kcal/mol) in the binding pocket without constraints.

I first wanted to determine if these compounds would mimic ilicicolin H within the binding pocket. Molecular docking of these compounds in the active site showed how they not only bound to the same site as ilicicolin H, but also better explored the cavity just outside of the binding pocket (much like the previous binding studies indicated). Further investigations also showed that when the key N32 hydrogen bond was constrained for binding as indicated by Singh and coauthors, SAM-derivatives bound in a more effective manner than ilicicolin H; suggesting that the simplified chromene tricycle may be sufficient to replace the complex ilicicolin H decalin (**Figure 3.8**). Importantly, when this restraint was removed, ilicicolin H bound most effectively, however docking scores of **3.41** and **3.38** were similar to that of ilicicolin H further purporting the scaffold simplification of ilicicolin H may produce potent analogs (**Figure 3.7**). Taking these results into consideration planned my synthetic route towards producing these notable compounds. I decided to begin initial synthetic efforts with methylated pyridinone aldehydes.

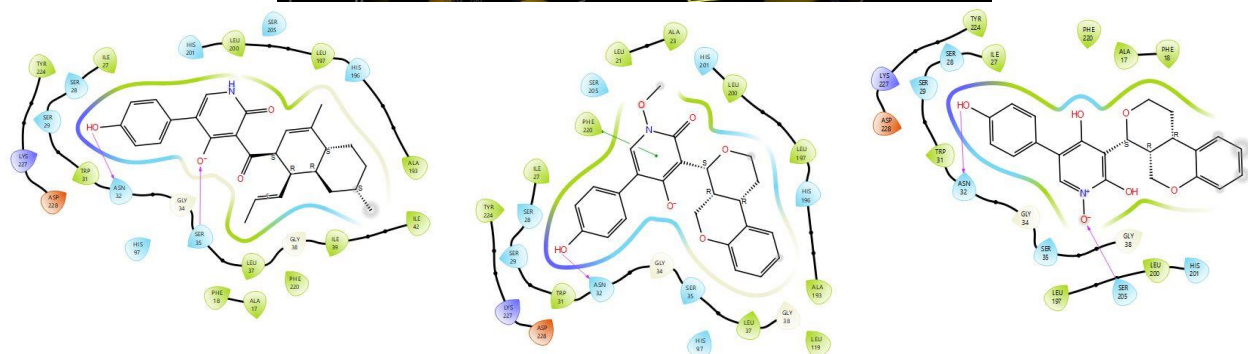


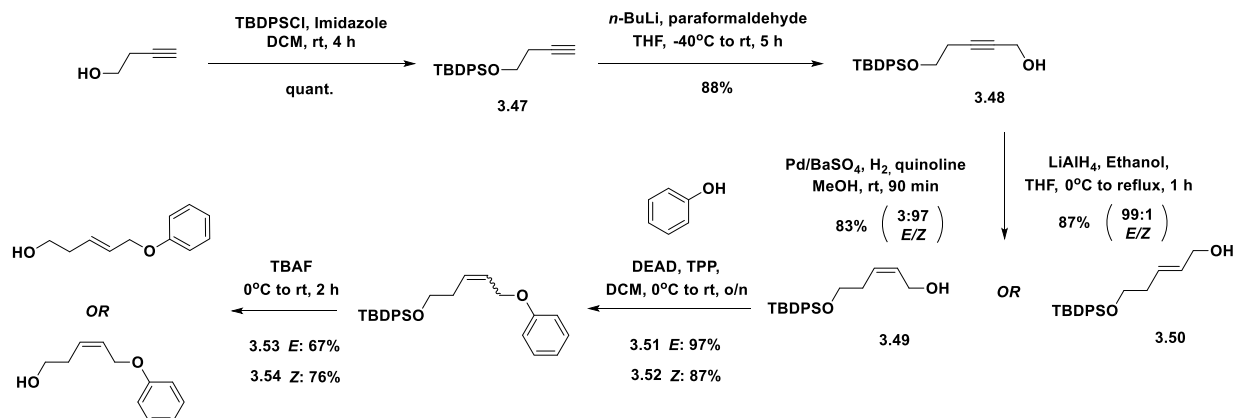
Figure 3.8: Docked structures **3.1**,

3.45 and **3.41** in the Q_i site of the bc_1 complex when key N-32 hydrogen bond is restrained. Docking scores are as follows: **3.45** (Blue) -5.573 kcal/mol, **3.41**

(Pink) -5.474 kcal/mol, ilicicolin H (**3.1**) (Green) -5.068 kcal/mol.

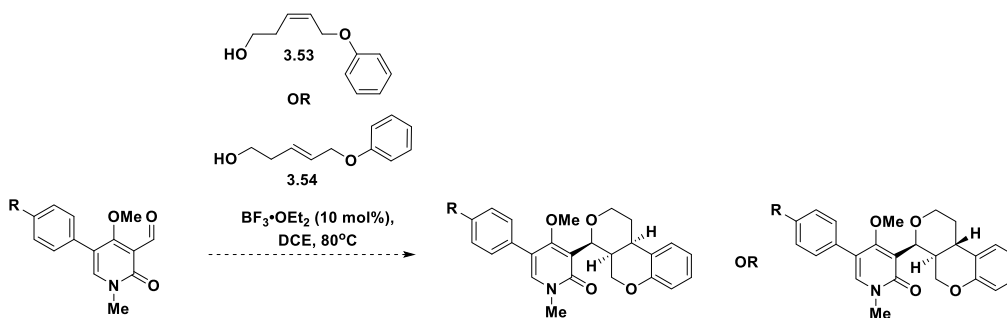
I envisioned that the pentacyclic compounds could be formed through a tandem Prins/Friedel-Crafts reaction and alcohols for both cis and trans products could be formed from the same alkyne precursor, after selective E or Z hydrogenation. Taking some inspiration from Satteyyanaidu and coauthors, synthesis of **3.53** and **3.54** starts from the TBDPS protection of propargyl alcohol.⁴⁴ Subsequent addition into paraformaldehyde cleanly furnished alkynol **3.48** in good yield. From here either reduction poisoned palladium gives the Z alkene in good yield with high selectivity (97:3). Alternatively, reduction with LiAlH_4 in ethanol gives the Z alkene (99:1). Mitsunobu coupling of these homoallylic alcohols with phenol smoothly affords ethers **3.51** and

3.52. Lastly, TBAF deprotection gives alcohols primed for the Tandem Prins/Friedel-Crafts reaction.



Scheme 3.12: Synthetic route to homoallylic alcohol tandem partners **3.53** and **3.54**.

With both alcohols in hand, I've begun optimization of conditions to produce pyridinone N-methylated derivatives of these compounds for biological testing against relevant fungal strains of *Candida*. Initial attempts at this reaction in DCM only returned starting material, however recent changes to DCE have showed full conversion to product via LCMS in just two hours. Purification of these compounds has been difficult thus far though efforts are ongoing to characterize products. If efforts here are fruitless then compounds will be purified by mass guided LMCS or by preparatory HPLC.



Scheme 3.13: Tandem Prins/ Friedel Crafts cyclization.

3.3. Conclusions

Though there were a few roadblocks in synthesizing derivatives of these 4-hydroxypyridinones has come about in the short time since the project was started, troubleshooting has been relatively successful. We currently are able to arylate and formylate the C-5 and C-3 positions on the pyridinone ring for all intended western fragments in modest yield. Though efforts are ongoing to transform the C-3 formyl group to a homoallylic alcohol, at current, we believe that chimera derivatives of ilicicolin H are the most feasible analogs to generate given the success of the chemistry of its building blocks. As such we will focus on completing and fully characterizing these compounds in the immediate future for initial biological evaluation to further guide analog development for this project.

3.4 Chapter 3 References

- (1) Shlezinger, N.; Irmer, H.; Dhingra, S.; Beattie, S. R.; Cramer, R. A.; Braus, G. H.; Sharon, A.; Hohl, T. M. Sterilizing Immunity in the Lung Relies on Targeting Fungal Apoptosis-like Programmed Cell Death. *Science* (1979) **2017**, 357 (6355), 1037–1041.
- (2) Kwon-Chung, K. J.; Sugui, J. A. *Aspergillus Fumigatus*—What Makes the Species a Ubiquitous Human Fungal Pathogen? *PLoS Pathog.* **2013**, 9 (12), 1–4.
- (3) Brakhage, A. A.; Liebmann, B. *Aspergillus Fumigatus* Conidial Pigment and CAMP Signal Transduction: Significance for Virulence. *Med. Mycol.* **2005**, 43 (SUPPL.1), S75–S82.
- (4) Brakhage, A. A.; Langfelder, K. MENACING MOLD: The Molecular Biology of *Aspergillus Fumigatus*. *Annu. Rev. Microbiol.* **2002**, 56, 433–455.
- (5) Dagenais, T. R. T.; Keller, N. P. Pathogenesis of *Aspergillus Fumigatus* in Invasive Aspergillosis. *Clin. Microbiol. Rev.* **2009**, 22 (3), 447–465.
- (6) Bongomin, F.; Gago, S.; Oladele, R. O.; Denning, D. W. Global and Multi-National Prevalence of Fungal Diseases—Estimate Precision. *J. Fungi* **2017**, 3 (4).
- (7) Salmanton-García, J.; Sprute, R.; Stemler, J.; Bartoletti, M.; Dupont, D.; Valerio, M.; Garcia-Vidal, C.; Falces-Romero, I.; Machado, M.; de la Villa, S.; Schroeder, M.; Hoyo, I.; Hanses, F.; Ferreira-Paim, K.; Giacobbe, D. R.; Meis, J. F.; Gangneux, J. P.; Rodríguez-Guardado, A.; Antinori, S.; Sal, E.; Malaj, X.; Seidel, D.; Cornely, O. A.; Koehler, P. COVID-19–Associated Pulmonary Aspergillosis, March–August 2020. *Emerg. Infect. Dis.* **2021**, 27 (4), 1086.

- (8) Dupont, D.; Menotti, J.; Turc, J.; Miossec, C.; Wallet, F.; Richard, J. C.; Argaud, L.; Paulus, S.; Wallon, M.; Ader, F.; Persat, F. Pulmonary Aspergillosis in Critically Ill Patients with Coronavirus Disease 2019 (COVID-19). *Med. Mycol.* **2021**, *59* (1), 110–114.
- (9) Bartoletti, M.; Pascale, R.; Cricca, M.; Rinaldi, M.; Maccaro, A.; Bussini, L.; Fornaro, G.; Tonetti, T.; Pizzilli, G.; Francalanci, E.; Giuntoli, L.; Rubin, A.; Moroni, A.; Ambretti, S.; Trapani, F.; Vatamanu, O.; Ranieri, V. M.; Castelli, A.; Baiocchi, M.; Lewis, R.; Giannella, M.; Viale, P.; Group, P. S.; Raumer, L.; Guerra, L.; Tumietto, F.; Cascavilla, A.; Zamparini, E.; Verucchi, G.; Coladonato, S.; Ianniruberto, S.; Attard, L.; Volpato, M. T. F.; Virgili, G.; Rossi, N.; Del Turco, E. R.; Guardigni, V.; Fasulo, G.; Dentale, N.; Fulgaro, C.; Legnani, G.; Campaci, E.; Basso, C.; Zuppiroli, A.; Passino, A. S.; Tesini, G.; Angelelli, L.; Badeanu, A.; Rossi, A.; Santangelo, G.; Dauti, F.; Koprivika, V.; Roncagli, N.; Tzimas, I.; Liuzzi, G. M.; Baxhaku, I.; Pasinelli, L.; Neri, M.; Zanaboni, T.; Dell’Omo, F.; Gori, A.; Zavatta, I.; Antonini, S.; Pironi, C.; Piccini, E.; Esposito, L.; Zuccotti, A.; Urbinati, G.; Pratelli, A.; Sarti, A.; Semprini, M.; Evangelisti, E.; D’Onofrio, M.; Sasdelli, G. Epidemiology of Invasive Pulmonary Aspergillosis Among Intubated Patients With COVID-19: A Prospective Study. *Clin. Infect. Dis.* **2021**, *73* (11), e3606–e3614.
- (10) Alanio, A.; Dellière, S.; Fodil, S.; Bretagne, S.; Mégarbane, B. Prevalence of Putative Invasive Pulmonary Aspergillosis in Critically Ill Patients with COVID-19. *Lancet Respir. Med.* **2020**, *8* (6), e48–e49.
- (11) Lin, S. J.; Schranz, J.; Teutsch, S. M. Aspergillosis Case-Fatality Rate: Systematic Review of the Literature. *Clin. Infect. Dis.* **2001**, *32* (3), 358–366.
- (12) Fisher, M. C.; Denning, D. W. The WHO Fungal Priority Pathogens List as a Game-Changer. *Nat. Rev. Microbiol.* **2023**, *21* (4), 211–212.
- (13) Neofytos, D.; Horn, D.; Anaissie, E.; Steinbach, W.; Olyaei, A.; Fishman, J.; Pfaller, M.; Chang, C.; Webster, K.; Marr, K. Epidemiology and Outcome of Invasive Fungal Infection in Adult Hematopoietic Stem Cell Transplant Recipients: Analysis of Multicenter Prospective Antifungal Therapy (PATH) Alliance Registry. *Clin. Infect. Dis.* **2009**, *48* (3), 265–273.
- (14) Verweij, P. E.; Ananda-Rajah, M.; Andes, D.; Arendrup, M. C.; Brüggemann, R. J.; Chowdhary, A.; Cornely, O. A.; Denning, D. W.; Groll, A. H.; Izumikawa, K.; Kullberg, B. J.; Lagrou, K.; Maertens, J.; Meis, J. F.; Newton, P.; Page, I.; Seyedmousavi, S.; Sheppard, D. C.; Viscoli, C.; Warris, A.; Donnelly, J. P. International Expert Opinion on the Management of Infection Caused by Azole-Resistant *Aspergillus fumigatus*. *Drug Resist. Updat.* **2015**, *21–22*, 30–40.
- (15) van der Linden, J. W. M.; Snelders, E.; Kampinga, G. A.; Rijnders, B. J. A.; Mattsson, E.; Debets-Ossenkopp, Y. J.; Kuijper, E. J.; van Tiel, F. H.; Melchers, W. J. G.; Verweij, P. E. Clinical Implications of Azole Resistance in *Aspergillus fumigatus*, the Netherlands, 2007–2009. *Emerg. Infect. Dis.* **2011**, *17* (10), 1854.
- (16) Bertini, I.; Cavallaro, G.; Rosato, A. Cytochrome c: Occurrence and Functions. *Chem. Rev.* **2006**, *106* (1), 90–115.
- (17) Hayakawa, S.; Mlnato, H.; Katagiri, K. The Ilicicolins, Antibiotics from *Cylindrocladium ilicicola*. *J. Antibiot. (Tokyo)* **1971**, *24* (9), 653–654.
- (18) Singh, S. B.; Liu, W.; Li, X.; Chen, T.; Shafiee, A.; Card, D.; Abruzzo, G.; Flattery, A.; Gill, C.; Thompson, J. R.; Rosenbach, M.; Dreikorn, S.; Hornak, V.; Meinz, M.; Kurtz, M.; Kelly, R.; Onishi, J. C. Antifungal Spectrum,

In Vivo Efficacy, and Structure–Activity Relationship of Illicicolin H. *ACS Med. Chem. Lett.* **2012**, 3 (10), 814–817.

- (19) Rotsaert, F. A. J.; Ding, M. G.; Trumpower, B. L. Differential Efficacy of Inhibition of Mitochondrial and Bacterial Cytochrome Bc 1 Complexes by Center N Inhibitors Antimycin, Illicicolin H and Funiculosin. *Biochim. Biophys. Acta – Bioenerg.* **2008**, 1777 (2), 211–219.
- (20) Kim, J.-C.; Lee, Y.-W. Sambutoxin, a New Mycotoxin Produced by Toxic Fusarium Isolates Obtained from Rotted Potato Tubers. *Appl. Environ. Microbiol.* **1994**, 60 (12), 4380–4386.
- (21) Kawai, K.; Suzuki, T.; Kitagawa, A.; Kim, J.-C.; Lee, Y.-W. A NOVEL RESPIRATORY CHAIN INHIBITOR, SAMBUTOXIN FROM Fusarium Sambucinum. *Cereal Res. Commu.* **25** (3), 325–326.
- (22) Jayasinghe, L.; Abbas, H. K.; Jacob, M. R.; Herath, W. H. M. W.; Dhammika Nanayakkara, N. P. N-Methyl-4-Hydroxy-2-Pyridinone Analogues from Fusarium Oxysporum. *J. Nat. Prod.* **2006**, 69 (3), 439–442.
- (23) Breinholt, J.; Ludvigsen, S.; Rassing, B. R.; Rosendahl, C. N.; Nielsen, S. E.; Olsen, C. E. Oxysporidinone: A Novel, Antifungal N-Methyl-4-Hydroxy-2-Pyridone from Fusarium Oxysporum. *J. Nat. Prod.* **1997**, 60 (1), 33–35.
- (24) Kumarihamy, M.; Fronczek, F. R.; Ferreira, D.; Jacob, M.; Khan, S. I.; Nanayakkara, N. P. D. Bioactive 1,4-Dihydroxy-5-Phenyl-2-Pyridinone Alkaloids from Septoria Pistaciarum. *J. Nat. Prod.* **2010**, 73 (7), 1250–1253.
- (25) Kumarihamy, M.; Khan, S. I.; Jacob, M.; Tekwani, B. L.; Duke, S. O.; Ferreira, D.; Dhammika Nanayakkara, N. P. Antiprotozoal and Antimicrobial Compounds from the Plant Pathogen Septoria Pistaciarum. *J. Nat. Prod.* **2012**, 75, 883–889.
- (26) Zhang, R.; Zhang, D.; Guo, Y.; Zhou, G.; Jiang, Z.; Dong, D. Vilsmeier Reaction of Enaminones: Efficient Synthesis of Halogenated Pyridin-2(1H)-Ones. *J. Org. Chem.* **2008**, 73 (23), 9504–9507.
- (27) Ziegler, D. S.; Wei, B.; Knochel, P. Improving the Halogen–Magnesium Exchange by Using New Turbo-Grignard Reagents. *Chem. Eur. J.* **2019**, 25 (11), 2695–2703.
- (28) Jones, A. C.; May, J. A.; Sarpong, R.; Stoltz, B. M. Toward a Symphony of Reactivity: Cascades Involving Catalysis and Sigmatropic Rearrangements. *Angew. Chem. Int. Ed.* **2014**, 53 (10), 2556–2591.
- (29) Ramachandran, P. V.; Pratihara, D.; Biswas, D. Synthesis of 4-Substituted Homoallylic Alcohols via a One-Pot Tandem Lewis-Acid Catalyzed Crotylboration-[3,3]-Sigmatropic Rearrangement. *ChemComm.* **2005**, No. 15, 1988–1989.
- (30) Veeraraghavan Ramachandran, P.; Gagare, P. D. One-Pot Allyl-/Crotylboration-Prins Cyclization of Aldehydes. *Tetrahedron Lett.* **2011**, 52 (34), 4378–4381.
- (31) Chen, M.; Roush, W. R. Highly (E)-Selective BF₃·Et₂O-Promoted Allylboration of Chiral Nonracemic α -Substituted Allylboronates and Analysis of the Origin of Stereocontrol. *Org. Lett.* **2010**, 12 (12), 2706–2709.
- (32) Williams, D. R.; Bremmer, M. L.; Brown, D. L.; D’Antuono, J. Total Synthesis of (\pm)-Illicicolin H. *J. Org. Chem.* **1985**, 50 (15), 2807–2809.

- (33) Fujita, Y.; Oguri, H.; Oikawa, H. The Relative and Absolute Configuration of PF1140. *J. Antibiot.* **2005**, *58* (6), 425–427.
- (34) Kemami Wangun, H. V.; Hertweck, C. Epicoccarines A, B and Epipyridone: Tetramic Acids and Pyridone Alkaloids from an *Epicoccum* Sp. Associated with the Tree Fungus *Pholiota Squarrosa*. *Org. Biomol. Chem.* **2007**, *5* (11), 1702–1705.
- (35) Isaka, M.; Tanticharoen, M.; Kongsaree, P.; Thebtaranonth, Y. Structures of Cordypyridones A-D, Antimalarial N-Hydroxy- and N-Methoxy-2-Pyridones from the Insect Pathogenic Fungus *Cordyceps Nipponica*. *J. Org. Chem.* **2001**, *66* (14), 4803–4808.
- (36) McBrien, K. D.; Gao, Q.; Huang, S.; Kloor, S. E.; Wang, R. R.; Pirnik, D. M.; Neddermann, K. M.; Bursuker, I.; Kadow, K. F.; Leet, J. E. Fusaricide, a New Cytotoxic N-Hydroxypyridone from *Fusarium* Sp. *J. Nat. Prod.* **1996**, *59* (12), 1151–1153.
- (37) Kamauchi, H.; Kimura, Y.; Ushiwatari, M.; Suzuki, M.; Seki, T.; Takao, K.; Sugita, Y. Synthesis and Antifungal Activity of Polycyclic Pyridone Derivatives with Anti-Hyphal and Biofilm Formation Activity against *Candida Albicans*. *Bioorg. Med. Chem. Lett.* **2021**, *37*, 127845.
- (38) Mller-Schiffmann, A.; Sticht, H.; Korth, C. Hybrid Compounds: From Simple Combinations to Nanomachines. *BioDrugs* **2012**, *26* (1), 21–31.
- (39) Morphy, R.; Kay, C.; Rankovic, Z. From Magic Bullets to Designed Multiple Ligands. *Drug. Discov. Today* **2004**, *9* (15), 641–651.
- (40) Cheng, H.; Shen, Y. Q.; Pan, X. Y.; Hou, Y. P.; Wu, Q. Y.; Yang, G. F. Discovery of 1,2,4-Triazole-1,3-Disulfonamides as Dual Inhibitors of Mitochondrial Complex II and Complex III. *New J. Chem.* **2015**, *39* (9), 7281–7292.
- (41) Li, Y.; Lei, S.; Liu, Y. Design, Synthesis and Fungicidal Activities of Novel 1,2,3-Triazole Functionalized Strobilurins. *ChemistrySelect* **2019**, *4* (3), 1015–1018.
- (42) Li, H. C.; Chai, B. S.; Li, Z. N.; Yang, J. C.; Liu, C. L. Synthesis and Fungicidal Activity of Novel Strobilurin Analogues Containing Substituted N-Phenylpyrimidin-2-Amines. *Chin. Chem. Lett.* **2009**, *20* (11), 1287–1290.
- (43) Zuccolo, M.; Kunova, A.; Musso, L.; Forlani, F.; Pinto, A.; Vistoli, G.; Gervasoni, S.; Cortesi, P.; Dallavalle, S. Dual-Active Antifungal Agents Containing Strobilurin and SDHI- Based Pharmacophores. *Sci. Rep.* **2019**, *9*, 11377.
- (44) Sattayyanaidu, V.; Chandrashekhar, R.; Reddy, B. V. S.; Lalli, C. Modulating Prins Cyclization versus Tandem Prins Processes for the Synthesis of Hexahydro-1H-Pyrano[3,4-c]Chromenes. *European. J. Org. Chem.* **2021**, *2021* (1), 138–145.

Chapter 4: Experimental Details

4.1 Fungal growth inhibition assays

Antifungal assays were performed by Corteva AgriscienceTM. Antifungal assays *Alternaria solani*, *Botrytis cinerea*, *Colletotrichum orbiculare*, *Magnaporthe grisea*, *Phytophthora infestans*, *Pythium irregulare*, *Ustilago maydis* and *Zymoseptoria tritici* were carried out in 96-well flat-bottomed microtiter plates (Techno Plastic Products, Trasadingen, Switzerland), with each well containing a total assay volume of 200 μL . The growth medium employed was Difco YNB (6.7 g L^{-1} , yeast nitrogen base without amino acids; BD Diagnostic Systems, Sparks, MD) supplemented with 2 g of glucose and 3 g each of potassium dihydrogen phosphate and dipotassium hydrogen phosphate L^{-1} . Initial inoculum density was adjusted to 250,000 spores mL^{-1} for *C. orbiculare*, 100,000 spores mL^{-1} for *B. cinerea*, *P. infestans* and *Z. tritici*, 50,000 spores mL^{-1} for *U. maydis*, 40,000 spores mL^{-1} for *M. grisea* and 10,000 spores mL^{-1} for *A. solani*. For inoculum of *P. irregulare*, a liquid culture was grown to an absorbance reading of 7000 OD, measured using a Spectronic20D+ spectrophotometer (Milton Roy, Warminster, PA) set at a wavelength of 450 nm. Serial dilutions of each material were prepared in DMSO and 2 μL aliquots were added to the wells. To enable better comparison of analogs differing significantly in biological activity, each compound was tested at eight doses using a five-fold dilution ranging from 10 to 0.00013 $\mu\text{g/mL}$. Immediately after addition of spore suspensions, initial cell density readings were determined using a NepheloStar nephelometer (BMG LABTECH Gmb, Ortenberg, Germany). After incubation in a New Brunswick Innova 44 incubator (Eppendorf, Inc., Enfield, CT) for 48 h at 20 °C (*A. solani*, *B. cinerea*, *M. grisea*, *P. infestans*, *P. irregulare* and *U. maydis*) or 72 h at 20 °C (*Z. tritici*) or 120 h at 28 °C (*C. orbiculare*), the plates were read in the NepheloStar a second time to assess growth. Percentage

growth inhibition was calculated by reference to control wells containing growth media and inoculum amended with 1% DMSO.

4.2 Chemistry: General notes

NMR spectra: NMR spectra were recorded using the following spectrometers: Bruker Avance 600 (600/150 MHz), Varian Inova 600 (600/150 MHz), Varian Inova 500 (500/125 MHz), Varian Inova 400 (400/100 MHz), VNMR 400 (400/100 MHz), or Mercury 300 (300/75 MHz). Chemical shifts are quoted in ppm relative to tetramethylsilane and with the indicated solvent as an internal reference (proton NMRs: $\text{CDCl}_3 = 7.26$; $(\text{CD}_3)_2\text{CO} = 2.05$; $\text{D}_2\text{O} = 4.79$; $(\text{CD}_3)_2\text{SO} = 2.50$; $\text{CD}_3\text{OD} = 3.31$). The following abbreviations are used to describe signal multiplicities: s (singlet), d (doublet), t (triplet), q (quartet), m (multiplet), br (broad), dd (doublet of doublets), dt (doublet of triplets), etc.

Mass spectra: Accurate mass spectra were recorded on a Thermo LTQ-FTMS using either APCI or ESI techniques.

Infrared spectra: Infrared spectra were obtained using a Thermo Nicolet Nexus 670 FTIR spectrophotometer.

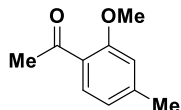
Specific rotation: Specific rotation measurements were made with a 1 dm path length using a Perkin Elmer 341 Polarimeter with a sodium lamp set to 589 nm.

Reaction setup, monitoring, and purification: Non-aqueous reactions were performed under an atmosphere of argon, in flame-dried glassware, with HPLC-grade solvents purified on a Pure Process Technology purification system. Amine bases were freshly distilled from CaH_2 before use. All other chemicals were used as received from Oakwood, TCI America, Sigma-Aldrich,

Alfa Aesar, AK Scientific, Enamine, or Strem. Brine refers to a saturated aqueous solution of sodium chloride. Reactions were monitored via thin-layer chromatography (TLC) using EMD Millipore TLC silica gel aluminum plates with KMnO₄, vanillin, *p*-anisaldehyde, or ninhydrin stain. Purification via column chromatography refers to purification on a Biotage Isolera flash chromatography purification system using a silica gel column and an increasing gradient of ethyl acetate in hexanes, diethyl ether in hexanes, or methanol in dichloromethane. Compounds that underwent biological testing were assessed for purity via analytical HPLC using an Agilent Technologies 1200 Series HPLC instrument and an acetonitrile in water solvent system with 0.1% formic acid.

4.3. Chemistry: Synthesis procedures and characterization

4.3.1. Chapter 2

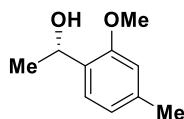


1-(2-methoxy-4-methylphenyl)ethan-1-one (2.2)

To a flame dried 100 mL round bottom flask was added 2'-hydroxy-4'-methylacetophenone (9.91 g, 66.0 mmol, 1.0 equiv) and potassium carbonate (36.5 g, 138 mmol, 4.0 equiv). The flask was sealed with a septum and evacuated and backfilled with argon three times. To this was added dry DMF (66 mL, 1M) and the resulting mixture was allowed to stir at room temperature for 10 minutes. Iodomethane (12.3 mL, 198 mmol, 3.0 equiv) was added slowly and the resulting mixture was heated to 55°C and stirred for 5 hours. The product mixture was diluted with DCM:H₂O (1:1, 120 mL), and aqueous layer was washed with DCM twice (2 x 200 mL). The combined organic layers were washed with saturated sodium bicarbonate, brine, dried over anhydrous MgSO₄ and concentrated via rotary evaporator. The resulting crude mixture was purified by silica column chromatography using a hexanes: ethyl acetate solvent system (0-20%) to yield product as a white solid (9.76 g, 90% yield). This compound is known in the literature and matches reported spectra.¹

R_f = 0.59 (2:1 hexanes: ethyl acetate)

¹H NMR (399 MHz, Chloroform-*d*) δ 7.68 (d, J = 7.9 Hz, 1H), 6.81 (d, J = 7.9 Hz, 1H), 6.77 (s, 1H), 3.90 (s, 3H), 2.59 (s, 3H), 2.38 (s, 3H).



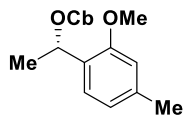
(R)-1-(2-methoxy-4-methylphenyl)ethan-1-ol (2.3)

To a flamed dried 100 mL flask was added **2.2** (1.0 g, 6.1 mmol, 1.0 equiv) and S-CBS catalyst (0.169 g, 0.61 mmol, 0.1 equiv) and this flask was sealed with a septum then evacuated and backfilled with argon three times. To this was added toluene (30.5 mL, 0.2M) and the solution was cooled down to -78°C. $\text{BH}_3 \cdot \text{THF}$ (1.5 eq, 9.15 mL, 9.15 mmol) in toluene (5 mL, 2M) was added slowly to the flask and the resulting solution was allowed to stir for 30 mins. The reaction was quenched with HCl (0.5M) and diluted with DCM. The aqueous layer was washed twice with DCM and organic layers were combined, washed with saturated sodium bicarbonate, brine and dried over anhydrous MgSO_4 . This was concentrated via rotary evaporator to afford product as a colorless oil (1.01 g, quantitative yield).

$R_f = 0.47$ (2:1 hexanes: ethyl acetate)

$^1\text{H NMR}$ (399 MHz, Chloroform-*d*) δ 7.20 (d, $J = 7.6$ Hz, 1H), 6.77 (d, $J = 7.6$, 1H), 6.70 (s, 1H), 5.05 (p, $J = 6.3$ Hz, 1H), 3.85 (s, 3H), 2.61 (d, $J = 5.3$ Hz, 1H), 2.35 (s, 4H), 1.50 (d, $J = 6.5$ Hz, 3H).

$[\alpha]_D^{20} = -7.9^\circ$ ($c = 1.0$, CHCl_3)



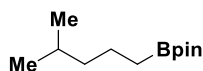
(R)-1-(2-methoxy-4-methylphenyl)ethyl diisopropylcarbamate (2.4)

To a flame dried 3 neck flask was added **2.3** (0.682 g, 4.1 mmol, 1.0 equiv) and N,N-diisopropylcarbamoyl chloride (0.704 g, 4.3 mmol, 1.05 equiv). The flask was outfitted with a reflux condenser, sealed with a septum then evacuated and backfilled with argon three times. These solids were dissolved in DCM (8.2 mL, 0.5 M) and freshly distilled triethylamine (0.600 mL, 4.3 mmol, 1.05 equiv) was added. The resulting solution was heated to reflux and stirred for 48 hours. The reaction was quenched with water and the organic layer was separated. The aqueous layer was washed twice with DCM and the combined organic layers were washed with brine and dried over MgSO₄. This was concentrated via rotary evaporator and the crude product was purified by silica column chromatography using a hexanes: ethyl acetate solvent system (0-25%) to afford the product as a colorless oil (0.868 g, 72% yield).

R_f = 0.47 (3:1 hexanes: ethyl acetate)

¹H NMR (399 MHz, Chloroform-*d*) δ 7.23 (dd, *J* = 7.8, 1.5 Hz, 1H), 6.76 (d, *J* = 7.6 Hz, 1H), 6.67 (d, *J* = 1.6 Hz, 1H), 6.14 (q, *J* = 6.5 Hz, 1H), 3.81 (s, 3H), 2.33 (s, 2H), 1.48 (d, *J* = 6.5 Hz, 3H), 1.28 – 1.17 (m, 12H).

$[\alpha]_D^{20} = +9.1^\circ$ (*c* = 1.0, CHCl₃)



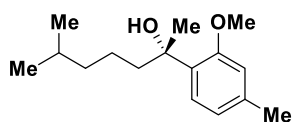
4,4,5,5-tetramethyl-2-(4-methylpentyl)-1,3,2-dioxaborolane (2.5)

To a flamed dried 3 neck flask was added Mg⁰ shavings (0.656g, 27 mmol, 3.0 equiv) and said flask was outfitted with a reflux condenser, sealed with a septum and evacuated and backfilled with argon three times. THF (10 mL, 0.9M) was added and 1-bromo-4-methylpentane (1.31mL,

9.0 mmol, 1.0 equiv) was added dropwise to the stirring suspension. This mixture was heated at reflux for 4 hours. A solution of 2-isopropoxy-4,4,5,5-tetramethyl-1,3,2-dioxaborolane (1.9 mL, 9.3 mmol, 1.03 equiv) was made and cooled to -78°C and the Grignard solution was added slowly dropwise to the cooled *iproBpin* solution via cannula and the resulting mixture was stirred for 20 minutes. The mixture was allowed to warm to room temperature, then cooled to 0°C where saturated NH_4Cl was added to quench the solution. This mixture was allowed to stir overnight. Product was extracted with diethyl ether, washed with brine, dried over MgSO_4 , and concentrated via rotary evaporator. Crude product was purified by silica chromatography using a hexanes: ethyl acetate solvent system (0-25%) to afford product as a slightly yellow oil (1.13 g, 59% yield).

$R_f = 0.68$ (4:1 hexanes: ethyl acetate)

$^1\text{H NMR}$ (399 MHz, $\text{Chloroform-}d$) δ 1.52 (dh, $J = 13.2, 6.6$ Hz, 1H), 1.46 – 1.34 (m, 2H), 1.24 (d, $J = 0.5$ Hz, 11H), 1.20 – 1.13 (m, 2H), 0.86 (dd, $J = 6.6, 0.4$ Hz, 4H), 0.75 (t, $J = 7.9$ Hz, 2H).



(S)-2-(2-methoxy-4-methylphenyl)-6-methylheptan-2-ol (2.6)

Synthesis by Aggarwal Borylation: A flame dried 15 mL round bottom flask was evacuated and backfilled with argon three times then a solution of **2.4** (0.123 g, 0.42 mmol, 1.0 equiv) in freshly distilled diethyl ether (1.7 mL, 0.25 M) was added and the solution was cooled to -78°C . To this, freshly titrated *s*-BuLi (0.452M, 2.76 mL, 1.26 mmol, 3.0 equiv) was added slowly ensuring that the reaction did not go over -70°C . This was allowed to stir for 15 minutes then a solution of

pinacol borane ester **2.5** (0.132 g, 0.63 mmol, 1.5 equiv) in freshly distilled diethyl ether (0.63 mL, 1M) was prepared and slowly added to the reaction vessel. The resulting solution was stirred at -78°C for 2 hours. A solution of $\text{MgBr}_2 \cdot \text{OEt}_2$ (0.163 g, 0.63 mmol, 1.5 equiv) was added and the reaction was warmed to room temperature and stirred overnight. To this, THF (2.8 mL, 0.15M) with BHT (3.1 mg) was added then the resulting solution was cooled to 0°C. NaOH (2M, 1.47 mL, 2.94 mmol, 7.0 equiv) and 30% H_2O_2 (11.8 eq, 0.51 mL, 5.0 mmol) were added and the resulting solution was warmed to room temperature and stirred overnight. The reaction was diluted with water (5 mL) and product was extracted with diethyl ether, washed with brine, dried over MgSO_4 then concentrated via rotary evaporator. Purification by silica column chromatography using a hexanes: ethyl acetate solvent system (0-25%) to afford the product as a colorless oil (0.032 g, 30% yield).

Synthesis by asymmetric Grignard addition: To a flame dried flask was added was added **2.2** (224 g, 0.6 mmol, 2.0 equiv) and the flask was sealed with a septum then evacuated and backfilled with argon three times. Toluene: ether (6:1, 3 mL, 0.2M) was added and the mixture was agitated for 5 minutes at room temperature then cooled to -78°C. Freshly prepared Grignard reagent (0.346M, 0.87 mL, 0.3 mmol, 1.0 equiv) was added dropwise slowly and this mixture was agitated at -78°C for 2 hours. The reaction was quenched by addition saturated NH_4Cl and the mixture was allowed to warm to room temperature and stir overnight. A 3:1 solution of IPA:water was added to the mixture followed by hexanes and the aqueous layer was washed three times with hexanes. A few drops of glacial acetic acid was added to the combined organic layer and this solution was passed through a 6 cm plug of silica in a glass Pasteur pipette followed by 50: 50 hexanes: ethyl acetate. The organic fractions were combined, washed with water, brine, and then dried over anhydrous MgSO_4 and concentrated via rotary evaporator.

Ligand was recovered from the silica plug by eluting with 50:40:10 hexanes: ethyl acetate: triethylamine and concentrated via rotary evaporator to yield crude **2.6**. Crude product was purified by silica column chromatography using a hexanes: ethyl acetate solvent system (0-25%) to afford the product as a colorless oil (0.042, 51% yield).

R_f = 0.65 (2:1 hexanes: ethyl acetate)

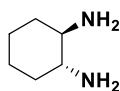
^1H NMR (399 MHz, Chloroform-*d*) δ 7.13 (d, J = 7.8 Hz, 1H), 6.75 (ddd, J = 7.8, 1.6, 0.7 Hz, 1H), 6.73 (s, 1H), 4.10 (s, 1H), 3.88 (s, 3H), 2.34 (s, 3H), 1.93 – 1.73 (m, 2H), 1.54 (s, 3H), 1.48 (dq, J = 13.2, 6.5 Hz, 1H), 1.34 – 1.18 (m, 1H), 1.17 – 1.02 (m, 2H), 0.82 (d, J = 6.6 Hz, 6H).

^{13}C NMR (100 MHz, cdCl_3) δ 187.12, 137.72, 126.42, 121.19, 112.10, 74.86, 55.11, 42.35, 39.21, 27.67, 27.23, 27.21, 22.45, 22.42, 22.10.

ν_{max} , cm^{-1} (film): 3417, 2925, 2879, 1473, 1248.

HRMS: APCI (m/z) calcd for $\text{C}_{16}\text{H}_{25}\text{O}$ [$\text{M}+\text{H}^+$]: 233.18999, found 233.18937

$[\alpha]_{\text{D}}^{20}$ = -15.2° (c = 1.0, CHCl_3)

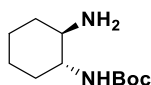


(1R,2R)-Cyclohexane-1,2-diamine (2.7)

(1R,2R)-cyclohexane-1,2-diamine-tartrate (29.6 g, 112 mmol, 1.0 equiv) was added to a 1000 mL flask and suspended in DCM (245 mL). To this, NaOH (10.9 g, 271 mmol, 2.4 equiv) dissolved in a water:brine mixture (150 mL, 1:1 ratio) was added slowly. After dissolution of the precipitate, the resulting mixture was allowed to stir at room temperature for 1 hour under a

stream of inert gas. The organic layer was separated and the aqueous layer was washed with DCM (4 x 100 mL). The combined organic layers were dried over anhydrous MgSO_4 and solvent was dried via rotary evaporator to afford the product as a crystalline, white solid (7.17g, 56% yield). This compound is known in the literature.²

^1H NMR (399 MHz, Chloroform- d) δ 2.35 – 2.26 (m, 2H), 1.91 – 1.81 (m, 2H), 1.76 – 1.62 (m, 2H), 1.34 – 1.21 (m, 2H), 1.18 – 1.07 (m, 2H).

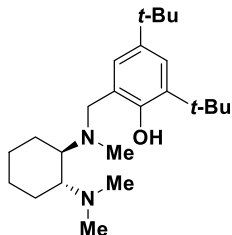


Tert-butyl (1R,2R)-2-aminocyclohexylcarbamate (2.8)

To a flame dried 100 mL flask was added HCl (1.0 eq, 0.95 mL, 37% aq) dissolved in methanol (10 mL) and cooled to 0°C. **2.7** (1.0 eq, 1.06 g, 9.25 mmol) dissolved in methanol (1.25 mL) was added dropwise and this mixture was allowed to warmed to room temperature. Di-tert-butyl dicarbonate (1.0 eq, 2.02 g, 9.25 mmol) dissolved in methanol (11.3 mL) was slowly added to the diamine hydrochloride mixture dropwise over a period of 2 hours and the total mixture was stirred for an additional 2 hours. Solvent was removed under reduced pressure and solids were washed and concentrated via rotary evaporator 3 times using diethyl ether. Remaining solids were treated with 2M NaOH (31 mL) and free amine was extracted with DCM (2 x 20 mL). Organic extracts were combined, washed with water, brine and dried over anhydrous MgSO_4 . Solvent was removed via rotary evaporator afford product as a slightly yellow solid (1.29 g, 65% yield). This compound is known in the literature.²

¹H NMR (399 MHz, Chloroform-d) δ 4.90 (s, 1H), 3.27 (s, 1H), 2.01 (d, J = 12.4 Hz, 2H), 1.71 (dd, J = 12.4, 3.2 Hz, 2H), 1.64 (s, 2H), 1.46 (s, 1H), 1.42 (d, J = 1.1 Hz, 9H), 1.38 – 1.10 (m, 4H).

$[\alpha]_D^{20} = +25^\circ$ (c = 1.0, CHCl₃)



2,4-di-tert-butyl-6-((((1R,2R)-2-(dimethylamino)cyclohexyl)(methyl)amino)methyl)phenol
(2.10)

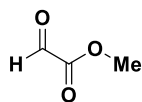
To a flame dried 100 mL flask was added **2.8** (0.643 g, 3.0 mmol, 1.0 equiv) dissolved in methanol (15 mL). To this solution was added 3,5-di-tert-butyl-2-hydroxy benzaldehyde (0.703 g, 3.0 mmol, 1.0 equiv) and the resulting mixture was stirred for 6 hours at room temperature. Sodium borohydride (0.227 g, 6.0 mmol, 2.0 equiv) was added to the mixture slowly over 20 minutes and this mixture was left to stir overnight. After 12 hours the reaction was quenched by the addition of saturated sodium bicarbonate and product was extracted with diethyl ether (3 x 20 mL), washed with water and concentrated via rotary evaporator to yield intermediate **2.9** as a white solid. This compound was dissolved in a mixture of DCM: TFA (1:2, 10 mL) and allowed to stir for 12 hours. This mixture was cooled and basified with concentrated KOH to pH 12 and the product was extracted with diethyl ether (3 x 20 mL), washed with water then dried over anhydrous MgSO₄. Removal of solvent yielded dark brown solids, which were dissolved in DCM and acetic acid (glacial, 0.5 mL) was added followed by formaldehyde (2 mL, 37%, aq.) and sodium triacetoxyborohydride (3.81 g, 18.0 mmol, 6.0 equiv). The resulting mixture was

allowed to stir for 12 hours at room temperature then quenched with saturated sodium bicarbonate. Product was extracted with diethyl ether (3 x 15 mL), washed with H₂O and concentrated via rotary evaporator to yield crude ligand as a sticky brown solid. Subsequent purification by silica column chromatography using a hexanes: ethyl acetate solvent system (0-30%) afforded pure ligand as a white crystalline solid (0.674 g, 60% yield). This compound is known in the literature.²

¹H NMR (600 MHz, Chloroform-*d*) δ 7.18 (d, J = 2.4 Hz, 1H), 6.83 (d, J = 2.4 Hz, 1H), 3.92 (d, J = 12.8 Hz, 1H), 3.20 (s, 1H), 2.52 (td, J = 10.8, 3.3 Hz, 2H), 2.25 (s, 6H), 2.20 (s, 3H), 2.03 – 1.97 (m, 2H), 1.84 – 1.76 (m, 2H), 1.42 (s, 9H), 1.28 (s, 9H), 1.21 – 1.11 (m, 4H)

¹³C NMR (151 MHz, CDCl₃) δ 154.56, 139.09, 135.33, 124.49, 123.08, 122.51, 64.01, 63.83, 54.32, 39.37, 35.03, 34.03, 31.76, 29.65, 25.75, 25.58, 23.92, 22.07.

$[\alpha]_D^{20} = -27^\circ$ (c = 1.0, CHCl₃)

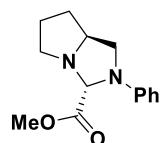


Methyl 2-oxoacetate (2.11)

To a flamed dried 2 necked 25 mL flask was added glyoxylic acid monohydrate (3.6 g, 39 mmol, 1.0 equiv) and p-toluenesulfonic acid (0.100g, 0.6 mmol, 0.015 equiv). This flask was outfitted with a reflux condenser, sealed with septa and evacuated and backfilled with argon three times. Solids were then dissolved in methyl dimethoxyacetate (4.77 mL, 29 mmol, 0.74 equiv) and the resulting mixture was heated to 80°C and stirred for 18 hours. The reaction mixture was cooled to 0°C and phosphorous pentoxide (3.97 g, 28 mmol, 0.71 equiv) was slowly added. The reaction

mixture was heated to 80°C again and stirred for 4 hours. Product was distilled under vacuum from the reaction mixture as needed (2.75 g, 80% yield). This compound is known in the literature.³

¹H NMR (399 MHz, Chloroform-*d*) δ 9.41 (s, 1H), 3.94 (s, 1H)

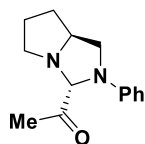


Methyl (3R,7aS)-2-phenylhexahydro-1H-pyrrolo[1,2-c]imidazole-3-carboxylate (2.12)

In a flame dried 10 mL round bottom flask was added (S)-(+)-2-(anilinomethyl)pyrrolidine (0.106 g, 0.6 mmol, 1.0 equiv) and freshly distilled **2.11** (0.058 g, 0.66 mmol, 1.1 equiv). The flask was capped with a septum and evacuated and backfilled with nitrogen three times. To this, toluene (3 mL, 2M) was added and the resulting solution was stirred at room temperature for 16 hours. Crude product was concentrated via rotary evaporator and purified by silica column chromatography using a hexanes: ethyl acetate solvent system (0-25%) to afford product as a colorless oil (0.142 g, 96% yield). This compound is known in the literature and matched reported spectra.⁴

R_f = 0.24 (4:1 hexanes: ethyl acetate)

¹H NMR (399 MHz, Chloroform-*d*) δ 7.23 (dd, J = 8.7, 7.4 Hz, 1H), 6.75 (tt, J = 7.3, 1.1 Hz, 1H), 6.55 (dd, J = 8.8, 1.1 Hz, 1H), 4.84 (s, 1H), 4.10 (qd, J = 7.1, 3.5 Hz, 1H), 3.72 (s, 1H), 3.67 (t, J = 8.0 Hz, 1H), 3.33 (ddd, J = 9.4, 6.9, 4.1 Hz, 1H), 3.17 (dd, J = 8.3, 6.4 Hz, 1H), 2.73 (td, J = 9.0, 7.3 Hz, 1H), 2.23 – 2.14 (m, 1H), 1.98 – 1.85 (m, 1H), 1.84 – 1.75 (m, 1H).



1-((3R,7aS)-2-phenylhexahydro-1H-pyrrolo[1,2-c]imidazol-3-yl)ethan-1-one (2.13)

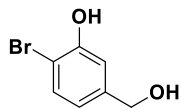
To a flame dried three necked 15 mL round bottom flask was added magnesium chloride (0.053g, 0.55 mmol, 1.1 equiv). The flask was outfitted with a reflux condenser, sealed with septa and heated under vacuum to 100°C for 1 hour. After being evacuated and backfilled with argon three times, a solution of **2.12** (0.124 g, 0.5 mmol, 1.0 equiv) in THF (5 mL, 0.1M) was prepared and added. The mixture was stirred at reflux for 1 hour then cooled to -78°C where a diethyl ether solution of MeMgBr (0.33 mL, 1.0 mmol, 1.1 equiv) was added slowly dropwise and allowed to stir for 20 minutes. The reaction was then quenched immediately with saturated NH₄Cl crude product was extracted with ethyl acetate, washed with brine, dried over anhydrous MgSO₄ then concentrated via rotary evaporator. Purification by silica column chromatography using a hexanes: ethyl acetate system afforded product as a colorless oil (0.097 g, 84% yield). Spectra matched literature reports.⁴

R_f = 0.38 (4:1 hexanes: ethyl acetate)

¹H NMR (399 MHz, Chloroform-*d*) δ 7.22 (dd, *J* = 8.7, 7.3 Hz, 2H), 6.76 (tt, *J* = 7.3, 1.1 Hz, 1H), 6.49 (dd, *J* = 8.8, 1.0 Hz, 2H), 4.38 (s, 1H), 3.94 (qd, *J* = 7.0, 4.7 Hz, 1H), 3.79 (dd, *J* = 8.5, 7.1 Hz, 1H), 3.21 (ddd, *J* = 10.1, 7.1, 5.1 Hz, 1H), 3.14 (dd, *J* = 8.5, 6.6 Hz, 1H), 2.84 (dt, *J* = 10.1, 7.3 Hz, 1H), 2.18 – 2.07 (m, 1H), 2.12 (s, 3H), 2.00 – 1.90 (m, 1H), 1.90 – 1.80 (m, 1H), 1.77 – 1.67 (m, 1H).

[α]_D²⁰ = +20.5 (*c* 1.00, chloroform) (*S,R*)

$[\alpha]_{\text{D}}^{20} = -21.4$ (c 1.00, chloroform) (*R,S*)

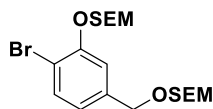


2-bromo-5-(hydroxymethyl)phenol (2.14)

To a base bath and flamed dried 500 mL round bottom flask was added methyl-4-bromo-3-hydroxybenzoate (5.0 g, 21.7 mmol, 1.0 equiv). The flask was capped with a septum and evacuated and backfilled with argon three times. Solids were dissolved in DCM (217 mL, 0.1 M) and cooled to 0°C. A 1M solution of DiBALH (71.6 mL, 71.6 mmol, 3.3 equiv) was added slowly via cannula and this solution was allowed to stir for 4 hours. The reaction was quenched by the addition of a saturated Rochelle's salt solution and crude product was extracted with ethyl acetate, washed with brine, dried over MgSO₄ and concentrated via rotary evaporator to afford product as a white solid (4.04 g, 92% yield). Spectra matched literature reports.⁴

$R_f = 0.14$ (4:1 hexanes: ethyl acetate)

¹H NMR (399 MHz, Chloroform-*d*) δ 7.44 (d, $J = 8.2$ Hz, 1H), 7.04 (d, $J = 2.0$ Hz, 0H), 6.82 (dd, $J = 8.2, 2.0$ Hz, 1H), 5.52 (s, 1H), 4.64 (s, 2H), 1.68 (s, 1H).

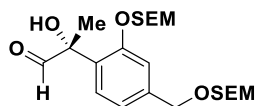


(2-(((4-bromo-3-((2-(trimethylsilyl)ethoxy)methoxy)benzyl)oxy)methoxy)ethyl)trimethylsilane (2.15)

To a base bathed and flamed dried 250 mL flask was added NaH as a 60% mineral oil suspension (2.33 g, 58.2 mmol, 3.0 equiv). The flask was capped with a septum and evacuated and backfilled with argon three times. To this, THF (16.2 mL, 3.6M) was added and the resulting mixture was cooled to 0°C. A solution of **2.14** (3.94 g, 19.4 mmol, 1.0 equiv) in THF (24.3 mL, 0.8M) was added slowly dropwise and this solution was allowed to stir for one hour at 0°C. A solution of SEMCl (13.7 mL, 77.6 mmol, 4.0 equiv) in THF (32.3 mL, 2.4M) and the resulting solution was allowed to warm up to room temperature and stir overnight. Crude product was extracted with ethyl acetate, washed with brine, dried over MgSO₄ and concentrated via rotary evaporator. Purification by silica column chromatography using a hexanes: ethyl acetate system (0-25%) afforded product as a yellow oil (6.30 g, 70% yield). Spectra matched literature reports.⁴

R_f = 0.75 (4:1 hexanes: ethyl acetate)

¹H NMR (399 MHz, Chloroform-d) δ 7.50 (d, J = 8.0 Hz, 1H), 7.16 (d, J = 1.9 Hz, 1H), 6.87 (dd, J = 8.0, 1.9 Hz, 1H), 5.30 (s, 2H), 4.74 (s, 2H), 4.54 (s, 2H), 3.84 – 3.78 (m, 2H), 3.64 – 3.59 (m, 2H), 0.97 – 0.92 (m, 4H), 0.02 (s, 9H), -0.00 (s, 9H). Spectral data are consistent with published values.



(R)-2-hydroxy-2-(2-((2-(trimethylsilyl)ethoxy)methoxy)-4-(((2-(trimethylsilyl)ethoxy)methoxy)methyl)phenyl)propanal (2.16)

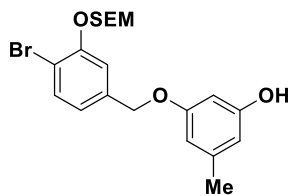
To a flamed dried three neck 15 mL flask was added Mg⁰ shavings (6.0 eq, 0.248 g, 10.2 mmol). The flask was outfitted with a reflux condenser, capped with septa and evacuated and backfilled

with argon three times. A solution of **2.15** (2.0 eq, 1.58 g, 3.4 mmol) in THF (6.8 mL, 0.5M) was added, followed by dibromoethane (0.5 eq, 0.07 mL, 0.85 mmol) and the resulting mixture was heated to reflux for 4 hours then cooled to -78°C . A solution of **2.13** (1.0 eq, 0.392 g, 1.7 mmol) was added slowly via syringe and resulting solution was allowed to stir at -78°C for 2 hours. Saturated NH_4Cl and water were added to the reaction to quench and crude intermediate was extracted ethyl acetate, washed with brine, dried over MgSO_4 and concentrated via rotary evaporator to yield crude hydroxy aminal. This was dissolved in diethyl ether (17 mL, 0.1 M) and cooled to 0°C and dilute hydrochloric acid (17 mL, 2%) was added. This was allowed to stir at 0°C for 15 hours. The organic layer was separated, and the aqueous layer was washed with ethyl acetate three times. Combined organic layers were washed with water, brine, dried over MgSO_4 and concentrated via rotary evaporator. Purification by silica column chromatography using a hexanes: diethyl ether system (0-35%) afforded product as a colorless oil (0.649 g, 85% yield). Spectra matched literature reports.⁴

$R_f = 0.22$ (4:1 hexanes: diethyl ether)

^1H NMR (399 MHz, Chloroform- d) δ 9.78 (s, 1H), 7.48 (d, $J = 7.9$ Hz, 1H), 7.14 (d, $J = 1.6$ Hz, 1H), 7.05 (dd, $J = 7.9, 1.6$ Hz, 1H), 5.26 (d, $J = 6.9$ Hz, 1H), 5.23 (d, $J = 6.9$ Hz, 1H), 4.75 (s, 2H), 4.58 (s, 2H), 4.04 (s, 1H), 3.69 – 3.64 (m, 4H), 1.67 (s, 3H), 0.97 – 0.93 (m, 4H), 0.02 (s, 9H), 0.00 (s, 9H). Spectral data are consistent with published values.

$[\alpha]_D^{20} = -50.1^{\circ}$ ($c = 1.0$, CHCl_3)



3-((4-bromo-3-((2-(trimethylsilyl)ethoxy)methoxy)benzyl)oxy)-5-methylphenol (**2.19**)

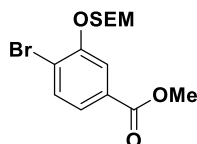
To a flame dried 5 dram vial was added **2.17** (0.061 g, 0.44 mmol, 1.0 equiv) and triphenylphosphine (0.150 g, 0.57 mmol, 1.3 equiv) then equipped with a magnetic stir bar. The vial was then filled and backfilled with argon three times. In a second 5 dram vial **2.18** (0.147 g, 0.44 mmol, 1.0 equiv) was dissolved in dry THF (0.8 mL) and the resulting solution was transferred to the first vial charged with the monoprotected orcinol and triphenylphosphine. The solution was cooled to 0°C and allowed to stir for 5 minutes before azodicarboxylate of choice (0.48 mmol, 1.1 equiv) was added and the resulting solution was stirred at 0°C for a further 15 minutes. The ice bath was removed and the reaction was stirred at room temperature overnight. The reaction was concentrated via rotovap and the residue was purified by silica chromatography using a hexanes: ethyl acetate gradient (0-15%) to give the intended product as an off yellow oil (0.66 g, 33% yield).

R_f = 0.32 (4:1 hexanes: ethyl acetate)

¹H NMR (400 MHz, Chloroform-*d*) δ 7.53 (d, *J* = 8.1 Hz, 1H), 7.22 (d, *J* = 1.9 Hz, 1H), 6.94 (dd, *J* = 8.1, 1.9 Hz, 1H), 6.38 (ddd, *J* = 2.2, 1.5, 0.8 Hz, 1H), 6.29 – 6.21 (m, 2H), 5.31 (s, 2H), 4.95 (s, 2H), 4.70 (s, 1H), 3.89 – 3.73 (m, 2H), 2.26 (s, 3H), 1.02 – 0.87 (m, 2H), 0.00 (s, 9H).

¹³C NMR (101 MHz, CDCl₃) δ 159.89, 156.59, 154.18, 140.80, 138.00, 133.50, 121.92, 115.26, 112.30, 109.17, 108.42, 99.63, 93.69, 69.44, 66.88, 21.74, 18.14, -1.27.

HRMS: APCI (*m/z*) calcd for C₂₉H₄₉O₄Si₂ [M+H⁺]: 517.31773, found 517.31664.



methyl 4-bromo-3-((2-(trimethylsilyl)ethoxy)methoxy)benzoate (2.20)

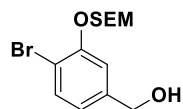
To a base bathed and flamed dried 250 mL flask was added NaH as a 60% mineral oil suspension (0.779 g, 19.5 mmol, 1.5 equiv) . The flask was capped with a septum and evacuated and backfilled with argon three times. To this, THF (140 mL) was added and the resulting mixture was cooled to 0°C. A solution of methyl 4-bromo-3-hydroxybenzoate (3.00g, 13.0 mmol, 1.0 equiv) in THF (100 mL) was added slowly dropwise and this solution was allowed to stir for one hour at 0°C. SEMCl (2.60 g, 15.6 mmol, 1.2 equiv) was then added neat and the resulting solution was allowed to warm up to room temperature and stir overnight. Crude product was extracted with ethyl acetate, washed with brine, dried over MgSO₄ and concentrated via rotary evaporator. Purification by silica column chromatography using a hexanes: ethyl acetate system (0-20%) afforded product as a yellow oil (4.47 g, 95.4% yield).

R_f = 0.59 (4:1 hexanes: ethyl acetate)

¹H NMR (399 MHz, Chloroform-*d*) δ 7.80 (d, *J* = 1.8 Hz, 1H), 7.61 (d, *J* = 8.3 Hz, 1H), 7.55 (dd, *J* = 8.3, 1.9 Hz, 1H), 5.35 (s, 2H), 3.91 (s, 3H), 3.84 – 3.78 (m, 3H), 0.99 – 0.93 (m, 3H), - 0.00 (s, 9H).

ν_{max}, cm⁻¹ (film): 2972, 2931, 1717, 1578, 1306.

HRMS APCI (*m/z*) calcd for C₁₄H₂₀O₄BrSi [M-H⁺]: 359.03197, found 359.03276.



(4-bromo-3-((2-(trimethylsilyl)ethoxy)methoxy)phenyl)methanol (2.17)

To a base bath and flamed dried 100 mL round bottom flask was added solid LiAlH_4 (0.506 g, 13.34 mmol, 2.2 equiv). The flask was capped with a septum and evacuated and backfilled with argon three times. Anhydrous THF (50 mL) was added and the resulting solution was cooled to 0°C . A solution of **2.20** (2.197 g, 6.08 mmol, 1.0 equiv) was added slowly via syringe and this solution was stirred at 0°C 1 hour. The reaction was quenched by the addition of a saturated Rochelle's salt solution and crude product was extracted with ethyl acetate, washed with brine, dried over MgSO_4 and concentrated via rotary evaporator to afford product as a clear oil (2.03 g, 95% yield).

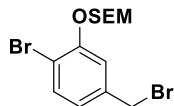
$R_f = 0.16$ (4:1 hexanes: ethyl acetate)

$^1\text{H NMR}$ (500 MHz, $\text{Chloroform-}d$) δ 7.50 (d, $J = 8.1$ Hz, 1H), 7.17 (d, $J = 1.5$ Hz, 1H), 6.87 (ddd, $J = 8.1, 1.8, 0.6$ Hz, 1H), 5.29 (s, 2H), 4.62 (d, $J = 4.6$ Hz, 2H), 3.88 – 3.72 (m, 2H), 1.02 – 0.89 (m, 2H), -0.00 (s, 4H).

$^{13}\text{C NMR}$ (126 MHz, cdcl_3) δ 153.96, 141.76, 133.28, 121.21, 114.55, 93.42, 66.73, 64.65, 17.99, -1.43.

ν_{max} , cm^{-1} (film): 3340, 2951, 2895, 1247, 831.

HRMS: APCI (m/z) calcd for $\text{C}_{13}\text{H}_{20}\text{O}_3\text{BrSi}$ [M-H^+]: 331.003706, found 331.03685.



(2-((2-bromo-5-(bromomethyl)phenoxy)methoxy)ethyl)trimethylsilane (2.21)

To a flame dried 250 mL flask was added triphenylphosphine (3.66 g, 14.0 mmol, 1.5 equiv).

The flask was equipped with a magnetic stir bar and purged with argon three times. A solution of **2.17** (3.10 g, 9.30 mmol, 1.0 equiv) in DCM (70 mL) was added and the resulting mixture was cooled to 0°C and allowed to stir for 5 minutes. A suspension of NBS (2.48 g, 14.0 mmol, 1.5 equiv) in DCM (23 mL) was slowly via syringe over 10 minutes to the stirring solution of **2.17**.

The cooling bath was removed and the reaction was stirred at room temperature for one hour.

The color of the solution changed from clear, to a pale yellow, to a pale orange. The reaction was quenched with saturated NH₄Cl. The aqueous layer was extracted with DCM (3 x 50 mL) and this organic layer was a deep orange/peach color. The organic layer was washed with brine leaving a deep ruby color. Once dried over MgSO₄ a pale orange/peach filtrate was left which which was concentrated *in vacuo*. Crude product was purified by silica column chromatography using a hexanes: ethyl acetate system (0-20%) afforded product as a clear oil (3.31 g, 90% yield).

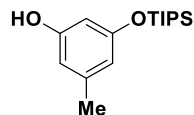
R_f = 0.59 (4:1 hexanes: ethyl acetate)

¹H NMR (600 MHz, Chloroform-*d*) δ 7.50 (d, *J* = 8.1 Hz, 1H), 7.20 (d, *J* = 2.0 Hz, 1H), 6.94 – 6.91 (m, 1H), 5.31 (s, 2H), 4.42 (s, 2H), 3.84 – 3.79 (m, 2H), 0.99 – 0.95 (m, 2H), 0.01 (s, 9H).

¹³C NMR (101 MHz, CDCl₃) δ 154.20, 138.52, 133.66, 123.54, 116.72, 112.99, 93.67, 66.92, 32.77, 18.12, -1.26.

ν_{max}, cm⁻¹ (film): 2948, 2870, 1473, 1255, 831.

HRMS: APCI (m/z) calcd for $C_{13}H_{19}O_2Br_2Si$ $[M-H^+]$: 392.95156, found 392.95281.



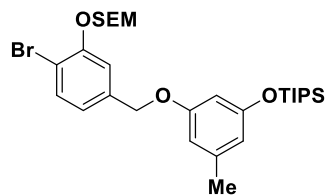
3-methyl-5-((triisopropylsilyl)oxy)phenol (2.22)

To a flame dried 250 mL flask equipped with a magnetic stir bar was added orcinol (2.01 g, 16.2 mmol, 1.0 equiv) and imidazole (1.65 g, 24.3 mmol, 1.5 equiv). This flask was purged and backfilled with argon three times. To this was added DCM (81 mL) and after stirring for 15 minutes TIPSCl (3.123 g, 3.47 mL, 16.2 mmol, 1.0 equiv) was added. The solution slowly started to turn clear and the resulting solution was allowed to stir for 18 hrs. To this was added saturated sodium bicarbonate (40 mL) and the solution once again became clear in color. The organic layer was removed and dried with $MgSO_4$ then concentrated via rotovap. The resulting crude product was purified by column chromatography (0-30% gradient, hexanes : ethyl acetate) leaving a off white amorphous solid (2.31 g, 51% yield). Spectra matched those reported in the literature.⁵

R_f = 0.54 (hexanes: ethyl acetate)

1H NMR (400 MHz, Chloroform- d) δ 6.31 (tt, J = 1.5, 0.7 Hz, 1H), 6.25 (td, J = 1.8, 0.7 Hz, 1H), 6.22 (t, J = 2.3 Hz, 1H), 5.00 (s, 1H), 2.23 (s, 3H), 1.32 – 1.18 (m, 3H), 1.10 (d, J = 7.4 Hz, 18H).

^{13}C NMR (101 MHz, $CDCl_3$) δ 157.20, 156.32, 140.36, 113.59, 109.14, 104.50, 21.57, 18.05, 12.79.



(3-((4-bromo-3-((2-(trimethylsilyl)ethoxy)methoxy)benzyl)oxy)-5-methylphenoxy)triisopropylsilane (2.23)

To a flame dried 4 dram vial equipped with a magnetic stir bar was added **2.21** (1.09 g, 2.75 mmol, 1.0 equiv) and **2.22** (0.850 g, 3.03 mmol, 1.1 equiv) followed by anhydrous DMF (5.00 mL). This solution was then cooled to 0°C using an ice bath and to this was added potassium carbonate (0.457 g, 3.3 mmol, 1.2 equiv). The resulting solution was heterogenous and the vessel was filled and backfilled with argon three times. A fresh septum was then used to cap the vial and the solution was allowed to stir overnight for 8 hours. The reaction was quenched by the addition of saturated ammonium chloride followed by water. The mixture was then diluted with DCM (2 mL) and shaken to extract the desired product. This process was repeated three times (3 x 2 mL) with DCM and the combined organic layer was washed with water, brine and dried over MgSO₄. Product was obtained by silica gel chromatography using a slow hexanes: ethyl acetate gradient (0-20%) (product starts to elute around 8% EtOAc). The resulting product was a clear oil (1.406 g, 86% yield).

R_f = 0.62 (4:1 hexanes: ethyl acetate)

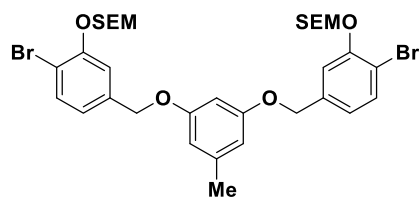
¹H NMR (600 MHz, Chloroform-*d*) δ 7.52 (d, *J* = 8.1 Hz, 1H), 7.22 (s, 1H), 6.94 (d, *J* = 8.1 Hz, 1H), 6.39 (s, 1H), 6.33 (s, 1H), 6.26 (s, 1H), 5.30 (s, 2H), 4.94 (s, 2H), 3.85 – 3.77 (m, 2H), 2.25

(d, $J = 1.4$ Hz, 3H), 1.24 – 1.15 (m, 3H), 1.07 (d, $J = 7.8$ Hz, 18H), 0.99 – 0.92 (m, 2H), 0.00 (s, 9H).

^{13}C NMR (101 MHz, CDCl_3) δ 159.42, 157.03, 154.21, 140.06, 138.22, 133.42, 121.83, 115.11, 113.90, 112.14, 108.74, 104.06, 93.69, 69.35, 66.83, 21.79, 18.12, 18.06, 12.78, -1.28.

ν_{max} , cm^{-1} (film): 2950, 2893, 2866, 1587, 1164.

HRMS: APCI (m/z) calcd for $\text{C}_{29}\text{H}_{38}\text{O}_4\text{BrSi}_2$ [$\text{M}+\text{H}^+$]: 595.2269, found 595.22715.

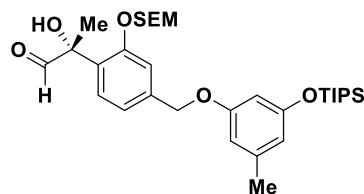


(((((((5-methyl-1,3-phenylene)bis(oxy))bis(methylene))bis(6-bromo-3,1-phenylene))bis(oxy))bis(methylene))bis(oxy))bis(ethane-2,1-diyl))bis(trimethylsilane) (2.24)

$R_f = 0.48$ (4:1 hexanes: ethyl acetate)

^1H NMR (600 MHz, $\text{Chloroform-}d$) δ 7.53 (d, $J = 8.1$ Hz, 2H), 7.23 (d, $J = 1.8$ Hz, 2H), 6.94 (dd, $J = 8.1, 1.9$ Hz, 2H), 6.41 (d, $J = 2.1$ Hz, 2H), 6.39 (t, $J = 2.2$ Hz, 1H), 5.31 (s, 4H), 4.95 (s, 4H), 3.82 – 3.79 (m, 4H), 2.29 (s, 3H), 1.02 – 0.89 (m, 4H), -0.00 (s, 18H).

ν_{max} , cm^{-1} (film): 2951, 2866, 1249, 1096, 835.



(R)-2-hydroxy-2-(4-((3-methyl-5-((triisopropylsilyl)oxy)phenoxy)methyl)-2-((2-(trimethylsilyl)ethoxy)methoxy)phenyl)propanal ((-)-2.25)

To a flamed dried 5 dram vial **2.23** (0.750 g, 1.26 mmol, 1.0 equiv) was added . This vial was then capped with septa and evacuated and backfilled with argon three times. Anhydrous THF (8 mL) was then added and the resulting solution was cooled to -78°C with a dry ice acetone bathe. TMEDA was then added (0.183 g, 1.57 mmol, 1.5 equiv) followed by *n*-BuLi (0.101 mg, 629 μL , 2.5 M, 1.57 mmol, 1.25 equiv) and this mixture was allowed to stir at -78°C for 1.5 hours. To this, a solution of **2.13** (0.435 g, 1.89 mmol, 1.5 equiv) in THF (2 mL) was added slowly and the resulting solution was allowed to stir at -78°C for 5 hours. Saturated NH_4Cl and water were added to the reaction to quench and crude intermediate was extracted ethyl acetate, washed with brine, dried over MgSO_4 and concentrated via rotary evaporator to yield crude hydroxy aminal. This was dissolved in diethyl ether (10 mL, 0.1 M) and cooled to 0°C and dilute hydrochloric acid (10 mL, 2% aq) was added. This was allowed to stir at 0°C for 15 hours. The organic layer was separated, and the aqueous layer was washed with ethyl acetate three times. Combined organic layers were washed with water, brine, dried over MgSO_4 and concentrated via rotary evaporator. Purification by silica column chromatography using a hexanes: diethyl ether system (0-30%) afforded product as a colorless oil (0.482 g, 65% yield).

R_f = 0.19 (4:1 hexanes: diethyl ether)

^1H NMR (600 MHz, Chloroform-*d*) δ 9.79 (d, J = 0.6 Hz, 1H), 7.51 (d, J = 7.9 Hz, 1H), 7.20 (d, J = 1.5 Hz, 1H), 7.11 (ddt, J = 7.9, 1.6, 0.8 Hz, 1H), 6.41 – 6.36 (m, 1H), 6.33 (ddd, J = 2.0, 1.3, 0.7 Hz, 1H), 6.28 (dt, J = 2.8, 1.4 Hz, 1H), 5.29 – 5.19 (m, 2H), 4.98 (s, 2H), 3.75 – 3.65 (m, 2H), 2.25 (s, 3H), 1.67 (s, 3H), 1.24 – 1.17 (m, 3H), 1.07 (d, J = 7.4 Hz, 18H), 0.96 – 0.92 (m, 2H), 0.00 (s, 9H).

^{13}C NMR (101 MHz, CDCl_3) δ 201.25, 159.53, 157.05, 154.57, 140.08, 139.64, 128.92, 127.64, 121.11, 113.87, 113.39, 108.76, 108.67, 104.03, 93.08, 93.05, 78.29, 69.48, 67.08, 21.81, 18.08, 12.79, -1.30.

ν_{max} , cm^{-1} (film): 2948, 2894, 2867, 1737, 1589.

HRMS: APCI (m/z) calcd for $\text{C}_{32}\text{H}_{53}\text{O}_6\text{Si}_2$ [$\text{M}+\text{H}^+$]: 589.33752, found 589.33744.

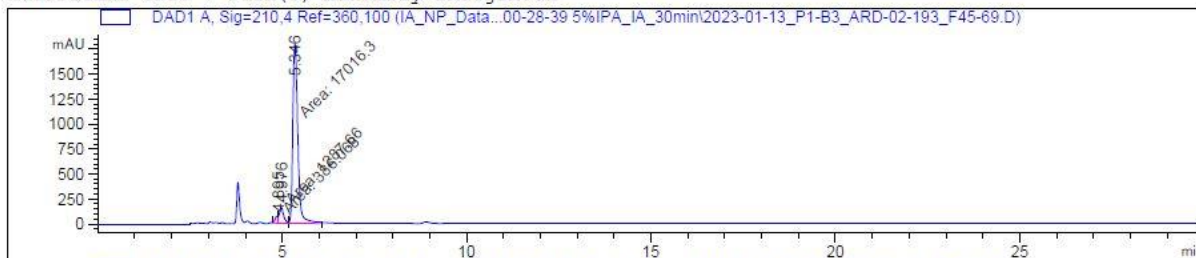
$[\alpha]_{\text{D}}^{20}$ = -39° (c = 1.0, CHCl_3)

Data File C:\Users\P...-01-13 00-28-39 5%IPA_IA_30min\2023-01-13_P1-B3_ARD-02-193_F45-69.D
Sample Name: ARD-02-193_F45-69

```
=====
Acq. Operator   : SYSTEM                      Seq. Line :    2
Sample Operator : SYSTEM
Acq. Instrument : Normal Phase                Location  : P1-B-03
Injection Date  : 1/13/2023 12:45:04 AM       Inj       :    1
                                           Inj Volume: 5.000  $\mu\text{L}$ 

Method          : C:\Users\Public\Documents\ChemStation\1\Data\IA_NP_Data\2023-01-13 00-28-39 5%
                  IPA_IA_30min\5_IPA_IA_FIXED_1.0mL-min_30min.M (Sequence Method)
Last changed    : 10/1/2022 2:20:02 PM by SYSTEM
Method Info     : Date Created: 09/27/2022
                  Created By: Patrick Gross
                  %IPA: 5
                  Column: IA
                  Flowrate: 1.0 mL/min
                  Runtime: 30.0 min
                  Wavelengths: 210nm, 230nm, 254nm, 280nm
```

Additional Info : Peak(s) manually integrated



Sorted By : Signal
Multiplier : 1.0000
Dilution : 1.0000
Do not use Multiplier & Dilution Factor with ISTDs

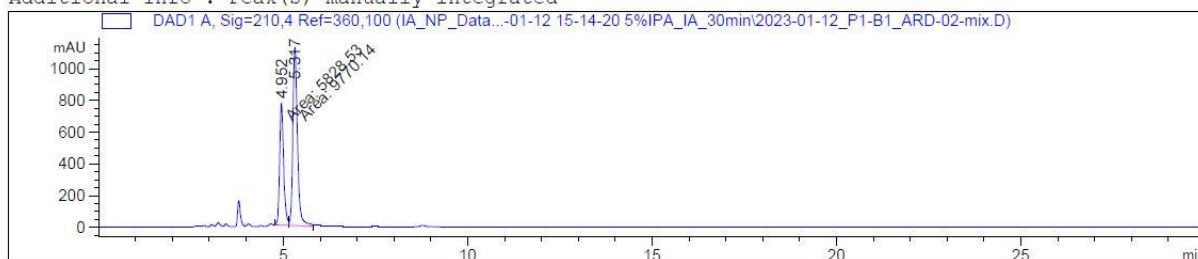
Signal 1: DAD1 A, Sig=210,4 Ref=360,100

| Peak # | RetTime [min] | Type | Width [min] | Area [mAU*s] | Height [mAU] | Area % |
|--------|---------------|------|-------------|--------------|--------------|---------|
| 1 | 4.895 | MF | 0.0935 | 386.06790 | 68.82710 | 2.0656 |
| 2 | 4.976 | FM | 0.1341 | 1287.66211 | 160.01558 | 6.8896 |
| 3 | 5.346 | FM | 0.1581 | 1.70163e4 | 1794.29236 | 91.0448 |

Data File C:\Users\P...ta\2023-01-12 15-14-20 5%IPA_IA_30min\2023-01-12_P1-B1_ARD-02-mix.D
Sample Name: ARD-02-mix

```
=====
Acq. Operator   : SYSTEM                               Seq. Line :    2
Sample Operator : SYSTEM
Acq. Instrument : Normal Phase                         Location  : P1-B-01
Injection Date  : 1/12/2023 3:30:47 PM                 Inj       :    1
                                                    Inj Volume: 5.000 µl
Method          : C:\Users\Public\Documents\ChemStation\1\Data\IA_NP_Data\2023-01-12 15-14-20 5%
                  IPA_IA_30min\5_IPA_IA_FIXED 1.0mL-min_30min.M (Sequence Method)
Last changed    : 10/1/2022 2:20:02 PM by SYSTEM
Method Info     : Date Created: 09/27/2022
                  Created By: Patrick Gross
                  %IPA: 5
                  Column: IA
                  Flowrate: 1.0 mL/min
                  Runtime: 30.0 min
                  Wavelengths: 210nm, 230nm, 254nm, 280nm
```

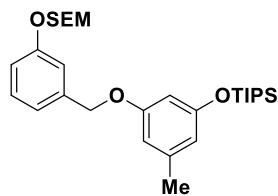
Additional Info : Peak(s) manually integrated



Sorted By : Signal
Multiplier : 1.0000
Dilution : 1.0000
Do not use Multiplier & Dilution Factor with ISTDs

Signal 1: DAD1 A, Sig=210,4 Ref=360,100

| Peak # | RetTime [min] | Type | Width [min] | Area [mAU*s] | Height [mAU] | Area % |
|--------|---------------|------|-------------|--------------|--------------|---------|
| 1 | 4.952 | MF | 0.1262 | 5828.53076 | 769.45557 | 37.3656 |
| 2 | 5.317 | FM | 0.1450 | 9770.14258 | 1123.30493 | 62.6344 |

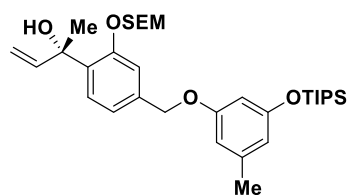


triisopropyl(3-methyl-5-((3-((2-(trimethylsilyl)ethoxy)methoxy)benzyl)oxy)phenoxy)silane
(2.26)

R_f = 0.66 (4:1 hexanes: diethyl ether)

$^1\text{H NMR}$ (600 MHz, Chloroform-*d*) δ 7.28 (t, J = 7.9 Hz, 1H), 7.09 (d, J = 2.0 Hz, 1H), 7.04 (dt, J = 7.5, 0.8 Hz, 1H), 6.99 (ddd, J = 8.2, 2.6, 1.0 Hz, 1H), 6.41 (ddd, J = 2.3, 1.4, 0.8 Hz, 1H), 6.32 (ddd, J = 2.2, 1.4, 0.7 Hz, 1H), 6.30 (t, J = 2.3 Hz, 1H), 5.22 (s, 2H), 4.98 (s, 3H), 3.80 – 3.66 (m, 2H), 2.26 (s, 3H), 1.25 – 1.17 (m, 3H), 1.08 (d, J = 7.3 Hz, 18H), 0.99 – 0.93 (m, 2H), 0.00 (s, 9H).

HRMS: APCI (m/z) calcd for $\text{C}_{29}\text{H}_{49}\text{O}_4\text{Si}_2$ [$\text{M}+\text{H}^+$]: 517.31773, found 517.31664.



(S)-2-(4-((3-methyl-5-((triisopropylsilyl)oxy)phenoxy)methyl)-2-((2-(trimethylsilyl)ethoxy)methoxy)phenyl)but-3-en-2-ol ((-)-2.27)

To a flame dried 10 mL round bottom flask equipped with a magnetic stir bar was added methyltriphenylphosphonium bromide (0.409 g, 1.15 mmol, 2.25 equiv) and potassium tert-butoxide (0.143 g, 1.27 mmol, 1.27 equiv). The flask was capped with a septum and evacuated

and backfilled with argon three times. THF (2 mL) was added and a bright yellow color immediately developed. This mixture was allowed to stir for 4 hours. To this, aldehyde (-)-**2.25** (0.300 g, 0.509 mmol, 1.0 equiv) was added and the resulting mixture was allowed to stir for 12 hours at room temperature. The reaction was quenched with saturated NH_4Cl and crude product was extracted with ethyl acetate, washed with brine, dried over MgSO_4 , and concentrated via rotary evaporator. Purification by silica column chromatography using a hexanes: ethyl acetate system (0-20%) afforded product as a colorless oil (0.209 g, 70% yield).

$R_f = 0.54$ (hexanes: ethyl acetate)

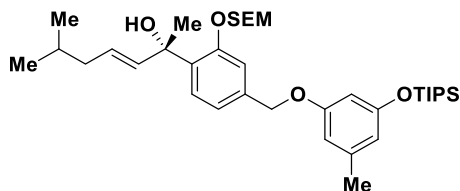
^1H NMR (600 MHz, CHCl_3 -*d*) δ 7.36 (d, $J = 7.9$ Hz, 1H), 7.22 (s, 1H), 7.06 (d, $J = 7.9$ Hz, 1H), 6.42 (t, $J = 1.9$ Hz, 1H), 6.36 – 6.33 (m, 1H), 6.31 (t, $J = 2.3$ Hz, 1H), 6.19 (dd, $J = 17.3$, 10.6 Hz, 1H), 5.33 – 5.24 (m, 2H), 5.16 (dd, $J = 17.3$, 1.2 Hz, 1H), 5.05 (dd, $J = 10.6$, 1.2 Hz, 1H), 4.98 (s, 2H), 4.24 (s, 1H), 3.76 (dtd, $J = 21.8$, 9.5, 8.4 Hz, 2H), 2.27 (s, 3H), 1.69 (s, 3H), 1.22 (ddt, $J = 14.2$, 9.7, 6.9 Hz, 3H), 1.09 (d, $J = 7.4$ Hz, 18H), 0.97 (dd, $J = 8.8$, 7.9 Hz, 2H), 0.02 (s, 9H).

^{13}C NMR (126 MHz, CDCl_3) δ 159.36, 156.74, 154.95, 144.92, 139.72, 137.74, 133.49, 126.64, 120.43, 113.51, 113.45, 111.36, 108.45, 103.77, 92.76, 74.62, 69.33, 66.68, 27.29, 21.51, 17.80, 17.58, 12.51, -1.57.

ν_{max} , cm^{-1} (film): 2952, 2861, 2155, 2029, 1594.

HRMS: APCI (m/z) calcd for $\text{C}_{33}\text{H}_{55}\text{O}_5\text{Si}_2$ [$\text{M}+\text{H}^+$]: 587.35825, found 587.35895.

$[\alpha]_{\text{D}}^{20} = -3.75$ (c 0.24, chloroform)



(S,E)-6-methyl-2-(4-((3-methyl-5-((triisopropylsilyl)oxy)phenoxy)methyl)-2-((2-(trimethylsilyl)ethoxy)methoxy)phenyl)hept-3-en-2-ol (2.28)

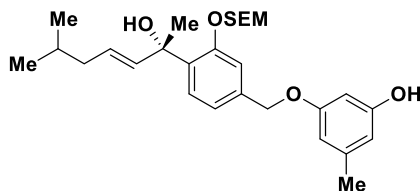
To a flame dried 6 dram vial equipped with a magnetic stir bar was added **2.27** (0.047 g, 0.08 mmol, 1.0 equiv), along with Grubbs II generation catalyst (0.007 g, 0.8 μ mol, 0.1 equiv). The vial was sealed with a septum and evacuated and backfilled with argon three times. To this DCM (0.5 mL, 0.15M) was added followed by 4-methylpentene (0.05 mL, 0.4 mmol, 5.0 equiv) and the resulting mixture was allowed to stir for 24 hours before being concentrated via rotary evaporator. Purification by preparative thin layer chromatography (PTLC) using a toluene: diethyl ether eluent system (7:1) afforded product as a colorless oil (0.034 g, 73% yield).

R_f = 0.69 (7:1 toluene: ether)

¹H NMR (600 MHz, Chloroform-*d*) δ 7.33 (d, J = 7.9 Hz, 1H), 7.21 (d, J = 1.5 Hz, 1H), 7.03 (ddd, J = 7.9, 1.7, 0.8 Hz, 1H), 6.40 (ddd, J = 2.2, 1.5, 0.7 Hz, 1H), 6.32 (ddd, J = 2.1, 1.4, 0.8 Hz, 1H), 6.29 (td, J = 2.3, 0.6 Hz, 1H), 5.78 (dt, J = 15.5, 1.3 Hz, 1H), 5.52 (dt, J = 15.5, 7.2 Hz, 1H), 5.27 (d, J = 1.6 Hz, 2H), 4.96 (s, 2H), 3.81 – 3.70 (m, 2H), 2.25 (s, 3H), 1.92 – 1.89 (m, 2H), 1.66 (s, 3H), 1.60 (hept, J = 6.8 Hz, 1H), 1.25 – 1.16 (m, 3H), 1.07 (d, J = 7.3 Hz, 18H), 1.00 – 0.94 (m, 2H), 0.86 (dd, J = 6.6, 3.3 Hz, 6H), 0.00 (s, 9H).

¹³C NMR (101 MHz, CDCl₃) δ 159.67, 157.03, 155.38, 140.01, 138.04, 137.76, 134.65, 127.01, 126.98, 120.73, 113.88, 113.78, 108.70, 104.05, 93.35, 74.57, 69.66, 66.95, 41.77, 28.54, 28.13, 22.51, 22.47, 21.80, 18.17, 18.08, 12.79, -1.26.

HRMS: ESI (m/z) calcd for $C_{27}H_{62}O_5ClSi_2$ $[M+Cl]^-$: 677.38298, found 677.38285.



(S,E)-3-((4-(2-hydroxy-6-methylhept-3-en-2-yl)-3-((2-(trimethylsilyl)ethoxy)methoxy)benzyl)oxy)-5-methylphenol (2.29)

A flame dried 6 dram vial equipped with a magnetic stirring bar containing **2.28** (0.055 g, 86 μ mol, 1.0 equiv) was evacuated and backfilled with argon three times. To this was added anhydrous THF (0.86 mL, 0.1M) and the resulting solution was cooled to 0°C. TBAF (0.13 mL, 0.13 mmol, 1.5 eq) was then slowly added and this was allowed to stir for 1 hour at 0°C. The reaction was quenched by the addition of saturated NH_4Cl . Water and ethyl acetate were added and the organic layer was separated. The aqueous layer was washed with water, brine, dried over anhydrous $MgSO_4$ and concentrated via rotary evaporator. Purification by silica column chromatography using a hexanes: ethyl acetate system (0-30%) afforded product as an amorphous solid (0.40 g, 95% yield).

R_f = 0.18 (4:1 hexanes: ethyl acetate)

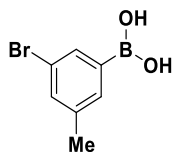
1H NMR (600 MHz, Chloroform- d) δ 7.35 (d, J = 7.9 Hz, 1H), 7.21 (s, 1H), 7.02 (d, J = 7.9 Hz, 1H), 6.36 (s, 1H), 6.25 (d, J = 16.7 Hz, 2H), 5.80 – 5.76 (m, 1H), 5.56 – 5.49 (m, 1H), 5.29 (s, 2H), 4.87 – 4.74 (m, 2H), 4.37 (s, 1H), 3.82 – 3.70 (m, 2H), 2.25 (s, 3H), 1.91 (t, J = 7.0 Hz, 2H), 1.68 (s, 3H), 1.63 – 1.56 (m, 1H), 1.00 – 0.94 (m, 2H), 0.89 – 0.84 (m, 6H), -0.01 (d, J = 1.1 Hz, 9H).

^{13}C NMR (101 MHz, CDCl_3) δ 160.00, 156.91, 155.33, 140.69, 137.80, 137.63, 134.54, 127.26, 127.09, 121.07, 114.18, 109.06, 108.41, 99.12, 93.29, 74.91, 69.56, 67.08, 41.74, 28.53, 27.99, 22.49, 21.72, 18.20, -1.28.

ν_{max} , cm^{-1} (film): 3321, 2953, 2898, 1594, 1148.

HRMS: APCI (m/z) calcd for $\text{C}_{28}\text{H}_{41}\text{O}_6\text{Si}$ [$\text{M}-\text{H}^+$]: 486.28015, found 485.27147.

$[\alpha]_{\text{D}}^{20} = -0.4$ (c 0.14, chloroform)



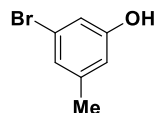
(3-bromo-5-methylphenyl)boronic acid (2.30)

To a flame dried 50 mL round bottom flask equipped with a magnetic stir bar was added 3,5-dibromotoluene (0.500 g, 2.0 mmol, 1.0 equiv). The flask was capped with a septum and evacuated and backfilled with argon three times. To this, THF (8 mL, 0.25M) was added and this solution was allowed to cool down to -78°C before addition of tert-butyllithium (1.17 mL, 2.0 mmol, 1.0 equiv). The resulting solution was allowed to stir for 30 mins at -78°C .

Triisopropylborate (0.553 mL, 2.4 mmol, 1.2 equiv) was then added and the solution was stirred for 3 hours. Saturated NH_4Cl was added and the solution was left to quench overnight. Product was extracted with ethyl acetate, washed with brine, dried over anhydrous MgSO_4 and concentrated on rotary evaporator to yield intended product without further purification (0.391 g, 91% yield). Spectra matched literature reports.⁶

$R_f = 0.16$ (2:1 hexanes: ethyl acetate)

$^1\text{H NMR}$ (399 MHz, Chloroform-*d*) δ 6.91 (tt, $J = 1.8, 0.7$ Hz, 1H), 6.82 (ddq, $J = 2.1, 1.8, 0.6$ Hz, 1H), 6.58 (ddt, $J = 2.1, 1.4, 0.7$ Hz, 1H), 2.28 (p, $J = 0.7$ Hz, 3H).

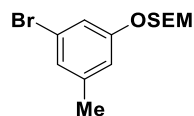


3-bromo-5-methylphenol (2.31)

To a flame dried 50 mL round bottom flask was added **2.30** (0.376 g, 1.75 mmol, 1.0 equiv) followed by potassium hydroxide (0.196 g, 3.5 mmol, 2.0 equiv) in water (7 mL, 0.5M). To this was added hydrogen peroxide (0.891 mL (30%wt), 8.75 mmol, 5.0 equiv) and the resulting was allowed to stir at room temperature for 1 hour. The reaction was brought to a pH of 7 using HCl (1M). Purification by silica column chromatography using a hexanes: ethyl acetate system (0-30%) afforded product as a peach colored solid (0.222 g, 68% yield). Spectra matched literature reports.⁶

$R_f = 0.50$ (2:1 hexanes: ethyl acetate)

$^1\text{H NMR}$ (399 MHz, Chloroform-*d*) δ 6.91 (tq, $J = 1.2, 0.7$ Hz, 1H), 6.82 (ddt, $J = 1.8, 1.3, 0.6$ Hz, 1H), 6.58 (ddq, $J = 2.0, 1.3, 0.7$ Hz, 1H), 2.28 (h, $J = 0.6$ Hz, 3H).



(2-((3-bromo-5-methylphenoxy)methoxy)ethyl)trimethylsilane (2.32)

To a base bathed and flamed dried 15 mL round bottom flask was added NaH as a 60% mineral oil suspension (0.138 g, 3.45 mmol, 1.5 equiv). The flask was capped with a septum and evacuated and backfilled with argon three times. To this, THF (2.16 mL, 1.6M) was added and the resulting mixture was cooled to 0°C. A solution of **2.31** (0.430 g, 2.3 mmol, 1.0 equiv) in THF (1.8 mL, 1.3M) was added slowly dropwise and this solution was allowed to stir for one hour at 0°C. A solution of SEMCl (0.488 mL, 2.76 mmol, 1.2 equiv) in THF (0.92 mL, 3M) and the resulting solution was allowed to warm up to room temperature and stir overnight. Crude product was extracted with ethyl acetate, washed with brine, dried over MgSO₄ and concentrated via rotary evaporator. Purification by silica column chromatography using a hexanes: ethyl acetate system (0-20%) afforded product as a clear oil (0.582g, 80% yield).

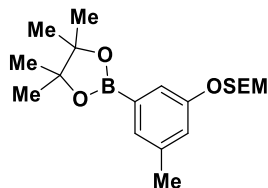
R_f = 0.61 (4:1 hexanes: ethyl acetate)

¹H NMR (500 MHz, Chloroform-d) δ 7.02 (td, J = 2.2, 0.6 Hz, 1H), 6.96 (tt, J = 1.5, 0.7 Hz, 1H), 6.78 (ddt, J = 2.2, 1.5, 0.7 Hz, 1H), 5.18 (d, J = 0.6 Hz, 2H), 3.76 – 3.71 (m, 2H), 2.29 (t, J = 0.7 Hz, 2H), 0.99 – 0.93 (m, 2H), 0.00 (d, J = 0.6 Hz, 9H).

¹³C NMR (126 MHz, CDCl₃) δ 158.20, 141.16, 125.64, 122.47, 116.76, 115.95, 93.04, 66.53, 21.41, 18.18, -1.28.

ν_{max}, cm⁻¹ (film): 2952, 2922, 2898, 1248, 856.

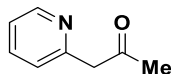
HRMS: APCI (*m/z*) calcd for C₁₃H₂₀BrO₂Si [M-H⁺]: 316.04942, found 315.04155.



trimethyl(2-((3-methyl-5-(4,4,5,5-tetramethyl-1,3,2-dioxaborolan-2-yl)phenoxy)methoxy)ethyl)silane (2.33)

To a flame dried flask equipped with a magnetic stir bar was added **2.32** (0.644 g, 2.03 mmol, 1.0 equiv), B₂pin₂ (1.29 g, 5.08 mmol, 2.5 equiv) and KOAc (0.996 g, 10.15 mmol, 5.0 equiv). The flask was with argon three times then 1,4-dioxane (169 mL) was added. This mixture was sparged while stirring with argon for 10 minutes prior to the addition of Pd(dppf)Cl₂•DCM (0.149 g, 0.203 mmol, 0.1 equiv). The vessel was recapped and the mixture was sparged with argon for an additional 10 minutes. The flask was then sealed, heated to 100°C and left to stir overnight. The resulting mixture was diluted with ethyl acetate and washed with water. The aqueous layer was washed ethyl acetate (3 x 50 mL), washed with brine, dried over MgSO₄ and concentrated *in vacuo*. The residue was purified by silica gel chromatography using a hexanes: ethyl acetate solvent system (0-25%) to afford the desired boronate ester as a clear oil (0.576 g, 78% yield).

¹H NMR: (600 MHz, Chloroform-*d*) δ 7.02 (ddd, *J* = 2.4, 1.8, 0.6 Hz, 1H), 6.95 (ddd, *J* = 2.5, 1.6, 0.7 Hz, 1H), 6.77 (ddd, *J* = 2.2, 1.4, 0.7 Hz, 1H), 5.17 (s, 2H), 3.78 – 3.74 (m, 2H), 2.29 (q, *J* = 0.7 Hz, 2H), 1.33 (s, 12H), 0.00 (s, 9H).



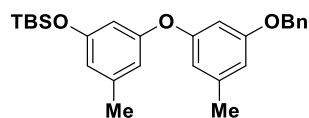
1-(pyridin-2-yl)propan-2-one (2.34)

To a flame dried base bathed and argon purged 250 mL round bottom flask was added 2-methylpyridine (2.96 mL, 32 mmol, 1.0 equiv). To this THF (60 mL) was added and the resulting solution was cooled to 0°C. Afterwards *n*-BuLi (32 mmol, 1.0 equiv) was added dropwise and the reaction was stirred for 45 min at 0 °C. Acetonitrile (1.56 mL, 3.32 mmol, 1.0 equiv) was added dropwise and the mixture was allowed to warm to room temperature and stir for 3 hours. Crude product was extracted with 30 ml of 3N-sulfuric acid, then washed with diethyl ether (2 x 25 mL). The resulting solution was made alkaline with 2M NaOH, then extracted once again with DCM (2 x 25 mL). The organic layer was dried over MgSO₄ and concentrated *in vacuo*. Crude product was purified by column chromatography using a hexanes to ethyl acetate gradient (10-40%) to afford intended product as a yellow oil (1.77 g, 41% yield).

This is a known compound and spectra matches literature reports. ⁷

R_f = (0.13 3:1 hexanes: ethyl acetate)

¹H NMR (399 MHz, Chloroform-*d*) δ 8.57 (d, *J* = 4.9 Hz, 1H), 7.66 (td, *J* = 7.7, 1.8 Hz, 4H), 7.24 – 7.16 (m, 8H), 3.92 (s, 8H), 2.23 (s, 8H).

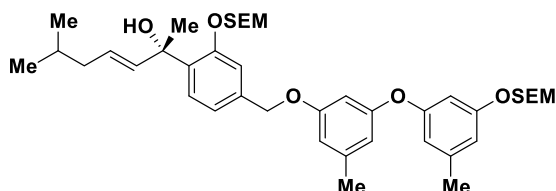
**1-bromo-3-(3-methoxy-5-methylphenoxy)-5-methylbenzene (2.9.5)**

To a flame dried vial equipped with Teflon coated metal stir bar were added **2.18** (0.205 g, 0.86 mmol, 2.0 equiv), **2.51** (0.139 g, 0.43 mmol, 1.0 equiv), boric acid (0.053 g, 0.86 mmol, 2

equiv), copper(II) acetate (0.080 g, 0.44 mmol, 1.0 equiv), and 4Å MS (200 mg) in anhydrous acetonitrile under argon. The vial was sealed and heated to reflux for 24 hours. The solution was cooled to room temperature, diluted with methylene chloride, and filtered over celite. The filtrate was washed with brine, dried over MgSO_4 , and concentrated *in vacuo*. The title compound was purified on silica column chromatography using a hexanes: ethyl acetate solvent system (0-20%) and isolated as a clear yellow oil (0.099 g, 53% yield).

$R_f = 0.63$ (4:1 hexanes: ethyl acetate)

$^1\text{H NMR}$: (400 MHz, CHCl_3) δ 7.42 – 7.34 (m, 5H), 6.53 (dd, $J = 2.1, 1.2$ Hz, 1H), 6.43 (t, $J = 2.2$ Hz, 1H), 6.40 (tq, $J = 2.0, 0.7$ Hz, 2H), 6.31 (ddd, $J = 2.8, 2.0, 0.6$ Hz, 1H), 4.98 (s, 2H), 2.27 (s, 3H), 2.24 (s, 3H), 0.94 (s, 9H), 0.16 (s, 6H).



(S,E)-6-methyl-2-(4-((3-methyl-5-(3-methyl-5-((2-(trimethylsilyl)ethoxy)methoxy)phenoxy)methyl)-2-((2-(trimethylsilyl)ethoxy)methoxy)phenyl)hept-3-en-2-ol (2.35)

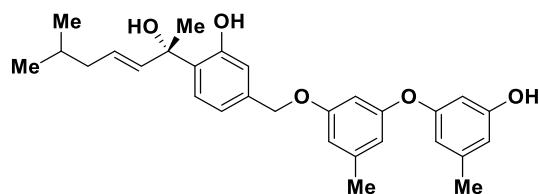
In a 1 dram vial equipped with a magnetic stir bar was added **2.29** (6 mg, 0.001 mmol, 1.00 equiv.), $\text{Pd}_2(\text{dba})_3$ (0.5 mg, 0.5 μmol , 4.00 mol%) and tBuXPhos (0.8 mg, 2 μmol , 16.0 mol%) under an argon atmosphere. These solids were dissolved in anhydrous dioxane (0.15 mL) at

room temperature. Then, crushed $\text{K}_3\text{PO}_4 \cdot \text{H}_2\text{O}$ (9 mg, 0.04 mmol, 3.00 equiv.) and **2.32** (5 mg, 0.012 mmol, 1.20 equiv.) were added, the vessel was sealed and the mixture stirred at 100 °C for 16 h. Then, water (1 mL) was added and the mixture extracted with diethyl ether (3×1 mL), dried over MgSO_4 , filtered and the solvent was removed *in vacuo*. The residue was purified by column chromatography using a hexanes: ethyl acetate system (0-20%) to yield **2.35** as colourless oil (6.4 mg, 70% yield). *This intermediate was found to be unstable.

$R_f = 0.55$ (4:1 hexanes: ethyl acetate)

^1H NMR: (500 MHz, Chloroform- d) δ 7.34 (d, $J = 7.9$ Hz, 1H), 7.22 (d, $J = 1.6$ Hz, 1H), 7.05 – 7.00 (m, 1H), 6.61 (ddt, $J = 2.2, 1.4, 0.8$ Hz, 1H), 6.54 (ddt, $J = 2.2, 1.4, 0.8$ Hz, 1H), 6.52 (t, $J = 2.2$ Hz, 1H), 6.46 (d, $J = 2.1$ Hz, 2H), 6.44 (dq, $J = 2.1, 1.0$ Hz, 1H), 5.78 (dq, $J = 15.5, 1.2$ Hz, 1H), 5.52 (dt, $J = 15.7, 7.1$ Hz, 1H), 5.27 (s, 2H), 5.17 (s, 2H), 4.95 (s, 2H), 4.17 (s, 1H), 3.83 – 3.69 (m, 4H), 2.28 (s, 6H), 1.90 (tt, $J = 7.0, 0.8$ Hz, 2H), 1.66 (s, 3H), 1.60 (dq, $J = 13.6, 6.9$ Hz, 1H), 1.01 – 0.91 (m, 4H), 0.86 (ddd, $J = 6.6, 2.8, 0.7$ Hz, 6H), -0.00 (dd, $J = 2.6, 0.7$ Hz, 18H).

HRMS: ESI (m/z) calcd for $\text{C}_{41}\text{H}_{62}\text{O}_7\text{ClSi}_2$ $[\text{M}+\text{Cl}]^-$: 757.37281, found 756.36921



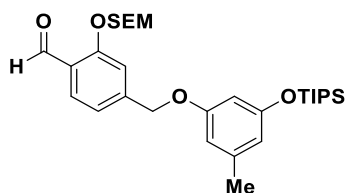
(S,E)-5-((3-(3-hydroxy-5-methylphenoxy)-5-methylphenoxy)methyl)-2-(2-hydroxy-6-methylhept-3-en-2-yl)phenol (2.36)

A flame dried 6 dram vial equipped with a magnetic stir bar was evacuated and backfilled with argon three times. To this was added a solution of **2.35** (2.5 mg, 3.5 μ mol, 1.0 equiv) in DMPU (0.3 mL, 0.01 M) and along with TBAF (55 μ L, 55 μ mol, 16.0 equiv) and this mixture was allowed to stir for 1.5 hours at 80°C. Water and diethyl ether were added to quench the reaction and the organic layer was separated. The aqueous layer was washed with water, brine, dried over anhydrous MgSO_4 and concentrated via rotary evaporator. Purification by silica column chromatography using a hexanes: diethyl ether system (0-50%) afforded product as a colorless oil (1.2 mg, 76% yield). *This intermediate was found to be unstable in ambient conditions.

R_f = 0.15 (4:1 hexanes : ethyl acetate)

^1H NMR: (500 MHz, Chloroform- d) δ 8.88 (s, 1H), 7.03 (d, J = 7.9 Hz, 1H), 6.89 (d, J = 1.7 Hz, 1H), 6.87 – 6.83 (m, 1H), 6.54 (t, J = 1.8 Hz, 1H), 6.45 – 6.43 (m, 1H), 6.43 – 6.42 (m, 2H), 6.41 (td, J = 1.6, 0.8 Hz, 1H), 6.23 (t, J = 2.3 Hz, 1H), 5.81 – 5.74 (m, 1H), 5.69 (dt, J = 15.3, 6.7 Hz, 1H), 4.94 (s, 2H), 2.28 (s, 4H), 2.27 (s, 5H), 1.97 (t, J = 6.9 Hz, 3H), 1.72 (s, 3H), 1.65 (dt, J = 13.4, 6.7 Hz, 1H), 0.89 (dd, J = 6.7, 2.1 Hz, 6H).

HRMS: APCI (m/z) calcd for $\text{C}_{29}\text{H}_{33}\text{O}_5$ [$\text{M}-\text{H}^+$]: 461.23207, found 461.23335



4-((3-methyl-5-((triisopropylsilyl)oxy)phenoxy)methyl)-2-((2-(trimethylsilyl)ethoxy)methoxy)benzaldehyde (2.37)

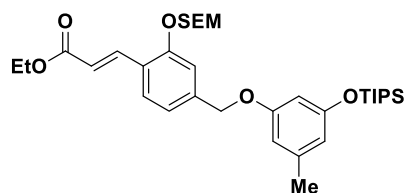
To a flamed dried vial was added **2.23** (0.248 g, 0.416 mmol, 1.0 equiv). This vial was then capped with septa and evacuated and backfilled with argon three times. Anhydrous THF (4.16 mL, 0.1 M) was then added and the resulting solution was cooled to -78°C with a dry ice acetone bath. TMEDA was then added (0.016 mL, 0.125 mmol, 1.25 equiv) followed by *n*-BuLi (1.25 eq, 60 μmL , 0.125 mmol) and this mixture was allowed to stir at -78°C for 1.5 hours. To this, DMF (0.059 mL, 0.624 mmol, 1.5 equiv) was added and the resulting mixture was allowed to warm to room temperature and stirred for 1 hour. The reaction was quenched by the addition of saturated NH_4Cl . Water and ethyl acetate were added and the organic layer was separated. The organic layer was separated and the aqueous layer was washed with ethyl acetate three times. Combined organic layers were washed with brine, dried over MgSO_4 and concentrated via rotary evaporator. Purification by silica column chromatography using a hexanes: ethyl acetate solvent system (0-20%) afforded product as a colorless oil (0.227, 80% yield).

$R_f = 0.49$ (4:1 hexanes: ethyl acetate)

^1H NMR: (500 MHz, CHCl_3 -d) δ 10.46 (d, $J = 0.8$ Hz, 1H), 7.84 (d, $J = 7.9$ Hz, 1H), 7.29 (s, 1H), 7.12 (dp, $J = 7.9, 0.7$ Hz, 1H), 6.40 (ddt, $J = 2.3, 1.6, 0.8$ Hz, 1H), 6.34 (ddt, $J = 2.2, 1.5, 0.7$ Hz, 1H), 6.27 (t, $J = 2.3$ Hz, 1H), 5.34 (s, 2H), 5.04 (s, 2H), 3.81 – 3.77 (m, 2H), 2.26 (s, 3H), 1.25 – 1.15 (m, 3H), 1.07 (d, $J = 7.4$ Hz, 18H), 1.01 – 0.93 (m, 2H), 0.00 (d, $J = 0.7$ Hz, 9H).

^{13}C NMR: (101 MHz, CDCl_3) δ 189.55, 160.27, 159.25, 157.08, 146.12, 140.17, 128.73, 124.92, 120.17, 114.06, 113.48, 108.77, 104.03, 93.31, 69.36, 67.12, 21.79, 18.17, 18.05, 12.78, -1.28.

HRMS: APCI (m/z) calcd for $\text{C}_{30}\text{H}_{49}\text{O}_5\text{Si}_2$ [$\text{M}-\text{H}^+$]: 545.3113, found 545.31113.



ethyl (E)-3-(4-((3-methyl-5-((triisopropylsilyl)oxy)phenoxy)methyl)-2-((2-(trimethylsilyl)ethoxy)methoxy)phenyl)acrylate (2.38)

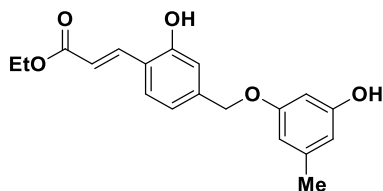
To a stirred solution of ethyl diethylphosphonoacetate (0.087 g, 0.39 mmol, 1.3 equiv) in THF (1.3 mL, 0.3M) was added NaH (60% in mineral oil, 0.160 g, 0.39 mmol, 1.3 equiv) at 0°C under argon atmosphere. After stirring for 30 min at room temperature, **2.37** (0.163 g, 0.3 mmol, 1.0 eq) in THF (0.75 mL, 0.4 M) was slowly added. The resultant mixture was stirred for 1 hour at room temperature, quenched with water and extracted with EtOAc. The organic layer was washed with water and brine, dried over MgSO₄ and concentrated *in vacuo*. The resultant residue was purified by column chromatography on silica gel chromatography using a hexanes to ethyl acetate system (0-20%) to yield **2.38** as a pale yellow oil (0.148 g, 80% yield).

R_f = 0.49 (4:1 hexanes: ethyl acetate)

¹H NMR: (400 MHz, Chloroform-*d*) δ 8.00 (d, *J* = 16.2 Hz, 1H), 7.52 (d, *J* = 8.0 Hz, 1H), 7.23 (d, *J* = 1.1 Hz, 1H), 7.07 – 7.04 (m, 1H), 6.50 (d, *J* = 16.2 Hz, 1H), 6.40 (ddt, *J* = 3.0, 2.3, 1.2 Hz, 1H), 6.33 (ddd, *J* = 2.2, 1.4, 0.7 Hz, 1H), 6.27 (t, *J* = 2.3 Hz, 1H), 5.30 (s, 2H), 4.99 (s, 2H), 4.27 (q, *J* = 7.1 Hz, 2H), 3.81 – 3.74 (m, 2H), 2.26 (s, 3H), 1.34 (t, *J* = 7.1 Hz, 3H), 1.25 – 1.15 (m, 3H), 1.07 (d, *J* = 7.2 Hz, 18H), 0.99 – 0.91 (m, 2H), 0.00 (s, 9H).

¹³C NMR: (101 MHz, CDCl₃) δ 167.59, 159.47, 157.04, 156.55, 141.18, 140.09, 139.74, 128.72, 123.69, 120.55, 118.86, 113.90, 113.67, 108.77, 104.04, 93.24, 69.60, 66.80, 60.53, 21.80, 18.16, 18.06, 14.52, 12.79, -1.27.

HRMS: APCI (m/z) calcd for $C_{34}H_{55}O_6Si_2$ $[M-H^+]$: 615.35317, found 615.35307.



ethyl (E)-3-(2-hydroxy-4-((3-hydroxy-5-methylphenoxy)methyl)phenyl)acrylate (2.39)

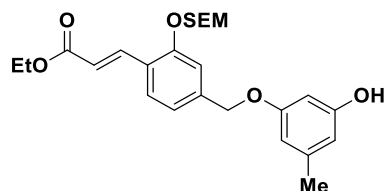
A flame dried 5 dram vial equipped with a magnetic stir bar was evacuated and backfilled with argon three times. To this was added a solution of **2.38** (13 mg, 19 μ mol, 1.0 equiv) in DMPU (0.19 mL, 0.01 M) along with TBAF (0.30 mL, 0.30 mmol, 16.0 equiv) this mixture was allowed to stir for 1.5 hours at 80°C. Water and diethyl ether were added to quench the reaction and the organic layer was separated. The aqueous layer was washed with water, brine, dried over anhydrous $MgSO_4$ and concentrated via rotary evaporator. Purification by silica column chromatography using a hexanes: diethyl ether system afforded product as an orange solid (10 mg, 78% yield). *This intermediate was found to be relatively unstable in deuterated solvents other than acetone.

R_f = 0.11 (4:1 hexanes: ethyl acetate)

1H NMR: (600 MHz, Acetone- d_6) δ 9.19 (s, 1H), 8.21 (s, 1H), 7.98 (d, J = 16.2 Hz, 1H), 7.62 (d, J = 8.0 Hz, 1H), 7.05 (s, 1H), 6.98 (d, J = 8.9 Hz, 1H), 6.62 (d, J = 16.1 Hz, 1H), 6.32 (ddt, J = 2.2, 1.5, 0.7 Hz, 1H), 6.28 (ddt, J = 2.1, 1.4, 0.7 Hz, 1H), 6.27 (td, J = 2.2, 0.6 Hz, 1H), 5.02 (s, 2H), 4.20 (q, J = 7.1 Hz, 2H), 2.20 (s, 3H), 1.28 (t, J = 7.1 Hz, 3H).

^{13}C NMR: (101 MHz, Acetone- d_6) δ 206.16, 167.59, 160.79, 159.31, 157.46, 142.64, 140.83, 140.40, 129.90, 121.66, 119.54, 118.79, 115.45, 109.79, 107.70, 100.26, 69.56, 60.57, 21.64, 14.67.

HRMS: APCI (m/z) calcd for $\text{C}_{19}\text{H}_{21}\text{O}_5$ $[\text{M}+\text{H}]^+$: 329.13835, found 329.13804.



ethyl (E)-3-(4-((3-hydroxy-5-methylphenoxy)methyl)-2-((2-(trimethylsilyl)ethoxy)methoxy)phenyl)acrylate (2.40)

A flame dried 6 dram vial containing **2.38** (0.049 g, 80 μmol , 1.0 eq) was evacuated and backfilled with argon three times. To this was added anhydrous THF (0.8 mL, 0.1M) and the resulting solution was cooled to 0°C . TBAF (0.13 mL, 0.12 mmol, 1.5 eq) was then slowly added and this was allowed to stir for 1 hour at 0°C . The reaction was quenched by the addition of saturated NH_4Cl . Water and ethyl acetate were added and the organic layer was separated. The aqueous layer was washed with water, brine, dried over anhydrous MgSO_4 and concentrated via rotary evaporator. Purification by silica column chromatography using a hexanes: ethyl acetate system (0-30%) afforded product as a clear oil (0.367 g, 99% yield).

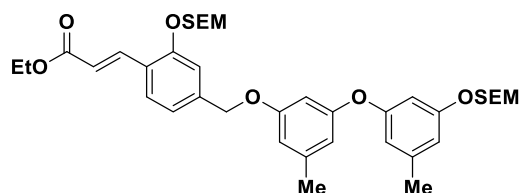
R_f = 0.24 (4:1 hexanes: ethyl acetate)

^1H NMR: (600 MHz, Chloroform- d) δ 8.00 (d, J = 16.2 Hz, 1H), 7.53 (d, J = 8.0 Hz, 1H), 7.23 (d, J = 1.6 Hz, 1H), 7.07 – 7.04 (m, 1H), 6.50 (d, J = 16.2 Hz, 1H), 6.38 (tt, J = 1.5, 0.7 Hz, 1H),

6.34 – 6.17 (m, 2H), 5.31 (s, 2H), 5.00 (s, 2H), 4.26 (q, $J = 7.1$ Hz, 2H), 3.94 – 3.65 (m, 2H), 2.27 (s, 3H), 1.34 (t, $J = 7.1$ Hz, 3H), 1.04 – 0.90 (m, 2H), -0.00 (s, 9H).

^{13}C NMR: (101 MHz, CDCl_3) δ 167.64, 159.78, 156.74, 156.36, 140.87, 140.59, 139.71, 128.67, 123.60, 120.51, 118.73, 113.66, 109.10, 108.13, 99.50, 93.05, 69.50, 66.70, 60.51, 21.62, 18.03, 14.37, -1.41.

HRMS: ESI (m/z) calcd for $\text{C}_{24}\text{H}_{34}\text{O}_6\text{ClSi}$ $[\text{M}+\text{Cl}]^-$: 493.18187, found 493.18241.



ethyl (E)-3-(4-((3-methyl-5-(3-methyl-5-((2-(trimethylsilyl)ethoxy)methoxy)phenoxy)phenoxy)methyl)-2-((2-(trimethylsilyl)ethoxy)methoxy)phenyl)acrylate (2.41)

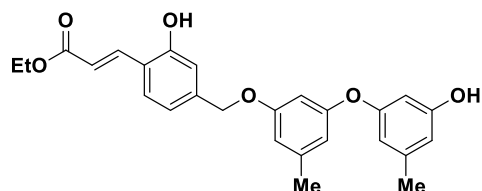
Under an argon atmosphere **2.40** (26 mg, 57 μmol , 1.00 equiv.), $\text{Pd}_2(\text{dba})_3$ (2.1 mg, 2.3 μmol , 4.00 mol%) and tBuXPhos (3.9 mg, 9.1 μmol , 16.0 mol%) were dissolved in anhydrous dioxane (0.3 mL) at room temperature. Then, crushed $\text{K}_3\text{PO}_4 \cdot \text{H}_2\text{O}$ (39 mg, 0.17 mmol, 3.00 equiv.) and **2.32** (22 mg, 0.022 μmol , 1.20 equiv.) were added, the vessel was sealed and the mixture stirred at 100 $^\circ\text{C}$ for 16 h. Then, water (1 mL) was added and the mixture extracted with diethyl ether (3 \times 1 mL), dried over MgSO_4 , filtered and the solvent was removed *in vacuo*. The residue was purified by column chromatography using a hexanes: ethyl acetate system (0-20%) to yield **2.41** as colorless oil (24 mg, 62%).

R_f = 0.55 (4:1 hexanes: ethyl acetate)

¹H NMR: (600 MHz, Chloroform-*d*) δ 8.00 (d, *J* = 16.2 Hz, 1H), 7.52 (d, *J* = 8.0 Hz, 1H), 7.22 (d, *J* = 1.6 Hz, 1H), 7.09 – 6.99 (m, 1H), 6.61 (ddt, *J* = 2.2, 1.4, 0.7 Hz, 1H), 6.54 (td, *J* = 1.8, 0.7 Hz, 1H), 6.52 – 6.51 (m, 1H), 6.44 (ddt, *J* = 3.2, 1.4, 0.7 Hz, 3H), 5.30 (s, 2H), 5.16 (s, 2H), 4.98 (s, 2H), 4.26 (q, *J* = 7.2 Hz, 2H), 3.82 – 3.70 (m, 4H), 2.29 – 2.28 (m, 3H), 2.28 – 2.27 (m, 3H), 1.34 (td, *J* = 7.2, 0.6 Hz, 3H), 0.97 – 0.92 (m, 4H), -0.01 (s, 18H).

¹³C NMR: (101 MHz, CDCl₃) δ 167.57, 159.78, 158.62, 158.25, 157.99, 156.51, 140.72, 140.68, 139.69, 128.76, 123.82, 120.68, 118.96, 113.84, 113.12, 112.52, 111.95, 110.78, 104.76, 103.05, 93.23, 93.04, 69.75, 67.24, 66.81, 66.40, 60.54, 29.85, 21.78, 18.17, 14.52, 14.27, -1.27.

HRMS: ESI (*m/z*) calcd for C₃₈H₅₄O₈ClSi₂ [M+Cl]⁻: 729.30512, found 729.30476.



ethyl (E)-3-(2-hydroxy-4-((3-(3-hydroxy-5-methylphenoxy)-5-methylphenoxy)methyl)phenyl)acrylate (2.42)

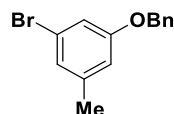
A flame dried 6 dram vial equipped with a magnetic stir bar was evacuated and backfilled with argon three times. To this was added a solution of **2.41** (1.0 eq, 13 mg, 19 μmol) in DMPU (0.19 mL, 0.01 M) along with TBAF (0.30 mL, 0.30 mmol, 16.0 eq) this mixture was allowed to stir for 1.5 hours at 80°C. Water and diethyl ether were added to quench the reaction and the organic layer was separated. The aqueous layer was washed with water, brine, dried over anhydrous

MgSO₄ and concentrated via rotary evaporator. Purification by silica column chromatography using a hexanes: diethyl ether system (0-50%) afforded product as a colorless oil (7.3 mg, 85% yield). *This intermediate was found to degrade rapidly in deuterated solvents.

R_f = 0.33 (1:1 hexanes: ethyl acetate)

¹H NMR: (600 MHz, Chloroform-*d*) δ 7.95 (d, *J* = 16.1 Hz, 1H), 7.45 (d, *J* = 7.9 Hz, 1H), 6.93 (dd, *J* = 8.0, 1.6 Hz, 1H), 6.84 (d, *J* = 1.5 Hz, 1H), 6.57 (d, *J* = 16.3 Hz, 1H), 6.51 (tq, *J* = 1.4, 0.7 Hz, 1H), 6.45 (ddt, *J* = 2.2, 1.4, 0.7 Hz, 1H), 6.44 – 6.38 (m, 3H), 6.27 (t, *J* = 2.3 Hz, 1H), 6.14 (s, 1H), 5.16 (s, 1H), 4.95 (s, 2H), 4.27 (q, *J* = 7.2 Hz, 2H), 2.28 (s, 3H), 2.26 (s, 3H), 1.34 (t, *J* = 7.1 Hz, 3H).

HRMS: ESI (*m/z*) calcd for C₂₆H₂₅O₆ [M-H]⁻: 433.16566, found 433.16461



1-(benzyloxy)-3-bromo-5-methylbenzene (2.47)

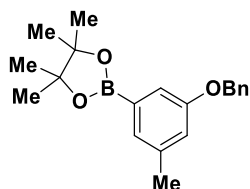
To a two necked flame dried 25 mL flask equipped with a magnetic stir bar was weighed **2.31** (0.500 g, 2.67 mmol, 1.0 equiv) and potassium carbonate (1.11 g, 8.02 mmol, 3.0 equiv). This flask was equipped with a reflux condenser then evacuated and backfilled with argon three times. To this was added MeCN (10.7 mL) from a drisolve bottle and the resulting solution was allowed to stir for 10 minutes. Lastly, benzyl bromide (0.480 g, 0.334 mL, 2.81 mmol, 1.05 equiv) was added via syringe and the resulting solution was heated to reflux and stirred for 20 hours. After stirring, the solution was allowed to cool to room temperature and water was added

to quench the solution. Crude product was extracted with ethyl acetate, washed with brine, dried over MgSO_4 and concentrated via rotary evaporator. Purification by silica column chromatography using a hexanes: ethyl acetate system (0-20%) afforded product as a clear non-viscous oil (0.589, 77% yield).

$R_f = 0.67$ (4:1 hexanes: ethyl acetate)

^1H NMR (^1H NMR (600 MHz, Chloroform-*d*) δ 7.44 – 7.37 (m, 4H), 7.37 – 7.32 (m, 1H), 6.97 – 6.94 (m, 1H), 6.95 (td, $J = 1.6, 0.7$ Hz, 1H), 6.73 (ddd, $J = 2.3, 1.5, 0.8$ Hz, 1H), 5.02 (s, 2H), 2.30 (d, $J = 0.7$ Hz, 3H).

^{13}C NMR (151 MHz, CDCl_3) δ 159.56, 141.22, 136.67, 128.77, 128.25, 127.63, 124.99, 122.62, 115.21, 114.92, 70.29, 21.44.



2-(3-(benzyloxy)-5-methylphenyl)-4,4,5,5-tetramethyl-1,3,2-dioxaborolane (2.48)

To a flame dried flask equipped with a magnetic stir bar was added **2.47** (0.366 g, 1.32 mmol, 1.0 equiv), B_2pin_2 (0.839 g, 3.30 mmol, 2.5 equiv) and KOAc (0.647 g, 6.60 mmol, 5.0 equiv). The flask was with argon three times then 1,4-dioxane (169 mL) was added. This mixture was sparged while stirring with argon for 10 minutes prior to the addition of $\text{Pd}(\text{dppf})\text{Cl}_2 \cdot \text{DCM}$ (0.097 g, 0.132 mmol, 0.1 equiv). The vessel was recapped and the mixture was sparged with argon for an additional 10 minutes. The flask was then sealed, heated to 100°C and left to stir

overnight. The resulting mixture was diluted with ethyl acetate and washed with water. The aqueous layer was washed ethyl acetate (3 x 50 mL), washed with brine, dried over MgSO_4 and concentrated *in vacuo*. The residue was purified by silica gel chromatography using a hexanes: ethyl acetate solvent system (0-25%) to afford the desired boronate ester as a sticky yellow oil (0.261 g, 61% yield).

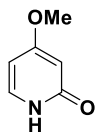
R_f = (0.73 1:1 hexanes: ethyl acetate)

^1H NMR: (600 MHz, Chloroform-*d*) δ 7.48 – 7.43 (m, 2H), 7.43 – 7.37 (m, 2H), 7.36 – 7.31 (m, 1H), 7.29 – 7.25 (m, 2H), 6.96 – 6.91 (m, 1H), 5.08 (s, 2H), 2.34 (s, 3H), 1.35 (s, 12H).

^{13}C NMR: (101 MHz, CDCl_3) δ 158.62, 139.14, 137.42, 128.64, 128.44, 127.97, 127.68, 119.59, 116.87, 83.95, 70.04, 25.01, 21.39.

HRMS: APCI (m/z) calcd for $\text{C}_{20}\text{H}_{26}\text{O}_3\text{B}$ [$\text{M}+\text{H}^+$]: 324.20058, found 324.20031

4.3.2 Chapter 3

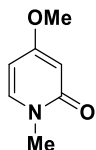


4-methoxypyridin-2(1H)-one (3.6)

To a flame dried 500 mL 3 necked round bottom flask was added 4-methoxypyridine-1-oxide (5.00 g, 40.0 mmol, 1.0 equiv) as a solid. The flask was equipped with a reflux condenser then was capped then filled and backfilled with argon three times. Acetic anhydride (148 mL) was added and the solution was heated to reflux under an argon atmosphere for 24 hours. As it stirs the reaction should turn dark brown/ black in color. After cooling to room temperature the crude mixture was concentrated under reduced pressure to remove excess acetic anhydride. The black residue was redissolved in 100 mL of a H₂O : MeOH (1:1) solution and stirred for 24 hours. The resulting solution was concentrated under reduced pressure then purified by silica gel chromatography (0-10% MeOH in DCM) to afford a brown solid as the intended product.

¹H NMR: (400 MHz, Chloroform-*d*) δ 13.00 (s, 1H), 7.21 (d, J = 7.3 Hz, 1H), 5.96 (dd, J = 7.3, 2.5 Hz, 1H), 5.87 (d, J = 2.5 Hz, 1H), 3.77 (s, 3H).

¹³C NMR: (101 MHz, CDCl₃) δ 169.90, 167.56, 134.73, 101.34, 97.18, 55.50.



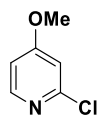
4-methoxy-1-methylpyridin-2(1H)-one (3.7)

To a flame dried 50 mL 3 necked flask was added **3.6** (900 mg, 7.19 mmol, 1.0 equiv) and potassium carbonate (1.99 g, 14.4 mmol, 2 equiv). The flask was equipped with a reflux condenser and purged with argon three times. DMF (20.8 mL) was added and the mixture was allowed to stir for 5 minutes. Methyl iodide (1.53 g, 675 μ L, 10.8 mmol, 1.5 equiv) was added dropwise and the solution was allowed to stir overnight at 60°C. The following day additional methyl iodide (751 mg, 225 μ L, 3.6 mmol, 0.5 equiv) was added and the solution was allowed to continue stirring at 60°C for another 6 hours. The reaction was cooled to room temperature and potassium carbonate was filtered off and washed 3 times with DCM (3x10 mL). All filtrate was collected and concentrated under reduced pressure. The crude mixture was then purified by silica gel chromatography (0-10% MeOH in DCM) to afford an orange brown solid as the intended product.

R_f = 0.51 (9:1 DCM: MeOH)

¹H NMR: (400 MHz, Chloroform-*d*) δ 7.10 (d, *J* = 7.4 Hz, 1H), 6.01 – 5.71 (m, 2H), 3.73 (s, 3H), 3.45 (s, 3H).

¹³C NMR: (101 MHz, CDCl₃) δ 168.24, 164.62, 138.07, 100.70, 97.25, 55.51, 36.82.



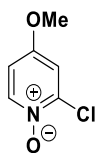
2-chloro-4-methoxypyridine (3.9)

To a flame dried 250 mL round bottom flask equipped with a magnetic stir bar was added **3.7** (2.86 g, 22.8 mmol, 1.0 equiv) followed by POCl₃ (28 mL). The flask was purged with argon and heated at 95 °C for 16 hours. Excess POCl₃ was removed *in vacuo* and the residue was

cooled with an ice bath then neutralized slowly with saturated sodium bicarbonate. This aqueous solution was extracted three times with ethyl acetate (3x 100 mL), washed with brine, dried over MgSO_4 then concentrated *in vacuo*. Product was purified via silica gel chromatography using (10-30% hexanes: ethyl acetate) to obtain intended product as amber oil (2.29 g, 70% yield). This compound is known in the literature matches reported spectra.⁸

^1H NMR: (400 MHz, Chloroform-*d*) δ 8.07 (td, $J = 5.7, 2.6$ Hz, 1H), 6.73 (dt, $J = 5.8, 2.3$ Hz, 1H), 6.66 (ddd, $J = 5.5, 4.1, 2.5$ Hz, 1H), 3.78 – 3.72 (m, 4H).

^{13}C NMR: (101 MHz, CDCl_3) δ 167.22, 152.43, 150.11, 109.66, 109.39, 55.55.



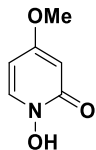
2-chloro-4-methoxypyridine 1-oxide (3.10)

To a flame dried 250 mL flask was added *m*-chloroperoxybenzoic acid (7.21 g, 41.8 mmol, 2.0 equiv) then dry DCM (42 mL) was added. To this solution was added **3.9** (3.00 g, 20.9 mmol, 1.00 equiv). This was allowed to stir at room temperature for 40 hours. A saturated solution of Na_2CO_3 was added and the biphasic solution was stirred for 30 minutes. Crude product was then extracted with DCM, extracts were dried with MgSO_4 , and concentrated via rotovap. The residue was purified on a silica gel plug (CH_2Cl_2 then acetone) to give 2.1 g (63%) the intended *N*-oxide as an off white solid.

$R_f = 0.37$ (9:1 DCM: MeOH)

¹H NMR: (400 MHz, Chloroform-*d*) δ 8.21 (d, $J = 7.4$ Hz, 1H), 6.99 (d, $J = 3.4$ Hz, 1H), 6.77 (dd, $J = 7.4, 3.4$ Hz, 1H), 3.84 (s, 3H).

¹³C NMR: (101 MHz, CDCl₃) δ 157.35, 142.58, 140.86, 111.95, 111.38, 56.50.

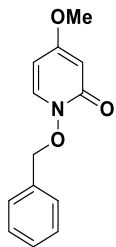


1-hydroxy-4-methoxypyridin-2(1H)-one (3.11)

To a flame dried 100 mL round bottom flask was added n-oxide **3.10** (1.6 g, 10 mmol, 1.0 equiv). The flask was filled and backfilled with argon three times then dry MeCN (8.5 mL) was added. To this suspension TFAA (13 mL, 90 mmol, 9.0 equiv) was added and the solution was stirred at room temperature for 16 hours. Once the reaction was complete by TLC, solid sodium bicarbonate was added followed by methanol and solids were filtered off. The filtrate was concentrated and purified by silica chromatography (0-10% MeOH in DCM) to obtain 1.0 g (71%) of intended product as a yellow orange solid.

¹H NMR: (400 MHz, Chloroform-*d*) δ 7.59 (d, $J = 7.6$ Hz, 1H), 6.03 (d, $J = 2.8$ Hz, 1H), 5.98 (dd, $J = 7.7, 3.0$ Hz, 1H), 3.76 (s, 3H).

¹³C NMR: (101 MHz, CDCl₃) δ 167.03, 160.35, 133.59, 99.75, 96.83, 55.94.

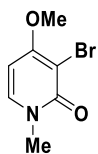


1-(benzyloxy)-4-methoxypyridin-2(1H)-one (3.12)

To a flame dried 100 mL 3 necked round bottom flask was added pyridinone **3.11** (.800 g, 5.67 mmol, 1.0 equiv) and potassium carbonate (2.35 g, 17.0 mmol, 3.0 equiv). The flask was equipped with a reflux condenser then filled and backfilled with argon three times. Anhydrous DMF was added (14.2 mL) and the solution was stirred vigorously for two minutes. Benzyl bromide (1.16 g, 809 μ L, 6.80 mmol, 1.2 equiv) was added dropwise and the resulting mixture was heated to 80 °C for 16 hours. Once cooled, solid potassium carbonate was filtered off and the residue was washed with DCM (3 x 10 mL). The filtrate was combined and concentrated under reduced pressure. Crude product was purified via silica chromatography (0-10% MeOH in DCM) to give 1.29 g (98%) of intended product as a beige solid.

¹H NMR: (400 MHz, Chloroform-*d*) δ 7.41-7.34 (m, 5H), 6.92 (d, J = 7.8 Hz, 1H), 5.97 (d, J = 3.1 Hz, 1H), 5.61 (dd, J = 7.9, 3.1 Hz, 1H), 5.23 (s, 2H), 3.73 (s, 3H).

¹³C NMR: (101 MHz, CDCl₃) δ 167.24, 160.20, 136.23, 134.03, 130.22, 129.41, 128.85, 98.90, 98.68, 78.59, 55.81.



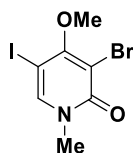
3-bromo-4-methoxy-1-methylpyridin-2(1H)-one (3.14)

To a flame 50 mL dried round bottom flask was added **3.7** (0.700 g, 5.03 mmol, 1.0 equiv) in DCM and AcOH (8:2) (17.5 mL). After stirring for 2 mins at room temperature bromine (1.85 g, 596 μ L, 11.6 mmol, 2.3 equiv) was slowly added and the solution was left to stir for 15 hrs at room temperature. The reaction was then concentrated via rotovap and the residue was quenched by the addition of saturated aqueous sodium thiosulfate (25 mL). To solution was added aqueous potassium carbonate (25 mL) and DCM (25 mL). The aqueous layer was then washed a further three times with DCM (25 mL). The organic layers were then combined, dried over MgSO_4 , and concentrated in vacuo. The residue was then purified by column chromatography using silica and DCM/acetone (0-20%) gradient afford 0.951 g (87%) of 3-bromo-4-methoxy-1-methylpyridin-2(1H)-one as an off white solid. This compound is known in the literature and matches literature reports.⁹

R_f = 0.27 (8:2 DCM: Acetone)

^1H NMR: (400 MHz, Chloroform-*d*) δ 7.31 (d, J = 7.6 Hz, 1H), 6.06 (d, J = 7.6 Hz, 1H), 3.92 (s, 3H), 3.56 (s, 3H).

^{13}C NMR: (101 MHz, CDCl_3) δ 164.27, 160.29, 137.67, 98.73, 94.37, 75.47, 56.87, 38.24.

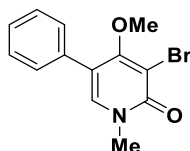
**3-bromo-5-iodo-4-methoxy-1-methylpyridin-2(1H)-one (3.15)**

A solution of the bromopyridone **3.14** (950 mg; 4.36 mmol, 1.0 equiv) and N-iodosuccinimide (1.18 g, 5.23 mmol, 1.2 equiv) in 11.8 mL MeCN was treated with trifluoroacetic acid (101 μ L, 1.31 mmol, 0.3 equiv) and the reaction mixture was stirred at room temperature for 15 h and then concentrated in vacuo. The residue was diluted with DCM (10 mL) and washed with aqueous $\text{Na}_2\text{S}_2\text{O}_3$ (20 mL) and 1N NaOH (20 mL). The aqueous layer was extracted with DCM (2 x 20 mL) and the combined organic layers were dried (MgSO_4) and concentrated in vacuo to give 1.43 g (95%) of iodobromopyridone as a solid of satisfactory purity which was taken forward without purification. This compound is known in the literature and matches literature reports.⁹

R_f = 0.65 (8:2 DCM: Acetone)

$^1\text{H NMR}$: (400 MHz, Chloroform-*d*) δ 7.63 (s, 1H), 3.94 (s, 3H), 3.58 (s, 3H).

$^{13}\text{C NMR}$: (101 MHz, CDCl_3) δ 164.76, 160.36, 142.45, 107.31, 65.47, 60.75, 38.39.



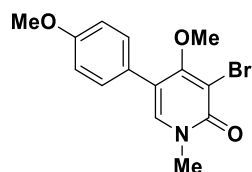
3-bromo-4-methoxy-1-methyl-5-phenylpyridin-2(1H)-one (**3.16**)

To a flask under argon was added **3.15** (2.40 g, 6.98 mmol, 1.0 equiv), phenylboronic acid (1.02 g, 8.37 mmol, 1.2 equiv), and TPPTS (0.620 g, 1.09 mmol, 0.16 equiv) in 80.0 mL 3:1 MeCN:water. This solution was sparged with argon for 10 minutes prior to the addition of $\text{Pd}(\text{OAc})_2$ (93.9 mg, 419 μ mol, 0.06 equiv). The solution was sparged with argon for an additional 10 minutes, then diisopropylamine (3.15 mL, 22.3 mmol, 3.2 eq) was added. The reaction vessel was sealed with electrical tape and left to stir at 80°C overnight. Solvents

removed *in vacuo* and the resulting crude was directly subjected to purification by column chromatography (10% acetone in DCM) to give the desired coupling adduct as an off white solid (1.8388 g, 90%). This compound is known in the literature and matches literature reports.⁹

¹H NMR: (400 MHz, Chloroform-*d*) δ 7.41 (d, J = 4.0 Hz, 5H), 7.28 (s, 1H), 3.63 (s, 3H), 3.54 (s, 3H).

¹³C NMR: (101 MHz, CDCl₃) δ 164.60, 160.27, 136.95, 133.76, 128.86, 128.80, 128.05, 117.66, 107.87, 60.35, 38.46.

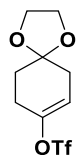


3-bromo-4-methoxy-5-(4-methoxyphenyl)-1-methylpyridin-2(1H)-one (3.17)

To a flask under argon was added **3.15** (1.60 g, 4.65 mmol, 1.0 equiv), (4-methoxyphenyl)boronic acid (0.848 g, 5.58 mmol, 1.2 equiv), and TPPTS (0.381 g, 0.670 mmol, 0.16 equiv) in 80.0 mL 3:1 MeCN:water. This solution was sparged with argon for 10 minutes prior to the addition of Pd(OAc)₂ (62.7 mg, 279 μ mol, 0.06 equiv). The solution was sparged with argon for an additional 10 minutes, then diisopropylamine (2.10 mL, 14.9 mmol, 3.2 eq) was added. The reaction vessel was sealed with electrical tape and left to stir at 80°C overnight. Solvents removed *in vacuo* and the resulting crude was directly subjected to purification by column chromatography (10% acetone in DCM) to give the desired coupling adduct as an off white solid (1.13 g, 75%). This compound is known in the literature and matches literature reports.⁹

¹H NMR: (400 MHz, Chloroform-*d*) δ 7.32 (d, J = 8.2 Hz, 2H), 7.23 (s, 1H), 6.94 (d, J = 8.1 Hz, 2H), 3.84 (s, 3H), 3.62 (s, 3H), 3.53 (s, 3H).

¹³C NMR: (101 MHz, CDCl₃) δ 164.69, 160.20, 159.50, 136.55, 129.97, 125.94, 117.36, 114.26, 107.84, 60.20, 55.44, 38.41.

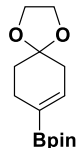


1,4-dioxaspiro[4.5]dec-7-en-8-yl trifluoromethanesulfonate (3.18)

To a flame-dried flask under argon was added 1,4-dioxaspiro[4.5]decan-8-one (1.50 g, 9.60 mmol, 1.0 equiv) and phenyl triflimide (3.77 g, 10.6 mmol, 1.1 equiv), which were then dissolved in 50.0 mL anhydrous THF. This solution was chilled to -78°C in a dry ice-acetone bath, after which 1M LiHMDS in THF (10.6 mL, 10.6 mmol, 1.1 equiv) was slowly added. The solution was then removed from the ice bath and left to stir at room temperature overnight. Reaction was quenched with the addition of water and THF was removed *in vacuo*. The mixture was transferred to a separatory funnel and extracted with ether. Combined organic phases washed with 1M NaOH and brine then dried over sodium sulfate and concentrated *in vacuo* to give crude product. Purification by column chromatography (10% EtOAc in hexanes) gave the desired triflate as a clear, light-yellow oil (2.5251 g, 91% yield). This compound is known and matches reported spectra.¹⁰

¹H NMR: (600 MHz, Chloroform-*d*) δ 5.66 (td, J = 3.9, 2.1 Hz, 1H), 4.06 – 3.92 (m, 4H), 2.54 (tq, J = 6.4, 2.1 Hz, 2H), 2.41 (dd, J = 4.3, 2.3 Hz, 2H), 1.90 (t, J = 6.6 Hz, 2H).

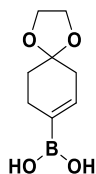
^{13}C NMR: (101 MHz, CDCl_3) δ 148.32, 120.24, 115.96, 106.27, 64.84, 34.29, 31.15, 26.53.



4,4,5,5-tetramethyl-2-(1,4-dioxaspiro[4.5]dec-7-en-8-yl)-1,3,2-dioxaborolane (3.19)

To a flame-dried flask under argon was added of B_2pin_2 (3.34 g, 13.1 mmol, 1.5 equiv), KOAc (2.58 g, 26.3 mmol, 3.0 equiv), and **3.18** (2.53 g, 8.76 mmol, 1.0 equiv) in 60.0 mL anhydrous 1,4-dioxane. This mixture was sparged with argon for 10 minutes prior to the addition of $\text{Pd}(\text{dppf})\text{Cl}_2 \cdot \text{DCM}$ (715 mg, 876 μmol , 0.1 equiv), after which the mixture was sparged with argon for an additional 10 minutes then heated to 85°C and left to stir overnight. The slurry was diluted in EtOAc and filtered through a pad of Celite. Filtrate transferred to a separatory funnel where the organic phase was washed with saturated NaHCO_3 and brine then dried over sodium sulfate and concentrated *in vacuo*. Purification by column chromatography (20% EtOAc in hexanes) afforded the desired boronate ester as a light-brown solid (2.1173 g, 90% yield). This compound is known in the literature.¹¹

^1H NMR: (600 MHz, Chloroform-*d*) δ 6.46 (dp, $J = 3.5, 1.8$ Hz, 1H), 3.98 (s, 4H), 2.45 – 2.28 (m, 4H), 1.75 – 1.70 (m, 2H), 1.26 (s, 12H).



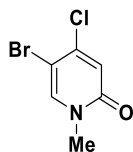
(1,4-dioxaspiro[4.5]dec-7-en-8-yl)boronic acid (3.20)

To a flask was added **3.19** (150 mg, 564 μmol , 1.0 equiv), NaIO_4 (362 mg, 1.69 mmol, 3.0 equiv), and NH_4OAc (130 mg, 1.69 mmol, 3.0 equiv) in 12 mL 1:1 acetone:water.* This slurry was left to stir at room temperature for 3 days. The mixture was filtered and washed with ether, then transferred to a separatory funnel. The aqueous phase was extracted generously with additional ether, then the combined organic phases were dried over sodium sulfate and concentrated *in vacuo* to give crude boronic acid as an orange-brown oil (83.1 mg, 80% yield). This material was used in the next reaction without further purification.

*Alternatively, silica can also be added to small-scale reaction mixtures (10:1 $\text{SiO}_2\text{:NaIO}_4$) to accelerate the reaction time to 16 hours and improve reaction yields (up to 95% isolated yield). Silica must be removed by vacuum filtration prior to aqueous workup.

*This compound is known in the literature.¹²

^1H NMR: (400 MHz, DMSO) δ 6.31 (s, 1H), 3.87 (s, 3H), 2.23 (s, 2H), 2.17 (s, 2H), 1.59 (t, J = 6.5 Hz, 2H).

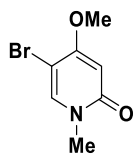
**5-bromo-4-chloro-1-methylpyridin-2(1H)-one (3.21)**

To a flame dried 25 mL round bottom flask equipped with a magnetic stirbar was added 5-bromo-4-chloropyridin-2(1H)-one (2.00 g, 9.60 mmol, 1.0 equiv), and cesium carbonate (4.28 g, 13.1 mmol, 1.37 equiv). The flask was filled and backfilled argon three times and anhydrous DMF

(8.9 mL, 0.4 M) was added. Methyl iodide (1.89 g, 13.3 mmol, 1.39 equiv) was added dropwise to the suspension and this was stirred at an ambient temperature for 4 hours. The mixture was poured into a separatory funnel containing 1:1 saturated aqueous sodium chloride: water (100 mL) and extracted with ethyl acetate (2 x 50 mL). The organic layer was washed with saturated aqueous sodium chloride, dried with MgSO₄, and concentrated in vacuo. The residue was triturated with 10 mL of 10 % ethyl acetate/hexanes. The solids were collected and vacuum dried to provide product. The filtrate was evaporated and the residue purified by flash chromatography (silica gel, 0-100% ethyl acetate/hexanes) to provide a total of 1.45 g (68% yield) of product. This compound is known in the literature and matches reported spectra.¹³

R_f = 0.44 (9:1 DCM:MeOH)

¹H NMR: (600 MHz, Chloroform-*d*) δ 7.55 (s, 1H), 6.77 (s, 1H), 3.53 (s, 3H).

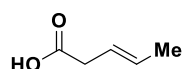


5-bromo-4-methoxy-1-methylpyridin-2(1H)-one (3.22)

To a flame bae bathed three necked flask was added **3.21** (0.250 g, 1.12 mmol, 1.0 equiv). The flask was then charged with a magnetic stir bar, equipped with a reflux condenser and filled and backfilled with argon three times. To this was added 0.5 M sodium methoxide in methanol (4.5 mL, 2.25 mmol). The solution was heated to 60°C and allowed to stir for 16 hours. The mixture was then cooled to room temperature and partitioned with water and ethyl acetate (10 mL). The organic layer was then washed with brine, dried over anhydrous MgSO₄, and concentrated *in*

vacuo. The resulting solid was triturated with an ethyl acetate heptanes solution (10%) to give product as an orange solid (0.178 g, 73% yield). The compound is known in the literature and matches reports.¹³

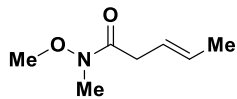
¹H NMR: (600 MHz, Chloroform-*d*) δ 7.42 (d, J = 1.2 Hz, 1H), 5.98 (d, J = 1.7 Hz, 1H), 3.85 (d, J = 1.3 Hz, 3H), 3.48 (d, J = 1.4 Hz, 3H).



(E)-pent-3-enoic acid (3.23)

To an oven-dried 25 mL round bottom flask equipped with a magnetic stir bar was added a solution of piperidine (22.7 μ L, 0.229 mmol, 0.04 equiv) in DMSO (1 mL) under an argon atmosphere. Then, acetic acid (13.1 μ L, 0.229 mmol, 0.04 equiv) was added. The solution was stirred at room temperature for 5 min. After that, a solution of malonic acid (1.20 g, 11.5 mmol, 2.01 equiv) in DMSO (5.75 mL) and propanal (0.333 g, 5.73 mmol, 1.0 equiv) were subsequently added to the flask. The resulting solution was stirred at room temperature for 25 min, and then was heated to 100°C and stirred overnight. The solution was cooled to room temperature, diluted with water (10 mL) and extracted with Et₂O (15 mL \times 3). The combined organic layers were washed with water (10 mL \times 3) and brine, dried over anhydrous MgSO₄, filtered and concentrated in *vacuo*. The residue was purified by flash column chromatography on silica gel (eluent: Hexanes/EtOAc; 0-20%) to give the intended product as a colorless oil.

¹H NMR: (600 MHz, Chloroform-*d*) δ 5.61 (dqt, J = 15.0, 6.2, 1.2 Hz, 1H), 5.53 (dtq, J = 15.3, 6.9, 1.5 Hz, 1H), 3.07 (dp, J = 6.9, 1.3 Hz, 2H), 1.71 (dq, J = 6.4, 1.4 Hz, 3H).

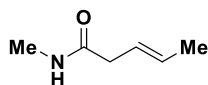


(E)-N-methoxy-N-methylpent-3-enamide (3.24)

To a flame dried 250 mL round bottom flask was added acid **3.23** (0.700 g, 6.99 mmol, 1.00 equiv), N,O-dimethylhydroxylamine (0.427 g, 6.99 mmol, 1.00 equiv), EDC (2.01 g, 10.5 mmol, 1.50 equiv) and HOBt (1.80 g, 10.5 mmol, 1.50 equiv). The flask was filled and backfilled with argon three times and then the reactants were dissolved in anhydrous DCM. Then triethylamine (2.92 mL, 21.0 mmol, 3.00 equiv) was added dropwise. This resulting mixture was allowed to stir overnight at room temperature. The solution was concentrated via rotovap (careful as the product is slightly volatile) and the crude residue was dissolved in EtOAc. The crude solution was washed with water, saturated NaHCO₃, brine, dried over MgSO₄ and concentrated in vacuo. This crude product was purified column chromatography on silica using a 3:1 Hexanes to Ethyl acetate solvent system (0.424 g, 74% yield).

R_f = 0.23 (3:1 Hexanes: Ethyl acetate)

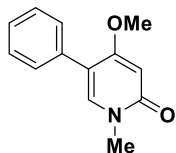
¹H NMR: (600 MHz, Chloroform-*d*) δ 5.62 – 5.52 (m, 2H), 3.68 (s, 3H), 3.17 (s, 3H), 3.15 (s, 2H), 1.69 (dq, *J* = 4.0, 1.3 Hz, 3H).



(E)-N-methylpent-3-enamide (3.25)

R_f = 0.33 (8:2 DCM Acetone)

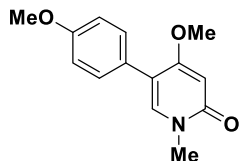
¹H NMR: (600 MHz, Chloroform-*d*) δ 5.78 (s, 1H), 5.63 – 5.54 (m, 1H), 5.53 – 5.44 (m, 1H), 2.91 – 2.86 (m, 2H), 2.76 (dd, *J* = 4.9, 1.1 Hz, 3H), 1.68 (dh, *J* = 5.0, 1.2 Hz, 3H).



4-methoxy-1-methyl-5-phenylpyridin-2(1H)-one (3.26.1)

¹H NMR: (600 MHz, Chloroform-*d*) δ 7.44 – 7.30 (m, 5H), 7.18 (s, 1H), 6.04 (s, 1H), 3.79 (s, 3H), 3.54 (s, 3H).

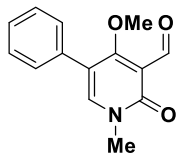
*Peaks shown in and pulled from crude NMR with unreacted Weinreb amide.



4-methoxy-1-methyl-5-(4-methoxyphenyl)pyridin-2(1H)-one (3.36.2)

¹H NMR: (600 MHz, Chloroform-*d*) δ 7.31 – 7.26 (m, 2H), 7.14 (s, 1H), 6.95 – 6.90 (m, 2H), 6.04 (s, 1H), 3.83 (s, 3H), 3.79 (s, 3H), 3.54 (s, 3H).

*Peaks shown in and pulled from crude NMR with unreacted Weinreb amide.



4-methoxy-1-methyl-2-oxo-5-phenyl-1,2-dihydropyridine-3-carbaldehyde (3.27)

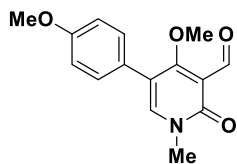
To a flame dried 3 dram vial was added 1-propanol and this was sparged for 20 minutes. To this was added **3.16** (0.300 g, 1.02 mmol, 1.0 equiv), potassium vinyl trifluoroborate (0.273 g, 2.04 mmol, 2.0 equiv), Et₃N (0.711 mL, 5.10 mmol, 5.0 equiv) and PdCl₂(dppf)•CH₂Cl₂ adduct (0.083 g, 0.102 mmol, 0.1 equiv). This was sparged for 5 minutes then the 5 dram vial was sealed with electrical tape and the resulting solution was stirred at 90°C for 24 hours. The reaction mixture was diluted with EtOAc and washed with water. The solvent was removed and the crude material was diluted with THF (4.62 mL) and water (4.62 mL). Osmium tetroxide (4.0% in tert-butanol) (0.211 mL, 0.102 mmol, 0.1 equiv) and sodium periodate (0.654 g, 3.06 mmol, 3.0 equiv) was added and the mixture was stirred at rt for 3 hours. The reaction color turned from a deep red to an olive-green color (grey/green). The reaction mixture was diluted with EtOAc and washed with water. The solvent was removed, and the crude material was purified via silica gel chromatography (20% Acetone in DCM) to give intended product as an off white/yellow solid (0.151 g, 61% yield).

R_f = 0.26 (4:1 DCM: Acetone)

¹H NMR: (600 MHz, Chloroform-*d*) δ 10.40 (d, *J* = 0.8 Hz, 1H), 7.51 (s, 1H), 7.43 – 7.32 (m, 5H), 3.72 (d, *J* = 0.7 Hz, 3H), 3.57 (s, 3H).

¹³C NMR: (126 MHz, cdcl₃) δ 189.88, 170.46, 163.77, 143.54, 133.35, 129.11, 128.77, 128.10, 117.35, 63.13, 37.36.

HRMS: APCI (m/z) calcd for $C_{14}H_{14}O_3N$ [$M+H^+$]: 244.09682, found 244.09636



**4-methoxy-5-(4-methoxyphenyl)-1-methyl-2-oxo-1,2-dihydropyridine-3-carbaldehyde
(3.28)**

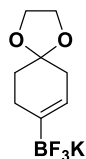
To a flame dried 3 dram vial was added 1-propanol and this was sparged for 20 minutes. To this was added **3.17** (0.330 g, 1.02 mmol, 1.0 equiv), potassium vinyl trifluoroborate (0.273 g, 2.04 mmol, 2.0 equiv), Et_3N (0.711 mL, 5.10 mmol, 5.0 equiv) and $PdCl_2(dppf) \cdot CH_2Cl_2$ adduct (0.083 g, 0.102 mmol, 0.1 equiv). This was sparged for 5 minutes then the 5 dram vial was sealed with electrical tape and the resulting solution was stirred at $90^\circ C$ for 24 hours. The reaction mixture was diluted with EtOAc and washed with water. The solvent was removed and the crude material was diluted with THF (4.62 mL) and water (4.62 mL). Osmium tetroxide (4.0% in tert-butanol) (0.211 mL, 0.102 mmol, 0.1 equiv) and sodium periodate (0.654 g, 3.06 mmol, 3.0 equiv) was added and the mixture was stirred at rt for 3 hours. The reaction color turned from a deep red to an olive-green color (grey/green). The reaction mixture was diluted with EtOAc and washed with water. The solvent was removed, and the crude material was purified via silica gel chromatography (20% Acetone in DCM) to give intended product as an off white/yellow solid (0.198 g, 71% yield).

$R_f = 0.35$ (4:1 DCM: Acetone)

^1H NMR: (600 MHz, Chloroform-*d*) δ 10.42 (d, J = 1.6 Hz, 1H), 7.47 (d, J = 1.3 Hz, 1H), 7.31 – 7.25 (m, 2H), 6.97 – 6.92 (m, 2H), 3.85 (d, J = 1.3 Hz, 3H), 3.73 (d, J = 1.5 Hz, 3H), 3.58 (d, J = 1.3 Hz, 3H).

^{13}C NMR: (126 MHz, cdCl_3) δ 190.00, 170.60, 163.81, 159.57, 143.20, 130.32, 125.54, 117.13, 114.25, 114.17, 63.04, 55.46, 37.36.

HRMS: APCI (m/z) calcd for $\text{C}_{15}\text{H}_{16}\text{O}_4\text{N}$ [$\text{M}+\text{H}^+$]: 274.10738, found 274.10703

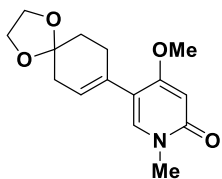


trifluoro(1,4-dioxaspiro[4.5]dec-7-en-8-yl)-l4-borane, potassium salt (3.29)

To a flask was added **3.19** (2.11 g 7.96 mmol, 1.0 equiv) and KHF_2 (2.49 g, 31.8 mmol, 4.0 equiv) in 72 mL of 3:1 acetone:water. This mixture was left to stir at room temperature overnight. Solvents were removed *in vacuo* to give a crude white solid. This solid was washed generously with hot MeCN and subjected to vacuum filtration. The combined filtrates were concentrated *in vacuo* to give the desired trifluoroborate salt as a white solid (1.52 g, 77% yield).

^1H NMR: (400 MHz, $\text{DMSO}-d_6$) δ 5.30 (s, 1H), 3.82 (s, 4H), 2.06 – 1.96 (m, 4H), 1.47 (t, J = 6.4 Hz, 2H).

^{13}C NMR: (101 MHz, DMSO) δ 108.81, 63.75, 41.09, 36.50, 31.84, 28.63, 26.53.



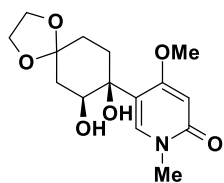
4-methoxy-1-methyl-5-(1,4-dioxaspiro[4.5]dec-7-en-8-yl)pyridin-2(1H)-one (3.30)

To a flame-dried flask under argon was added **3.15** (635 mg, 1.85 mmol, 1.0 equiv) and **3.29** (545 mg, 2.22 mmol, 1.2 equiv) in 13 mL of 1-propanol. This solution was sparged with argon for 10 minutes prior to the addition of Pd(dppf)Cl₂•DCM (151 mg, 185 μmol, 0.1 equiv). The mixture was sparged with argon for an additional 10 minutes then triethylamine (1.29 mL, 9.24 mmol, 5.0 equiv) was added. The reaction vessel was sealed with electrical tape and the mixture was allowed to stir at 90°C overnight. The mixture was filtered through a pad of Celite and washed with EtOAc. The filtrate was concentrated *in vacuo* to give the crude product as a black oil. Purification by column chromatography (0-10% acetone in DCM) gave the product as an impure mixture of the desired coupling adduct and a protodehalogenated byproduct, which was taken forward into the next reaction.

¹H NMR: (600 MHz, Chloroform-*d*) δ 7.14 (s, 1H), 5.67 (td, *J* = 3.8, 2.0 Hz, 1H), 4.01 (s, 4H), 3.84 (s, 3H), 3.56 (s, 3H), 2.49 (ddt, *J* = 6.6, 4.5, 2.1 Hz, 2H), 2.41 (q, *J* = 2.4 Hz, 2H), 1.86 (t, *J* = 6.5 Hz, 2H).

¹³C NMR: (101 MHz, CDCl₃) δ 164.71, 160.21, 135.45, 132.41, 125.08, 118.85, 107.27, 64.51, 60.24, 56.76, 38.10, 36.27, 31.31, 28.12.

HRMS: APCI (*m/z*) calcd for C₁₅H₁₉O₄NBr [M+H⁺]: 356.0492, found 356.04905



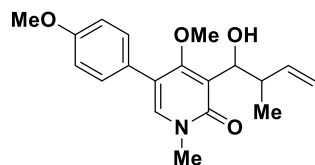
5-((7S,8S)-7,8-dihydroxy-1,4-dioxaspiro[4.5]decan-8-yl)-4-methoxy-1-methylpyridin-2(1H)-one (3.31)

To a flask was added AD-mix- α (787 mg, 1.01 mmol, 1.8 equiv) and methanesulfonamide (53.4 mg, 561 μ mol, 1.0 eq) in 6.0 mL 1:1 tBuOH:water. This slurry was allowed to stir at room temperature for 30 minutes prior to the addition of 200 mg (561 μ mol, 1.0 eq) of crude **3.30**. This mixture was left to continue stirring at room temperature overnight. The reaction was quenched by addition of 0.7 g sodium sulfite to the mixture followed by an additional hour of stirring. Then, the mixture was transferred to a separatory funnel and the aqueous phase was extracted vigorously with DCM. The combined organic phases were washed with 1M NaOH then dried over sodium sulfate and concentrated *in vacuo*. Purification by column chromatography (0-10% MeOH in DCM) afforded the desired diol as an off-white solid (15 mg, 7% yield).

^1H NMR: (400 MHz, Chloroform-*d*) δ 7.56 (s, 1H), 4.59 – 4.50 (m, 1H), 4.09 (s, 3H), 4.06 – 3.93 (m, 4H), 3.96 – 3.88 (m, 1H), 3.54 (s, 3H), 3.28 (d, J = 1.9 Hz, 1H), 2.21 – 2.08 (m, 1H), 2.05 – 1.88 (m, 4H), 1.72 (ddd, J = 13.7, 4.3, 2.5 Hz, 1H).

^{13}C NMR: (101 MHz, CDCl_3) δ 165.56, 160.62, 137.36, 120.47, 109.05, 105.85, 74.19, 69.76, 64.64, 64.57, 61.81, 39.10, 38.45, 32.55, 30.03.

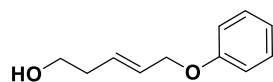
HRMS: APCI (m/z) calcd for $\text{C}_{15}\text{H}_{21}\text{O}_6\text{NBr}$ [$\text{M}+\text{H}^+$]: 390.05468, found 390.05468



3-(1-hydroxy-2-methylbut-3-en-1-yl)-4-methoxy-1-methyl-5-phenylpyridin-2(1H)-one (3.33)

R_f = 0.66 (4:1 DCM: Acetone)

^1H NMR: (600 MHz, Chloroform-*d*) δ 7.34 – 7.28 (m, 2H), 7.19 (s, 1H), 6.97 – 6.91 (m, 2H), 6.02 (ddd, J = 17.2, 10.3, 7.9 Hz, 1H), 5.44 (d, J = 11.2 Hz, 1H), 5.14 – 5.06 (m, 2H), 4.69 (dd, J = 11.1, 8.4 Hz, 1H), 3.84 (s, 3H), 3.55 (s, 3H), 3.35 (s, 3H), 2.81 – 2.75 (m, 1H), 0.98 (d, J = 6.9 Hz, 3H).



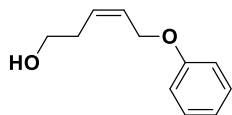
(E)-5-phenoxy-pent-3-en-1-ol (3.53)

*This compound is known in the literature.¹⁴

R_f = 0.14 (4:1 Hexanes : Ethyl Acetate)

^1H NMR: (400 MHz, Chloroform-*d*) δ 7.33 – 7.24 (m, 2H), 6.96 (dt, J = 7.4, 1.1 Hz, 1H), 6.94 – 6.89 (m, 2H), 5.92 – 5.77 (m, 2H), 4.51 – 4.50 (m, 2H), 3.70 (t, J = 6.3 Hz, 2H), 2.37 (dt, J = 6.4, 3.9, 1.1 Hz, 2H).

^{13}C NMR: (101 MHz, CDCl_3) δ 158.65, 131.12, 129.57, 128.12, 120.96, 114.85, 68.44, 61.85, 35.83.



(Z)-5-phenoxy-3-en-1-ol (3.54)

*This compound is known in the literature.¹⁴

R_f = 0.16 (4:1 Hexanes: Ethyl acetate)

¹H NMR: (600 MHz, Chloroform-*d*) δ 7.32 – 7.26 (m, 2H), 6.96 (tt, *J* = 7.4, 1.0 Hz, 1H), 6.95 – 6.90 (m, 2H), 5.93 – 5.86 (m, 1H), 5.73 (dt, *J* = 10.7, 7.6, 1.4 Hz, 1H), 4.60 (ddd, *J* = 6.4, 1.5, 0.7 Hz, 2H), 3.70 (t, *J* = 6.3 Hz, 2H), 2.46 – 2.40 (m, 2H).

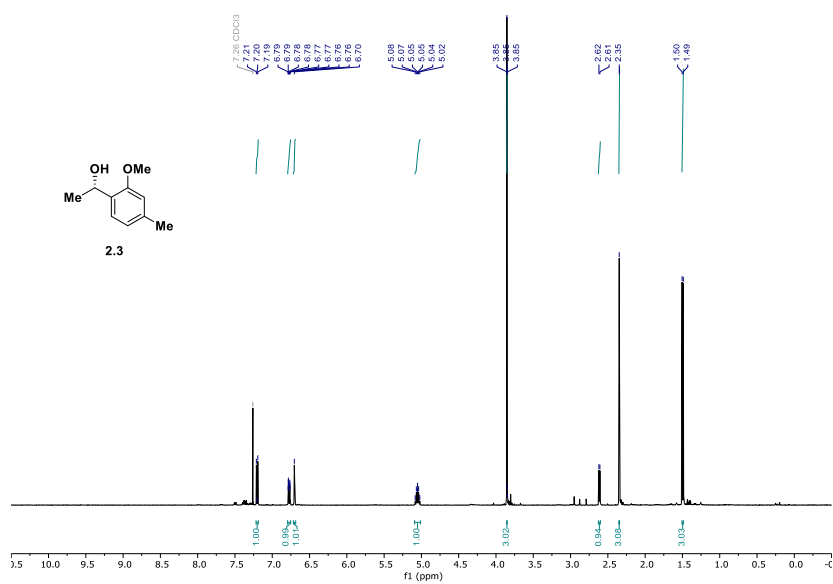
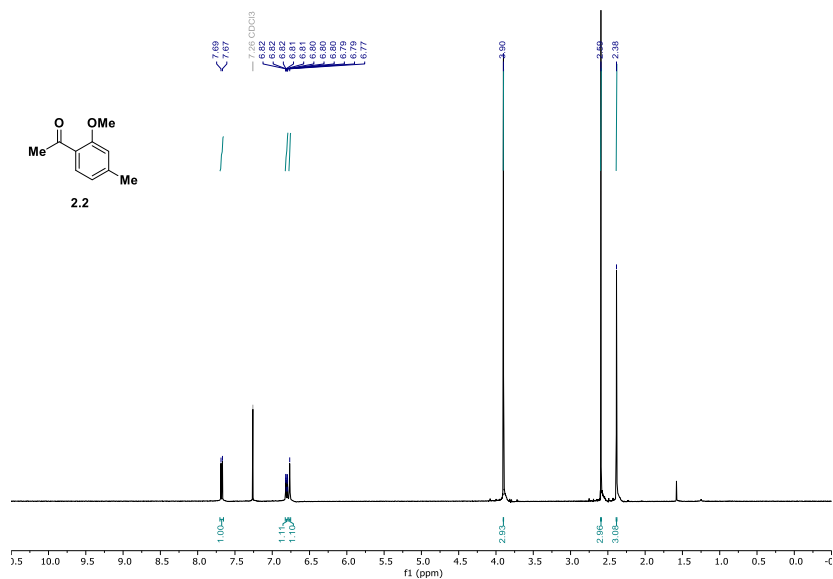
¹³C NMR: (101 MHz, CDCl₃) δ 158.61, 130.51, 129.59, 127.88, 121.04, 114.82, 63.78, 31.39.

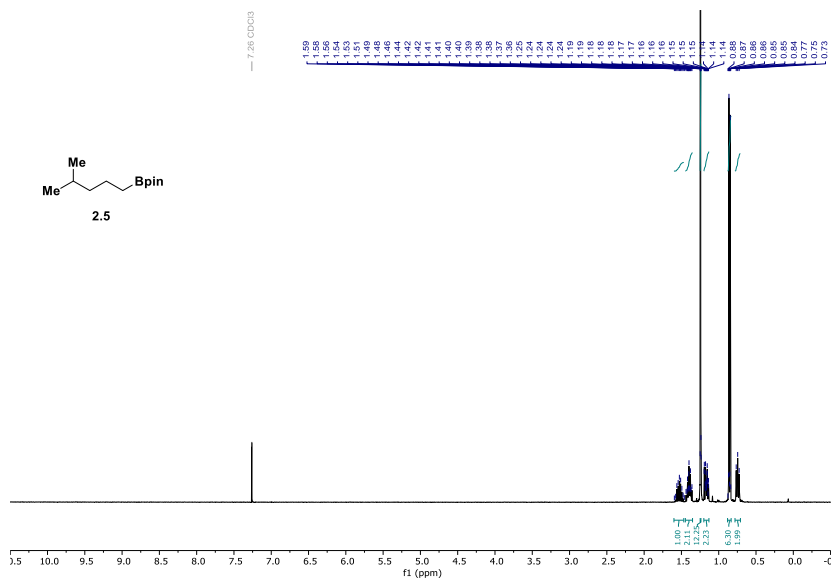
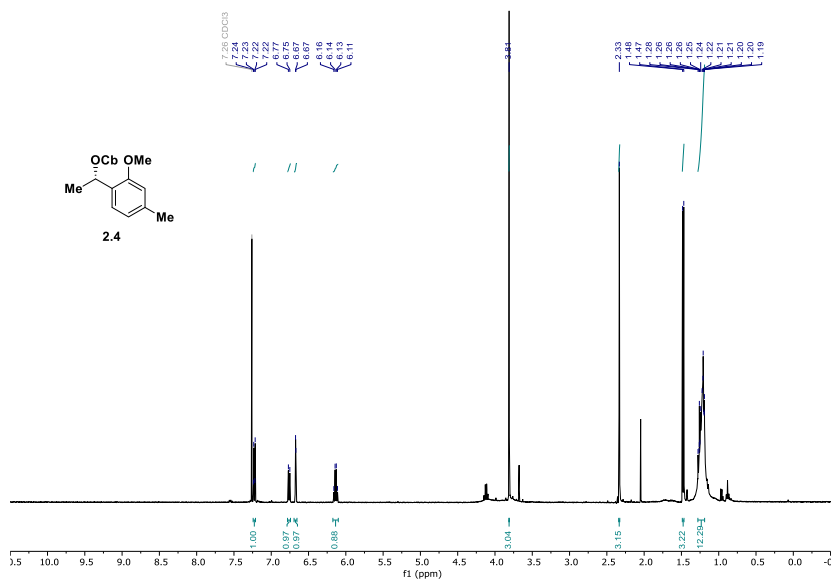
4.4. SI References

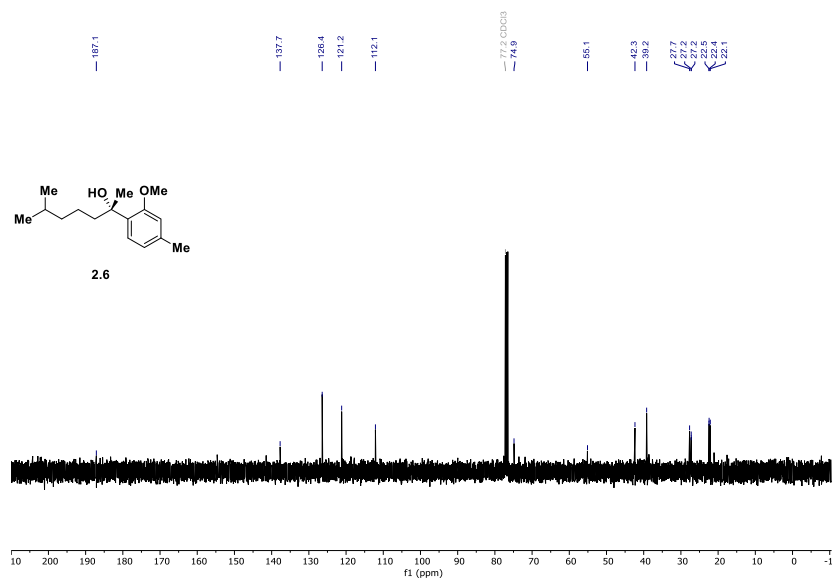
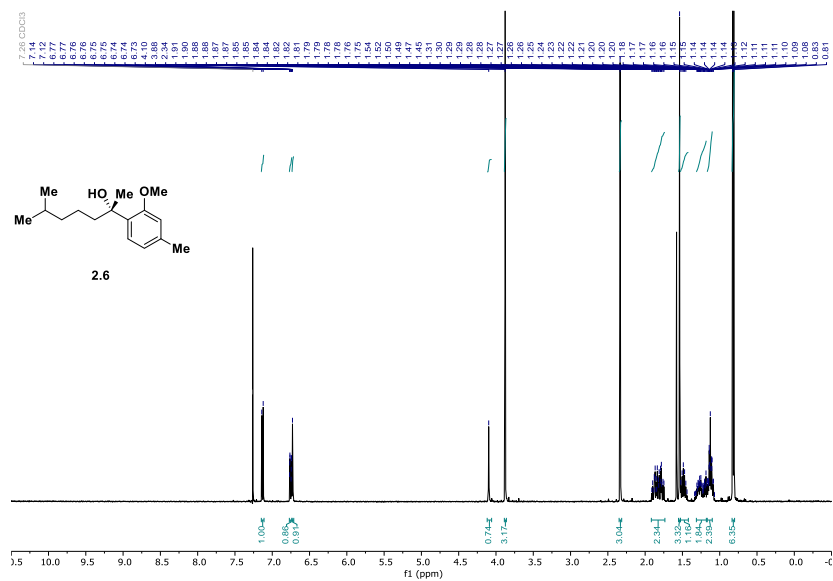
- (1) Blair, D. J.; Fletcher, C. J.; Wheelhouse, K. M. P.; Aggarwal, V. K.; Blair, D. J.; Fletcher, C. J.; Aggarwal, V. K.; Wheelhouse, K. M. P. Stereocontrolled Synthesis of Adjacent Acyclic Quaternary-Tertiary Motifs: Application to a Concise Total Synthesis of (–)-Filiformin. *Angew. Chem. Int. Ed.* **2014**, 53 (22), 5552–5555.
- (2) Bieszczad, B.; Gilheany, D. G. Asymmetric Grignard Synthesis of Tertiary Alcohols through Rational Ligand Design. *Angew. Chem. Int. Ed.* **2017**, 56 (15), 4272–4276.
- (3) Foster, M. S.; Oldham, C. D.; May, S. W. Looking Glass Mechanism-Based Inhibition of Peptidylglycine α -Amidating Monooxygenase. *Tetrahedron Asymm.* **2011**, 22 (3), 283–293.
- (4) Ito, S.; Zhang, C.; Hosoda, N.; Asami, M. Asymmetric Total Synthesis of (+)-Curcutetraol and (+)-Sydonol. *Tetrahedron* **2008**, 64 (42), 9879–9884.
- (5) Mikula, H.; Skrinjar, P.; Sohr, B.; Ellmer, D.; Hametner, C.; Fröhlich, J. Total Synthesis of Masked Alternaria Mycotoxins—Sulfates and Glucosides of Alternariol (AOH) and Alternariol-9-Methyl Ether (AME). *Tetrahedron* **2013**, 69 (48), 10322–10330.
- (6) Zhao, C.; Wu, M.; Huang, Z. Process for Preparing 3-Methyl-5-Methoxybenzenesulfonyl Chloride. Faming Zhuanli Shenqing: China 2017, p 11pp.

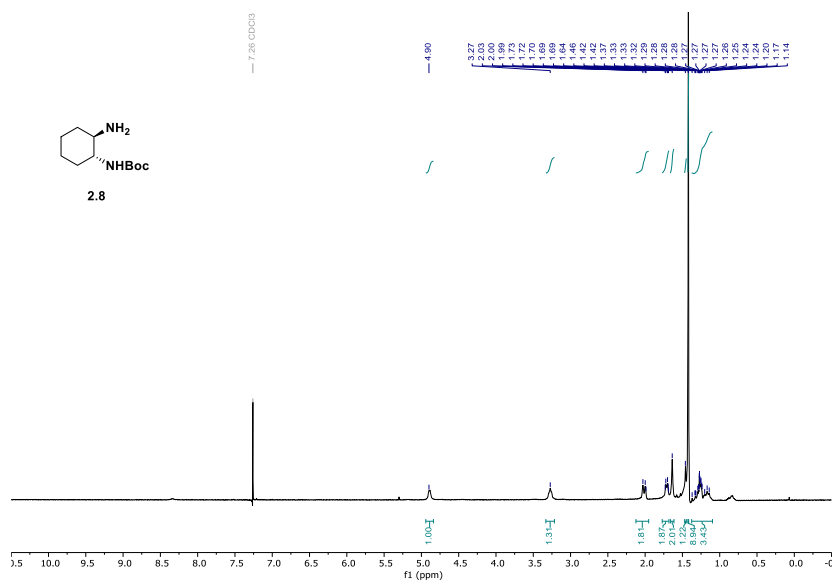
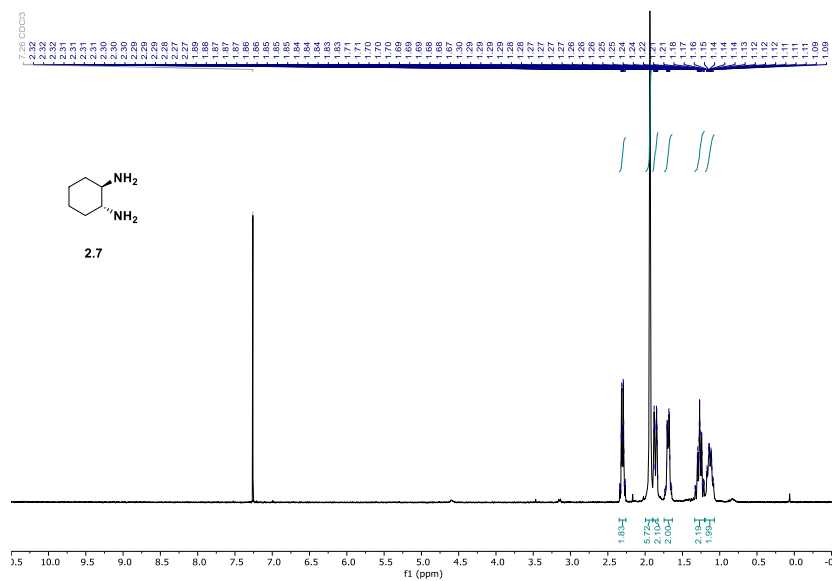
- (7) Zhang, Q.; Wang, D.; Wang, X.; Ding, K. (2-Pyridyl)Acetone-Promoted Cu-Catalyzed O-Arylation of Phenols with Aryl Iodides, Bromides, and Chlorides. *J. Org. Chem.* **2009**, *74* (18), 7187–7190.
- (8) Anderson, R. J.; Hill, J. B.; Morris, J. C. Concise Total Syntheses of Variolin B and Deoxyvariolin B. *J. Org. Chem.* **2005**, *70* (16), 6204–6212.
- (9) Conreux, D.; Bossharth, E.; Monteiro, N.; Desbordes, P.; Vors, J. P.; Balme, G. Flexible Strategy for Differentially 3,5-Disubstituted 4-Oxypyridin-2(1H)- Ones Based on Site-Selective Pd-Catalyzed Cross-Coupling Reactions. *Org Lett.* **2007**, *9* (2), 271–274.
- (10) Mitschke, N.; Christoffers, J.; Wilkes, H. A Straightforward Synthesis of Trideuterated α -Terpinene for Mechanistic Studies. *Eur. J. Org. Chem.* **2020**, *2020* (31), 4893–4899.
- (11) Gong, L.; Li, C.; Yuan, F.; Liu, S.; Zeng, X. Chromium-Catalyzed Selective Borylation of Vinyl Triflates and Unactivated Aryl Carboxylic Esters with Pinacolborane. *Org Lett.* **2022**, *24* (17), 3227–3231.
- (12) Gutiérrez-Bonet, Á.; Popov, S.; Emmert, M. H.; Hughes, J. M. E.; Nolting, A. F.; Ruccolo, S.; Wang, Y. Asymmetric Synthesis of Tertiary and Secondary Cyclopropyl Boronates via Cyclopropanation of Enantioenriched Alkenyl Boronic Esters. *Org Lett.* **2022**, 3455–3460.
- (13) Wang, L.; Pratt, J. K.; Soltwedel, T.; Sheppard, G. S.; Fidanze, S. D.; Liu, D.; Hasvold, L. A.; Mantei, R. A.; Holms, J. H.; McClellan, W. J.; Wendt, M. D.; Wada, C.; Frey, R.; Hansen, T. M.; Hubbard, R.; Park, C. H.; Li, L.; Magoc, T. J.; Albert, D. H.; Lin, X.; Warder, S. E.; Kovar, P.; Huang, X.; Wilcox, D.; Wang, R.; Rajaraman, G.; Petros, A. M.; Hutchins, C. W.; Panchal, S. C.; Sun, C.; Elmore, S. W.; Shen, Y.; Kati, W. M.; McDaniel, K. F. Fragment-Based, Structure-Enabled Discovery of Novel Pyridones and Pyridone Macrocycles as Potent Bromodomain and Extra-Terminal Domain (BET) Family Bromodomain Inhibitors. *J. Med. Chem.* **2017**, *60* (9), 3828–3850.
- (14) Satteyyanaidu, V.; Chandrashekhar, R.; Reddy, B. V. S.; Lalli, C. Modulating Prins Cyclization versus Tandem Prins Processes for the Synthesis of Hexahydro-1H-Pyrano[3,4-c]Chromenes. *Eur. J. Org. Chem.* **2021**, *2021* (1), 138–145.

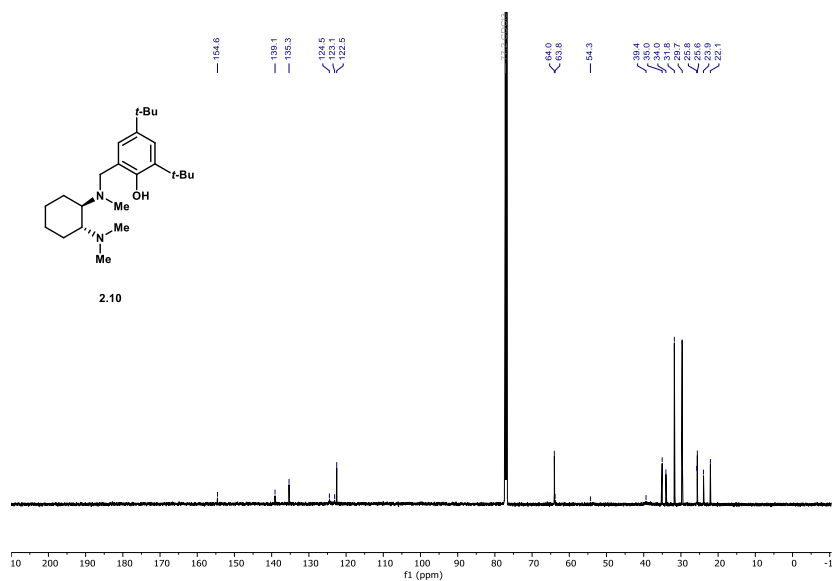
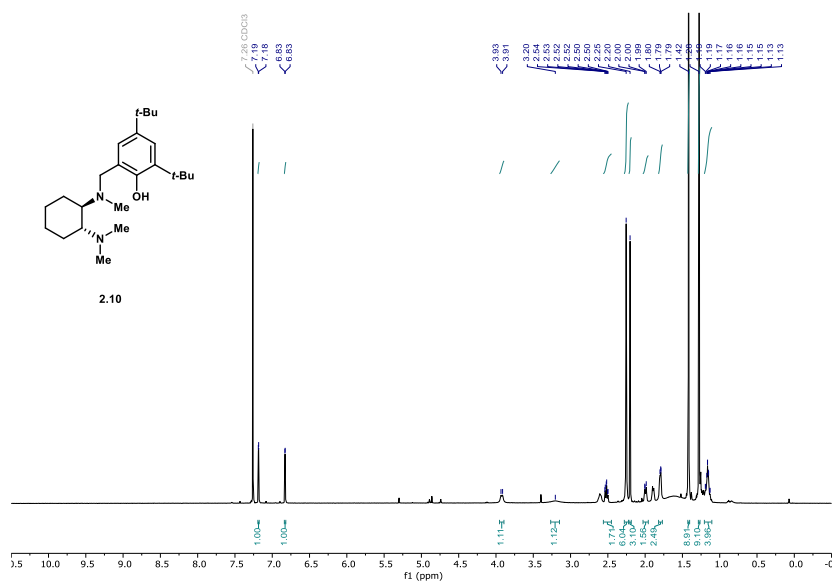
5.1 Appendix Chapter 2

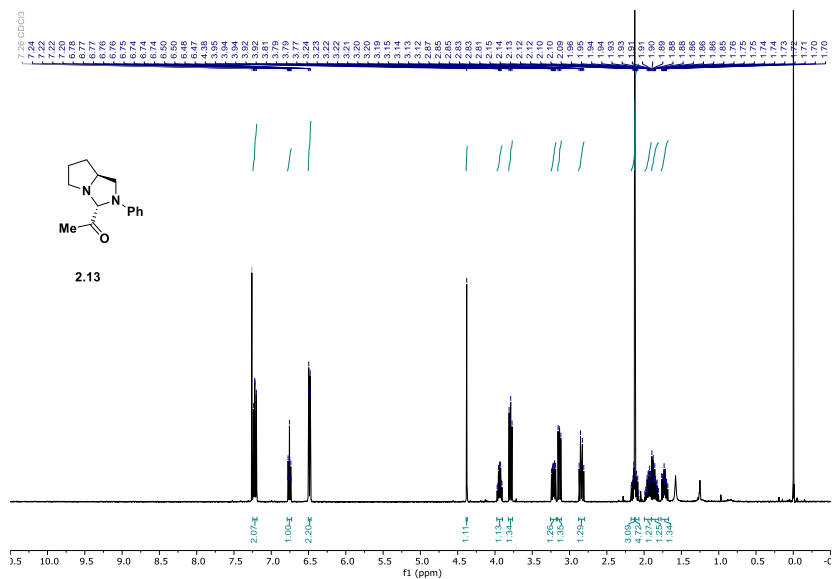
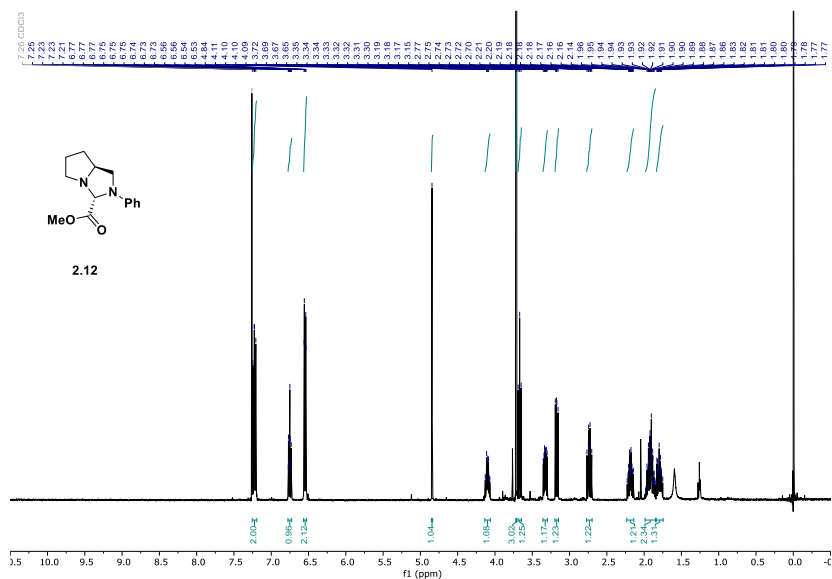


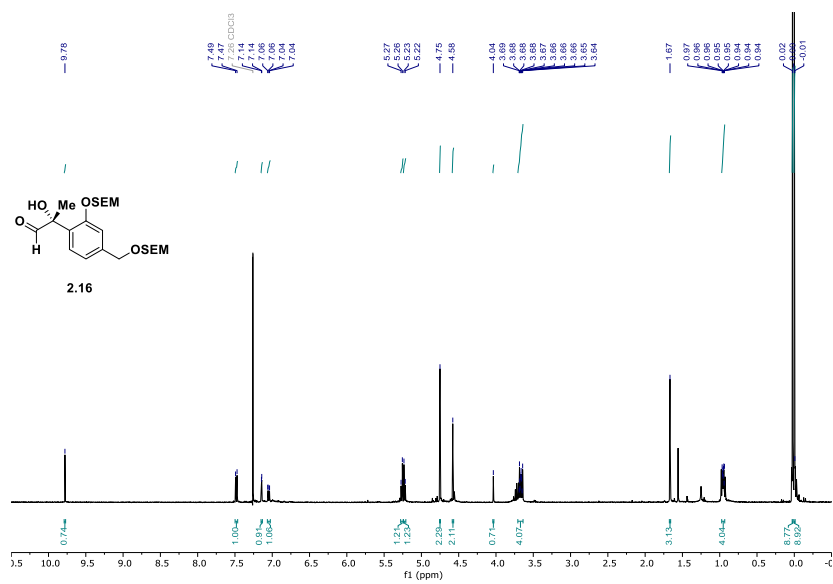
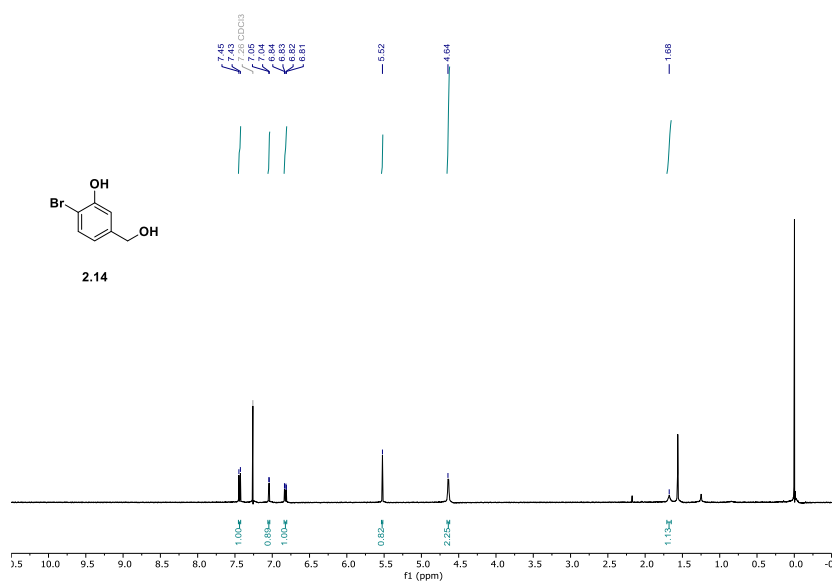


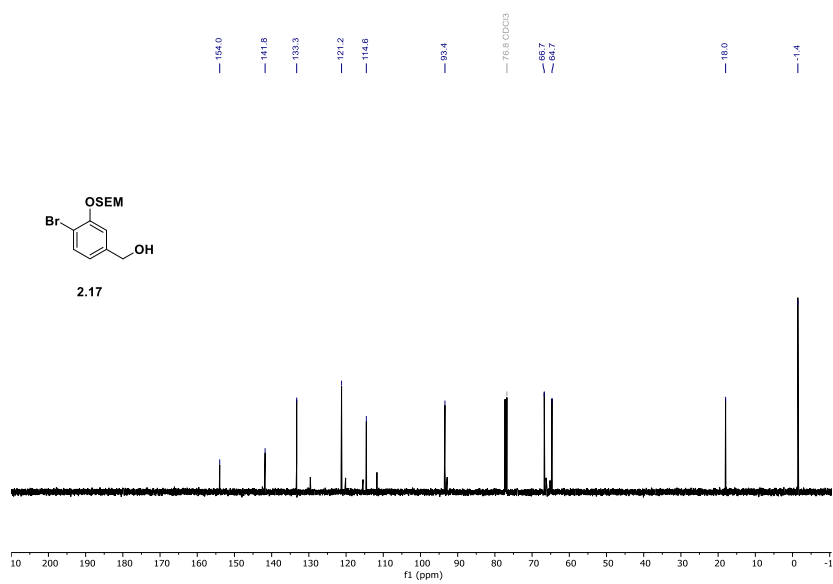
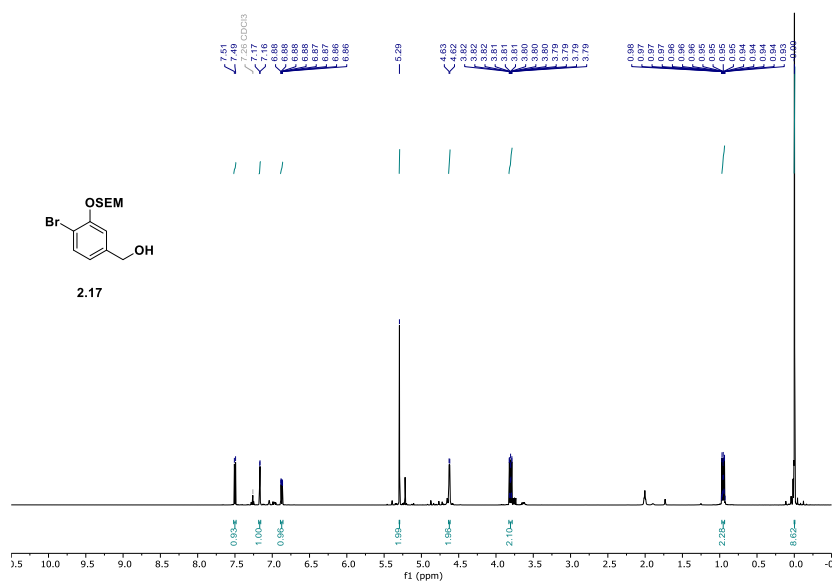


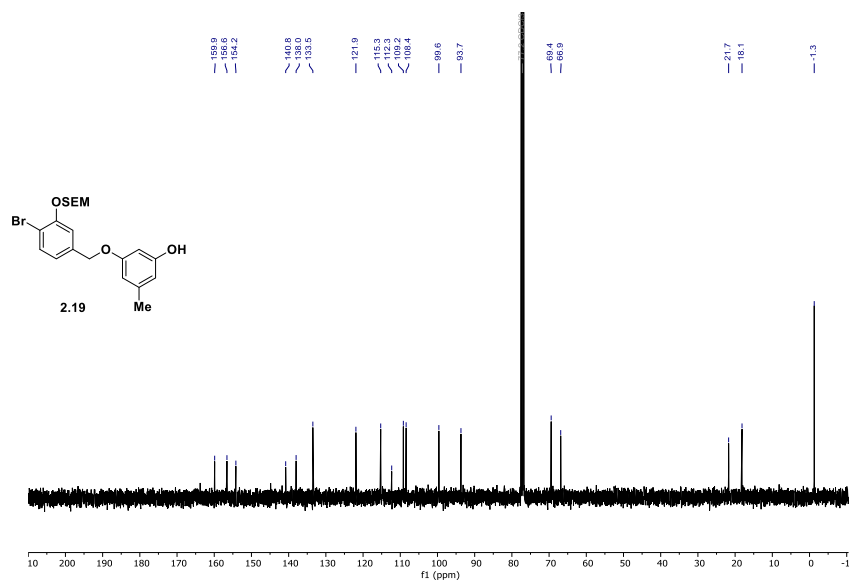
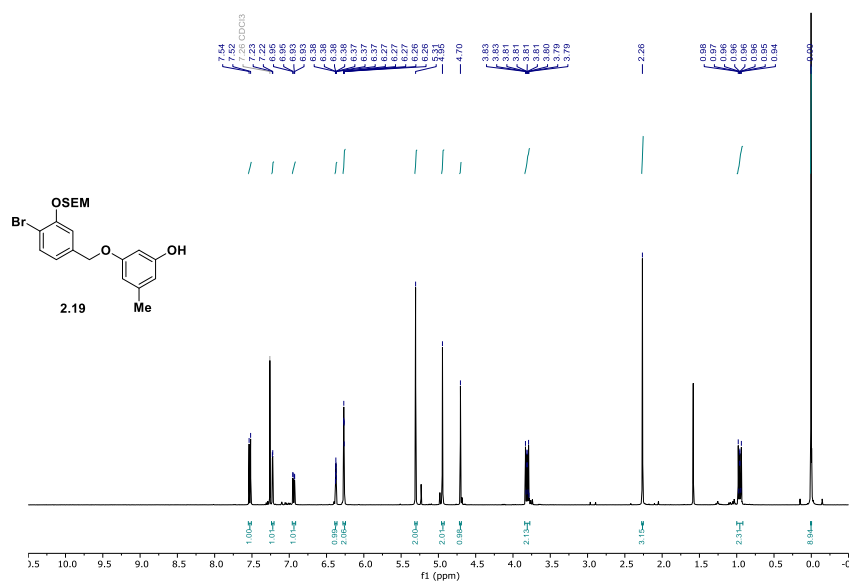


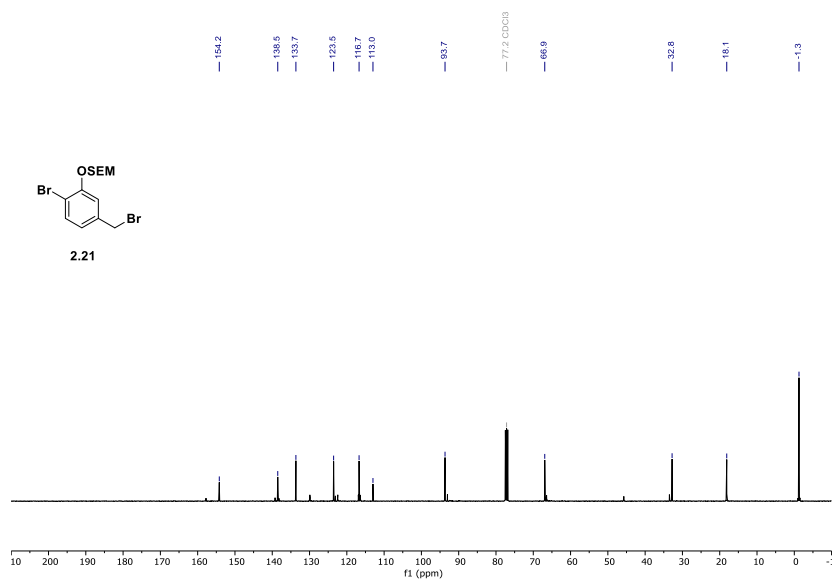
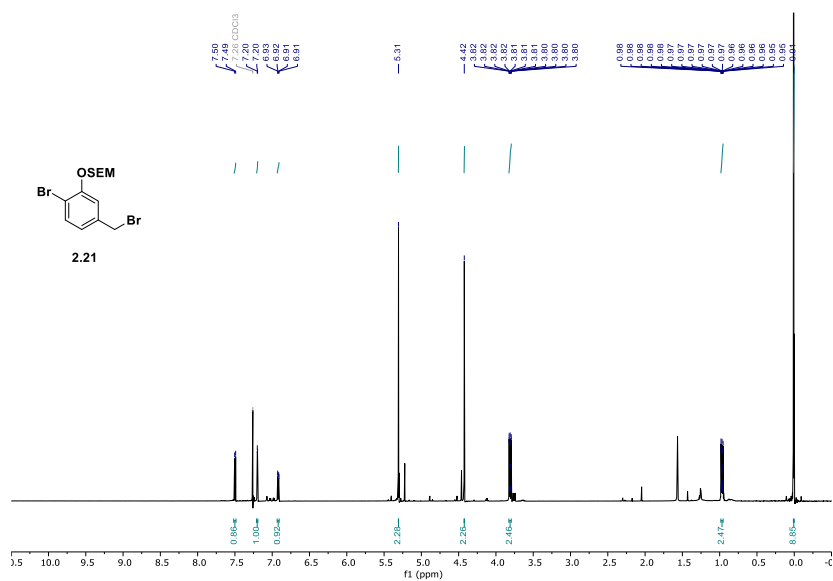


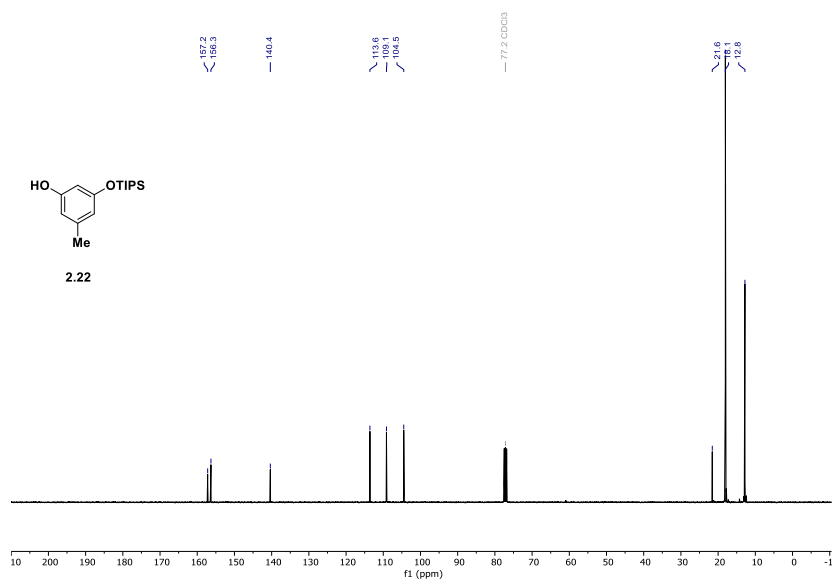
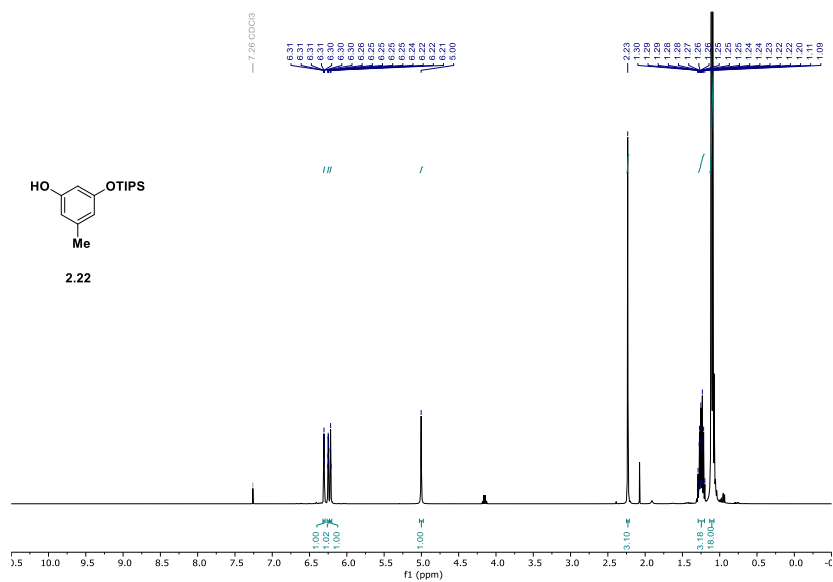


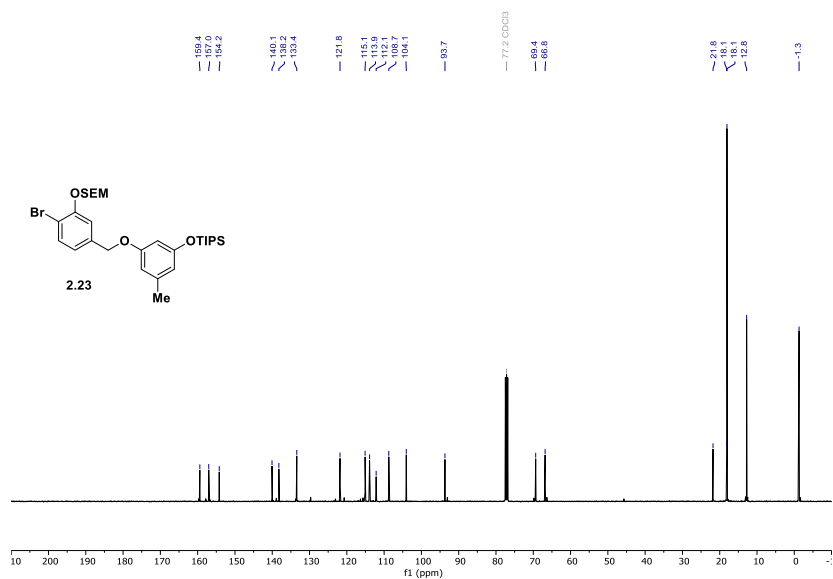
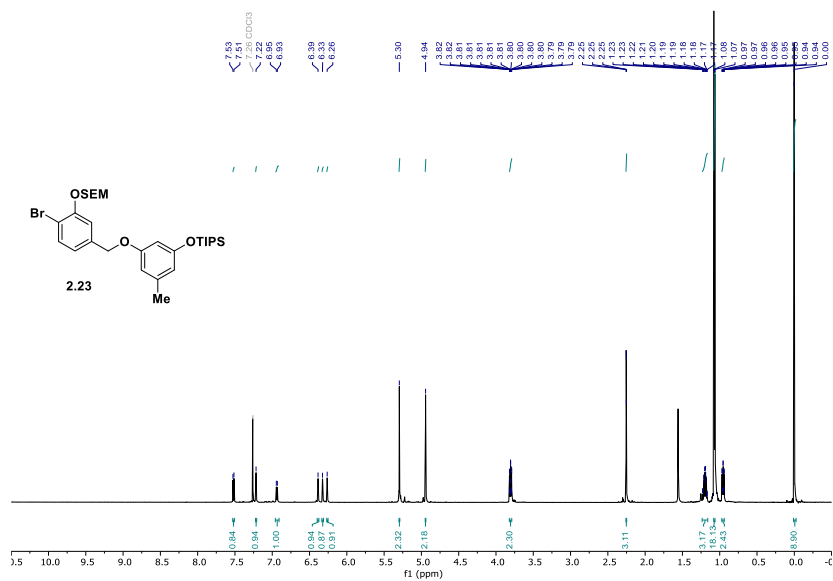


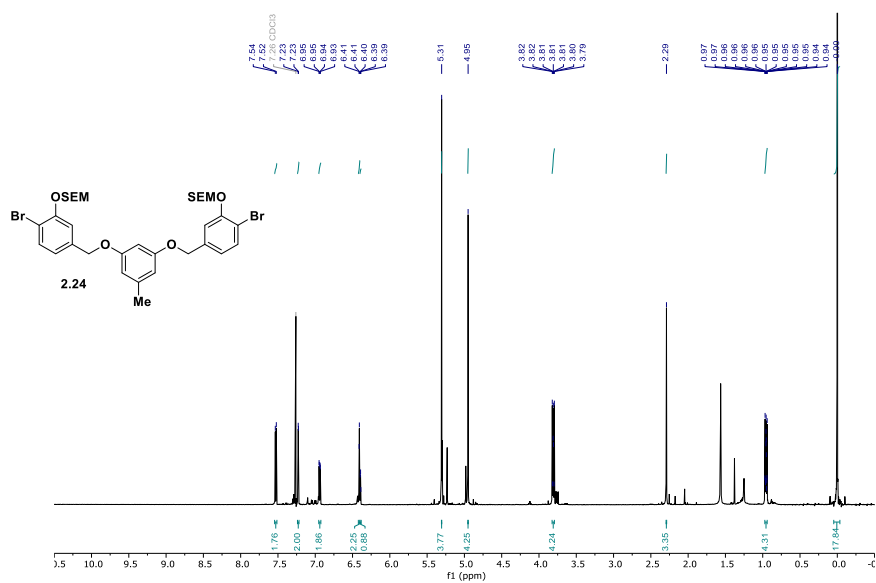


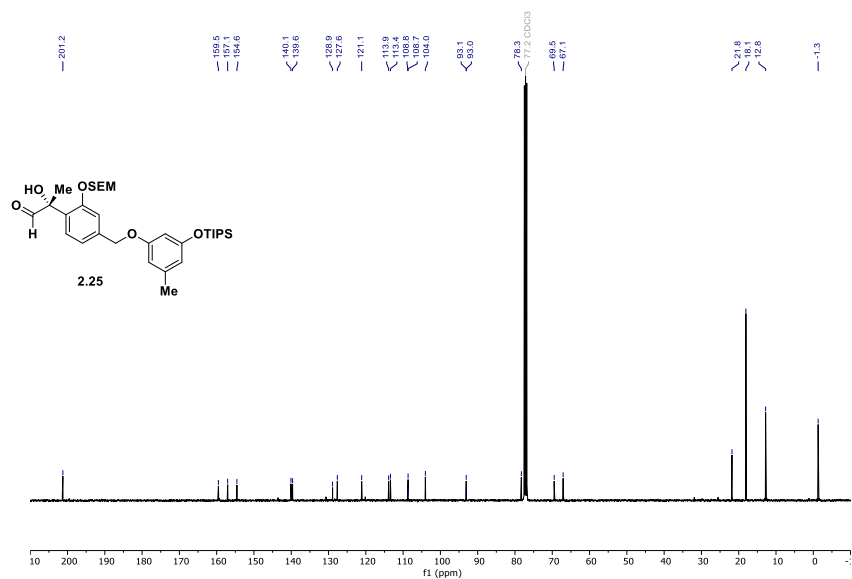
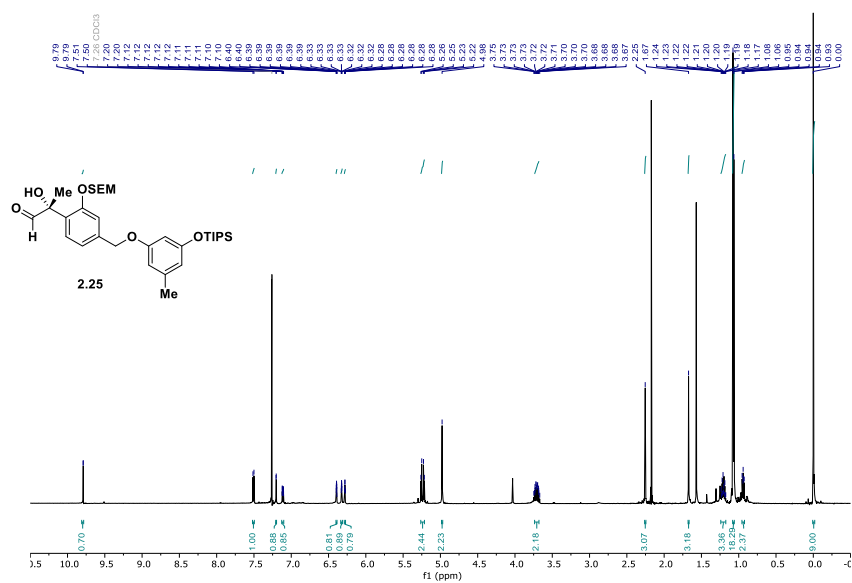


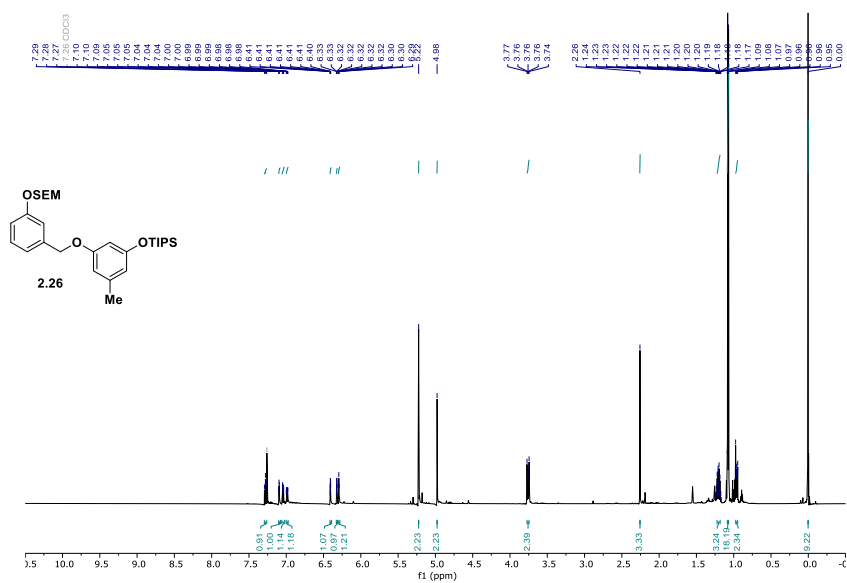


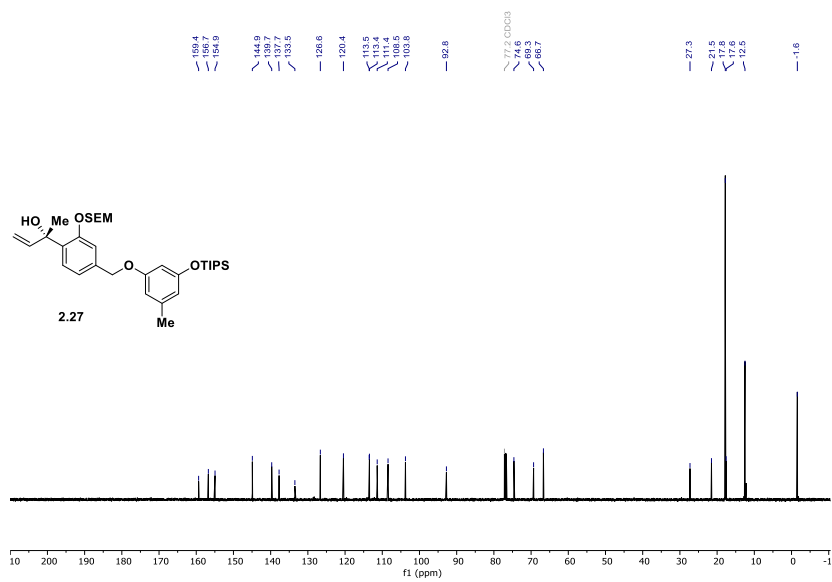
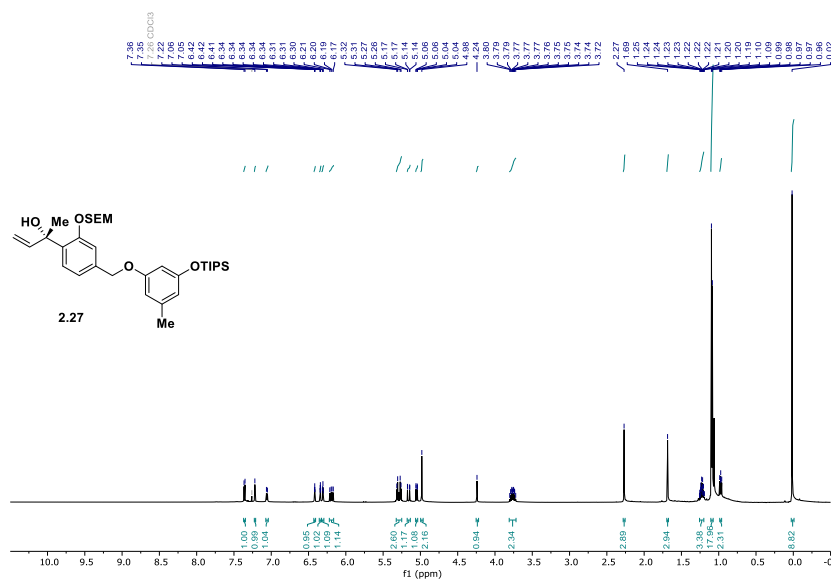


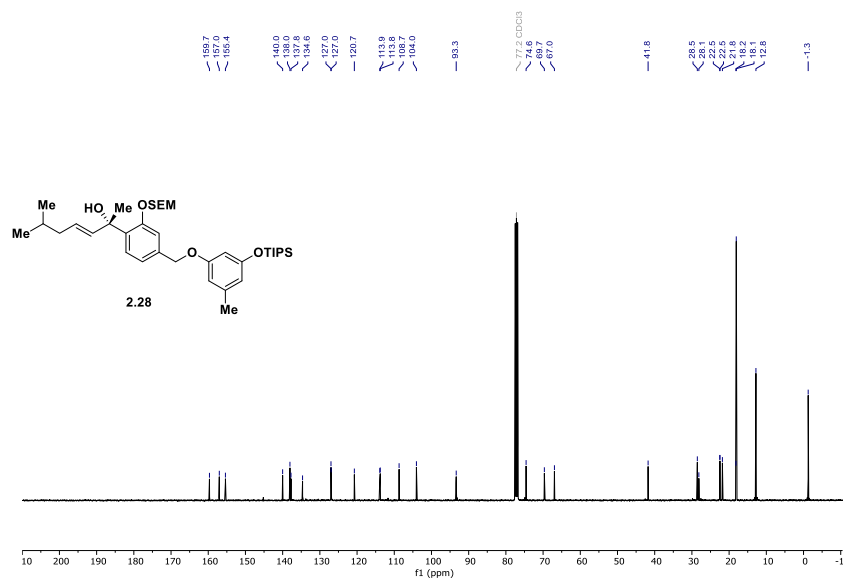
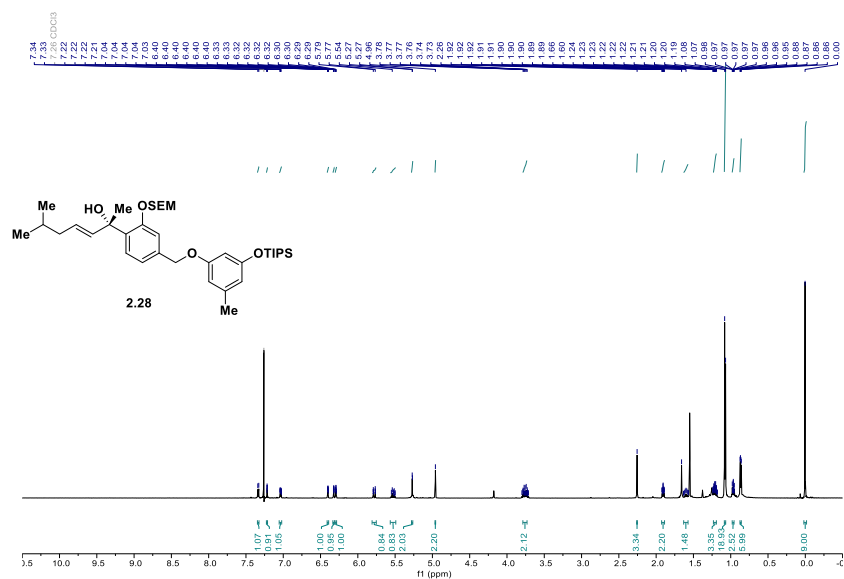


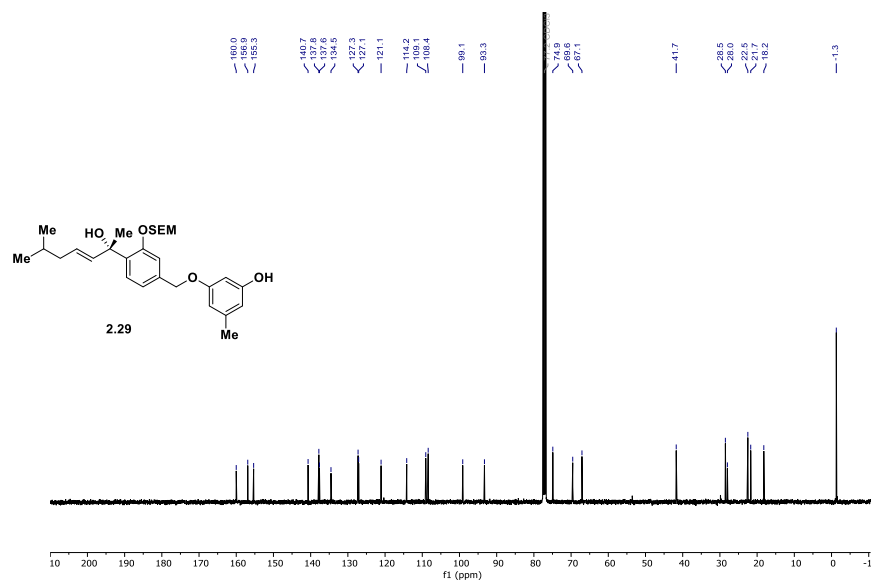
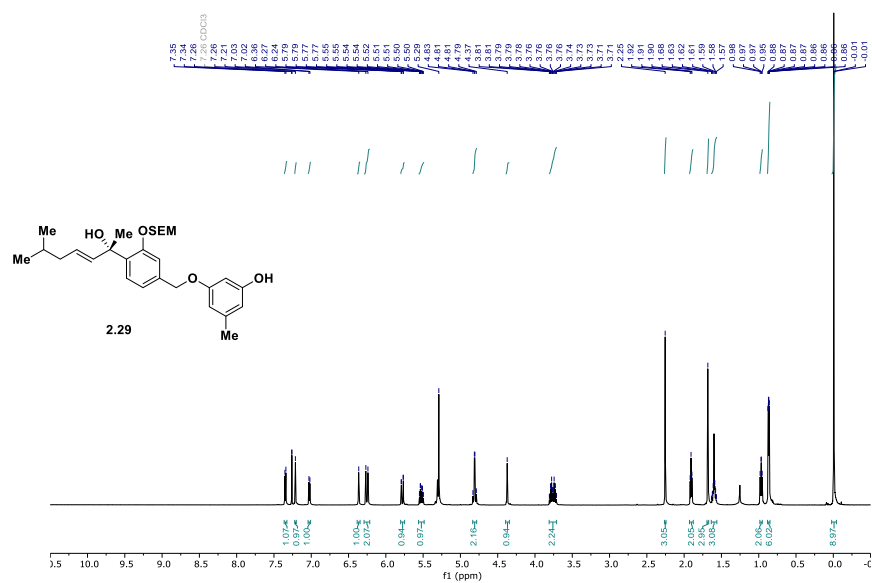


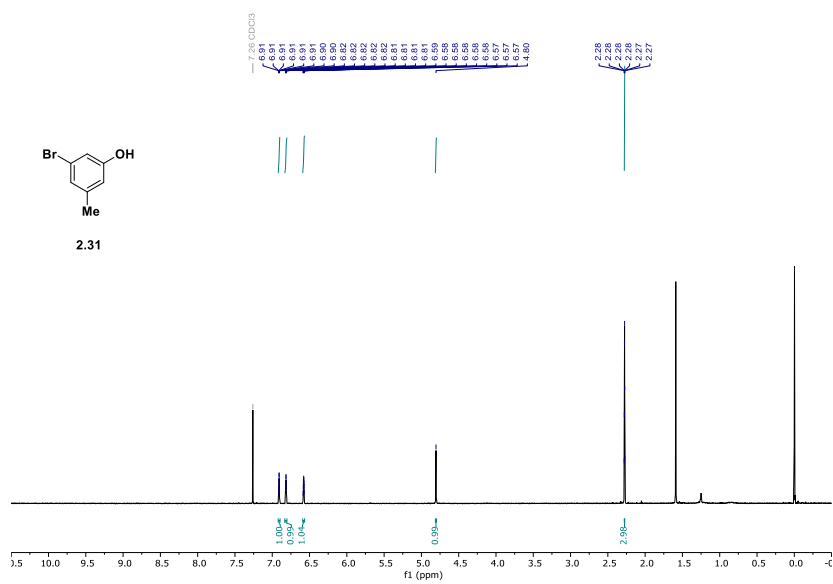
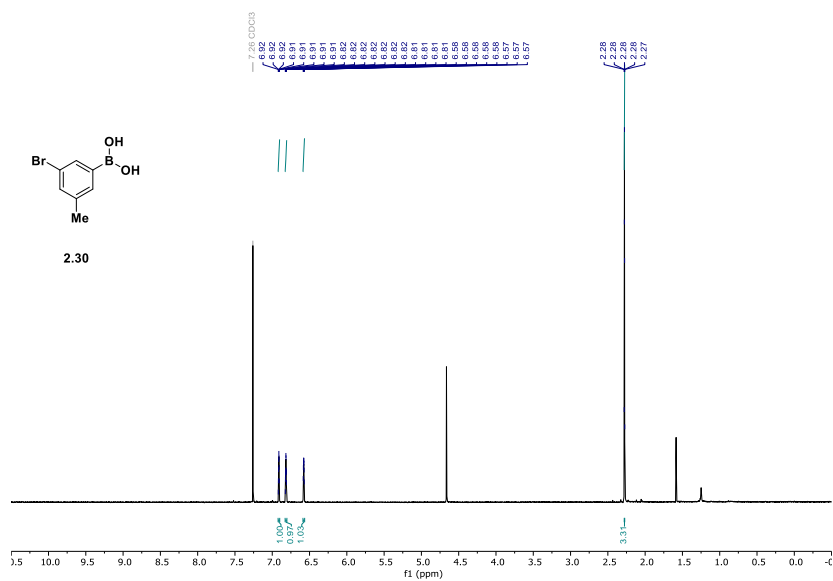


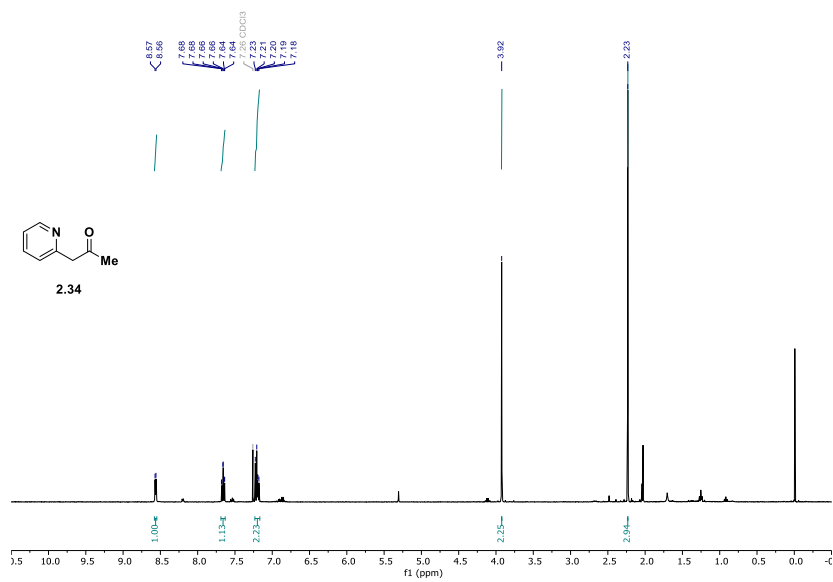
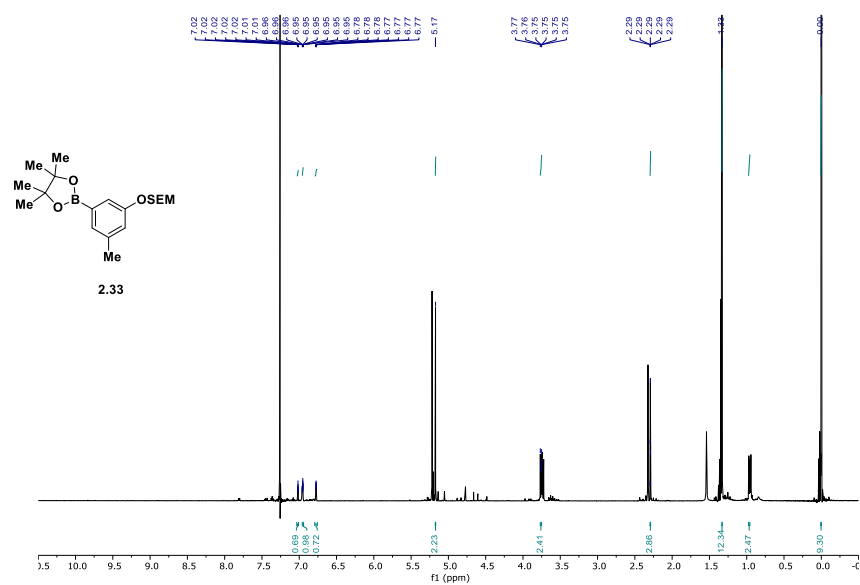


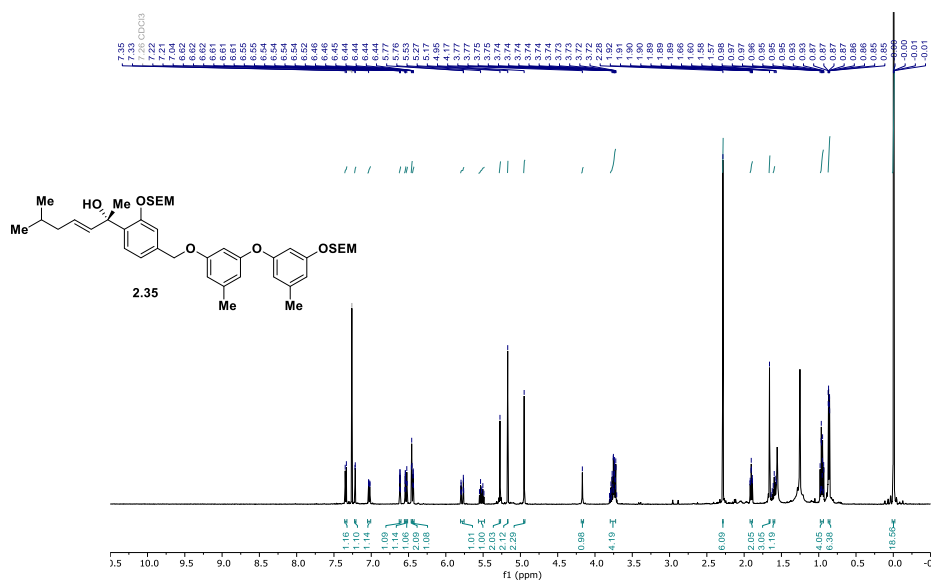
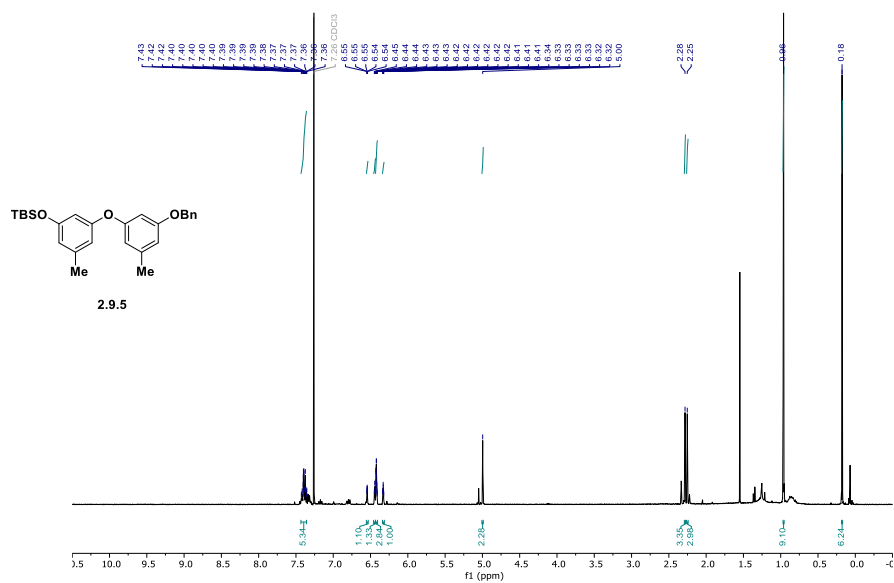


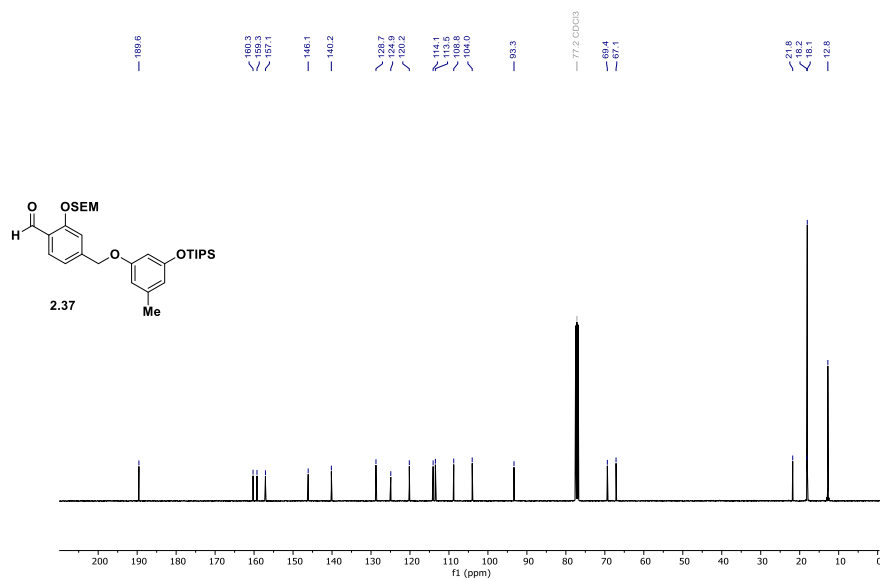


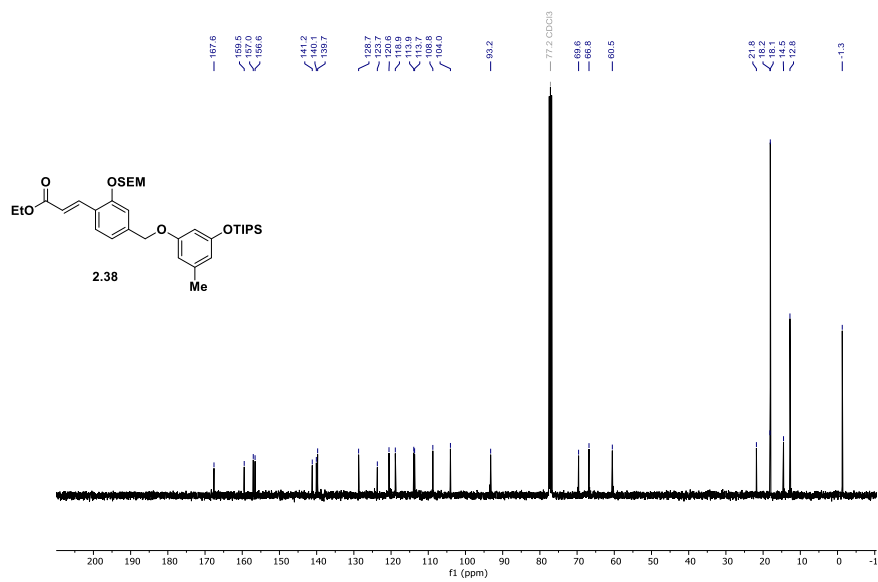
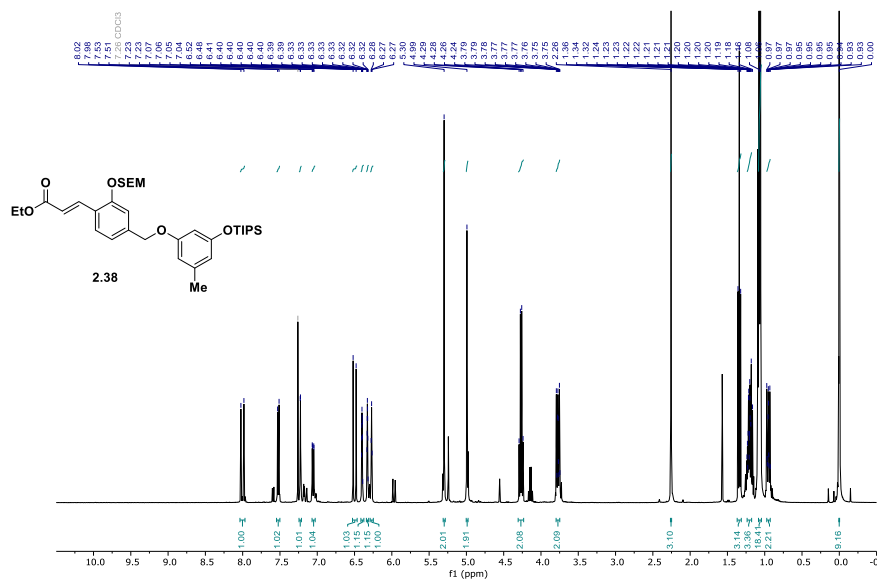


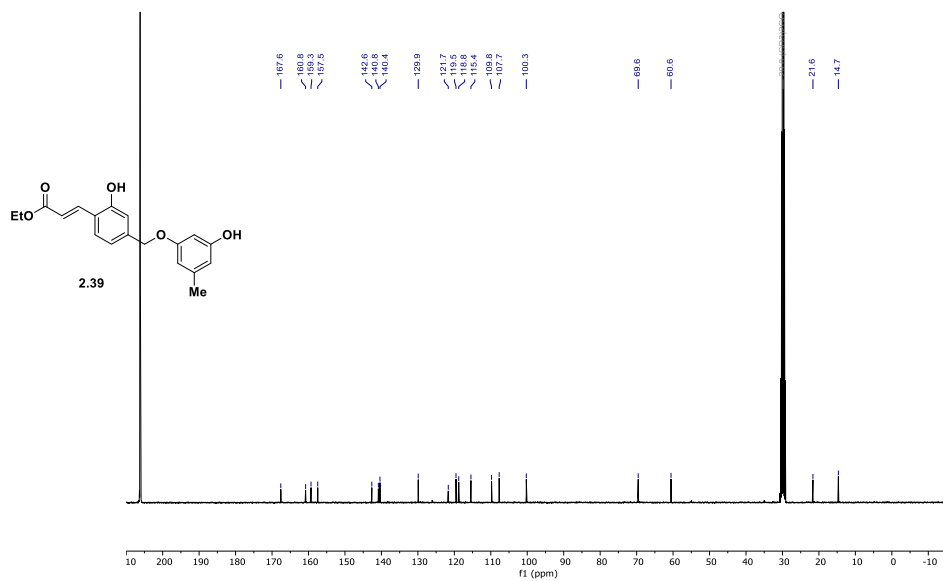
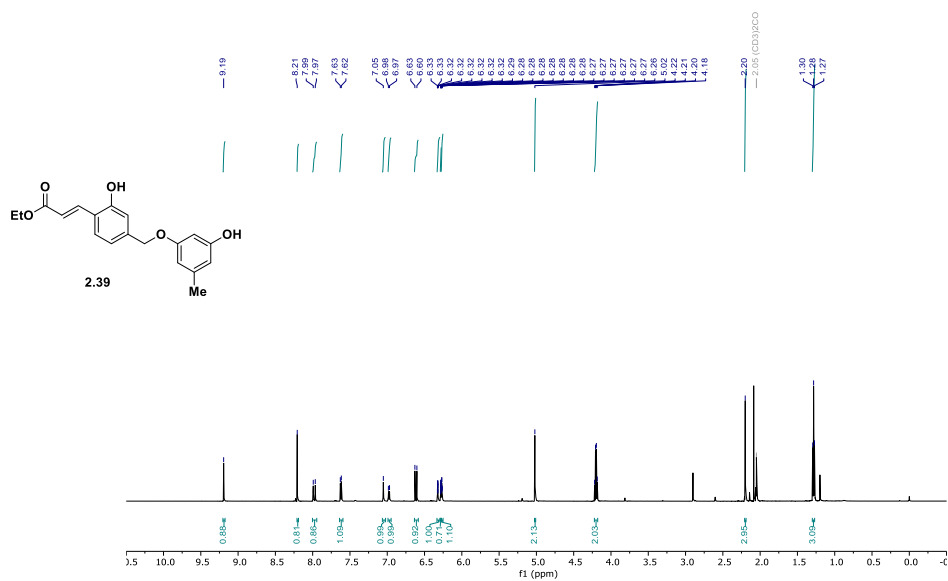


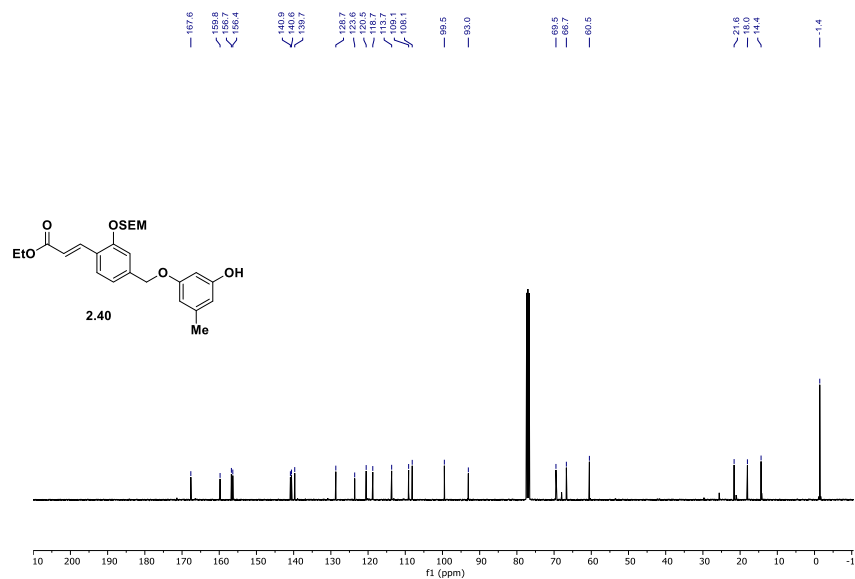
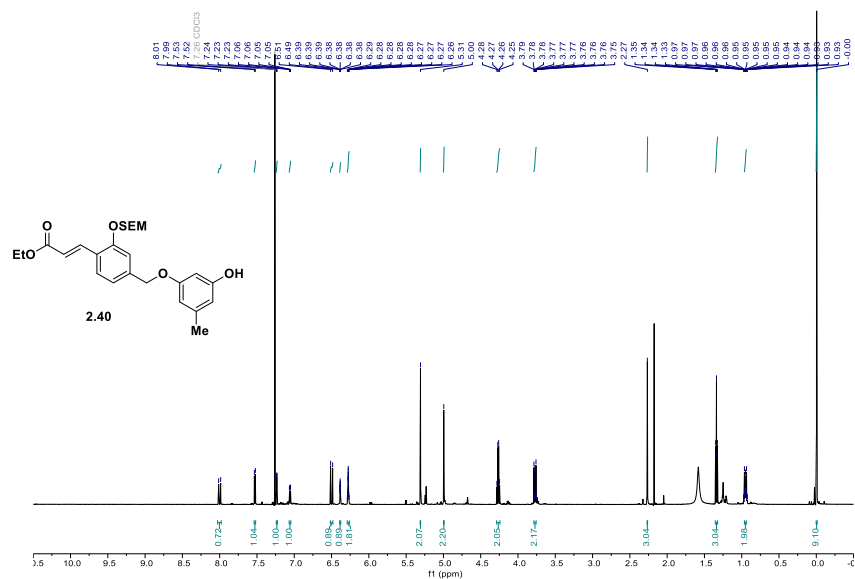


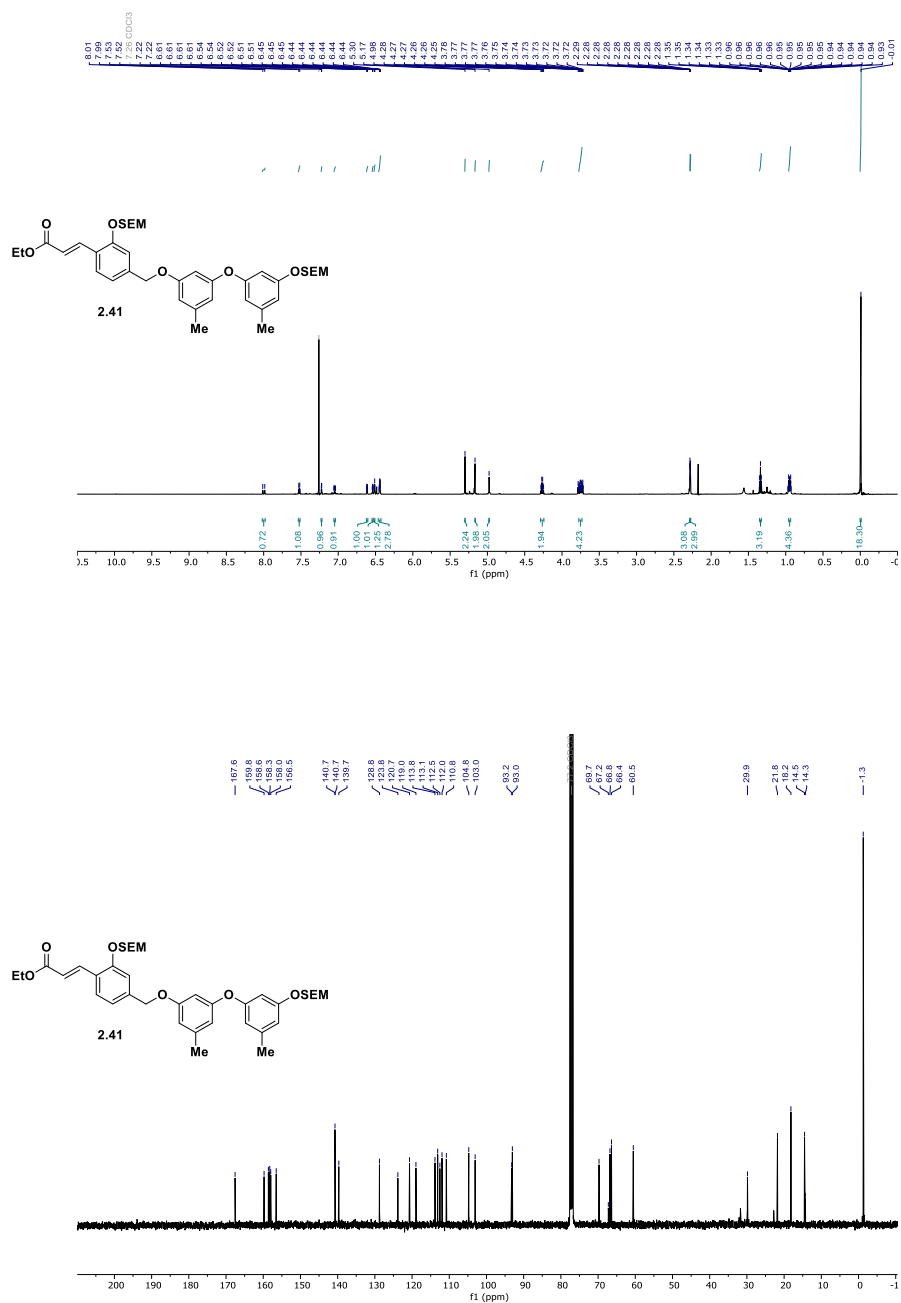


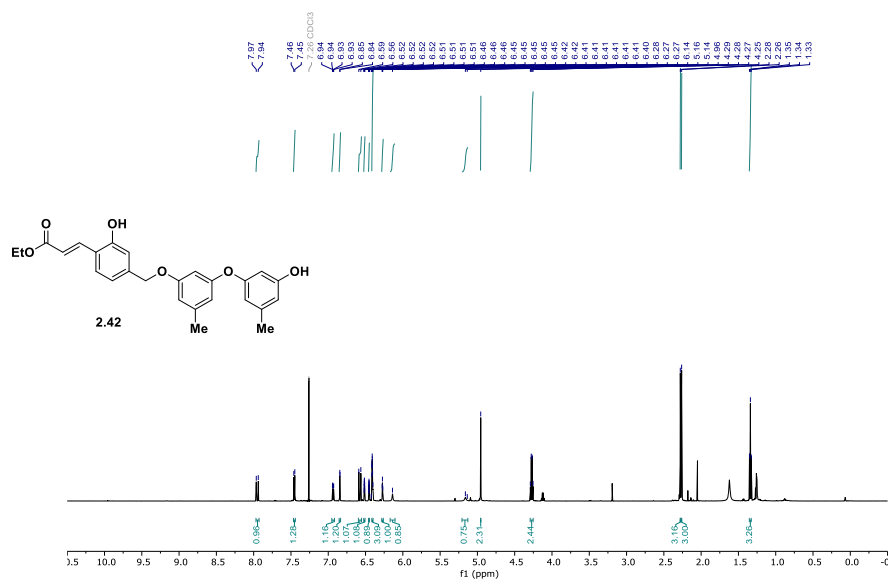


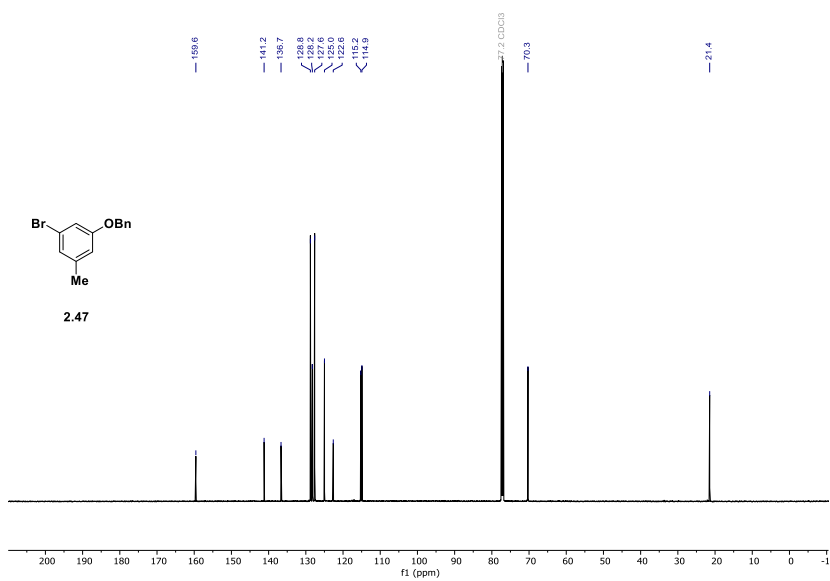
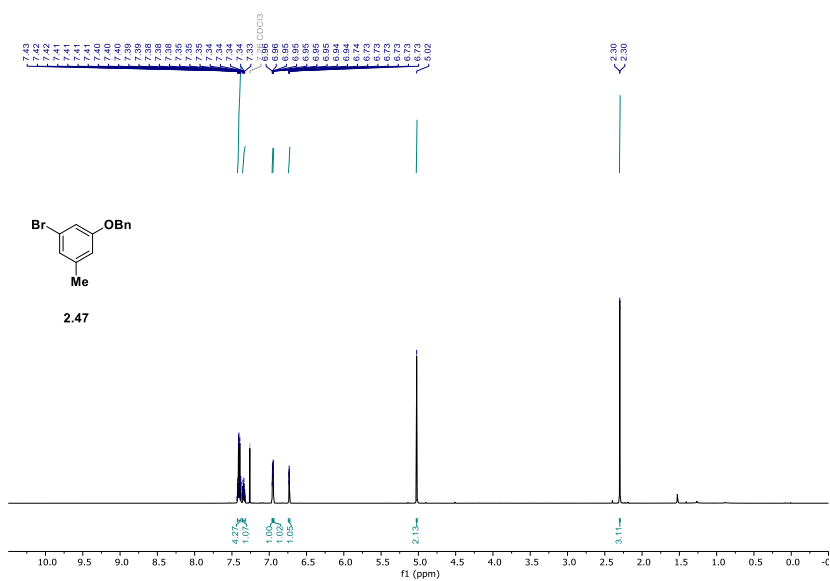


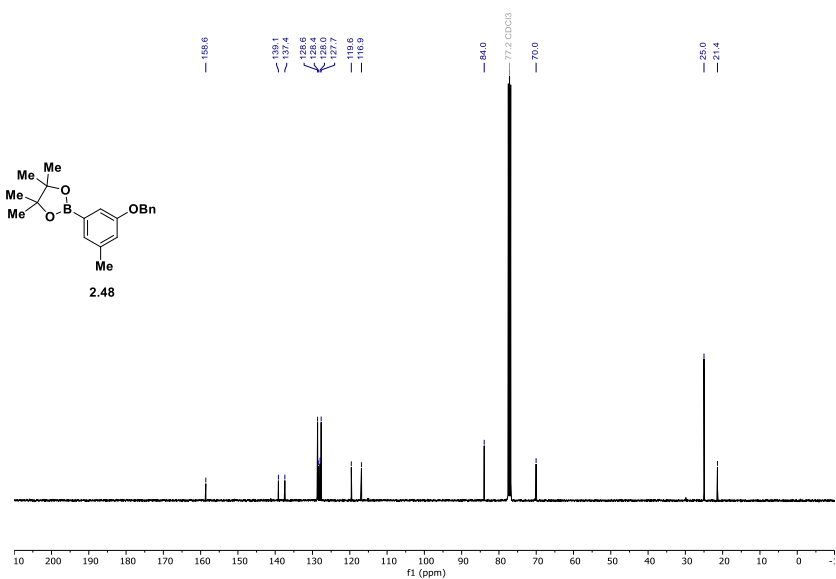
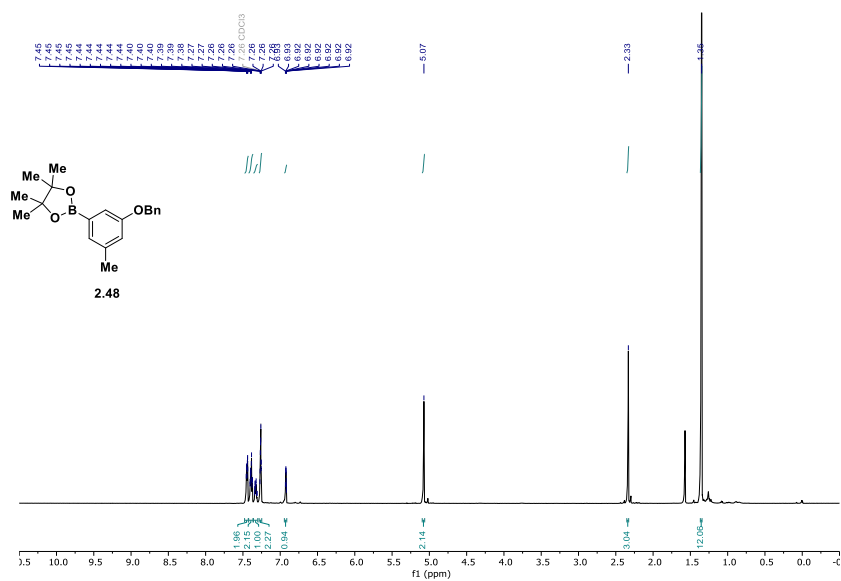












5.2 Appendix Chapter 3

